PLANT PROGRAMMED CELL DEATH REVISITED

EDITED BY: Paul McCabe, Francois Bouteau, Arunika Gunawardena and Joanna Kacprzyk

PUBLISHED IN: Frontiers in Plant Science

frontiers Research Topics

frontiers

ISSN 1664-8714
ISBN 978-2-88966-812-0
DOI 10.3389/978-2-88966-812-0

About Frontiers

Frontiers is more than just an open-access publisher of scholarly articles: it is a pioneering approach to the world of academia, radically improving the way scholarly research is managed. The grand vision of Frontiers is a world where all people have an equal opportunity to seek, share and generate knowledge. Frontiers provides immediate and permanent online open access to all its publications, but this alone is not enough to realize our grand goals.

Frontiers Journal Series

The Frontiers Journal Series is a multi-tier and interdisciplinary set of open-access, online journals, promising a paradigm shift from the current review, selection and dissemination processes in academic publishing. All Frontiers journals are driven by researchers for researchers; therefore, they constitute a service to the scholarly community. At the same time, the Frontiers Journal Series operates on a revolutionary invention, the tiered publishing system, initially addressing specific communities of scholars, and gradually climbing up to broader public understanding, thus serving the interests of the lay society, too.

Dedication to Quality

Each Frontiers article is a landmark of the highest quality, thanks to genuinely collaborative interactions between authors and review editors, who include some of the world's best academicians. Research must be certified by peers before entering a stream of knowledge that may eventually reach the public - and shape society; therefore, Frontiers only applies the most rigorous and unbiased reviews.
Frontiers revolutionizes research publishing by freely delivering the most outstanding research, evaluated with no bias from both the academic and social point of view. By applying the most advanced information technologies, Frontiers is catapulting scholarly publishing into a new generation.

What are Frontiers Research Topics?

Frontiers Research Topics are very popular trademarks of the Frontiers Journals Series: they are collections of at least ten articles, all centered on a particular subject. With their unique mix of varied contributions from Original Research to Review Articles, Frontiers Research Topics unify the most influential researchers, the latest key findings and historical advances in a hot research area! Find out more on how to host your own Frontiers Research Topic or contribute to one as an author by contacting the Frontiers Editorial Office: frontiersin.org/about/contact

PLANT PROGRAMMED CELL DEATH REVISITED

Topic Editors:
Paul McCabe, University College Dublin, Ireland
Francois Bouteau, Université Paris Diderot, France
Arunika Gunawardena, Dalhousie University, Canada
Joanna Kacprzyk, University College Dublin, Ireland

Citation: McCabe, P., Bouteau, F., Gunawardena, A., Kacprzyk, J., eds. (2021). Plant Programmed Cell Death Revisited. Lausanne: Frontiers Media SA.
doi: 10.3389/978-2-88966-812-0

Table of Contents

frontiers in Plant Science

EDITORIAL
published: 25 March 2021
doi: 10.3389/fpls.2021.672465

Editorial: Plant Programmed Cell Death Revisited

Joanna Kacprzyk[1]*, *Arunika H. L. A. N. Gunawardena*[2], *Francois Bouteau*[3] and *Paul F. McCabe*[1]

[1] School of Biology and Environmental Science, University College Dublin, Dublin, Ireland, [2] Biology Department, Dalhousie University, Halifax, NS, Canada, [3] Laboratoire Interdisciplinaire des Énergies de Demain, Université de Paris, Paris, France

Keywords: plant programmed cell death, abiotic stress, plant development, cell death proteases, transcription factors

Editorial on the Research Topic

Plant Programmed Cell Death Revisited

Plant life cannot exist without programmed cell death (PCD). Both plant developmental processes and responses to environmental factors are modulated by highly controlled, localized cell death events (Kacprzyk et al., 2011; Locato and De Gara, 2018). A detailed understanding of these essential pathways and their regulation is therefore required, especially in the light of challenges imposed on plant health and productivity by an increasingly volatile climate. Reassuringly, this Research Topic gathers contributions underscoring that the plant PCD research is coming out of age and indeed holds the potential to drive the development of novel stress tolerant crop cultivars.

The two review articles of this Topic discuss critical aspects of plant cell death pathway: its transcriptional control (Burke et al.) and the proteases involved in execution of cell death process (Balakireva and Zamyatnin). Burke et al. highlights the role of transcription factors (TFs) in the regulation of plant PCD occurring in response to abiotic and biotic environmental triggers, complementing a recent publication by Cubría-Radío and Nowack (2019), who focused on TFs involvement during developmental PCD. Burke et al. surveyed TFs from NAC, ERF and WKRY families that are involved in life-death decisions in response to environmental perturbations, including those modulating mitochondrial stress signaling. This work provides a starting point for integrative analysis of gene regulatory networks involved in PCD induced by abiotic and biotic stresses, and further elucidation of core transcriptional mechanisms driving the cell death processes in plants. Following PCD activation, proteolytic cascades are important elements of cell death pathways in animals, responsible for signal transduction (initiation caspases) and degradation of cellular components (effector caspases) (Crawford and Wells, 2011; Galluzzi et al., 2018). While canonical caspases are absent in plant genomes, numerous proteases have been shown to play a role in plant PCD, often displaying caspase-like specificity (Salvesen et al., 2016). In this Research Topic, Balakireva and Zamyatnin compare the key characteristics of protease function during cell death in animal and plant cells. The authors propose that proteolytic death-inducing cascades also exist in plant cells, although their participants are different in origin, but similar in function, to those described in animals (see Figure 1 in Balakireva and Zamyatnin). We expect that the application of increasingly accessible proteomics-based approaches will test this hypothesis in the near future.

The Original Research Articles from this topic uncover different aspects of both developmentally regulated and environmentally induced PCD modulation.

Dauphinee et al. used lace plant leaf morphogenesis, a unique model system for studying developmentally regulated PCD, to study the cross talk between cell death and autophagy. Authors demonstrate through the chemical modulation of autophagy, that the process does

OPEN ACCESS

Edited and reviewed by:
Abidur Rahman,
Iwate University, Japan

***Correspondence:**
Joanna Kacprzyk
joanna.kacprzyk@ucd.ie

Specialty section:
This article was submitted to Plant Cell Biology, a section of the journal Frontiers in Plant Science

Received: *25 February 2021*
Accepted: *02 March 2021*
Published: *25 March 2021*

Citation:
Kacprzyk J, Gunawardena AHLAN, Bouteau F and McCabe PF (2021) Editorial: Plant Programmed Cell Death Revisited. Front. Plant Sci. 12:672465. doi: 10.3389/fpls.2021.672465

not have a direct role in the induction of developmental PCD during lace plant leaf morphogenesis and primarily contributes to cell survival. These findings are an important contribution to the ongoing debate on the role of autophagy in plant cell death (Bozhkov, 2018).

The Earth's changing climate is leading to increased frequency of extreme weather events that may lead to severe crop damage. Thankfully, plants have developed diverse strategies to deal with environmental stresses, and PCD is part of this defense repertoire (Kacprzyk et al., 2011; Locato and De Gara, 2018). In this Research Topic, Pegg et al. provide novel insights into PCD-mediated formation of aerenchyma, a tissue comprising empty spaces that facilitates the gas exchange and consequently a key morphological adaptation for waterlogging tolerance (Mustroph, 2018). The study characterized the flooding-induced aerenchyma formation patterns and the associated cell wall carbohydrate modifications within the vascular stele of three Fabacea species (pea, chickpea, and runner bean). The authors identified a localized (and likely carefully controlled) pectin de-methyl-esterification as a putative mechanism paving the way for enzymatic degradation of cell walls and cell death in the aerenchyma forming tissues. Efforts to improve the flooding tolerance in legumes are likely to significantly benefit from this work. The theme of PCD in plant stress tolerance is continued by Chua et al. who explored the effect of the cyanobacteria *Nostoc muscorum* exometabolites on the heat-induced PCD in Arabidopsis root hairs. In their elegantly designed study, the authors demonstrate the suppression of stress-induced plant PCD due to uptake of cyanobacteria-derived proline. The findings suggest a novel mechanism for increased plant stress tolerance when Nostoc is used as a biofertilizer, and may therefore stimulate development of more effective strategies where Nostoc strains with increased proline secretion are generated. The rates of PCD in root hairs were also studied in this Research Topic as a potential marker for the variety stress tolerance (Chua et al.). These authors used the root hair assay (Kacprzyk et al., 2014) to score the PCD rates in barley and wheat seedlings and estimate their basal-, induced- and cross-stress tolerance. The stressed-induced PCD responses were an effective biomarker for preliminary identification of stress tolerant cereal varieties prior to large scale field testing, making the study highly relevant from an agricultural point of view.

Collectively, the contributions from the Research Topic emphasize the progress in the field of PCD research and its potential to deliver solutions from the laboratory to the farm. They also highlight the still unanswered questions about the death of plant cell—and hence the exciting opportunities for further research!

AUTHOR CONTRIBUTIONS

All authors listed have made a substantial, direct and intellectual contribution to the work, and approved it for publication.

ACKNOWLEDGMENTS

We thank the Frontiers editorial team for their help in making this Research Topic possible.

REFERENCES

Bozhkov, P. V. (2018). Plant autophagy: mechanisms and functions. *J. Exp. Bot.* 69, 1281–1285. doi: 10.1093/jxb/ery070

Crawford, E. D., and Wells, J. A. (2011). Caspase substrates and cellular remodeling. *Annu. Rev. Biochem.* 80, 1055–1087. doi: 10.1146/annurev-biochem-061809-121639

Cubría-Radío, M., and Nowack, M. K. (2019). Transcriptional networks orchestrating programmed cell death during plant development. *Curr. Top. Dev. Biol.* 131, 161–184. doi: 10.1016/bs.ctdb.2018.10.006

Galluzzi, L., Vitale, I., Aaronson, S. A., Abrams, J. M., Adam, D., Agostinis, P., et al. (2018). Molecular mechanisms of cell death: recommendations of the Nomenclature Committee on Cell Death 2018. *Cell Death Differ.* 25, 486–541. doi: 10.1038/s41418-017-0012-4

Kacprzyk, J., Daly, C. T., and McCabe, P. F. (2011). "Chapter 4–the botanical dance of death: programmed cell death in plants," in *Advances in Botanical Research*, Vol. 60, eds J. C. Kader and M. Delseny (Burlington, VT: Academic Press), 169–261. doi: 10.1016/B978-0-12-385851-1.00004-4

Kacprzyk, J., Devine, A., and McCabe, P. F. (2014). The root hair assay facilitates the use of genetic and pharmacological tools in order to dissect multiple signalling pathways that lead to programmed cell death. *PLoS ONE* 9:e94898. doi: 10.1371/journal.pone.0094898

Locato, V., and De Gara, L. (Eds.). (2018). "Programmed cell death in plants: an overview," in *Plant Programmed Cell Death: Methods and Protocols* (New York, NY: Springer New York), 1–8. doi: 10.1007/978-1-4939-7668-3_1

Mustroph, A. (2018). Improving Flooding Tolerance of Crop Plants. *Agronomy*, 8, 160. doi: 10.3390/agronomy8090160

Salvesen, G. S., Hempel, A., and Coll, N. S. (2016). Protease signaling in animal and plant-regulated cell death. *FEBS J.* 283, 2577–2598. doi: 10.1111/febs.13616

Conflict of Interest: The authors declare that the research was conducted in the absence of any commercial or financial relationships that could be construed as a potential conflict of interest.

frontiers in Plant Science

PERSPECTIVE
published: 04 June 2019
doi: 10.3389/fpls.2019.00704

Cutting Out the Gaps Between Proteases and Programmed Cell Death

Anastasia V. Balakireva[1] *and Andrey A. Zamyatnin Jr.*[1,2]*

[1] *Institute of Molecular Medicine, I.M. Sechenov First Moscow State Medical University, Moscow, Russia,* [2] *Belozersky Institute of Physico-Chemical Biology, Lomonosov Moscow State University, Moscow, Russia*

To date, many animal models for programmed cell death (PCD) have been extensively characterized and classified while such efforts in plant types of PCD still remain poorly understood. However, despite a wide range of functional differences between PCD types in animals and plants, it is certain that all of them are regulated through the recruitment of proteases. Most importantly, proteases are able to perform proteolysis that results in a gain or loss of protein function. This principle relies on the presence of proteolytic cascades where proteases are activated upon various upstream stimuli and which lead to repetitive cell death. While protease activation, proteolytic cascades and targeted substrates are described in detail mainly for nematode, human, and mice models of apoptosis, for plants, only fragmentary knowledge of protease involvement in PCD exists. However, recently, data on the regulation of general plant PCD and protease involvement have emerged which deepens our understanding of the molecular mechanisms responsible for PCD in plants. With this in mind, this article highlights major aspects of protease involvement in the execution of PCD in both animals and plants, addresses obstacles and advances in the field and proposes recommendations for further research of plant PCD.

Keywords: protease, cascade, processing, caspase, programmed cell death, plant, metacaspase

OPEN ACCESS

Edited by:
Paul McCabe,
University College Dublin, Ireland

Reviewed by:
Manuel Martinez,
Polytechnic University of Madrid, Spain
Barbara Baldan,
University of Padua, Italy

***Correspondence:**
Andrey A. Zamyatnin Jr.
zamyat@belozersky.msu.ru

Specialty section:
This article was submitted to Plant Cell Biology, a section of the journal Frontiers in Plant Science

Received: *12 February 2019*
Accepted: *13 May 2019*
Published: *04 June 2019*

Citation:
Balakireva AV and Zamyatnin AA Jr (2019) Cutting Out the Gaps Between Proteases and Programmed Cell Death. Front. Plant Sci. 10:704. doi: 10.3389/fpls.2019.00704

INTRODUCTION

Programmed cell death (PCD) is an integral part of any organism's life, and for animals PCD has been classified into apoptosis, autophagy and necrosis (Galluzzi et al., 2018). However, when it comes to classification of plant PCD, it is a rather complex matter. Morphologically, plant forms of PCD were classified into autolytic and non-autolytic types (Van Doorn et al., 2011), and where autolytic death implies a rupture of the tonoplast with the subsequent rapid clearance of the cytoplasm that causes the death of the cell. Non-autolytic PCD is characterized by such events happening after cells gave already died (Van Doorn, 2011). Functionally, PCD may occur during the normal development of a plant (dPCD) (Van Durme and Nowack, 2016), or be triggered by

pathogens (pPCD) (Huysmans et al., 2017), and which may result in a plant-specific form of PCD, for example, dying a hypersensitive response (HR) death (Balakireva and Zamyatnin, 2018).

Moreover, both dPCD and pPCD may exhibit mixed traits of autophagic, autolytic and non-autolytic forms simultaneously, which makes it difficult to distinguish dPCD and pPCD morphologically. Despite that obstacle, it is clear that the regulation of any type of PCD is held by proteases (Zamyatnin, 2015), and evidenced in both animals and plants, with apoptosis in animals being orchestrated mainly by the well-known caspases (aspartate-specific cysteine proteases). However, due to the presence of semirigid cell wall in plants, it is consequently accepted, that apoptosis is morphologically absent in plants (Locato and De Gara, 2018). Moreover, the caspases are absent in plants (Uren et al., 2000). Nevertheless, during plant PCD, caspase-like activity can be detected and is attributed to the alternative families of proteases, which include the metacaspases (Coll et al., 2014), vacuolar processing enzymes (VPEs) (Hatsugai et al., 2004, 2015), and the papain-like cysteine proteases (PLCP), etc., (Gilroy et al., 2007; Paireder et al., 2016), summarized in **Supplementary Table**. However, exactly how these proteases orchestrate PCD in plants is still largely unknown. In this article, we compare major aspects of protease function in PCD between animals and plants, address obstacles and advances in the field, and explore niches for research in the future.

PROTEASE INITIATION EVENTS: HOW ARE PCD PROTEASES ACTIVATED IN PLANTS?

The first step in the plant PCD by proteases is their activation, since all known PCD-related proteases in both animals and plants are synthetized as inactive zymogens and which require proteolytic processing in order to become enzymatically active. Most secreted zymogens have similar domain structures and contain a signal peptide, N-terminal and/or C-terminal autoinhibitory prodomains, and a catalytic domain. Hydrolysis of the autoinhibitory domains may happen autocatalytically or by other proteases, which triggers a conformational change that is indispensable for protease activity (**Figure 1A**).

Mechanistic Similarities Between Animal and Plant Protease Activation

It is widely accepted that inhibitors are essential for the regulation of protease activity in animals (Armstrong, 2006) and is evidenced for plants too. For example, during the embryonic development of *Nicotiana tabacum*, the mechanism triggering PCD of a structure involved solely in positioning the embryo proper within the seed – suspensor – is based on the antagonistic actions of two proteins, the protease inhibitor (cystatin NtCYS), and its target (cathepsin H-like protease NtCP14) (Zhao et al., 2013). Another example is the protease "Responsive to Desiccation-21" (RD21) and the activity of which is regulated through the irreversible inhibition by AtSerpin1 during PCD (Lampl et al., 2013). Moreover, recently it has been shown that there is cross-talk between the pathways for irreversible inhibition of RD21 (by AtSerpin1) and reversible inhibition, mediated by the water-soluble chlorophyll-binding protein (WSCP), which broadly contributes to the regulatory role of RD21 in innate immunity and development (Rustgi et al., 2017).

Inhibitors and activators of certain proteases are usually co-located within the same subcellular compartments (Van der Hoorn, 2004), which can differ in pH values. This can significantly affect protease activation status. One good example illustrating this point are lysosomal proteases, known as the human cathepsins, which are activated in the low pH, acidic environments within the lysosome. Interestingly, this is evidenced for plant vacuolar proteases as well, such as the *Arabidopsis* RD21 protease (Yamada et al., 2001), or its wheat homolog triticain-α (Savvateeva et al., 2015). The cysteine C13 protease legumain, which displays low-pH-dependent dimerization and activation is also another good example (Zauner et al., 2018).

Conversely, the activity of some proteases with a neutral pH optimum does depend greatly on their calcium-binding ability as in the case of mammalian membrane-bound proteases (Mellgren, 1987), which has been evidenced for plant proteases as well. Here, phytocalpain DEK1 is a calcium-dependent membrane-bound protease, the activity of which enhances significantly after binding to calcium (van der Hoorn, 2008) and serves as a good paradigm, as do the type II metacaspases (Bozhkov et al., 2005) and the MCA2 protein from *Arabidopsis thaliana* (Watanabe and Lam, 2011).

Other activators of caspase-3 in animals are reactive oxygen species (ROS) (Higuchi et al., 1998). Similarly, ROS are able to activate proteases in plants too. For example, caspase-like proteases (C1LP and C3LP) had increased activity resulting from reactive carbonyl species (RCS) which are downstream products of ROS and which consequently triggered PCD in *N. tabacum* (Biswas and Mano, 2016). Vacuolar cell death can also be regulated by ROS as oxygen radical directly cause vacuole membrane permeabilization and the release of RD21 and its consequent binding to AtSerpin1 in *A. thaliana* cells leading to PCD (Koh et al., 2016).

Taken together, we can conclude that the activation of proteases in animals and plants can happen through very similar mechanisms, as seen in animals and based on this proposition, does raise questions about how protease initiation may be triggered in plants mechanistically.

Does Plant Protease Activation Occur in a Similar Manner to Animals, During Cell Death?

During apoptosis, the extrinsic pathway of caspase activation requires the engagement of cell membrane receptors by a ligand, leading to the formation of the death-inducing signaling complex (DISC). The DISC activates caspase-8, which subsequently activates caspase-3 and caspase-7 (Crawford and Wells, 2011).

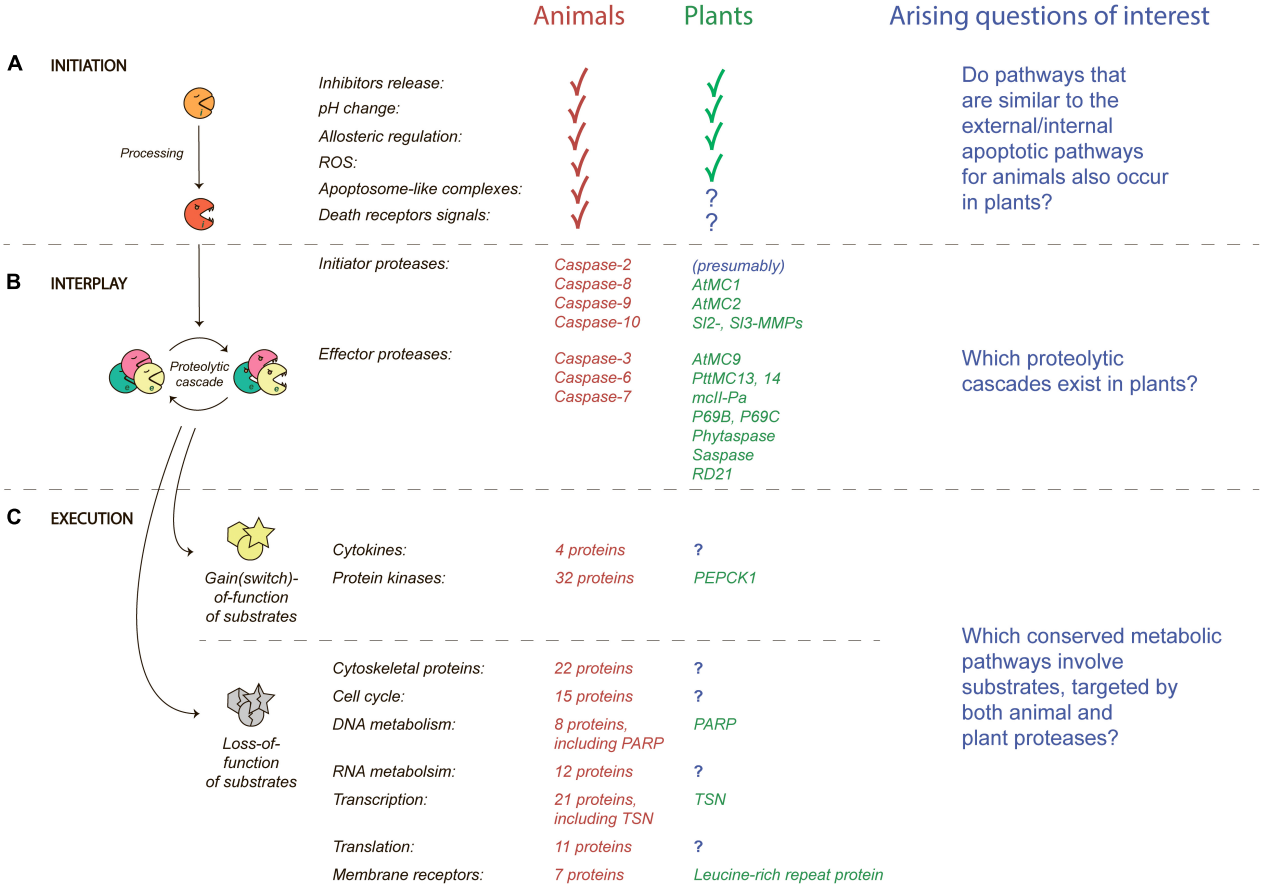

FIGURE 1 | A protease implementation in PCD. **(A)** Factors that affect activation of proteases (initiation); **(B)** protease cooperation after initiation (proteolytic cascade); and **(C)** effects on signal transduction by activated proteases (execution). Groups of caspase substrates were adapted from Fischer et al. (2003). Protease names, pathways that correspond to animals are indicated in red, and for plants – in green. Arising questions of interest are indicated by question marks and text in blue.

However, it is still unknown whether such death receptors can transduce such signals directly to the proteases in plants and therefore does require further investigation.

Alternatively, the intrinsic pathway of caspase activation requires the release of mitochondrial cytochrome *c* which induces the formation of a multiprotein complex called the apoptosome – a scaffold consisting of cytochrome *c* bound to dATP and the cytochrome *c* apoptotic protease activating factor 1 (Apaf1). The apoptosome activates caspase-9 through its N-terminal caspase recruitment domain (CARD) and caspase-9 subsequently activates caspase-3 and caspase-7 (Crawford and Wells, 2011). To date, there is no evidence that such multiprotein pro-death complexes capable of activating PCD-related proteases exist in plants. However, the presence of a similar mechanism has been indirectly observed for plants. Whereas in animals, recombinant Bax protein is responsible for the release of cytochrome *c* from mitochondria, it also induces a response similar to a HR and a cell death response in tobacco (Lacomme and Santa Cruz, 1999). Additionally, when expressed in tobacco, the antiapoptotic protein Bcl-xL can confer resistance to death induced by UV-B irradiation and by paraquat (Mitsuhara et al., 1999), or by *Tobacco mosaic virus* protein p50 (Solovieva et al., 2013). However, Bcl-2 family orthologs are absent in plants, and this process which is similar to apoptotic cell death is achieved through other unidentified proteins.

TRANSDUCTION OF A SIGNAL: WHICH PROTEOLYTIC CASCADES EXIST IN PLANTS?

Once a protease becomes active, it can change conformation and interact with other proteases (**Figure 1B**). As mentioned, the main executioners of apoptosis in animals are the caspases that act through the proteolytic cascades. Caspases can manage the two-step activation of PCD through the recruitment of initiator (caspases-2, -8, -9, -10) and effector (caspases-3, -6, -7) caspases (Crawford and Wells, 2011). How the initiator caspases cause the activation of effector caspases is through cleavages of a number of other proteases or proapoptotic substrates leading to death of the cell (Galluzzi et al., 2018). Apoptosis is characterized by YVADase, DEVDase, VEIDase and other activities (Kidd, 1998), which correspond to activities of caspases-1, -3, and -6, respectively.

Despite close homologs of caspases being absent in plants, proteases that belong to the same family of C14 cysteine proteases are present, called the metacaspases. Of interest is that metacaspases are lysine- and arginine-specific, unlike the aspartate-specific caspases, suggesting that metacaspases may not be directly responsible for similar caspase activities found in plants (Fagundes et al., 2015). However, type I metacaspases (AtMC1, AtMC2) are strongly associated with an autolytic type of PCD and plant immunity (Coll et al., 2010), whereas type II metacaspases from *Populus tremula* × *tremuloides* PttMC13 and PttMC14 are able to cleave PLCP, RD21 during xylem elements cell death (Bollhoner et al., 2018).

There are also many studies supporting the involvement of proteases other than metacaspases in plant PCD. Not only do cysteine proteases, such as VPEs, exhibit caspase-like activity (Hatsugai et al., 2004, 2009; Zhang et al., 2010), but proteasome subunit PBA1 (Hatsugai et al., 2009) and subtilases (Coffeen and Wolpert, 2004; Chichkova et al., 2010) were also shown to display same activity. Moreover, there are also proteases that do not exhibit caspase-like activity at all, but are closely associated with different types of PCD. For example, PLCPs are associated with pPCD [cathepsin B, RD21 (Gilroy et al., 2007; McLellan et al., 2009; Shindo et al., 2012)] and dPCD [CEP1, NtCP14, XCP1, XCP2 (Avci et al., 2008; Ruckh et al., 2012; Bollhoner et al., 2013; Salvesen et al., 2016)]. In addition, serine protease P69B is cleaved by apoplastic metalloproteases Sl2- and Sl3-MMPs (Li et al., 2015; Zimmermann et al., 2016) and regulates cell death in the tomato plant in response to *Botrytis cinerea* infection and *Pst*DC3000. Known examples of proteases that are involved in plant PCD are summarized in the **Supplementary Table**.

Based on the animal apoptotic pathway, the initiator-effector model was also proposed for the metacaspases (Rocha et al., 2017). Type I metacaspases undergo autocatalytic processing and can activate type II metacaspases. Due to the limited data, it is still difficult to assign the role of an initiator or effector protease for the "non-metacaspase" proteases that are involved in PCD. Moreover, there is a consensus, that cysteine proteases may not be universal regulators of PCD in plants as they are in animals (Sueldo and van der Hoorn, 2017) and may be they are unessential for plant PCD.

Recently, the question of whether proteolytic cascades exist in plants was addressed, and a specific requirement for two proteases to form a protease-substrate link was suggested (Paulus and van der Hoorn, 2019). It is certain, that although caspases are absent in plants, and caspase-like activity is not the only activity that characterizes plant PCD, it does lead to similar to animal apoptotic traits such as cytoplasm shrinkage, chromatin condensation, and nucleus fragmentation (Van Doorn et al., 2011). Based on this data, we believe that death-inducing cascades do exist in plants and their participants are different in origin, but similar in function. Recently, it was used for the identification of sites of hydrolysis by endogenous proteases during biotic stress (Balakireva et al., 2018). It was shown that during the early response of wheat to different pathogens, caspase-like and metacaspase-like activities are not required, while immune response is still triggered and, apparently, is held by some other proteases, which confirms our assumptions in a way.

EXECUTION OF A SIGNAL: IS PCD DERIVED FROM THE SAME SIGNALING PATHWAYS IN BOTH ANIMALS AND PLANTS?

It is true that plants and animals differ in a number of ways, firstly, due to photoautotrophic growth, absence of mobility and the presence of a semirigid cell wall. Independent evolution of animals and plants resulted in the development of analogous, but non-conserved protein structure and signaling pathways. One striking example is the animal Toll-like receptors. In plants, the equivalent is the receptor-like kinase (Ausubel, 2005). Both of them have a C-terminal leucine-rich repeat domain, and the cytoplasmic domains from the proteins are not conserved but are able to perform analogous functions. However, the downstream signaling events are very conserved among eukaryotic organisms such as the activation of mitogen-activated protease kinase (MAPK) cascades (Dong et al., 2002; Pitzschke et al., 2009).

Apoptosis itself is very conserved among metazoans and fungi (Crawford and Wells, 2011). Cleavage of a substrate by proteases at a specific site can result in two outcomes, the loss or gain of protein function (**Figure 1C**). In this manner, one effect of cleavage by caspases for a large number of their substrates was analyzed (Fischer et al., 2003) and made clear that the majority of substrates lose their function after hydrolytic cleavage which leads to a shutdown of almost all pathways essential for vital activity. However, some of the substrates become active after hydrolysis such as cytokines, protein kinases, and regulatory proteins essential for signal transduction.

It is very important to note that the analysis of caspase sites, their substrates and appropriate pathways in mice, *Drosophila* and *Caenorhabditis elegans*, which represent 600 million years of evolution, highlight that such sites are conserved over a relatively short evolutionary timeframe, in comparison to the lengthy timeframes of signaling pathways (Crawford et al., 2012). For example, the Tudor Staphylococcal Nuclease (TSN) protein is essential for the activation of transcription, mRNA splicing and RNA silencing, a pathway highly conserved among eukaryotes (Ausubel, 2005) in which TSN can be cleaved by both human caspase-3 and metacaspase mcII-Pa from Norway spruce (Sundstrom et al., 2009). Similarly, poly (ADP-ribose) polymerase (PARP) which is involved in the conserved pathway for DNA repair, is a substrate of human caspases and two metacaspases (MCA1 and MCA2) from the fungi *Podospora anserine* (Strobel and Osiewacz, 2013). Collectively, these findings indeed support the idea that eukaryotes share conserved signaling pathways that can be targeted by PCD proteases which are functionally similar but structurally unique (e.g., caspase-3 vs. metacaspase mcII-Pa, and others).

Additionally, another excellent example is a membrane receptor protein which can be cleaved by the tomato P69C protease and includes a leucine-rich repeat (Tornero et al., 1996). This protein can also be categorized into a group of membrane receptors that can also be targeted by caspases (**Figure 1C**). Finally, phosphoenolpyruvate carboxykinase 1 (PEPCK1) can be cleaved and activated by AtMC9 (Tsiatsiani et al., 2013). Other

examples of known substrates of plant proteases are summarized in the **Supplementary Table**.

CONCLUSION

Considering all the findings supporting the involvement of proteases in plant PCD, it is clear that this research area is relatively unexplored. To date, not a single proteolytic cascade in any plant has been linked to the PCD-related process. And the question posed is "why is the area of plan PCD so fragmentary?" Firstly, great emphasis has been placed on the study of human forms of PCD because of its immense therapeutic value and which serves as a good paradigm. Secondly, extrapolating such findings to the plant system has been slow due to a lack of methodology needed to yield findings in a timely manner. Thirdly, plant genomes contain many duplicated genes, especially in such organisms as hexaploid *Triticum aestivum*, which makes it difficult to perform knock-out studies.

To help matters, there has been some promising advances that have been recently introduced into plant science. "Big data" analytics are increasingly being used to discover hidden patterns, correlations and other insights from fragmented studies (Gharajeh, 2018). Additionally, genome-wide gene expression profiling and other "omics" technologies are indeed needed, started with proteomics approaches which are now becoming widely used for studying various aspects of plant death.

Plants do have their own features, their signaling networks do have a high level of functional redundancy. With similar parts of related pathways functionally compensating and substitutional for each other (Sewelam et al., 2016). Nevertheless, we believe that across eukaryotes its these pathways that are the most conserved rather than the regulatory proteins which constitute them. We assume that although proteases themselves (caspase vs. metacaspase) and their specificities (D-specific vs. R-, K-specific) are functionally giving rise to different morphologically diverse forms of PCD between animals and plants, such distinctions cannot be clearly made at this juncture in time.

DATA AVAILABILITY

All datasets analyzed for this study are cited in the manuscript and the **Supplementary Files**.

AUTHOR CONTRIBUTIONS

AZ conceived an original idea for a review. AB wrote the manuscript and created a figure.

FUNDING

This research was funded by the Russian Science Foundation (Grant # 16-15-10410).

ACKNOWLEDGMENTS

We are very grateful to Dr. Surinder M. Soond for his editorial work throughout the preparation of this manuscript.

SUPPLEMENTARY MATERIAL

The Supplementary Material for this article can be found online at: https://www.frontiersin.org/articles/10.3389/fpls.2019.00704/full#supplementary-material

REFERENCES

Armstrong, P. B. (2006). Proteases and protease inhibitors: a balance of activities in host-pathogen interaction. *Immunobiology* 211, 263–281. doi: 10.1016/j.imbio.2006.01.002

Ausubel, F. M. (2005). Are innate immune signaling pathways in plants and animals conserved? *Nat. Immunol.* 6, 973–979. doi: 10.1038/ni1253

Avci, U., Earl Petzold, H., Ismail, I. O., Beers, E. P., and Haigler, C. H. (2008). Cysteine proteases XCP1 and XCP2 aid micro-autolysis within the intact central vacuole during xylogenesis in *Arabidopsis* roots. *Plant J.* 56, 303–315. doi: 10.1111/j.1365-313X.2008.03592.x

Balakireva, A. V., Deviatkin, A. A., Zgoda, V. G., Kartashov, M. I., Zhemchuzhina, N. S., Dzhavakhiya, V. G., et al. (2018). Proteomics analysis reveals that caspase-like and metacaspase-like activities are dispensable for activation of proteases involved in early response to biotic stress in *Triticum aestivum* L. *Int. J. Mol. Sci.* 19:3991. doi: 10.3390/ijms19123991

Balakireva, A. V., and Zamyatnin, A. A. (2018). Indispensable role of proteases in plant innate immunity. *Int. J. Mol. Sci.* 19:629. doi: 10.3390/ijms19020629

Biswas, M. S., and Mano, J. (2016). Reactive carbonyl species activate caspase-3-like protease to initiate programmed cell death in plants. *Plant Cell Physiol.* 57, 1432–1442. doi: 10.1093/pcp/pcw053

Bollhoner, B., Jokipii-Lukkari, S., Bygdell, J., Stael, S., Adriasola, M., Muniz, L., et al. (2018). The function of two type II metacaspases in woody tissues of populus trees. *New Phytol.* 217, 1551–1565. doi: 10.1111/nph.14945

Bollhoner, B., Zhang, B., Stael, S., Denance, N., Overmyer, K., Goffner, D., et al. (2013). Post mortem function of AtMC9 in xylem vessel elements. *New Phytol.* 200, 498–510. doi: 10.1111/nph.12387

Bozhkov, P. V., Suarez, M. F., Filonova, L. H., Daniel, G., Zamyatnin, A. A., Rodriguez-Nieto, S., et al. (2005). Cysteine protease mcII-Pa executes programmed cell death during plant embryogenesis. *Proc. Natl. Acad. Sci. U.S.A.* 102, 14463–14468. doi: 10.1073/pnas.0506948102

Chichkova, N. V., Shaw, J., Galiullina, R. A., Drury, G. E., Tuzhikov, A. I., Kim, S. H., et al. (2010). Phytaspase, a relocalisable cell death promoting plant protease with caspase specificity. *EMBO J.* 29, 1149–1161. doi: 10.1038/emboj.2010.1

Coffeen, W. C., and Wolpert, T. J. (2004). Purification and characterization of serine proteases that exhibit caspase-like activity and are associated with programmed cell death in *Avena sativa*. *Plant Cell* 16, 857–873. doi: 10.1105/tpc.017947

Coll, N. S., Smidler, A., Puigvert, M., Popa, C., Valls, M., and Dangl, J. L. (2014). The plant metacaspase AtMC1 in pathogen-triggered programmed cell death and aging: functional linkage with autophagy. *Cell Death Differ.* 21, 1399–1408. doi: 10.1038/cdd.2014.50

Coll, N. S., Vercammen, D., Smidler, A., Clover, C., Van Breusegem, F., Dangl, J. L., et al. (2010). Arabidopsis type I metacaspases control cell death. *Science* 330, 1393–1397. doi: 10.1126/science.1194980

Crawford, E. D., Seaman, J. E., Ii, A. E. B., David, D. C., Babbitt, P. C., Burlingame, A. L., et al. (2012). Conservation of caspase substrates across metazoans suggests hierarchical importance of signaling pathways over specific targets and cleavage

site motifs in apoptosis. *Cell Death Differ.* 19, 2040–2048. doi: 10.1038/cdd.2012.99

Crawford, E. D., and Wells, J. A. (2011). Caspase substrates and cellular remodeling. *Annu. Rev. Biochem.* 80, 1055–1087. doi: 10.1146/annurev-biochem-061809-121639

Dong, C., Davis, R. J., and Flavell, R. A. (2002). MAP kinases in the immune response. *Annu. Rev. Immunol.* 20, 55–72. doi: 10.1146/annurev.immunol.20.091301.131133

Fagundes, D., Bohn, B., Cabreira, C., Leipelt, F., Dias, N., Bodanese-Zanettini, M. H., et al. (2015). Caspases in plants: metacaspase gene family in plant stress responses. *Funct. Integr. Genomics* 15, 639–649. doi: 10.1007/s10142-015-0459-7

Fischer, U., Jänicke, R. U., and Schulze-Osthoff, K. (2003). Many cuts to ruin: a comprehensive update of caspase substrates. *Cell Death Differ.* 10, 76–100. doi: 10.1038/sj.cdd.4401160

Galluzzi, L., Vitale, I., Aaronson, S. A., Abrams, J. M., Adam, D., Agostinis, P., et al. (2018). Molecular mechanisms of cell death: recommendations of the nomenclature committee on cell death 2018. *Cell Death Differ.* 25, 486–541. doi: 10.1038/s41418-017-0012-4

Gharajeh, M. S. (2018). Biological big data analytics. *Adv. Comput.* 109, 321–355. doi: 10.1016/bs.adcom.2017.08.002

Gilroy, E. M., Hein, I., van der Hoorn, R., Boevink, P. C., Venter, E., McLellan, H., et al. (2007). Involvement of cathepsin B in the plant disease resistance hypersensitive response. *Plant J.* 52, 1–13. doi: 10.1111/j.1365-313X.2007.03226.x

Hatsugai, N., Iwasaki, S., Tamura, K., Kondo, M., Fuji, K., Ogasawara, K., et al. (2009). A novel membrane fusion-mediated plant immunity against bacterial pathogens. *Genes Dev.* 23, 2496–2506. doi: 10.1101/gad.1825209

Hatsugai, N., Kuroyanagi, M., Yamada, K., Meshi, T., Tsuda, S., Kondo, M., et al. (2004). A plant vacuolar protease, VPE, mediates virus-induced hypersensitive cell death. *Science* 305, 855–858. doi: 10.1126/science.1099859

Hatsugai, N., Yamada, K., Goto-Yamada, S., and Hara-Nishimura, I. (2015). Vacuolar processing enzyme in plant programmed cell death. *Front. Plant Sci.* 6:234. doi: 10.3389/fpls.2015.00234

Higuchi, M., Honda, T., Proske, R. J., and Yeh, E. T. H. (1998). Regulation of reactive oxygen species-induced apoptosis and necrosis by caspase 3-like proteases. *Oncogene* 17, 2753–2760. doi: 10.1038/sj.onc.1202211

Huysmans, M., Lema, A. S., Coll, N. S., and Nowack, M. K. (2017). Dying two deaths programmed cell death regulation in development and disease. *Curr. Opin. Plant Biol.* 35, 37–44. doi: 10.1016/j.pbi.2016.11.005

Kidd, V. J. (1998). Proteolytic activities that mediate apoptosis. *Annu. Rev. Physiol.* 60, 533–573. doi: 10.1146/annurev.physiol.60.1.533

Koh, E., Carmieli, R., Mor, A., and Fluhr, R. (2016). Singlet oxygen-induced membrane disruption and serpin-protease balance in vacuolar-driven cell death. *Plant Physiol.* 171, 1616–1625. doi: 10.1104/pp.15.02026

Lacomme, C., and Santa Cruz, S. (1999). Bax-induced cell death in tobacco is similar to the hypersensitive response. *Proc. Natl. Acad. Sci.* 96, 7956–7961. doi: 10.1073/pnas.96.14.7956

Lampl, N., Alkan, N., Davydov, O., and Fluhr, R. (2013). Set-point control of RD21 protease activity by AtSerpin1 controls cell death in *Arabidopsis*. *Plant J.* 74, 498–510. doi: 10.1111/tpj.12141

Li, D., Zhang, H., Song, Q., Wang, L., Liu, S., Hong, Y., et al. (2015). Tomato Sl3-MMP, a member of the Matrix metalloproteinase family, is required for disease resistance against *Botrytis cinerea* and *Pseudomonas* syringae pv. tomato DC3000. *BMC Plant Biol.* 15:143. doi: 10.1186/s12870-015-0536-z

Locato, V., and De Gara, L. (2018). Programmed cell death in plants: an overview. *Methods Mol. Biol.* 1743, 1–8. doi: 10.1007/978-1-4939-7668-3_1

McLellan, H., Gilroy, E. M., Yun, B. W., Birch, P. R., and Loake, G. J. (2009). Functional redundancy in the *Arabidopsis* Cathepsin B gene family contributes to basal defence, the hypersensitive response and senescence. *New Phytol.* 183, 408–418. doi: 10.1111/j.1469-8137.2009.02865.x

Mellgren, R. L. (1987). Calcium-dependent proteases: an enzyme system active at cellular membranes? *FASEB J.* 1, 110–115. doi: 10.1096/fasebj.1.2.2886390

Mitsuhara, I., Malik, K. A., Miura, M., and Ohashi, Y. (1999). Animal cell-death suppressors Bcl-x(L) and Ced-9 inhibit cell death in tobacco plants. *Curr. Biol.* 9, 775–778.

Paireder, M., Mehofer, U., Tholen, S., Porodko, A., Schahs, P., Maresch, D., et al. (2016). The death enzyme CP14 is a unique papain-like cysteine proteinase with a pronounced S2 subsite selectivity. *Arch. Biochem. Biophys.* 603, 110–117. doi: 10.1016/j.abb.2016.05.017

Paulus, J. K., and van der Hoorn, R. A. L. (2019). Do proteolytic cascades exist in plants? *J. Exp. Bot.* 70, 1997–2002. doi: 10.1093/jxb/erz016

Pitzschke, A., Schikora, A., and Hirt, H. (2009). MAPK cascade signalling networks in plant defence. *Curr. Opin. Plant Biol.* 12, 421–426. doi: 10.1016/j.pbi.2009.06.008

Rocha, G. L., Fernandez, J. H., Oliveira, A. E. A., and Fernandes, K. V. S. (2017). "Programmed Cell Death-Related Proteases in Plants," in *Enzyme Inhibitors and Activators*, ed. O. D. Lopina (London: InTech).

Ruckh, J. M., Zhao, J.-W., Shadrach, J. L., van Wijngaarden, P., Rao, T. N., Wagers, A. J., et al. (2012). Rejuvenation of regeneration in the aging central nervous system. *Cell Stem Cell* 10, 96–103. doi: 10.1016/j.stem.2011.11.019

Rustgi, S., Boex-Fontvieille, E., Reinbothe, C., von Wettstein, D., and Reinbothe, S. (2017). Serpin1 and WSCP differentially regulate the activity of the cysteine protease RD21 during plant development in *Arabidopsis thaliana*. *Proc. Natl. Acad. Sci. U.S.A.* 114, 2212–2217. doi: 10.1073/pnas.1621496114

Salvesen, G. S., Hempel, A., and Coll, N. S. (2016). Protease signaling in animal and plant-regulated cell death. *FEBS J.* 283, 2577–2598. doi: 10.1111/febs.13616

Savvateeva, L. V., Gorokhovets, N. V., Makarov, V. A., Serebryakova, M. V., Solovyev, A. G., Morozov, S. Y., et al. (2015). Glutenase and collagenase activities of wheat cysteine protease Triticain-alpha: feasibility for enzymatic therapy assays. *Int. J. Biochem. Cell Biol.* 62, 115–124. doi: 10.1016/j.biocel.2015.03.001

Sewelam, N., Kazan, K., and Schenk, P. M. (2016). Global plant stress signaling: reactive oxygen species at the cross-road. *Front. Plant Sci.* 7:187. doi: 10.3389/fpls.2016.00187

Shindo, T., Misas-Villamil, J. C., Horger, A. C., Song, J., and van der Hoorn, R. A. (2012). A role in immunity for Arabidopsis cysteine protease RD21, the ortholog of the tomato immune protease C14. *PLoS One* 7:e29317. doi: 10.1371/journal.pone.0029317

Solovieva, A. D., Frolova, O. Y., Solovyev, A. G., Morozov, S. Y., and Zamyatnin, A. A. Jr. (2013). Effect of mitochondria-targeted antioxidant SkQ1 on programmed cell death induced by viral proteins in tobacco plants. *Biochemistry* 78, 1006–1012. doi: 10.1134/S000629791309006X

Strobel, I., and Osiewacz, H. D. (2013). Poly (ADP-Ribose) polymerase is a substrate recognized by two metacaspases of *Podospora anserina*. *Eukaryot. Cell* 12, 900–912. doi: 10.1128/EC.00337-12

Sueldo, D. J., and van der Hoorn, R. A. L. (2017). Plant life needs cell death, but does plant cell death need Cys proteases? *FEBS J.* 284, 1577–1585. doi: 10.1111/febs.14034

Sundstrom, J. F., Vaculova, A., Smertenko, A. P., Savenkov, E. I., Golovko, A., Minina, E., et al. (2009). Tudor staphylococcal nuclease is an evolutionarily conserved component of the programmed cell death degradome. *Nat. Cell Biol.* 11, 1347–1354. doi: 10.1038/ncb1979

Tornero, P., Mayda, E., Gómez, M. D., Cañas, L., Conejero, V., and Vera, P. (1996). Characterization of LRP, a leucine-rich repeat (LRR) protein from tomato plants that is processed during pathogenesis. *Plant J.* 10, 315–330. doi: 10.1046/j.1365-313X.1996.10020315.x

Tsiatsiani, L., Timmerman, E., De Bock, P.-J. J., Vercammen, D., Stael, S., van de Cotte, B., et al. (2013). The *Arabidopsis* METACASPASE9 Degradome. *Plant Cell* 25, 2831–2847. doi: 10.1105/tpc.113.115287

Uren, A. G., O'Rourke, K., Aravind, L. A., Pisabarro, M. T., Seshagiri, S., Koonin, E. V., et al. (2000). Identification of paracaspases and metacaspases: two ancient families of caspase-like proteins, one of which plays a key role in MALT lymphoma. *Mol. Cell* 6, 961–967. doi: 10.1016/s1097-2765(00)00094-0

Van der Hoorn, R. (2004). Activity profiling of papain-like cysteine proteases in plants. *Plant Physiol.* 135, 1170–1178. doi: 10.1104/pp.104.041467.1170

van der Hoorn, R. A. L. (2008). Plant proteases: from phenotypes to molecular mechanisms. *Annu. Rev. Plant Biol.* 59, 191–223. doi: 10.1146/annurev.arplant.59.032607.092835

Van Doorn, W. G. (2011). Classes of programmed cell death in plants, compared to those in animals. *J. Exp. Bot.* 62, 4749–4761. doi: 10.1093/jxb/err196

Van Doorn, W. G., Beers, E. P., Dangl, J. L., Franklin-Tong, V. E., Gallois, P., Hara-Nishimura, I., et al. (2011). Morphological classification of plant cell deaths. *Cell Death Differ.* 18, 1241–1246. doi: 10.1038/cdd.2011.36

Van Durme, M., and Nowack, M. K. (2016). Mechanisms of developmentally controlled cell death in plants. *Curr. Opin. Plant Biol.* 29, 29–37. doi: 10.1016/j.pbi.2015.10.013

Watanabe, N., and Lam, E. (2011). Arabidopsis metacaspase 2d is a positive mediator of cell death induced during biotic and abiotic stresses. *Plant J.* 66, 969–982. doi: 10.1111/j.1365-313X.2011.04554.x

Yamada, K., Matsushima, R., Nishimura, M., and Hara-Nishimura, I. (2001). A slow maturation of a cysteine protease with a granulin domain in the vacuoles of senescing *Arabidopsis* leaves. *Plant Physiol.* 127, 1626–1634. doi: 10.1104/pp.127.4.1626

Zamyatnin, A. A. (2015). Plant proteases involved in regulated cell death. *Biochemistry* 80, 1701–1715. doi: 10.1134/S0006297915130064

Zauner, F. B., Dall, E., Regl, C., Grassi, L., Huber, C. G., Cabrele, C., et al. (2018). Crystal structure of plant legumain reveals a unique two-chain state with pH-dependent activity regulation. *Plant Cell* 30, 686–699. doi: 10.1105/tpc.17.00963

Zhang, H., Dong, S., Wang, M., Wang, W., Song, W., Dou, X., et al. (2010). The role of vacuolar processing enzyme (VPE) from *Nicotiana benthamiana* in the elicitor-triggered hypersensitive response and stomatal closure. *J. Exp. Bot.* 61, 3799–3812. doi: 10.1093/jxb/erq189

Zhao, P., Zhou, X. M., Zhang, L. Y., Wang, W., Ma, L. G., Yang, L. B., et al. (2013). A bipartite molecular module controls cell death activation in the basal cell lineage of plant embryos. *PLoS Biol.* 11:e1001655. doi: 10.1371/journal.pbio.1001655

Zimmermann, D., Gomez-Barrera, J. A., Pasule, C., Brack-Frick, U. B., Sieferer, E., Nicholson, T. M., et al. (2016). Cell death control by matrix metalloproteinases. *Plant Physiol.* 171, 1456–1469. doi: 10.1104/pp.16.00513

Conflict of Interest Statement: The authors declare that the research was conducted in the absence of any commercial or financial relationships that could be construed as a potential conflict of interest.

frontiers in Plant Science

ORIGINAL RESEARCH
published: 22 October 2019
doi: 10.3389/fpls.2019.01198

The Function of Autophagy in Lace Plant Programmed Cell Death

*Adrian N. Dauphinee[1,2], Georgia L. Denbigh[1], Alice Rollini[1], Meredith Fraser[1], Christian R. Lacroix[3] and Arunika H. L. A. N. Gunawardena[1]**

[1] Department of Biology, Dalhousie University, Halifax, NS, Canada, [2] Department of Molecular Sciences, Swedish University of Agricultural Sciences, Uppsala, Sweden, [3] Department of Biology, University of Prince Edward Island, Charlottetown, PE, Canada

The lace plant (*Aponogeton madagascariensis*) is an aquatic monocot that utilizes programmed cell death (PCD) to form perforations throughout its mature leaves as part of normal development. The lace plant is an emerging model system representing a unique form of developmental PCD. The role of autophagy in lace plant PCD was investigated using live cell imaging, transmission electron microscopy (TEM), immunolocalization, and *in vivo* pharmacological experimentation. ATG8 immunostaining and acridine orange staining revealed that autophagy occurs in both healthy and dying cells. Autophagosome-like vesicles were also found in healthy and dying cells through ultrastructural analysis with TEM. Following autophagy modulation, there was a noticeable increase in vesicles and vacuolar aggregates. A novel cell death assay utilizing lace plant leaves revealed that autophagy enhancement with rapamycin significantly decreased cell death rates compared to the control, whereas inhibition of autophagosome formation with wortmannin or blocking the degradation of cargoes with concanamycin A had an opposite effect. Although autophagy modulation significantly affected cell death rates in cells that are destined to die, neither the promotion nor inhibition of autophagy in whole plants had a significant effect on the number of perforations formed in lace plant leaves. Our data indicate that autophagy predominantly contributes to cell survival, and we found no clear evidence for its direct involvement in the induction of developmental PCD during perforation formation in lace plant leaves.

Keywords: programmed cell death (PCD), autophagy, TEM, confocal microscopy, immunolocalization, ATG8, leaf development, perforation formation

OPEN ACCESS

Edited by:
Diane C. Bassham, Iowa State University, United States

Reviewed by:
Agnieszka Sirko, Institute of Biochemistry and Biophysics (PAN), Poland
Olga V. Voitsekhovskaja, Komarov Botanical Institute (RAS), Russia
Caiji Gao, South China Normal University, China
Suayib Üstün, University of Tuebingen, Germany

****Correspondence:***
Arunika H. L. A. N. Gunawardena
arunika.gunawardena@dal.ca

Specialty section:
This article was submitted to Plant Cell Biology, a section of the journal Frontiers in Plant Science

Received: *13 May 2019*
Accepted: *30 August 2019*
Published: *22 October 2019*

Citation:
Dauphinee AN, Denbigh GL, Rollini A, Fraser M, Lacroix CR and Gunawardena AHLAN (2019) The Function of Autophagy in Lace Plant Programmed Cell Death. Front. Plant Sci. 10:1198. doi: 10.3389/fpls.2019.01198

INTRODUCTION

Autophagy is a major catabolic pathway critical for the survival of eukaryotes as it enables cells to maintain homeostasis under stressful conditions such as nutrient deprivation or starvation (Klionsky et al., 2016). Autophagy plays a central role in many processes including programmed cell death (PCD), stress responses, and longevity (Floyd et al., 2015). It has been proposed that there are three classes of autophagy in plants: i) microautophagy which involves the direct passing of contents into a lytic vacuole; ii) macroautophagy is coordinated by evolutionarily conserved AuTophaGy-related (ATG) proteins and involves either the bulk or selective sequestration of cytoplasmic cargoes into double-membrane vesicles known as autophagosomes, which are then delivered to a lytic compartment for degradation; and iii) mega-autophagy, defined by cellular degradation following

the release of hydrolases from the vacuole after tonoplast rupture (Van Doorn and Papini, 2013; Marshall and Vierstra, 2018). Of these classes, macroautophagy, hereafter autophagy, is the only well-characterized form of autophagy in plants (Batoko et al., 2017) and is therefore the focus of this study.

Because of the significant involvement of autophagy in a wide range of developmental processes and stress responses, there has been a substantial effort to identify chemicals that modulate autophagic flux (**Figure 1**). Autophagy is an evolutionary conserved process in fungi, plants, and animals. In fact, a great deal of our understanding of the regulatory genes involved in autophagy originated from yeast (*Saccharomyces cerevisiae*) mutagenic screens (Tsukada and Ohsumi, 1993). There have been 40 ATG proteins identified in yeast to date, and among them is ATG8, which is a ubiquitin-like protein integral for autophagosome membrane formation (Shpilka et al., 2011; Avin-Wittenberg et al., 2018; Marshall and Vierstra, 2018). The central regulator of autophagy is the target of rapamycin (TOR) kinase, which comprised two complexes: TORC1 and TORC2 (Liu and Bassham, 2012). Autophagy is inhibited by TOR, and therefore compounds such as rapamycin (Ballou and Lin, 2008) and AZD 8055 (Din et al., 2012), which block TOR, lead to an increase in autophagic activity. A similar effect can be achieved through starvation, which also inhibits TOR (Kwak et al., 2012; Liu and Bassham, 2012; Heras-Sandoval et al., 2014). Autophagy can also be inhibited with compounds such as wortmannin or 3-methyladenine that interfere with vesicle nucleation by inhibiting phosphoinositide 3-kinase (Klionsky et al., 2016; Marshall and Vierstra, 2018). Additionally, autophagy can be inhibited indirectly toward the end of autophagic flux by halting the breakdown of autophagic bodies *via* raising the vacuolar pH through the specific inhibition of vacuolar ATPases with concanamycin A (Huss et al., 2002).

The lace plant (*Aponogeton madagascariensis*) is an aquatic monocot with a unique perforated morphology created by developmentally regulated PCD (**Figure 2A**; Gunawardena et al., 2004). The lace plant is an emerging model for studying PCD due to the predictability of perforation formation, its nearly transparent leaves that facilitate live cell imaging, and established sterile cultures for *in vivo* pharmacological experimentation (Gunawardena et al., 2006). The first visible sign that PCD is underway is the disappearance of anthocyanins (which are potent antioxidants) between longitudinal and transverse veins in spaces known as areoles (Gunawardena et al., 2004). The disappearance of anthocyanins provides a visual gradient of PCD within each areole (**Figures 2B, C**): non-PCD (NPCD; **Figure 2D**) cells retain anthocyanins throughout perforation formation; early-PCD (EPCD; **Figure 2E**) cells have lost anthocyanin and are fated to die but still have an abundance of chlorophyll pigmentation; and cells that are in the late-PCD (LPCD; **Figure 2F**) are mostly devoid of pigmentation and near death (Lord et al., 2011; Dauphinee et al., 2017). When observed with transmission electron microscopy (TEM), the PCD gradient highlights the degradation of LPCD compared to NPCD cells (**Figure 2G**). The dynamics and time-course analysis of lace plant PCD has been described in detail (Wertman et al., 2012), and preliminary evidence suggested that autophagy may be involved; however, its function in lace plant PCD remains unknown. Autophagy has been implicated in the regulation of various plant PCD systems and therefore warrants further investigation in lace plants. The purpose of this study is to elucidate the function of autophagy in developmental PCD during lace plant leaf development.

MATERIALS AND METHODS

Plant Material and *in Vivo* Experiments

Lace plant (*A. madagascariensis*) cultures were propagated according to Gunawardena et al. (2006). To test the effects of autophagy modulators on the formation of perforations, 40 ml septum-lidded vials were used (Sigma-Aldrich) according to Dauphinee et al. (2012). Plants were grown in magenta boxes under daylight deluxe fluorescent lighting (Phillips) on 12-h dark-light cycles at an intensity of 125 $\mu mol\, m^{-2} s^{-1}$ for approximately 4 weeks. They were then transferred to the vials and allowed to acclimate for 1 to 2 weeks. Once plants produced two to three perforated leaves, they were assigned randomly to a treatment group. Treatments were applied once to the liquid media and were dissolved in dimethyl sulfoxide (DMSO). The autophagy modulator treatments were optimized using a gradient of concentrations. The mock control treatment group received an equal volume of DMSO used for the autophagy modulator treatments. Optimal concentrations had no severe effects on leaf growth or showed signs of stress, which was observed at higher concentrations with the autophagy modulators. The optimized concentrations included 5 μM rapamycin (Enzo Scientific, BML-275), 1 μM AZD 8055 (AZD; ApexBio Technology, A8214), and 5 μM wortmannin (Cayman Chemical, 10010591).

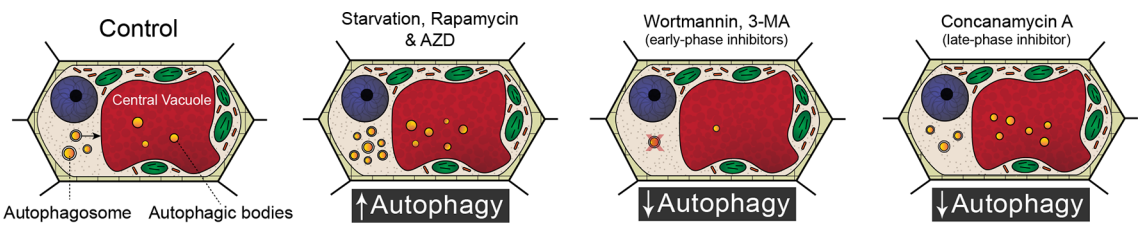

FIGURE 1 | Modulating autophagic flux. Compared to standard control conditions, starvation, rapamycin, and AZD 8055 increase the number of autophagosomes within a cell. Wortmannin and 3-methyladenine (3-MA) disrupt membrane formation and are therefore early phase inhibitors of autophagy. Concanamycin A inhibits the breakdown of autophagic bodies and cargoes in the vacuole.

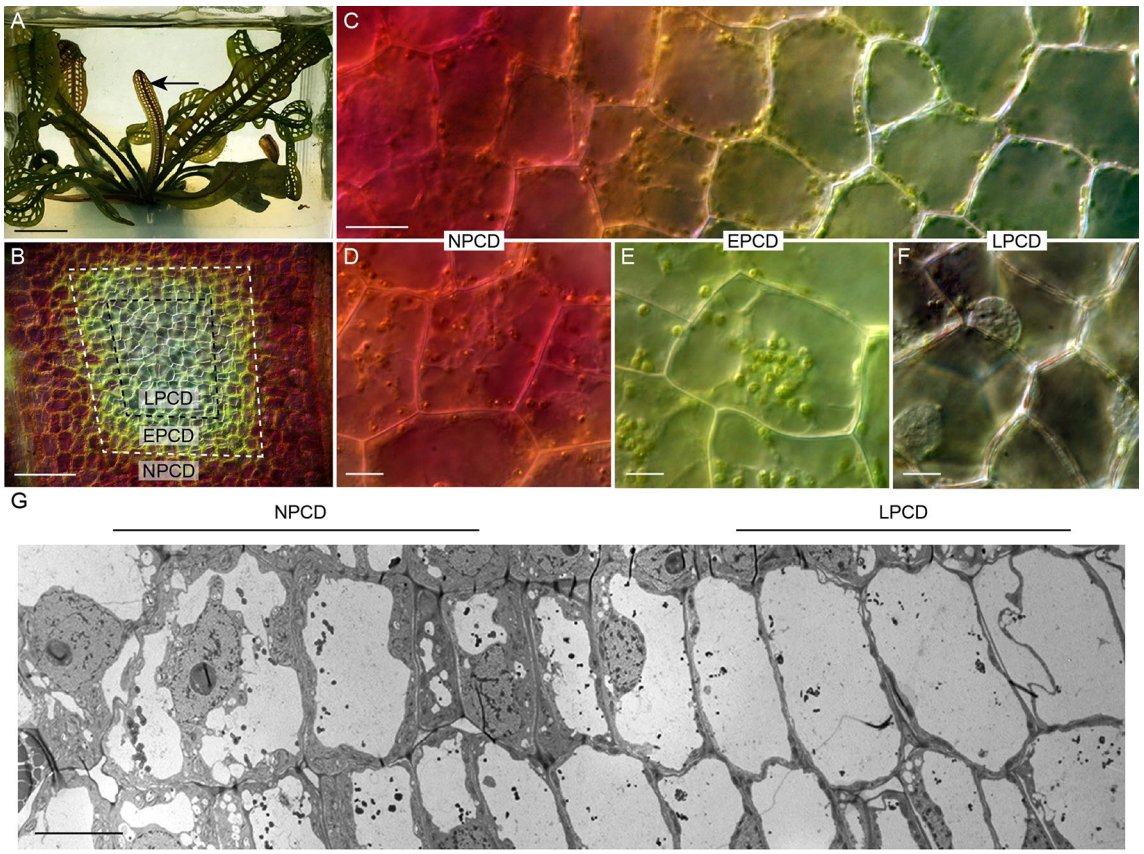

FIGURE 2 | The lace plant programmed cell death (PCD) model system. **(A)** Lace plant grown in axenic magenta box culture producing a window stage leaf (arrow) where PCD is actively occurring. Between the longitudinal and transverse veins is the areole **(B)**, and in the window stage of leaf development, there is a gradient of cell death **(C)**. **(D–F)** Higher magnification of representative cells along the gradient of cell death. **(D)** Non-PCD (NPCD) cells do not die during perforation formation. **(E)** Early-PCD (EPCD) cells have lost anthocyanin pigmentation and are undergoing PCD. **(F)** Late-PCD (LPCD) cells are nearly devoid of pigmentation and are near death. **(G)** Merged transmission electron microscopy (TEM) micrographs of the lace plant gradient of PCD. Scale bars: A = 1 cm; B = 80 μm; C = 20 μm; D–F = 10 μm; G = 20 μm.

Autophagy Modulation

Autophagy modulating compounds were also used for live cell imaging (described below) of detached window stage leaves. Autophagy modulation was achieved using the following treatments: distilled water (16 h starvation), 5 μM rapamycin, 1 μM AZD, 5 μM wortmannin, and 1 μM concanamycin A (Santa Cruz Biotechnology, sc-202111). For the cell death assay, leaves were mounted in treatment solution and observed continuously (video capture) for 6 h unless stated otherwise. Treatment times for the autophagy modulators were 3 h for TEM and live cell imaging experiments. The mock control treatment group received an equal volume of DMSO (BioShop Canada, DMS666).

Cell Death Assay and Live Cell Imaging

Window stage leaves were detached under sterile conditions and kept in distilled water for 16 h. Leaves were mounted in the designated treatment solution and placed on a custom grooved slide as per Wertman et al. (2012). The slide was then sealed with VALAP (a mixture of VAseline, LAnolin, and Paraffin wax) according to Kacprzyk et al. (2015). Videos were then captured on a Nikon Eclipse 90i microscope fitted with a DXM1200C digital camera using the audio video interleave recording function of NIS Elements AR 3.1 software (Nikon Instruments). Experiments ran for a maximum of 6 h or until all LPCD stage cells collapsed. A minimum of six independent replicates were carried out for each treatment. The number of dead cells (collapsed PMs) were counted prior to the beginning of the experiment and at the end of the observation period to determine the death rate per hour. Evans blue (Sigma-Aldrich, 46160) staining was used to facilitate the counting of dead cells at the end of the experiments and carried out according to Wertman et al. (2012).

ATG8 Immunolocalization

Intracellular detection of ATG8 was achieved in lace plant leaves using an adapted immunolocalization protocol (Pasternak et al., 2015; Mishra et al., 2017). Four independent replicates were carried out using window stage leaves taken from axenic cultures that were then rinsed gently with distilled water and fixed in 100% methanol at 37°C for 30 min. The tissues were then transferred to 800 μl of fresh 100% methanol and hydrophilized to a concentration of 20% methanol at 60°C through the addition of 200 μl of distilled water every 2 min for 32 min. Leaves were then

cut into 2-mm^2 pieces and rinsed in distilled water before being placed onto a multiwell slide. The leaf pieces were then allowed to dry on the slide for approximately 5 min until all excess liquid evaporated. Blocking was performed for 30 min at 37°C with 4% (w/v) low-fat milk in 1X MTSB (microtubule stabilization buffer: 7.5 g Pipes, 0.85 g EDTA, 0.61 g $MgSO_4$*$7H_2O$, and 1.25 g KOH, pH 7). Incubation with the ATG8 rabbit polyclonal primary antibody (Agrisera, AS14 2769) was done at 37°C for 30 min at a 1:1,000 dilution in MTSB. Negative controls were incubated with ATG8 preimmune serum (Agrisera, AS14 2769PRE) under the same conditions. Samples were then rinsed three times for 5 min each with MTSB. Secondary incubation was done with a 1:2,000 dilution of goat anti–rabbit Dylight® 488 polyclonal antibody (Agrisera, AS09 633) in MTSB. The samples were then rinsed as above and mounted in Mowiol (Sigma, 9000-89-5) prior to scanning with a Nikon Eclipse *Ti* C1 confocal system (Nikon). Z-stack images were analyzed and converted to maximum intensity projections using NIS Elements AR 3.1 software; fluorescent punctate structures (puncta) were counted automatically using ImageJ (particle analysis set to a lower brightness threshold of 75), and a central focal plane of the transmitted light channel was used to approximate the number of cells in the field of view. The data were normalized to the mean number of puncta in NPCD cells and expressed as the relative number of ATG8-positive puncta per cell.

ATG8 Immunoblotting

Three window stage leaves from sterile cultures were blot dried and had their midribs removed prior to freezing in liquid nitrogen. Tissues were macerated on ice in equal volumes of Pipes buffer (pH 6.8) and a protease inhibitor solution. The protease inhibitor solution consisted of a 1:2 ratio of two components (Component A: 10 mg/ml leupeptin and 10 mg/ml soybean trypsin inhibitor dissolved in Pipes buffer; Component B: 10 mg/ml pepstatin and 20 mg/ml phenylmethylsulfonyl fluoride dissolved in 95% ethanol). Following maceration, the samples were centrifuged for 15 min at 16,000 *g*. Total protein concentration of the supernatant was determined using the Bradford assay. A 1:1 mixture of sample to 2X Laemmli Buffer (Bio-Rad, 1610737) with 5% β-mercaptoethanol (v/v) was prepared prior to gel electrophoresis. A total of 10 μg of protein was loaded for each sample lane, along with 5 μl of the Precision Plus Protein Standards solution (Bio- Rad, 1610374) in a 8% to 16% sodium dodecyl sulfate (SDS) polyacrylamide Mini-PROTEAN TGX precast gel (Bio- Rad, 456- 1103). The gel was resolved at 100 V for 2 h in ice-cold running buffer (0.1% SDS [v/v], 25 mM Tris, and 192 mM glycine, 8.3 pH). Protein transfer to a 0.2 μm nitrocellulose membrane (Bio-Rad, 1610112) occurred overnight at 120 mA in a transfer buffer (20% methanol [v/v], 25 mM Tris, and 192 mM glycine, 8.3 pH) at room temperature.

Ponceau staining on the membrane was done for 5 min to confirm successful protein transfer. The membrane was then rinsed for 2 min in TBS-T (10 mM Tris, 140 mM NaCl, Tween-20, pH 7.4) prior to being scanned. The membrane was blocked in a 5% (w/v) low-fat milk powder TBS-T solution with mild shaking and then incubated overnight with the ATG8 primary antibody (detailed above) at a 1:10,000 dilution in TBS-T with 3% low-fat milk powder (w/v) at 2°C. The following day, the membrane was rinsed with mild shaking at 1-, 2-, and 3-min intervals in TBS-T. The secondary antibody (horseradish peroxidase–conjugated goat–anti-rabbit polyclonal; AS609 602, Agrisera) was applied at a 1:20,000 dilution in TBS-T for 30 min, and then the membrane was rinsed as described above with an additional 2-min rinse in Tris-buffered saline (10 mM Tris, 140 mM NaCl, 0.1%, pH 7.4). Clarity Western ECL substrate (Bio-Rad, 1705061) was used according to the manufacturer's instructions. Protein bands were resolved using an MF-ChemiBIS 3.2 gel documentation system (DNR Bio-Imaging).

Acridine Orange and Monodansylcadaverine Staining

Window stage leaves were taken from cultures and had their midrib removed prior to staining. The leaves were then cut into 2-mm^2 pieces prior to being placed in 30 μM acridine orange or a combination of acridine orange and 300 μM monodansylcadaverine (MDC) dissolved in phosphate-buffered saline. The leaf pieces were incubated at room temperature on a rotary shaker for 2 h at room temperature prior to being rinsed three times for 5 min with distilled water. Samples were mounted in distilled water and then imaged with confocal microscopy. Acridine orange was excited at 488 nm and detected at 525/25 nm (green) and 595/50 nm (red). Excitation of MDC was achieved with 405-nm light, and the emission filters for the dual stain experiments included 450/35 nm (blue), 525/25 nm (green), and 595/50 nm (red). Cyan, green, and magenta pseudocolors were applied for detecting blue, green, and red fluorescence, respectively, using ImageJ.

Transmission Electron Microscopy

Window stage lace plant leaves were taken from sterile cultures and treated (four independent replicates) for 3 h prior to having their midribs removed and sectioned into 2-mm^2 pieces. The leaf pieces were then fixed for a minimum of 2 h with 2.5% solution of glutaraldehyde in a 0.1 M sodium cacodylate buffer. The samples were then rinsed three times for 10 min each time, with the 0.1 M sodium cacodylate buffer. Secondary fixation with 1% osmium tetroxide was done for 48 h under vacuum (20 psi). The samples were then rinsed with distilled water briefly before being placed in 0.25% uranyl acetate at 4°C overnight. The samples were then dehydrated through a graduated series of acetone at 50%, 70%, 70%, 95%, 95%, 100%, and 100% for 10 min at each step of the process. Epon-Araldite resin was used to infiltrate the samples, initially in a 3:1 ratio of 100% acetone to resin for 3 h. This step was followed by transferring the samples to a 1:3 ratio of 100% acetone and resin overnight. The samples were then placed in 100% Epon-Araldite resin for 6 h, with the solution being refreshed once during that time. The embedded samples were then cured for 48 h at 60°C. Thin sections were cut using an Ultracut E Ultramicrotome (Reicher-Jung) with a diamond knife (100-nm thickness) and placed on formvar/carbon support film copper grids (Cedarlane, FCF205-CU-25). Staining was done using 2% aqueous uranyl acetate for 10 min, followed by two 5-min rinses with distilled water, 4 min in lead

citrate counterstain, and then a final quick rinse with distilled water. The samples were viewed with a JEM 1230 Transmission Electron Microscope (JEOL) at 80 kV, and images were captured using a Hamamatsu ORCA-HR digital camera.

Statistical Analysis and Data Representation

Data analysis and graphical representations used GraphPad Prism 5 software (GraphPad Software Inc.). Data are represented as mean ± standard error. Maximum intensity projections of confocal z-stacks were made using NIS Elements AR 3.1 software. Figures were prepared using Adobe Illustrator and Adobe Photoshop, and videos were assembled with Premiere Pro (CC; Adobe Systems Inc.). When necessary to improve clarity, adjustments to brightness, contrast, and exposure were made consistently with all replicates.

RESULTS

The Involvement of Autophagy in Lace Plant Developmental PCD

To assess whether autophagy occurs during lace plant PCD, immunostaining of NPCD and LPCD cells in fixed window stage leaves was carried out with ATG8 and DyLight 488 antibodies and a negative control with the α-ATG8 preimmune serum (**Figure 3A**). Both healthy (NPCD) and dying (LPCD) lace plant cells contained ATG8-positive puncta; however, there was a significant increase in puncta in LPCD cells (**Figure 3B**). Immunoblotting for ATG8 was also carried out using protein extracts of window stage leaves to verify ATG8 antibody binding in lace plant samples (**Figure 3C**). The lysotropic dye acridine orange was also used to compare autophagy in living NPCD and LPCD cells of window stage leaves (**Figure 4**; **Supplementary File 1**). There were fluorescent puncta in both NPCD and LPCD cells (white arrows, **Figure 4**). However, there were considerably more puncta in LPCD cells that had more red than green fluorescence. Vacuolar aggregates in LPCD cells were also positive for acridine orange staining (black arrow, **Figure 4**). Monodansylcadaverine and acridine orange dual staining was also performed in NPCD cells and revealed a similar staining pattern (**Supplementary File 2**).

Autophagy Modulation and Live Cell Imaging

Live cell imaging was used to determine the effects of autophagy modulation on NPCD and LPCD cells of lace plant window stage leaves (**Figure 5**; see also **Supplementary Files 3** and **4**). The negative control group represents leaves taken directly from culture, whereas all other treatment groups had a 16-h starvation period prior to a 3-h exposure to an autophagy modulator. Qualitative assessment of the micrographs and the corresponding **Supplementary Videos 3** and **4** suggest that autophagy modulation with 1 μM AZD, 5 μM rapamycin, and 1 μM concanamycin A led to the formation of large vacuolar aggregates (VA, **Figure 5**) and numerous small, spherical autophagosome-like vesicles (A, **Figure 5**) that were most distinguishable with time-lapse imaging (**Supplementary Files 3** and **4**). Wortmannin treatment also resulted in the formation of large vesicles in NPCD cells that appeared to contain organelles (Ve, NPCD, **Figure 5**; **Supplementary File 3**).

Ultrastructural Analysis

Window stage leaves exposed to autophagy modulators were also examined using TEM (**Figure 6**). In the mock control treatment group, some autophagosome-like structures were observed in NPCD and LPCD stage cells (A, **Figure 6**), along with numerous single-membrane vesicles that varied in size and shape (Ve, **Figure 6**). Late-PCD stage cells had vacuolar aggregates (VA), whereas NPCD cells had little to no material in the vacuole (**Figure 6**). Compared

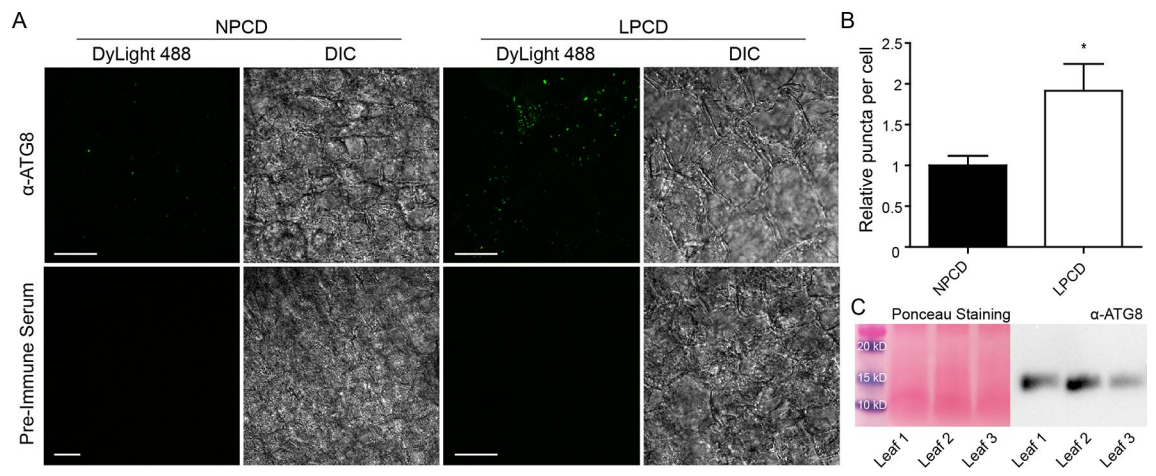

FIGURE 3 | (A) Nonprogrammed cell death (NPCD) and late-PCD (PCD) cells following immunostaining with α-ATG8 and DyLight 488. Fluorescent images represent maximum intensity projections and corresponding differential interference contrast (DIC) images are from a representative optical section. **(B)** Relative number of ATG8-positive puncta per cell for NPCD and LPCD cells (normalized to NPCD). n = 4 leaves from individual plants, Student *t* test, $^*P < 0.05$, error bar represents standard error. **(C)** Ponceau-stained membrane and corresponding immunoprobing for ATG8 in window stage leaves (n = 3) from individual plants. Scale bars: 10 μm.

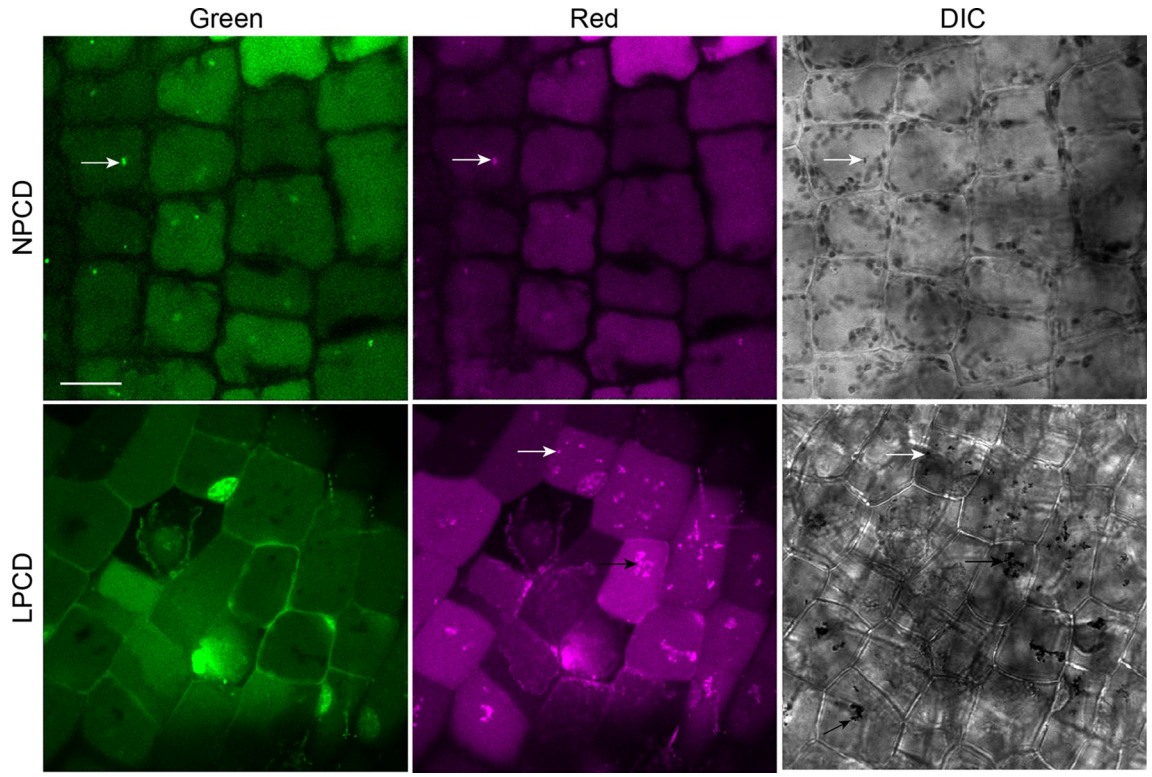

FIGURE 4 | Acridine orange staining in window stage leaves. Nonprogrammed cell death (NPCD) and late-programmed cell death (LPCD) stage cells were stained with 30 μM acridine orange. Fluorescent puncta were found in both cell types (white arrows), and large vacuolar aggregates were seen in LPCD cells (black arrow). Scale bar: 20 μm.

to the mock control treatment group, 5 μM rapamycin-treated cells had the highest number of visible small, single-membrane vesicles (Ve) and larger vacuolar aggregates (VA, **Figure 6**). Similarly, 1 μM concanamycin had noticeably larger vacuolar aggregates compared to the mock control treatment group (VA, **Figure 6**) and had many single-membrane vesicles (Ve, **Figure 6**).

Lace Plant Novel Cell Death Assay

To assess the effect of autophagy on cell death rate during lace plant development, a novel live cell imaging assay was developed (**Figure 7**; see also **Supplementary File 5**). Window stage areoles with one to three dead cells in the epidermal layer (asterisks, **Figure 7A**, and dashed box, **Figure 7C**) were selected to ensure that PCD was synchronized in the samples. Continuous videos were captured for the control, 5 μM rapamycin, 1 μM concanamycin A, and 5 μM wortmannin treatment groups (**Figure 7A**). At the end of experiments, DIC micrographs were taken (Final, **Figure 7A**) prior to Evans blue staining (Final + Evans blue; **Figures 7A, D**), which was done to facilitate scoring of dead cells in the epidermal layer. The rate of cell death (% of LPCD cells per hour) was determined for each treatment group (**Figure 7**B). Leaves of the mock control treatment group had a mean cell death rate of 6.59 ± 0.48 (% LPCD cells per hour). The 5 μM rapamycin treatment significantly reduced the rate of cell death to 2.56 ± 0.70 (% LPCD cells per hour). Conversely, the 1 μM concanamycin A and 5 μM wortmannin treatments significantly increased the rate of cell death rates in relation to the control to 13.10 ± 1.80 and 16.42 ± 1.39 (% LPCD cells per hour), respectively.

Autophagy Modulation and the Formation of Perforations

Lace plants grown in axenic cultures were treated with autophagy modulators including rapamycin and wortmannin to determine their effects on the formation of perforations (**Figure 8**). Mock control treatment group plants (**Figure 8A**) produced leaves with an average length of 8.37 ± 0.23 cm (**Figure 8D**) and developed 75 ± 6.66 perforations (**Figure 8E**). The length of leaves of rapamycin-treated plants (**Figure 8B**) were not significantly different (9 ± 0.70 cm), as well as the number of perforations formed (78 ± 10.58). Wortmannin-treated plants did not differ from the mock control treatment group in terms of perforations (73.43 ± 6.70) per leaf and leaf length (8.85 ± 0.84 cm). *In vivo* experiments were also carried out with 1 μM AZD, but similar to autophagy enhancement with rapamycin, there was no observable response in terms of formation of perforations and leaf lengths (data not shown).

DISCUSSION

Autophagy is a critical life process that allows for the degradation and repurposing of cytoplasmic constituents (Feng et al., 2014). In eukaryotes, autophagy plays a central role in development and

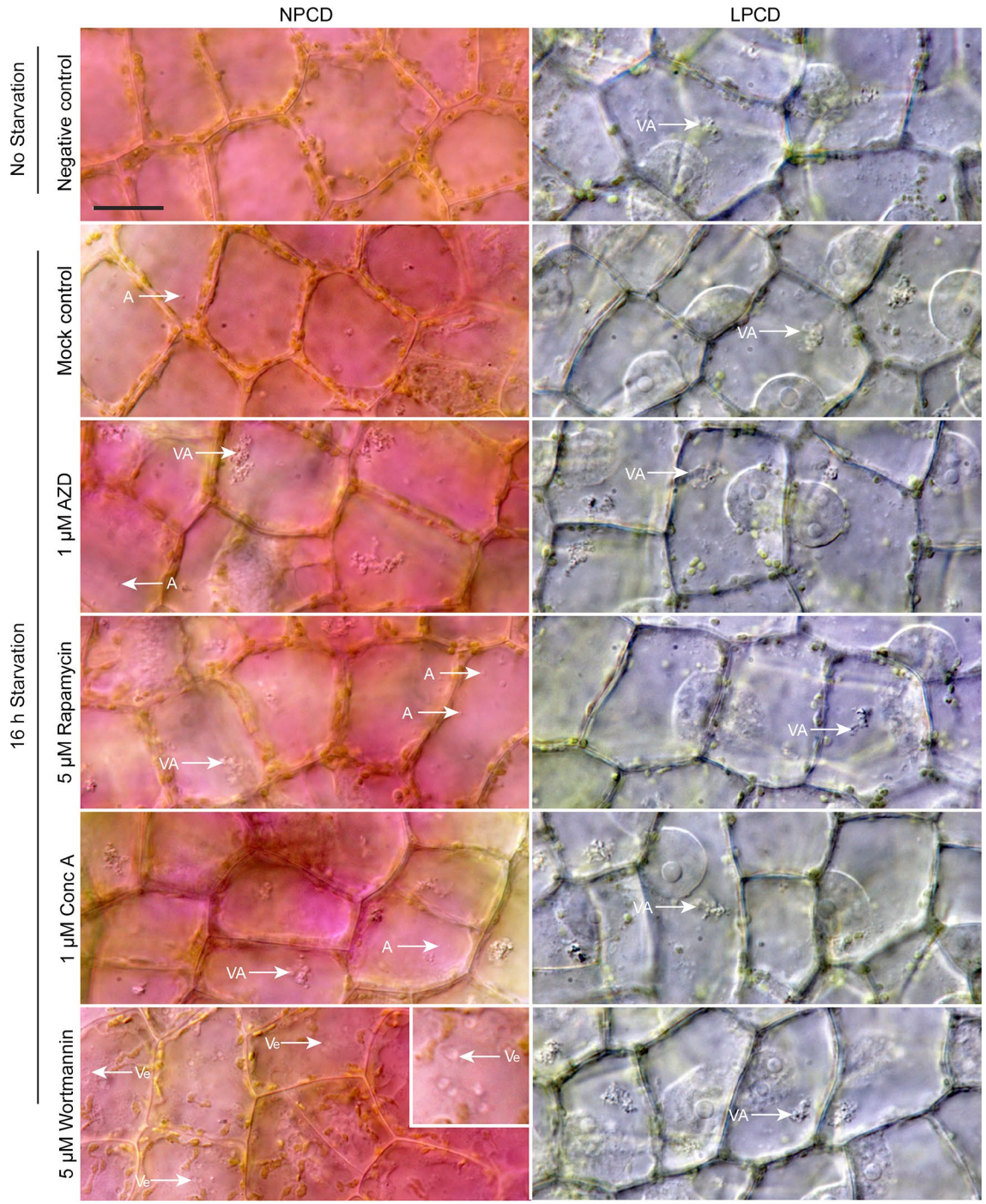

FIGURE 5 | Live cell imaging of non-programmed cell death (NPCD) and late-PCD (LPCD) cells in window stage leaves exposed to various conditions. The negative control was a sample taken directly from plants growing in the culture media. All other treatment groups were subjected to a 16-h starvation period in distilled water prior to 3-h exposure to one of the following: 0.05% DMSO (mock control), 1 μM AZD 8055 (AZD), 5 μM rapamycin, 1 μM concanamycin A (Conc A), or 5 μM wortmannin. VA = vacuolar aggregates, A = autophagosome-like vesicle, inset displays large, organelle-containing vesicles (Ve). n = 3 leaves from individual plants. Scale bar: 20 μm. For additional information see **Supplementary Files 3** and **4**.

is implicated in numerous human diseases including, but not limited to, cancer, diabetes, and neurodegeneration (Tsujimoto and Shimizu, 2005; Choi et al., 2013; Jiang and Mizushima, 2014). According to Mariño et al. (2014), there is a considerable interplay between the autophagy and PCD signaling pathways, and the modulation of autophagy can have antagonistic effects depending on the experimental conditions (Minina et al., 2014). In plants, autophagy can be induced by exposure to

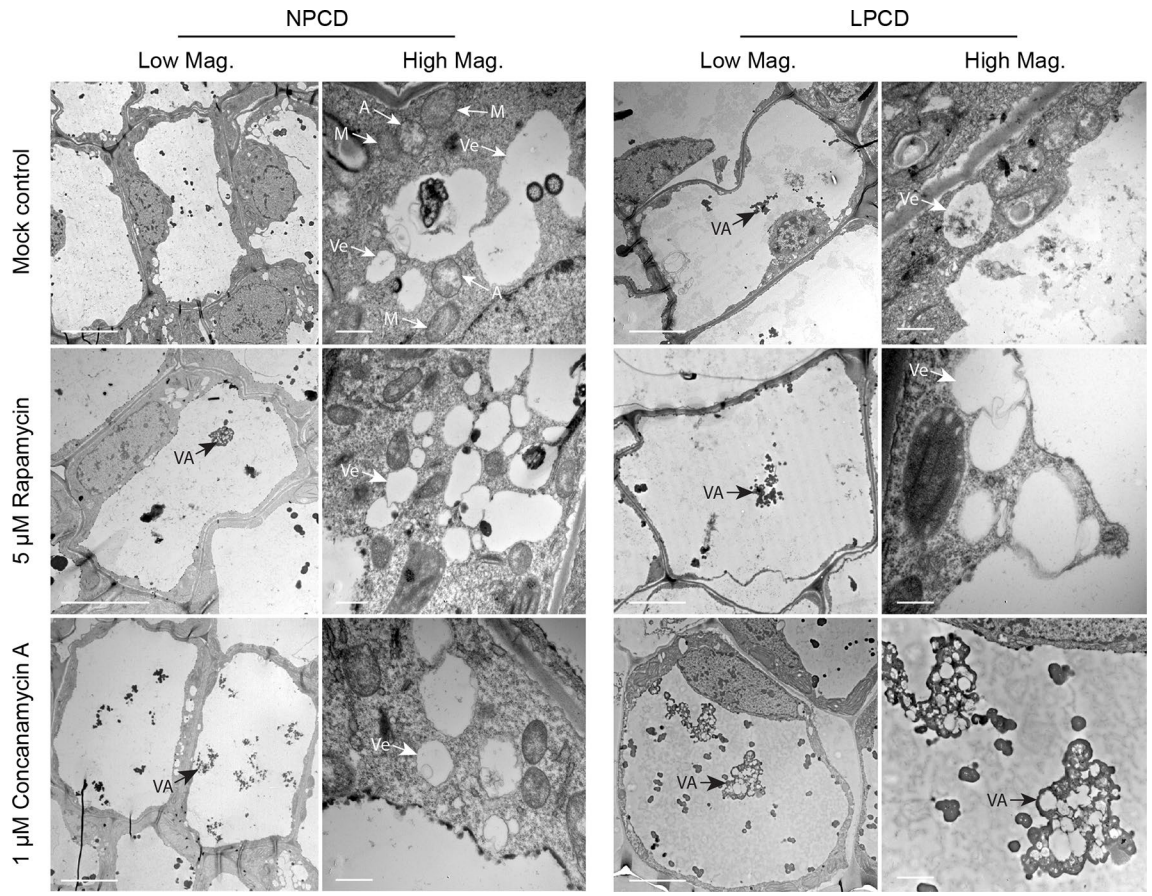

FIGURE 6 | Non-programmed cell death (NPCD) and late-PCD (PCD) cells treated with 0.05% DMSO (mock control), 5 µM rapamycin, or 1 µM concanamycin A. Note that concanamycin A–treated cells contained large vacuolar aggregates. A = autophagosome-like vesicle; M = mitochondria VA = vacuolar aggregate; Ve = single membrane vesicle. Scale bars: (Low Mag.) = 20 µm; (High Mag.) = 1 µm.

various abiotic stresses such as starvation, exposure to saline conditions, drought, and hydrogen peroxide (Liu and Bassham, 2012). Autophagy has also been implicated in PCD following the invasion of pathogens during the hypersensitive response, as well as developmental processes ranging from embryogenesis to senescence (Liu and Bassham, 2012; Minina et al., 2013; Hofius et al., 2018). Because of the involvement of autophagy in various plant PCD systems, we investigated the extent of its involvement during lace plant leaf development.

Autophagy and Lace Plant PCD

ATG8 and acridine orange positive puncta were observed in both healthy NPCD cells and dying cells, which indicates that autophagy occurs as part of normal homeostasis and during cellular degradation, respectively. A recent study showed that dying lace plant cells accumulate high levels of reactive oxygen species (ROS; Dauphinee et al., 2017). Autophagy is induced from various forms of stress including ROS, which may account for LPCD cells containing more ATG8-positive and acridine orange puncta compared to healthy NPCD cells. Our TEM observations of the lace plant PCD gradient confirmed the presence of double-membrane–bound autophagosome-like structures in NPCD and PCD cells (A, **Figure 6**). Additionally, numerous single-membrane vesicles (Ve, **Figure 6**) of varying shapes and sizes were found, having a similar appearance to the provacuoles formed during cellular degradation in the embryos of Norway spruce (*Picea abies*; Filonova et al., 2000; Minina et al., 2013) or autolysosomes in BY-2 cells (Takatsuka et al., 2017). The red fluorescence in LPCD cells stained with acridine orange suggests that the puncta are acidic vesicles and may serve a similar function to autolysosomes. Like acridine orange, MDC accumulates in acidic compartments (Klionsky et al., 2016), and previous work in the lace plant showed that NPCD cells contain ATG8 and MDC-positive puncta (Mishra et al., 2017). A general increase in the size of the vacuoles was observed as degradation of the cytoplasm advanced throughout PCD (**Figures 2** and **6**), which is commonly observed during developmental PCD in plants (Liu and Bassham, 2012). Vacuolar aggregates in lace plant cells that comprised electron-dense, degraded organelle material were also seen to increase in size as PCD

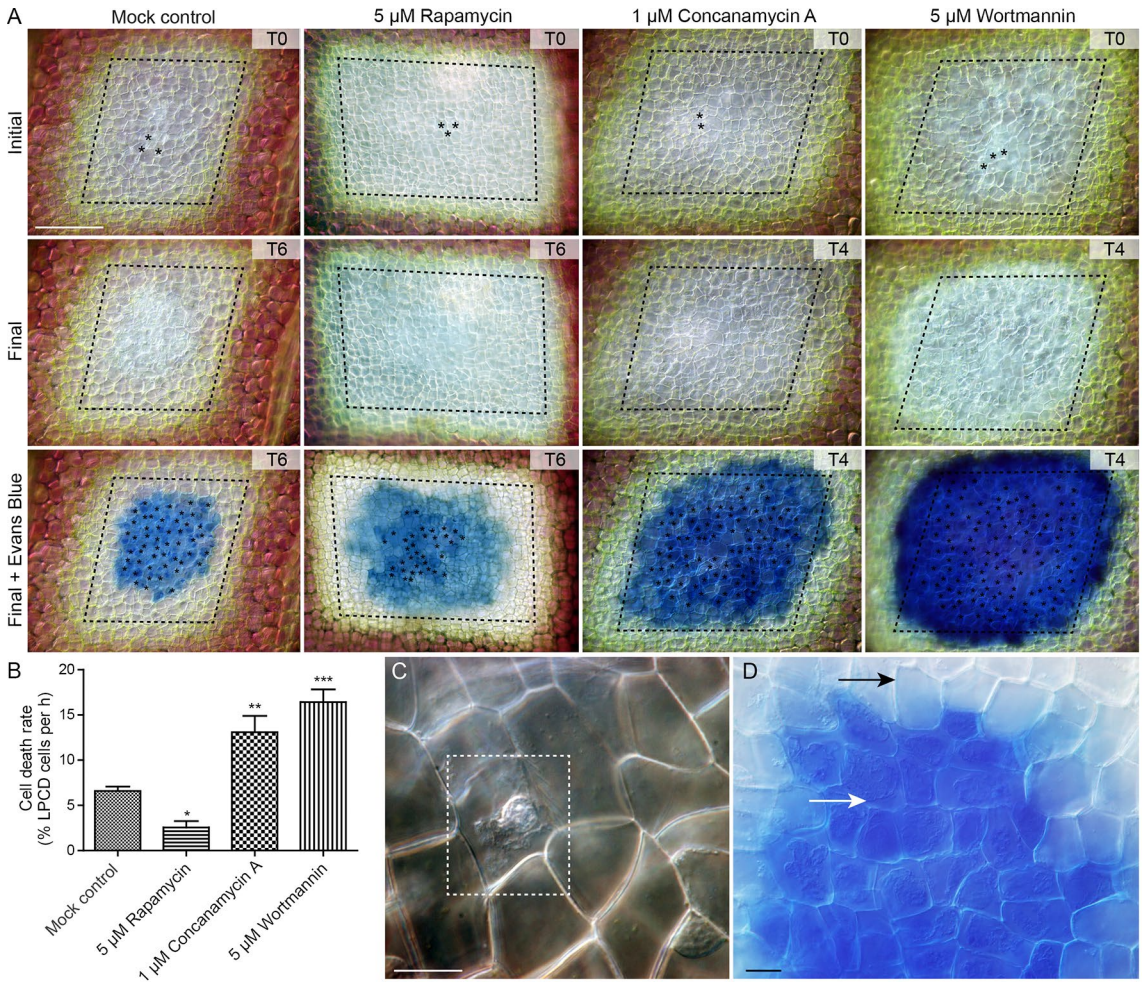

FIGURE 7 | Cell death assay. **(A)** Initial and final micrographs of window stage leaves. Evans blue staining was performed at the end of the experiments to facilitate the final scoring of cell death in epidermal cells (asterisks). Treatments included 0.05% DMSO (mock control), 5 μM rapamycin, 1 μM concanamycin A, or 5 μM wortmannin. T = time, rounded to the nearest h. **(B)** The rate of cell death was calculated as the % of late programmed cell death (LPCD) cells that died per hour. **(C)** High magnification view of unstained dead epidermal cell (dashed box) in a window stage leaf. Evans blue staining **(D)** was used to facilitate quantification of dead cells in the epidermis (white arrow) at the end of experiments. Black arrow = living cell with intact plasma membrane. One-way analysis of variance, Dunnett multiple-comparisons test, n ≥ 6 leaves from individual plants; ***$P < 0.001$; **$P < 0.01$; *$P < 0.05$). Error bars represent standard error. Scale bars: A = 150 μm; C and D = 5 μm. (For more details, see **Supplementary File 5**.)

progressed; this was consistent with preliminary lace plant TEM observations (Wertman et al., 2012).

Modulation of Autophagy in Lace Plants

Live cell and TEM observations showed that commercially available autophagy modulators are effective in lace plant cells. The effects of autophagy modulation were most pronounced in NPCD cells, where autophagosome-like vesicles were moving quickly and clearly visible using time-lapse live cell imaging (**Figure 5**; **Supplementary File 3**). Interestingly, wortmannin-treated window stage NPCD cells contained larger, slow-moving vesicles that appeared to have organelles within them. Similar vesicles were observed following cell death induction from high pH conditions (Dauphinee et al., 2014), suggesting these organelle-containing vesicles may form under stressful conditions in lace plant cells. The novel cell death assay presented here also highlights the advantages of using the lace plant model to study autophagy (**Figure 7**; **Supplementary File 5**). Our cell death assay results indicate that enhancement of autophagy led to prolonged lifespan in LPCD cells, and conversely, the inhibition of autophagy led to a greater rate of cell death. Although the autophagy-modulating compounds had effects at the cellular level, there was no observed effect *in vivo* on lace plant leaf development even at higher concentrations (data not shown). Therefore, autophagy modulation itself is not enough to significantly influence the formation of perforations or lace plant leaf development under optimal growth conditions. However, future experiments should be done to determine how modulation may affect lace plant development under stressful

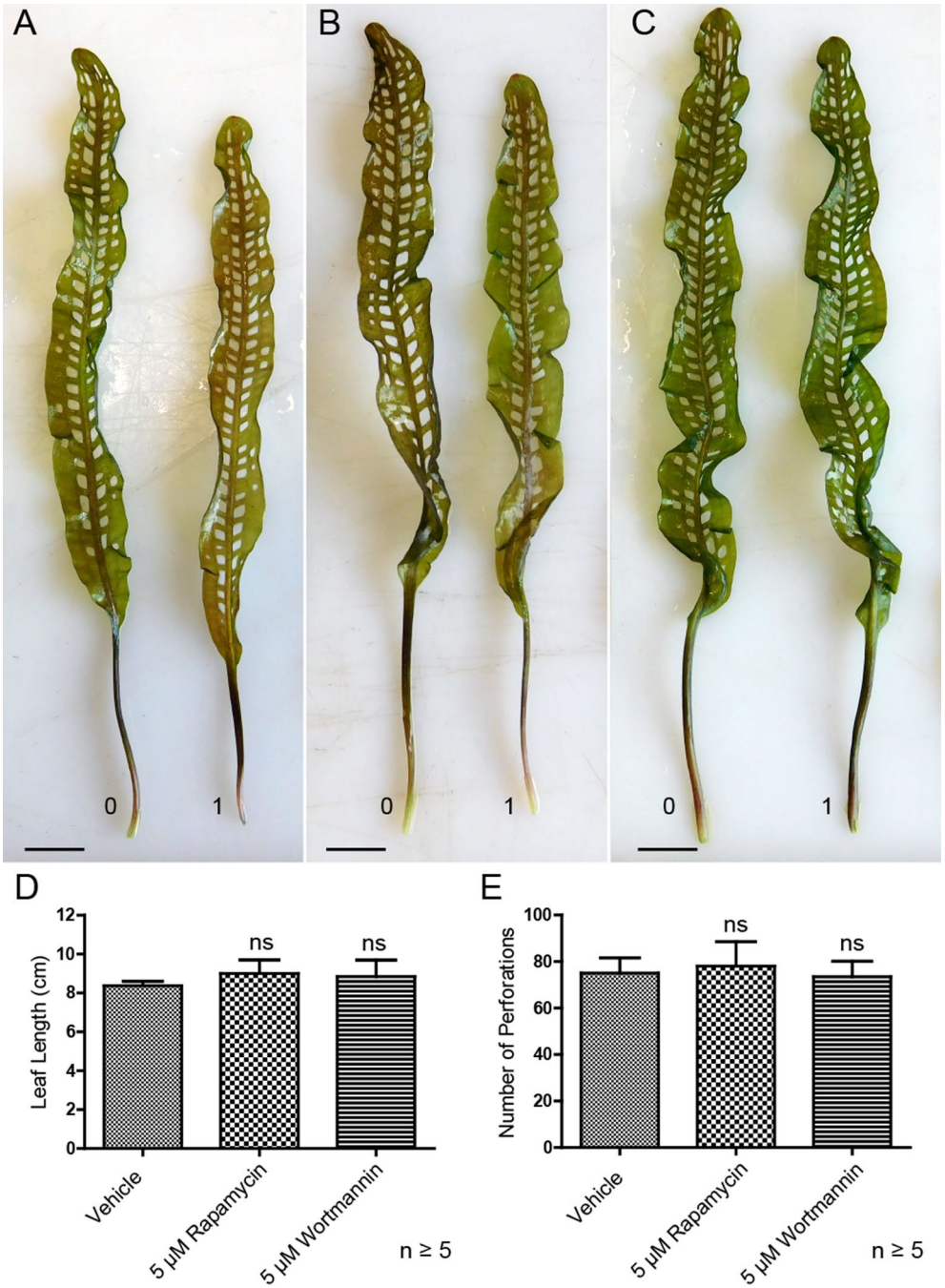

FIGURE 8 | Autophagy modulation *in vivo*. Representative leaves for the DMSO control **(A)**, 5 μM rapamycin **(B)**, and 5 μM wortmannin **(C)** treatment groups. Leaf 0 represents the last to develop prior to treatment application, and leaf 1 is the first to develop afterward. **(D)** Mean leaf lengths of mature leaves posttreatment. **(E)** The number of perforations in mature leaves following treatment. One-way analysis of variance, Dunnett multiple-comparisons test, n ≥ 5 plants, ns = non-significant, $P > 0.05$). Error bars represent standard error. Scale bars: 0.5 cm.

conditions. In terms of ultrastructural observations following autophagy modulation, the 5 μM rapamycin treatment generated a visible increase in vesicles that appeared to contain more electron-dense material compared to the control. Concanamycin A–treated specimens also had an abundance of vesicles and had the largest vacuolar aggregates, which was evident *via* TEM. Autophagic bodies found within the vacuoles of *Arabidopsis* roots (Merkulova et al., 2014) have a similar appearance at the light microscopy level to the vacuolar aggregates detailed here in the lace plant.

Conclusions and Future Work

Lace plant leaves provide an excellent system to study the role of autophagy on cell death or survival since both types of cells (NPCD and PCD) are simultaneously present within an areole of a window stage leaf. Although autophagy modulation led to delayed or enhanced cell death rates toward the later stages of PCD, our results indicate that autophagy is predominantly a survival mechanism in the lace plant, and we did not observe clear evidence for its direct involvement in the induction of developmental PCD under normal circumstances. The lace plant presents a tractable model for studying the core autophagy machinery *in planta*; however, more advanced tools are necessary to better understand this biochemical pathway. Future aims include genetic modification to create GFP–ATG8 lines and the establishment of autophagy-deficient mutants, which would be invaluable tools to understand autophagy in the emerging lace plant model system.

DATA AVAILABILITY STATEMENT

The raw data supporting the conclusions of this manuscript will be made available by the authors, without undue reservation, to any qualified researcher.

AUTHOR CONTRIBUTIONS

AD carried out experiments and wrote the manuscript. GD and AR contributed to whole plant and live cell imaging experiments. MF contributed to cell death assay experiments. CL participated in manuscript revisions. AG secured funding for the study, designed the experiments, contributed to manuscript revisions, and supervised all experimental work. All authors read and approved the final version.

FUNDING

This work was supported by AG's NSERC Discovery Grant (# 2017-04299) and Accelerator Supplements (# 2017-507825).

ACKNOWLEDGMENTS

We thank Dr. Joanna Kacprzyk (University College Dublin) for a critical review of this manuscript and The Killam Trusts and the Natural Sciences and Engineering Research Council (NSERC) of Canada for providing PhD funding to AD. Later, AD was supported by AG's NSERC Discovery accelerator supplements (DAS) as a postdoctoral. GD was supported by a Nova Scotia Research and Innovation Graduate Scholarship and AG's NSERC discovery grant. MF was supported by NSERC and Sarah Lawson Research Scholarships. Stephen Chew assisted with optimization of the live cell imaging assay and was supported by a Sarah Lawson Research Scholarship. We also thank Mary Ann Trevors (Dalhousie Facilities) for assistance with TEM including sample preparations.

SUPPLEMENTARY MATERIAL

The Supplementary Material for this article can be found online at: https://www.frontiersin.org/articles/10.3389/fpls.2019.01198/full#supplementary-material

SUPPLEMENTAL FILE 1 | Acridine orange staining in window stage leaves. Non-programmed cell death (NPCD) and late-programmed cell death (LPCD) stage cells were stained with acridine orange and observed using confocal microscopy. Acridine orange was excited at 488 nm and detected at 525/25 nm (green) and 595/50 nm (magenta). Actual acquisition time: 5 min. Scale bar: 15 µm. Video 1.MP4.

SUPPLEMENTAL FILE 2 | Acridine orange and monodansylcadaverine dual staining in window stage leaves. Non-programmed cell death (NPCD) were stained and observed using confocal microscopy. Fluorescent laser scanning confocal micrographs represent maximum intensity projections of z-stack acquisitions. Corresponding differential interference contrast (DIC) is taken from a single representative focal plane within the z-stack. Excitation with 405 and 488 nm light was used for MDC and acridine orange stains, respectively. Fluorescence emission was detected at 450/35 nm (cyan), 525/25 nm (green), and 595/50 nm (magenta). Scale bar: 20 µm. Image 1. TIF.

SUPPLEMENTAL FILE 3 | Live cell imaging time-lapse videos of non-programmed cell death (NPCD) window stage cells. Treatments include a negative control, mock control treatment group (DMSO), 1 µM AZD 8055, 5 µM rapamycin, 1 µM concanamycin A or 5 µM wortmannin. Negative control leaves were scanned immediately after removed from culture and all other groups had a 16-h starvation period in distilled water prior to treatment application. Click on individual videos to play/pause. Actual acquisition time: 5 min. Scale bar: 20 µm. For additional information see **Figure 4**. Presentation 1.PPTX (video files).

SUPPLEMENTAL FILE 4 | Live cell imaging time-lapse videos of late-programmed cell death (LPCD) window stage cells. Treatments include a negative control, mock control treatment group (DMSO), 1 µM AZD 8055, 5 µM rapamycin, 1 µM concanamycin A or 5 µM wortmannin. Negative control leaves were scanned immediately after removed from culture and all other groups had a 16-h starvation period in distilled water prior to treatment application. Click on individual videos to play/pause. Actual acquisition time: 5 min. Scale bar: 20 µm. For additional information see **Figure 4**. Presentation 2.PPTX (video files).

SUPPLEMENTAL FILE 5 | Cell death assay. Mock control treatment group (DMSO), 5 µM rapamycin, 1 µM concanamycin and 5 µM wortmannin-treated window stage leaves. Actual acquisition time: 4h (Concanamycin A, Wortmannin) – 6h (Control, Rapamycin). Scale bar:100 µm. Video 2.MP4.

REFERENCES

Avin-Wittenberg, T., Bozhkov, P. V., Masclaux-Daubresse, C., Sirko, A., Isono, E., Batoko, H., et al. (2018). Autophagy-related approaches for improving nutrient use efficiency and crop yield protection. *J. Exp. Bot.* 69, 1335–1353. doi: 10.1093/jxb/ery069

Ballou, L. M., and Lin, R. Z. (2008). Rapamycin and mTOR kinase inhibitors. *J. Chem. Biol.* 1, 27–36. doi: 10.1007/s12154-008-0003-5

Batoko, H., Dagdas, Y., Baluska, F., and Sirko, A. (2017). Understanding and exploiting autophagy signaling in plants. *Essays Biochem.* 61, 675–685. doi: 10.1042/EBC20170034

Choi, A. M. K., Ryter, S. W., and Levine, B. (2013). Autophagy in human health and disease. *N. Engl. J. Med.* 368, 651–662. doi: 10.1056/NEJMra1205406

Dauphinee, A. N., Warner, T. S., and Gunawardena, A. H. (2014). A comparison of induced and developmental cell death morphologies in lace plant (Aponogeton madagascariensis) leaves. *BMC Plant Biol.* 14, 389. doi: 10.1186/s12870-014-0389-x

Dauphinee, A. N., Wright, H., Rantong, G., and Gunawardena, A. H. L. A. N. (2012). The involvement of ethylene in programmed cell death and climacteric-like behaviour during the remodelling of lace plant (Aponogeton madagascariensis) leaves. *Botany* 90, 1237–1244. doi: 10.1139/b2012-093

Dauphinee, A. N., Fletcher, J. I., Denbigh, G. L., Lacroix, C. R., and Gunawardena, A. H. L. A. N. (2017). Remodelling of lace plant leaves: antioxidants and ROS are key regulators of programmed cell death. *Planta*, 246 (1), 1–15. doi: 10.1007/s00425-017-2683-y

Din, F. V. N., Valanciute, A., House, V. P., Zibrova, D., Green, K. A., Sakamoto, K., et al. (2012). Aspirin inhibits mTOR signaling, activates AMP-activated protein kinase, and induces autophagy in colorectal cancer. *Gastroenterology* 142, 1504–1524. doi: 10.1053/j.gastro.2012.02.050

Feng, Y., He, D., Yao, Z., and Klionsky, D. J. (2014). The machinery of macroautophagy. *Cell Res.* 24, 24–41. doi: 10.1038/cr.2013.168

Filonova, L. H., Bozhkov, P. V., Brukhin, V. B., Daniel, G., Zhivotovsky, B., and von Arnold, S. (2000). Two waves of programmed cell death occur during formation and development of somatic embryos in the gymnosperm, Norway spruce. *J. Cell Sci.* 113, 4399–4411.

Floyd, B. E., Soto-Burgos, J., and Bassham, D. C. (2015). To live or die: autophagy in plants, in *Plant programmed cell death*. Eds. A. H. Gunawardena and P. F. McCabe (Springer: Basel, Switzerland), 269–300. doi: 10.1007/978-3-319-21033-9_11

Gunawardena, A. H. L. A. N., Greenwood, J. S., and Dengler, N. G. (2004). Programmed cell death remodels lace plant leaf shape during development. *Plant Cell* 16, 60–73. doi: 10.1105/tpc.016188

Gunawardena, A. H. L. A. N., Navachandrabala, C., Kane, M., and Dengler, N. G. (2006). Lace plant: a novel system for studying developmental programmed cell death, in *Floriculture, ornamental and plant biotechnology: advances and tropical issues*. Ed. J. A. Teixeira da Silva (Middlesex: Global Science Books), 157–162.

Heras-Sandoval, D., Pérez-Rojas, J. M., Hernández-Damián, J., and Pedraza-Chaverri, J. (2014). The role of PI3K/AKT/mTOR pathway in the modulation of autophagy and the clearance of protein aggregates in neurodegeneration. *Cell Signal* 26, 2694–2701. doi: 10.1016/j.cellsig.2014.08.019

Hofius, D., Hafrén, A., Marshall, R. S., Bozhkov, P. V., Minina, E. A., Liu, Q., et al. (2018). Bacteria exploit autophagy for proteasome degradation and enhanced virulence in plants. *Plant Cell* 30, 668–685. doi: 10.1105/tpc.17.00815

Huss, M., Ingenhorst, G., König, S., Gaßel, M., Dröse, S., Zeeck, A., et al. (2002). Concanamycin A, the specific inhibitor of V-ATPases, binds to the VO subunit c. *J. Biol. Chem.* 277, 40544–40548. doi: 10.1074/jbc.M207345200

Jiang, P., and Mizushima, N. (2014). Autophagy and human disease. *Cell Cycle* 6, 1837–1849. doi: 10.1038/cr.2013.161

Kacprzyk, J., Dauphinee, A. N., Gallois, P., Gunawardena, A. H., and McCabe, P. F. (2015). Methods to study plant programmed cell death. *Methods Mol. Biol.* 1419, 145–160. doi: 10.1007/978-1-4939-3581-9

Klionsky, D. J., Abdelmohsen, K., Abe, A., Abedin, M. J., Abeliovich, H., Acevedo, A., et al. (2016). Guidelines for the use and interpretation of assays for monitoring autophagy (3rd edition). *Autophagy* 12, 1–222. doi: 10.1080/15548627.2015.1100356

Kwak, D., Choi, S., Jeong, H., Jang, J. H., Lee, Y., Jeon, H., et al. (2012). Osmotic stress regulates mammalian target of rapamycin (mTOR) complex 1 via c-Jun N-terminal kinase (JNK)–mediated raptor protein phosphorylation. *J. Biol. Chem.* 287, 18398–18407. doi: 10.1074/jbc.M111.326538

Liu, Y., and Bassham, D. C. (2012). Autophagy: pathways for self-eating in plant cells. *Annu. Rev. Plant Biol.* 63, 215–237. doi: 10.1146/annurev-arplant-042811-105441

Lord, C. E. N., Wertman, J. N., Lane, S., and Gunawardena, A. H. L. A. N. (2011). Do mitochondria play a role in remodelling lace plant leaves during programmed cell death? *BMC Plant Biol.* 11, 102. doi: 10.1186/1471-2229-11-102

Mariño, G., Niso-Santano, M., Baehrecke, E. H., and Kroemer, G. (2014). Self-consumption: the interplay of autophagy and apoptosis. Nature reviews. *Mol. Cell Biol.* 15 (2), 81–94. doi: 10.1038/nrm3735Q10

Marshall, R. S., and Vierstra, R. D. (2018). Autophagy: the master of bulk and selective recycling. *Annu. Rev. Plant Biol.* 69, 173–208. doi: 10.1146/annurev-arplant-042817-040606

Merkulova, E. A., Guiboileau, A., Naya, L., Masclaux-Daubresse, C., and Yoshimoto, K. (2014). Assessment and optimization of autophagy monitoring methods in arabidopsis roots indicate direct fusion of autophagosomes with vacuoles. *Plant Cell Physiol.* 55, 715–726. doi: 10.1093/pcp/pcu041

Minina, E. A., Bozhkov, P. V., and Hofius, D. (2014). Autophagy as initiator or executioner of cell death. *Trends Plant Sci.* 19, 692–697. doi: 10.1016/j.tplants.2014.07.007

Minina, E. A., Filonova, L. H., Fukada, K., Savenkov, E. I., Gogvadze, V., Clapham, D., et al. (2013). Autophagy and metacaspase determine the mode of cell death in plants. *J. Cell Biol.* 203, 917–927. doi: 10.1083/jcb.201307082

Mishra, P., Dauphinee, A. N., Ward, C., Sarkar, S., Gunawardena, A. H. L. A. N., and Manjithaya, R. (2017). Discovery of pan autophagy inhibitors through a high-throughput screen highlights macroautophagy as an evolutionarily conserved process across 3 eukaryotic kingdoms. *Autophagy* 13, 1556–1572. doi: 10.1080/15548627.2017.1339002

Pasternak, T., Tietz, O., Rapp, K., Begheldo, M., Nitschke, R., Ruperti, B., et al. (2015). Protocol: an improved and universal procedure for whole-mount immunolocalization in plants. *Plant Methods* 11, 50. doi: 10.1186/s13007-015-0094-2

Shpilka, T., Weidberg, H., Pietrokovski, S., and Elazar, Z. (2011). ATG8: an autophagy-related ubiquitin-like protein family. *Genome Biol.* 12, 1–11. doi: 10.1186/gb-2011-12-7-226

Takatsuka, C., Inoue-Aono, Y., and Moriyasu, Y., (2017). Isolation of autolysosomes from tobacco BY-2 Cells, in *Isolation of plant organelles and structures. Methods in molecular biology*, vol. 1511. Eds. Taylor, N., Millar, and A. (New York, NY: Humana Press). doi: 10.1007/978-1-4939-6533-5_12

Tsujimoto, Y., and Shimizu, S. (2005). Another way to die: autophagic programmed cell death. *Cell Death Differ.* 12, 1528–1534. doi: 10.1038/sj.cdd.4401777

Tsukada, M., and Ohsumi, Y. (1993). Isolation and charactization of autophagy-defective mutants of. *FEBS Lett.* 333, 169–174. doi: 10.1016/0014-5793(93)80398-E

Van Doorn, W. G., and Papini, A. (2013). Ultrastructure of autophagy in plant cells: a review. *Autophagy* 9, 1922–1936. doi: 10.4161/auto.26275

Wertman, J., Lord, C. E. N., Dauphinee, A. N., and Gunawardena, A. H. L. A. N. (2012). The pathway of cell dismantling during programmed cell death in lace plant (Aponogeton madagascariensis) leaves. *BMC Plant Biol.* 12, 1–17. doi: 10.1186/1471-2229-12-115

Conflict of Interest: The authors declare that the research was conducted in the absence of any commercial or financial relationships that could be construed as a potential conflict of interest.

frontiers in Plant Science

ORIGINAL RESEARCH
published: 26 November 2019
doi: 10.3389/fpls.2019.01539

Sorting the Wheat From the Chaff: Programmed Cell Death as a Marker of Stress Tolerance in Agriculturally Important Cereals

*Alysha Chua, Laurence Fitzhenry and Cara T. Daly**

Department of Science, Waterford Institute of Technology, Waterford, Ireland

Conventional methods for screening for stress-tolerant cereal varieties rely on expensive, labour-intensive field testing and molecular biology techniques. Here, we use the root hair assay (RHA) as a rapid screening tool to identify stress-tolerant varieties at the early seedling stage. Wheat and barley seedlings had stress applied, and the response quantified in terms of programmed cell death (PCD), viability and necrosis. Heat shock experiments of seven barley varieties showed that winter and spring barley varieties could be partitioned into their two distinct seasonal groups based on their PCD susceptibility, allowing quick data-driven evaluation of their thermotolerance at an early seedling stage. In addition, evaluating the response of eight wheat varieties to heat and salt stress allowed identification of their PCD inflection points (35°C and 150 mM NaCl), where the largest differences in PCD levels arise. Using the PCD inflection points as a reference, we compared different stress effects and found that heat-susceptible wheat varieties displayed similar vulnerabilities to salt stress. Stress-induced PCD levels also facilitated the assessment of the basal, induced and cross-stress tolerance of wheat varieties using single, combined and multiple individual stress exposures by applying concurrent heat and salt stress in a time-course experiment. Two stress-susceptible varieties were found to have low constitutive resistance as illustrated by their high PCD levels in response to single and combined stress exposure. However, both varieties had a fast, adaptive response as PCD levels declined at the other time-points, showing that even with low constitutive resistance, the initial stress cue primes cross-stress tolerance adaptations for enhanced resistance even to a second, different stress type. Here, we demonstrate the RHA's suitability for high-throughput analysis (~4 days from germination to data collection) of multiple cereal varieties and stress treatments. We also showed the versatility of using stress-induced PCD levels to investigate the role of constitutive and adaptive resistance by exploring the temporal progression of cross-stress tolerance. Our results show that by identifying suboptimal PCD levels *in vivo* in a laboratory setting, we can preliminarily identify stress-susceptible cereal varieties and this information can guide further, more efficiently targeted, field-scale experimental testing.

Keywords: programmed cell death, plant stress tolerance, root hair assay, cereals, basal tolerance, induced tolerance, stress phenotypes

OPEN ACCESS

Edited by:
Francois Bouteau, Paris Diderot University, France

Reviewed by:
Klára Kosová, Crop Research Institute (CRI), Czechia
Honghong Wu, Huazhong Agricultural University, China

****Correspondence:***
Cara T. Daly
CDALY@wit.ie

Specialty section:
This article was submitted to Plant Cell Biology, a section of the journal Frontiers in Plant Science

Received: *05 August 2019*
Accepted: *04 November 2019*
Published: *26 November 2019*

Citation:
Chua A, Fitzhenry L and Daly CT (2019) Sorting the Wheat From the Chaff: Programmed Cell Death as a Marker of Stress Tolerance in Agriculturally Important Cereals. Front. Plant Sci. 10:1539. doi: 10.3389/fpls.2019.01539

INTRODUCTION

The global population is estimated to reach 9.7 billion by 2050 (United Nations, 2017). Consequently, agriculture systems must be rooted solidly in practices that sustain and enhance our natural environments but must also evolve to meet rising food demands. Until recently, a relatively predictable climate has allowed commercial farmers to prioritise high-yielding crops over stress tolerant varieties. However, the potential gains of high-yielding varieties are redundant if plants are liable to succumb to stress as novel climate abnormalities cause crops to have more frequent encounters with unique abiotic and biotic stress combinations (Mittler, 2006). As a consequence of modified plant physiology and a weakened defence system, crop yield is negatively impacted as plants become more susceptible to pathogens and have lower competitive ability against weeds (Pandey et al., 2017). There is a growing consensus that we need to broaden the focus from production of high-yielding crops, to developing more stress-tolerant varieties as yield improvements must not come at the expense of environment and ecosystem damage (Coleman-Derr and Tringe, 2014; Meena et al., 2017).

Over the years, researchers have developed a diverse range of molecular biology techniques to investigate the different stress-response phases that underpin plant stress tolerance, such as transcriptomics (mRNA transcriptional and post-transcriptional analysis, e.g. micro-RNA and small interfering RNAs) (Chinnusamy et al., 2010), proteomics (2-dimensional liquid chromatography, polyacrylamide gel electrophoresis, difference gel electrophoresis) (Ahmad et al., 2016), metabolomics (gas/liquid chromatography-mass spectrometry, capillary electrophoresis and nuclear magnetic resonance spectroscopy) (Obata and Fernie, 2012), and phenomics (high-throughput phenotyping) (Singh et al., 2018). These high-throughput methods integrate large amounts of information to generate a high-resolution picture of the plant stress response but are often labour-intensive processes that involve significant technical expertise. In contrast, biochemical and physiological techniques are cheaper, quicker and offer useful stress biomarkers. One such biochemical marker is investigation of cellular oxidative damage. Used as a common measurement of plant stress tolerance, excessive reactive oxygen species (ROS) damage subcellular components and trigger programmed cell death (PCD) (Petrov et al., 2015). Common methods for quantifying oxidative damage include total antioxidant capacity, lipid peroxidation and measurement of non-enzymatic and enzymatic antioxidant levels (Elavarthi and Martin, 2010; Jambunathan, 2010). Other biomarkers include fluctuations in cell osmolyte levels which regulate cell volume and maintain osmotic balance during stress onset (Verslues, 2010), while ion quantification is used to screen plants for salt tolerance as the ability to partition and cycle ions through the different tissues is vital for surviving salt stress (Munns et al., 2010).

In the present work we show how PCD can be used as a quick effective tool to identify stress-tolerant cereal varieties. PCD is a normal facet of plant growth and development activated by developmental and environmental factors, but is also a protective mechanism during abiotic and biotic stress onset (Petrov et al., 2015). PCD describes a highly organised sequence of events that leads to the controlled disassembly of the cell and is characterised by the distinctive Ca^{2+}-dependent retraction of the cytoplasm (Kacprzyk et al., 2017). Conversely, necrosis is associated with uncontrolled Ca^{2+}-independent cell death that occurs when cells cannot withstand overwhelming cellular stress (Kacprzyk et al., 2017). Necrotic death is characterised by a loss of plasma membrane integrity, resulting in impaired osmoregulation and the cellular influx of water and ions, causing the cell to swell and rupture, releasing their cellular contents (Lockshin and Zakeri, 2004). PCD plays an important role in the plant response to a variety of environmental stresses as stress-induced PCD activation signifies that damaged cells are unable to cope with the prolonged redox imbalance (Petrov et al., 2015). PCD is activated as the cells' last act of preservation because of stress-induced oxidative damage to organelles and macromolecules (Wituszynska and Karpinski, 2013). Unlike necrotic death, selective PCD activation improves the overall chances of plant survival as it maintains tissue and organ integrity by eliminating damaged cells that accumulate during stress (Wituszynska and Karpinski, 2013). By eliminating cells in a controlled manner, the remaining plant cells can recycle the metabolic precursors from dying cells to increase the likelihood of cell survival (Hoang et al., 2016).

Stress-induced PCD has broad implications for global agricultural practises as it affects crop yield and productivity (Mittler and Blumwald, 2010). With the advance of rapidly changing climates all over the globe, there is a growing interest in developing methods for attenuating environmental stress-induced PCD to minimise crop yield losses (Kim et al., 2014; Hoang et al., 2016). Consequently, it is important for researchers to have an array of methods available to quantify PCD levels *in vivo*. Current methods rely on either the direct scoring of PCD based on its distinctive cell morphology, or indirectly by tracking PCD-triggering molecular signals (e.g. ROS, intracellular Ca^{2+} levels, and cyclic guanosine monophosphate) (Chen et al., 2018; Doccula et al., 2018; Terrón-Camero et al., 2018) and various mitochondrial markers (Xiao et al., 2018). Other indirect methods for quantifying PCD include the measurement of molecular markers generated under oxidative damage (reactive carbonyl species, DNA and lipid damage) (Mano and Biswas, 2018), or PCD executors such as mitogen-activated protein kinase (MAPK) signalling cascades (Wu and Jackson, 2018) and vacuolar processing enzyme (VPE) activity (Hatsugai and Hara-Nishimura, 2018). All of these methods have a wide range of applications for investigation of the different phases of the plant stress response, but it is important to remember that cells integrate multiple PCD-inducing signals across many different subcellular compartments, and not just a lone signal as measured by the aforementioned methods (Petrov et al., 2015). This was illustrated in work by Kacprzyk et al. (2017) who showed that chemical modulators that alter mitochondrial permeability transition, ATP synthesis and Ca^{2+} signalling also inhibit protoplast retraction in stressed cells, showing that multiple signalling pathways are acting collectively to modulate PCD. Perception of stress cues generates PCD-inducing signals at the endoplasmic reticulum (ER), chloroplast and mitochondria, but

each organelle has distinctive mechanisms for processing the signal (Petrov et al., 2015).

The intricate signalling networks modulating PCD emphasises the serious consequences the cellular decision to undergo PCD holds for the survival of the whole organism. Cells regulate PCD by balancing pro- and anti-apoptotic signals, and the decision to live or die depends on which direction the balance shifts. This highlights the biggest difference found between indirect and direct PCD quantification methods. Indirect methods track the progression of molecular markers, signalling networks or metabolic changes that stressed cells undergo, while direct PCD scoring shows the final outcome of the cells decision-making procedure, whether cells stay alive or undergo PCD.

This paper provides evidence that direct *in vivo* PCD scoring is a useful marker of stress tolerance in cereals as it integrates multiple stress inputs (and combinations thereof) to provide a cohesive picture of the stress response. Studies using direct PCD scoring methods generally involve *in vitro* plant cell cultures, but they can be labour intensive to establish and because of divergent mitotic patterns, not all plant species will have the right morphologies to form uniform suspension cultures (Cimini et al., 2018). More importantly, it is pertinent to assess the effects of PCD modulators in the whole plant context, as tissue-specific cells will not respond in a synchronised manner as would be seen in homogenous plant cell cultures (Reape et al., 2015). Given these points, using seedlings as an *in vivo* model system for investigating plant PCD offers a more accurate representation compared to artificially controlled reconstructions using *in vitro* methods (Kacprzyk et al., 2011; Reape et al., 2015). A novel model system involving root hairs for direct PCD scoring was demonstrated by Hogg et al. (2011) as root hairs are lateral single-celled extensions from root epidermal cells, are present in quantities large enough for sample enumeration, and are easily accessible for pharmacological treatment. The protocol developed was termed the root hair assay (RHA) and was used to establish heat stress response curves in *Arabidopsis* seedlings, and Hogg et al. (2011) also successfully extrapolated the assay to *Medicago truncatula*, *Zea mays*, and *Quercus robur* seedlings. Furthermore, Kacprzyk et al. (2014) demonstrated RHA use with genetic and pharmacological tools to assess the signalling networks regulating the PCD response in *Arabidopsis* seedlings.

In this paper, we build on these past works to show that stress-induced PCD levels can be a novel marker for identifying stress tolerance in cereal varieties of *Triticum aestivum* (wheat) and *Hordeum vulgare* (barley). Using the RHA as an early screening tool, we developed a protocol for identifying stress tolerant and susceptible cereal varieties by subjecting <2-day-old seedlings to increasing heat and salt stress intensities. By reviewing the dose-dependent response, we identified the 'inflection point' for each species and stress treatment. The inflection points indicate the stress dose which exhibited the largest variances in stress-induced PCD levels and once identified, these inflection points were then used to assess the basal, induced and cross-stress tolerance of wheat varieties by exposing plants to single, combined and multiple individual stresses. Single stress exposure involves the application of a single stress-factor, multiple individual stresses are non-overlapping repetitive stresses at different time-points, while combined stress is two or more stresses applied simultaneously that overlap to a certain degree (Pandey et al., 2017).

Basal tolerance was assessed using single and combined stress exposure as both treatments highlight the intrinsic ability of plants to survive stress by its baseline physiological state without prior stress exposure or acclimation (Arbona et al., 2017). Combined stress treatments are highly distinct from single stress-factor treatments as the former generates a unique stress phenotype that is distinct from the latter (Mittler, 2006; Rasmussen et al., 2013; Rivero et al., 2014). Rasmussen et al. (2013) divided the unique stress phenotype into five categories (prioritized, similar, combinatorial, cancelled and independent), but for simplicity's sake, we refer to the original stress phenotype categories devised by Mittler (2006) who divided the response into synergistic, antagonistic or neutral interactions, of which all five stress modes fall into (**Supplementary Figure 1A**). Finally, we used multiple individual stresses to study induced and cross-stress tolerance, the phenomenon where the initial stress exposure makes plants more resistant to other stress types (Walter et al., 2013; Rejeb et al., 2014; Pandey et al., 2017). As **Supplementary Figure 1B** illustrates, the first stress cue can either prime (positive and neutral) or predispose (negative) plants to recurrent stress exposure (Pandey et al., 2017). Priming enables plants to reach a new metabolic steady-state higher than its pre-stress levels by reprogramming the metabolome and making epigenetic changes; primed plants either become resistant to the second stress encounter without additive damage (neutral – maintains same steady state), or have improved tolerance (positive – higher metabolic steady state) (Tausz et al., 2004; Walter et al., 2013; Pandey et al., 2017). Conversely if the cell protective mechanisms are insufficient, predisposition makes plants more vulnerable to repetitive stresses because of lagging stress effects (e.g. excessive oxidative damage) that leads to degradation of the metabolic steady state and higher cell death rates (Tausz et al., 2004; Walter et al., 2013). The variety of responses to different stress exposures shown here demonstrates how stress-induced PCD levels can be used to screen for the formation of unique stress phenotypes, while at the same time, allowing examination of how basal, induced and cross-stress tolerance affects cereal survival.

MATERIALS AND METHODS

Seedling Preparation

Three spring barley varieties were provided by Seedtech®, while four spring wheat, four winter wheat and four winter barley varieties were supplied by KWS UK®. **Table 1** details the list of cereals and their identifier numbers used in these experiments. In temperate climates, spring and winter varieties differ in the season they are sown. Winter varieties require vernalisation in the cold to flower, while spring varieties do not. In barley, the vernalisation response is controlled by two major loci at *VRN-H1* and *VRN-H2*, while spring alleles have deletions in both loci that enables flowering without vernalization (Cockram et al., 2007). A similar scenario occurs in wheat, but five vernalization-responsive genes (*Vrn1–5*) have been identified (Cattivelli et al.,

TABLE 1 | Cereal Variety Identifier, Corresponding Species, Season and Provider.

Seed Identifier	Species	Season	Provider
SB1	*H. vulgare* (Barley)	Spring	Seedtech®
SB2			
SB3			
WB1	*H. vulgare* (Barley)	Winter	KWS UK®
WB2			
WB3			
WB4			
SW1	*T. aestivum* (Wheat)	Spring	KWS UK®
SW2			
SW3			
SW4			
WW1	*T. aestivum* (Wheat)	Winter	KWS UK®
WW2			
WW3			
WW4			

SB, spring barley; WB, winter barley; SB, spring wheat; WW, winter wheat.

2002), but the three major vernalization genes responsible for vernalization in both wheat and barley are *VRN1*, *VRN2* and *VRN3* (Distelfeld et al., 2009).

T. aestivum (Wheat) Seedling Preparation and Germination

Wheat seeds were soaked in sterile distilled water (SDW) at room temperature for 3 h. In a sterile flow cabinet, water was drained from seeds, a 20% bleach solution (Domestos® disinfectant: sodium hypochlorite 4.5 g per 100g) was added, and the mixture was shaken for 4 min and rinsed 5 times with SDW. Using sterile forceps, 10 surface-sterilised seeds were placed between two layers of sterile 10 mm Whatman™ filter paper (pre-soaked with 3 cm^3 SDW) in a Petri dish. Seeds were arranged far apart from one another to prevent roots from tangling after germination to minimise root hair damage. Plates were sealed with Parafilm, wrapped in foil and stratified at 4°C for at least two days to synchronise germination. To germinate seeds, plates were placed in a 21°C growth chamber (light regime: 33 µmol m^{-2} s^{-1}, 16-h light: 8-h darkness) and used for stress assays after 1 day of growth.

H. vulgare (Barley) Seedling Preparation and Germination

The procedure to prepare barley seedlings for testing was similar to the protocol used for wheat seedlings; however, barley seeds were left to grow for 2 days as initial testing (data not shown) showed inadequate germination levels after 1 day of growth.

Stress Application and Scoring of Cell Modes

Barley and wheat seedlings were transferred into Petri dishes under aseptic conditions with care to prevent mechanical damage which would inflate the background death levels of root hairs. SDW (2 cm^3) was pipetted into the germination plates and swirled to dislodge the roots from the filter paper. Seedlings were transferred to Petri dishes (containing 25 cm^3 SDW), heated for 10 min in a water bath at specific temperatures (25, 35, 45, 50, or 55°C) and returned to the 21°C growth chamber. Viability and cell death (PCD and necrosis) were scored 14–16 h after stress application to allow PCD morphology to develop fully as per Hogg et al. (2011).

The longest root in 1-day-old wheat seedlings was counted as shorter roots lacked sufficient root hair density for accurate cell mode enumeration. In contrast, 2-day-old barley seedlings have multiple roots (3–5) of approximately equal length. Preliminary RHA testing (data not shown) showed that barley roots on the same seedling have similar viability, PCD, and necrosis levels therefore because of the insignificant variability of roots from the same plant sample, subsequent heat stress curves only involved the enumeration of one root per barley seedling.

To score cell mode, the seedlings were stained with a 0.001% w/v fluorescein diacetate (FDA) solution for 2 min and examined using an Olympus BX61 microscope under a mercury lamp with a fluorescein isothiocyanate (FITC, wavelength 485 nm) filter. Using a combination of viability staining and cell death morphology, root hairs were scored as viable if they were fluorescent (FDA positive), PCD if they had a retracted cytoplasm and negative FDA stain, and necrotic if they did not possess a retracted cytoplasm and negative FDA stain. **Supplementary Figure 2A** depicts the different cell mode morphologies found in FDA-stained stressed and unstressed root hairs of *Arabidopsis thaliana*, the model organism in which the RHA was originally developed. Cereal root hairs display similar morphologies when viable, PCD or necrotic, but are longer and occur more frequently along the main root compared to *A. thaliana*. Consequently, it is difficult to take clear images of cereal roots depicting the different cell morphologies; hence we use *A. thaliana* images here to clearly illustrate cell death morphology in individual root hair cells. **Supplementary Figure 2B** shows cell death morphology in wheat root hairs but at a lower magnification. These are included because on occasion, salt-stressed wheat seedlings displayed mixed markers (retracted cytoplasm and FDA positive) because of plasmolysis (**Supplementary Figure 2B**). Under these circumstances, root hairs displaying mixed markers were rinsed with SDW and remounted on microscope slides without additional FDA staining. This removes excessive background FDA staining and makes it easier to distinguish between viable (strong fluorescence) and PCD (weak, almost imperceptible fluorescence) root hairs. At least 100 root hairs were scored per seedling across both sides of the primary root to provide an accurate representation of viable, PCD and necrosis levels. Each cell mode result is depicted as the percentage of cell mode over total number of root hairs, where viability% + PCD% + necrosis% = 100%.

Establishing Salt Stress Response Curves in *T. aestivum* Seedlings

1-day-old wheat seedlings were placed in Petri dishes filled with 25 cm^3 NaCl (50, 100, 150, 200 or 250 mM) for 5 min, before being transferred into new Petri dishes containing 25 cm^3 SDW.

Seedlings were returned to the 21°C growth chamber and scored 14-16 h after stress application.

Evaluating the Single, Combined and Multiple Stress Responses of *T. aestivum* Seedlings to Heat and Salt Stress

Eight wheat varieties were examined for their response to single, combined and multiple stresses. As a result of identifying the 35°C heat and 150 mM NaCl inflection points, 1-day-old wheat seedlings were subjected to heat (35°C) and/or salt (150 mM NaCl) stress at specific time-intervals. In the first data-set, samples were subjected to 35°C stress for 10 min at the 0-min mark, followed by 150 mM NaCl stress for 5 min at the 30, 60 and 120-min mark, followed by transfer into 25 cm^3 SDW. In the second data-set, samples were subjected to 150 mM NaCl stress for 5 min at the 0-min mark, transferred into SDW-containing plates, and followed by 35°C heat stress for 10 min at the 30, 60 and 120-min mark. **Figure 1** summarises the process used to examine basal and induced tolerance using single, combined and multiple individual stresses. Controls include single-stress (35°C only, or 150 mM NaCl only) and double-stress (heat and then salt (H+S) or, salt and then heat (S+H) at the 0-min mark).

Statistical Analysis

IBM® SPSS® Version 24 (RRID : SCR_002865) was used to analyse results for significant changes ($p < 0.05$) across stress treatments and cereal (barley and wheat) varieties. Statistical tests used include one-way ANOVA (Tukey or Dunnett Post-hoc Test), bivariate analysis (Pearson's correlation), and independent-samples *t*-test.

RESULTS

Thermotolerance of *H. vulgare* Varieties

Four winter barley (WB) and three spring barley (SB) varieties were tested for their thermotolerance by stressing 1-day-old seedlings for 10 min at temperatures ranging from 25 to 55°C. Based on the changing cell mode ratios across the temperature gradient, three threshold stress-responses were observed: 1) stress-tolerant (25°C) where PCD levels were at their lowest (and necrosis levels were negligible), 2) the viable/PCD 'inflection point' (35°C), and 3) the PCD zone (45–55°C) where the majority of root hairs died by PCD. We observed a clear distinction between spring and winter varieties as all three spring varieties had consistently lower PCD levels at low heat stress (25–35°C) compared to their four winter counterparts. The PCD levels of the spring barley varieties remained stable (10–17%) across 25°C and 35°C heat stress, unlike the winter varieties which increased when heat stress was increased from 25°C (35–40%) to 35°C (43–63%). Statistical analysis confirmed these observations: PCD levels only changed significantly ($p < 0.05$) in WB1, WB2, and WB4 seedlings when heat stress was increased from 25°C to 35°C but remained stable in the remaining varieties (**Supplementary Table 1**). A similar trend was noted at medium heat stress (45°C) where spring varieties remained more resistant to heat shock, with average PCD levels of 63%. In contrast, PCD levels of all four winter barley varieties

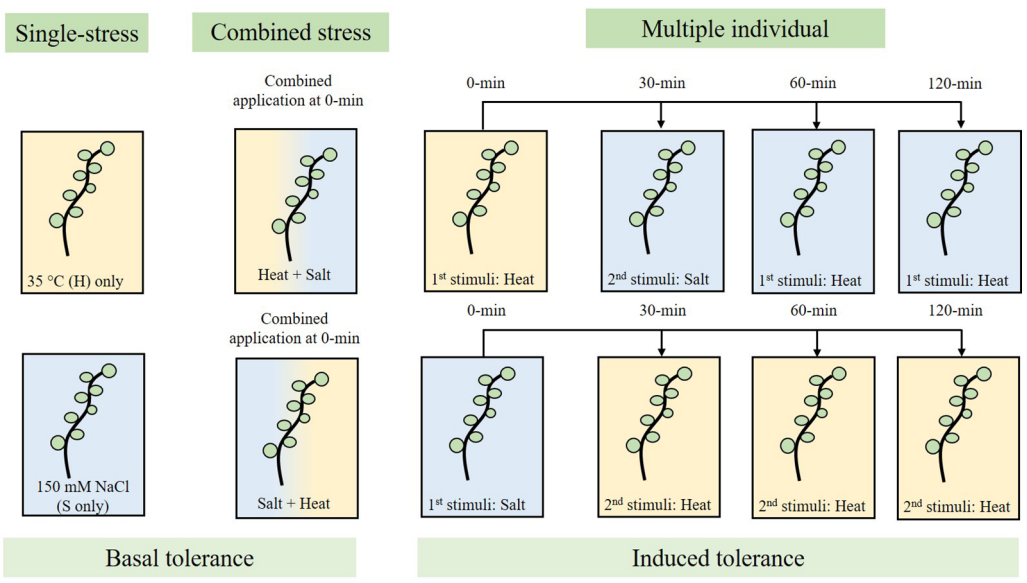

FIGURE 1 | Experimental workflow used to assess basal stress tolerance (single and combined), and induced stress tolerance (multiple individual) in wheat seedlings in response to 35°C heat (H) and/or 150 mM NaCl salt (S) stress. Single-stress involves the application of a single stress-factor (H only, or S only), combined stress involved the overlapping application of 35°C heat followed by salt stress (H+S; 0-min) and vice versa (S+H; 0-min), and multiple individual testing involves the application of the first stress stimuli (0-min), followed by application of the second stress stimuli at 30, 60, and 120-min.

were significantly higher (83–87%) at 45°C. At high stress (50–55°C), no difference was observed between winter and spring varieties as viability levels declined to ~0%, with PCD being the predominant cell death mode across all varieties. **Figure 2A** illustrates the clear thermotolerance differences between seasonal varieties; at low-to-medium heat shock, spring varieties were heat-tolerant, but winter barley varieties were heat-susceptible. Stress-induced PCD was the predominant cell mode across all varieties at 45°C, while necrosis levels were generally unchanged at temperatures up to 50°C, but started to increase at 55°C in WB3 and SB3 (**Figure 2B**).

Stress Tolerance of *T. aestivum* Varieties

Thermotolerance of *T. aestivum* Varieties

Four spring wheat (SW) and four winter wheat (WW) varieties were tested for their resilience to transient heat stress (**Figure 3**) and, again, three stress-response thresholds were identified: stress tolerant (25°C), viable/PCD inflection point (35°C), and the PCD zone (45–55°C). However, unlike the barley varieties, mixed tolerance was seen across both spring and winter varieties of wheat. At low heat stress (25°C), WW1 had the highest PCD levels (53.2%), followed by SW4 (36.8%) and SW3 (23.9%). We observed a comparable trend at 35°C as SW4, WW1, and WW4 had the highest PCD (46–47%) of all the varieties, with limited variance in viability and necrotic levels.

Distinctions between the thermotolerance of wheat varieties were detected as early as 35°C, which was determined as the viable/PCD inflection point; apart from WW2, WW3 and WW4 whose PCD levels rose significantly ($p < 0.05$) as heat shock increased from 25°C to 35°C, the remaining varieties maintained similar PCD levels (**Supplementary Table 2**). At higher heat stress (45°C), variations in PCD receded as most wheat varieties had ~80% PCD, although SW1, SW2 and WW4 lines still exhibitied remarkble heat resistance, with stress-induced PCD ranging from 63 to 71%. Beyond this point, viability declined to ~0%, with PCD remaining the primary death mode at 50°C and 55°C. Even at 55°C heat shock, necrotic levels remained remarkably stable across the wheat varieties and temperature gradient, apart from WW1 and WW2 seedlings that had a 2 to 3-fold increase in necrosis, compared to that seen at the 50°C data-point.

Evaluating *T. aestivum* Varieties for Salt Tolerance

Four spring wheat (SW1-4) and four winter wheat (WW1-4) varieties were tested for their tolerance to transient salt stress (**Figure 4**). Three stress-response thresholds were also detected: stress-tolerant (50–100 mM NaCl), the viable/PCD inflection point (150 mM NaCl), and the PCD zone (200–250 mM NaCl). At low salt stress (50–100 mM), we could clearly see the distinctions between the salt-tolerant and salt-susceptible varieties: SW1, SW2, WW3, WW4 were identified as the salt-tolerant lines as

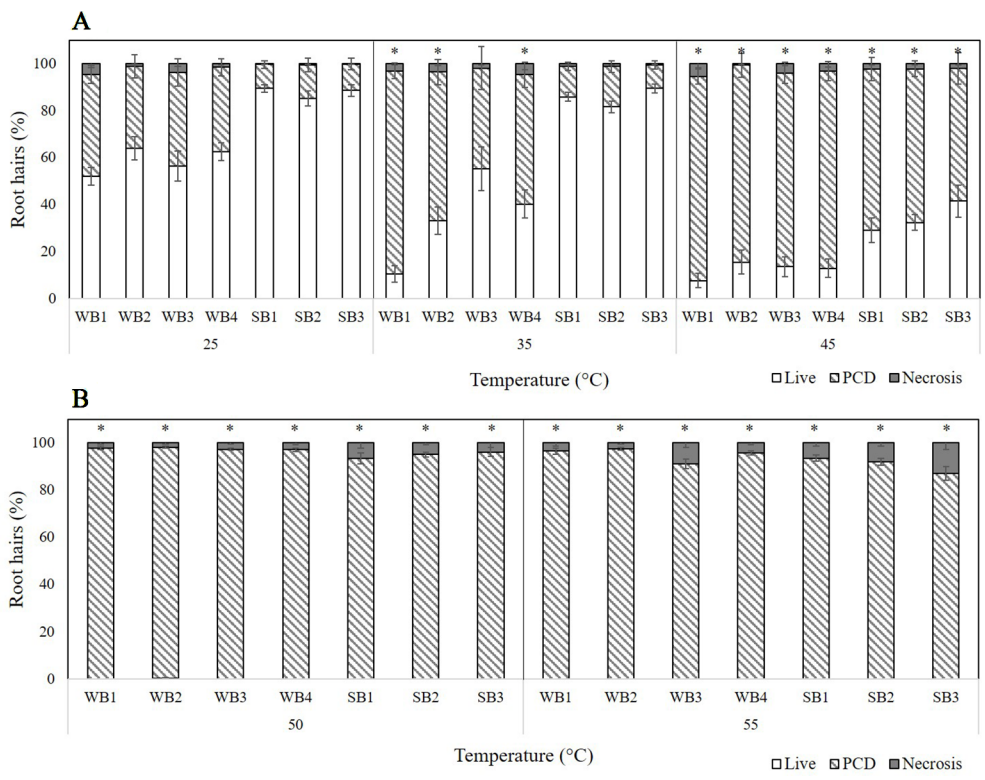

FIGURE 2 | Effect of **(A)** low-to-medium or **(B)** high heat stress on root hair viability and cell death (PCD and necrosis) levels in varieties of winter (WB1-4) and spring (SB1-3) barley. (*) marks PCD results significantly ($p < 0.05$) different from the 25°C dataset, using a one-way ANOVA Dunnett post-hoc test (**Supplementary Table 1**). Error bars = standard error of $n \geq 8$ replicates.

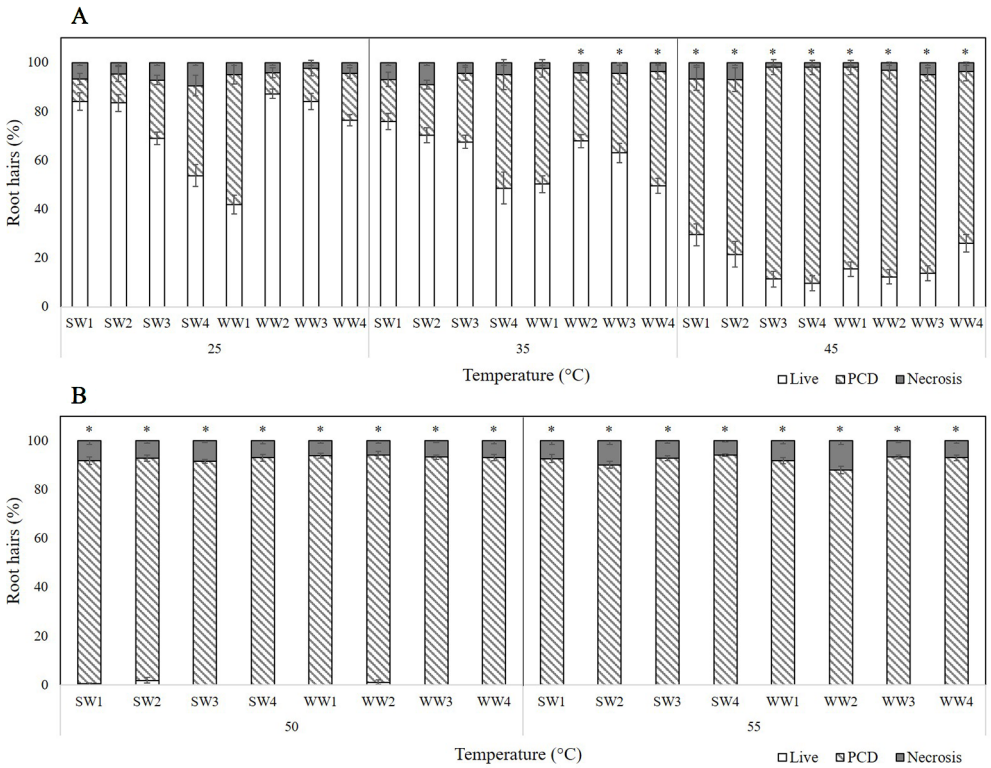

FIGURE 3 | Effect of **(A)** low-to-medium or **(B)** high heat stress on root hair viability and cell death (PCD and necrosis) levels of four spring wheat (SW1-4) and four winter wheat varieties (WW1-4). (*) marks PCD results significantly ($p < 0.05$) different from the 25°C dataset, using a one-way ANOVA Dunnett post-hoc test (**Supplementary Table 2**). Error bars = standard error of n ≥ 12 replicates.

they had the lowest stress-induced PCD (15–20%) of all the varieties. Discrepancies became even larger when effects were examined at 150 mM NaCl (viability/PCD inflection point); PCD predictably increased across all varieties but SW4, WW1, and WW2 had elevated PCD levels compared to the other varieties tested. WW1 and WW2 had PCD ranging from 37-44%, while SW4 had almost double PCD (62.6%) which equates to a 27.2% increase from its nearest 100 mM data-point (**Figure 4A**). The remaining five varieties had similar PCD ranging from 21–30%. Beyond this point, medium salt stress (200–250 mM) caused PCD to become the predominant cell mode over viable and necrotic cells. Interestingly, SW1 and SW2 still had the lowest PCD levels at 200 mM NaCl (64–68%), indicative of their salt tolerance, since the average PCD across the other varieties was 80.9%. Nevertheless, this discrepancy disappeared at higher 250 mM NaCl doses as PCD (85-93%) became similar across all eight varieties (**Figure 4B**). Necrosis levels did not change significantly in the experiment.

Screening *T. aestivum* Varieties for Dual Stress Tolerance

The discovery of the three distinct stress-response phases across all the heat and salt stress gradients tested in wheat prompted the preparation of a tolerance matrix (**Table 2**) to determine if varieties displayed dual tolerance to both heat and salt stress. As previously stated, the largest deviations in stress-induced PCD levels arise at the inflection point, making it easier to compare differences in the tolerance strength of the varieties. While we do see fluctuations at the other phases, stress-induced PCD levels tend to cluster too closely to pick out subtle variations between the investigated varieties. For example, PCD is generally low in the stress-tolerant zone, but predominantly high in the PCD zone. Consequently, we focused on performance at the viable/PCD inflection point to identify stress-tolerant or susceptible varieties.

The first stress-tolerant threshold (25°C; 50 mM NaCl) denotes the phase where the cell protective mechanisms are enough to repair oxidative damage therefore cells maintain high viability and low PCD levels. Bivariate analysis was used to measure the strength of association between heat and salt stress-induced PCD levels. We found statistically significant ($p < 0.05$) correlation between both variables, with a Pearson's correlation coefficient of 0.223 (n = 105), showing that PCD levels in heat shocked seedlings correlated with their salt-stressed counterparts. As illustrated in **Figures 5A**, **B** and **Table 2**, low salt tolerance was observed in SW3, SW4, WW1, and WW2 seedlings, with PCD ranging from 26–34%, compared to the remaining seedlings exhibiting PCD of 15-20%. Similar varieties were also found to be susceptible to minimal (25°C) heat stress, as elevated PCD levels were found in SW3 (23.9%), SW4 (36.8%) and WW1 (53.2%), and to a certain extent, WW4 (19.2%). PCD in the four remaining varieties was substantially different and averaged 10.8%.

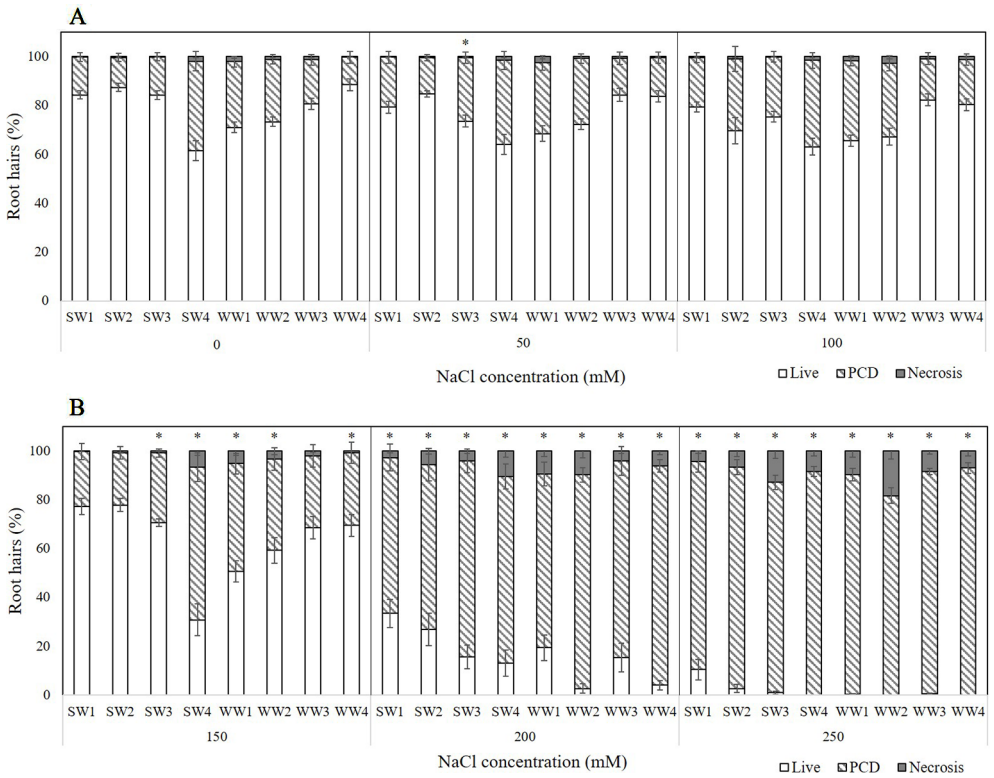

FIGURE 4 | Effect of **(A)** low or **(B)** medium-to-high salt stress on root hair viability and cell death (PCD and necrosis) levels of four spring wheat varieties (SW1-4) and four winter wheat varieties (WW1-4). (*) marks PCD results significantly ($p < 0.05$) different from the 0 mM NaCl (i.e. SDW control) dataset, using a one-way ANOVA Dunnett post-hoc test (**Supplementary Table 3**). Error bars = standard error of n ≥ 12 replicates.

TABLE 2 | Tolerance matrix examining the tolerance or susceptibility of wheat seedlings to salt or heat stress at different stress-response phases (stress-tolerant, viable/PCD inflection point and PCD zone) highlights SW1 and SW2 as stress tolerant varieties. Bivariate analysis (Pearson) found correlation between PCD levels of heat and salt-stressed seedlings in the stress-tolerant phase (n = 105) and viable/PCD inflection point (n = 115), but not in the PCD zone (n = 121).

Stress-response Phase	Stress Applied	Variety							
		SW1	SW2	SW3	SW4	WW1	WW2	WW3	WW4
Stress-tolerant	**25 °C**	++	++	x	x	x	++	+	+
	PCD (%)	9.1	11.86	23.86	36.84	53.21	8.66	13.68	19.19
	50 mM NaCl	+	++	x	x	x	x	++	++
	PCD (%)	20.4	15	26	34.4	29	26.9	15	15.9
	Pearson's correlation coefficient = 0.223*, p-value = 0.022, R^2 linearity = 0.050								
Viable/PCD inflection point	**35 °C**	++	++	+	x	x	+	+	x
	PCD (%)	17.3	20.7	28	46.5	47.4	28	32.7	46.7
	150 mM NaCl	++	++	+	x	x	x	+	+
	PCD (%)	22.5	21.5	28.5	62.6	44.3	37.3	29.4	29.7
	Pearson's correlation coefficient = 0.333*, p-value = 0.000, R^2 linearity = 0.111								
PCD zone	**45 °C**	++	+	x	x	x	x	x	+
	PCD (%)	63.8	71.5	86.9	88.3	82.6	84.5	81.3	70.3
	200 mM NaCl	++	++	x	+	+	x	x	x
	PCD (%)	63.8	67.6	80.1	76.5	71.1	87.4	80.5	89.7
	Pearson's correlation coefficient = -0.015, p-value = 0.867, R^2 linearity = 2.365 x 10^{-4}								

Key: 'X' = Stress-susceptible, '++' = stress-tolerant, '+' = moderately stress-tolerant.

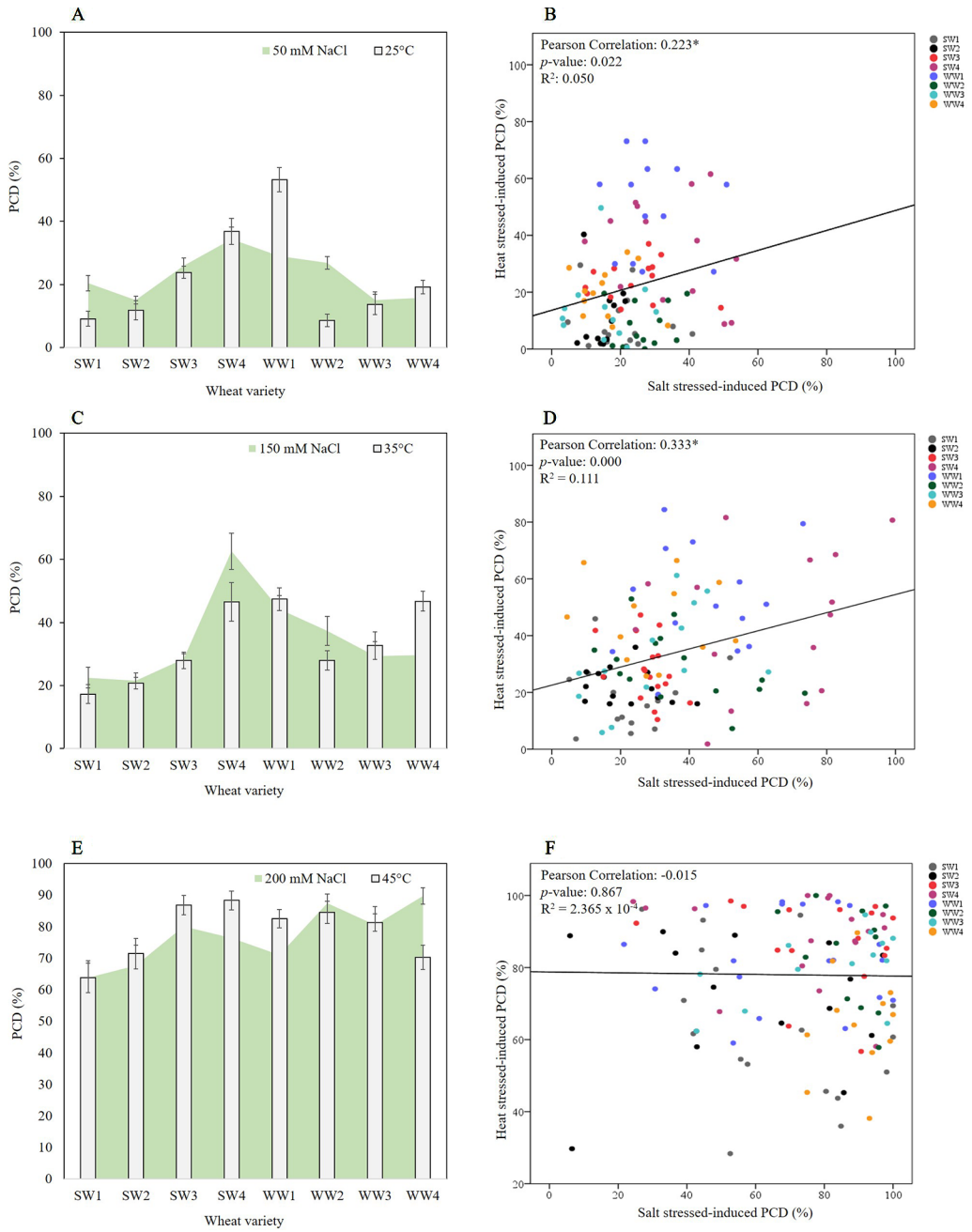

FIGURE 5 | Pearson correlation analysis between the tolerance/susceptibility of wheat varieties to salt and heat stress. Figures on the left column represent overlaid heat and salt datasets, while their respective scatterplots are shown on the right column. **(A, B)** Stress-tolerant phase of 25°C and 50 mM NaCl, **(C, D)** the viable/PCD inflection point of 35°C and 150 mM NaCl, and **(E, F)** the PCD zone of 45°C and 200 mM NaCl. Correlation was found between PCD levels of heat and salt-stressed seedlings in the stress-tolerant phase (0.223, *p*-value = 0.022 and n = 105) and viable/PCD inflection point (0.333, *p*-value = 0.000 and n = 115), but not in the PCD zone (-0.015, *p*-value = 0.867 and n = 121).

A similar trend was observed at the viable/PCD inflection point (35°C; 150 mM NaCl) shown in **Figures 5C, D** and **Table 2**. Compared to the stress-tolerant thresholds, a stronger correlation was noted here as we detected a highly statistically significant correlation of 0.333 ($p < 0.01$) between PCD levels of heat and salt-shocked seedlings (n = 115). At 150 mM NaCl, the highest PCD values were seen in SW4 (62.6%), WW1 (44.3%) and WW2 (37.3%), while the PCD levels in the other lines only ranged between 21-30%; the lowest PCD levels at 150 mM NaCl were seen in SW1 and SW2 which had ~22% PCD. Under 35°C heat stress, elevated PCD (~47%) was seen in SW4, WW1 and WW4, whereas the lowest PCD levels were seen in SW1 (17.3%) and SW2 (20.7%). Collectively, these results show that similar wheat varieties displayed dual tolerance (SW1 and

SW2) or susceptibility (SW4 and WW1) to independent heat and salt stress.

Finally, no significant correlation (-0.015, where $p > 0.05$ and n = 121) was found at the PCD zone (45°C; 200 mM NaCl) between heat and salt-stressed seedlings (**Figures 5E**, **F** and **Table 2**). At this stage, both stress intensities were high enough to overcome most of the differences in basal tolerance between wheat varieties; apart from SW1 and SW2 that maintained PCD levels lower than 70% at 200 mM NaCl (**Figures 5E**, **F**), the remaining six varieties averaged 80.9%. Similarly, at 45°C, SW1, SW2, and WW4 had the lowest PCD (64-72%), while the other five lines had PCD levels >81%.

Evaluation of *T. aestivum* Varieties for Basal, Induced and Cross-Stress Tolerance to Heat and Salt Stress

Three types of stress exposure were investigated in this final study: single, combined and multiple individual stresses. Basal tolerance of the seedlings was examined at the viable/PCD inflection point by applying a single (35°C heat or 150 mM NaCl) or combined stress (simultaneous application of heat and salt at the 0-min time-point). The adaptive tolerance was evaluated by administering the first stress trigger (heat or salt) at the 0-min mark, followed by the second stress across three time-points (30, 60 and 120 min). **Figure 6** depicts how each individual wheat variety responds to unique stress exposures as a function of their stress-induced PCD levels. Given that basal tolerance reflects the genetically pre-determined ability to withstand stress without prior exposure (Arbona et al., 2017), SW1 and SW2 were identified as varieties with high basal tolerance, while SW4 and WW2 were singled out as varieties with low basal tolerance, based on their performance against single and combined stress treatments (see section: *T. aestivum Cross-Stress Tolerance Depends on the Initial Stress Cue*). Interestingly, varieties with high basal tolerance (SW1 and SW2) had a slow induced tolerance response, unlike stress-susceptible SW4 and WW1 which adapted faster, as elaborated in the section *Individual T. aestivum Varieties Under Combined Stress Exposure Exhibit Varying Stress Responses*. By varying the initial stress cue, we observed a few interesting overall trends not immediately apparent from the data presented in **Figure 6**. For that reason, we merged the average stress-induced PCD levels of all eight varieties across the H+S, and S+H datasets (**Figure 7**) and the following trends were revealed. First, cross-stress tolerance experiments

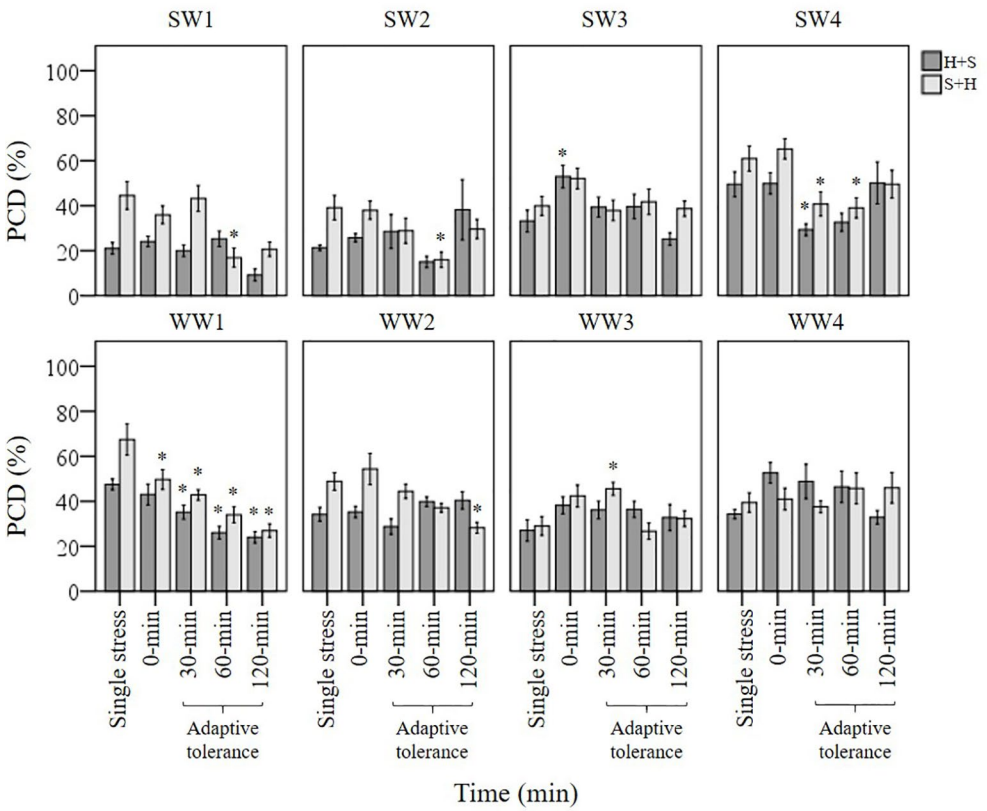

FIGURE 6 | Examining how single, combined and multiple individual stress exposures affects stress-induced PCD in wheat varieties. The initial stress cue (35°C heat or 150 mM NaCl) is applied at the 0-min mark, followed by the second stress application at different time-points (30, 60 and 120-min). (H+S) refers to heat stress as the initial cue, followed by salt stress, while (S+H) refers to salt stress as the first cue, followed by heat stress at the relevant time-points. (*) marks PCD results significantly ($p < 0.05$) different from the single-stress factor control (H-only or S-only), using a one-way ANOVA Dunnett post-hoc test (**Supplementary Table 4**). Error bars = standard error of n ≥ 4 replicates.

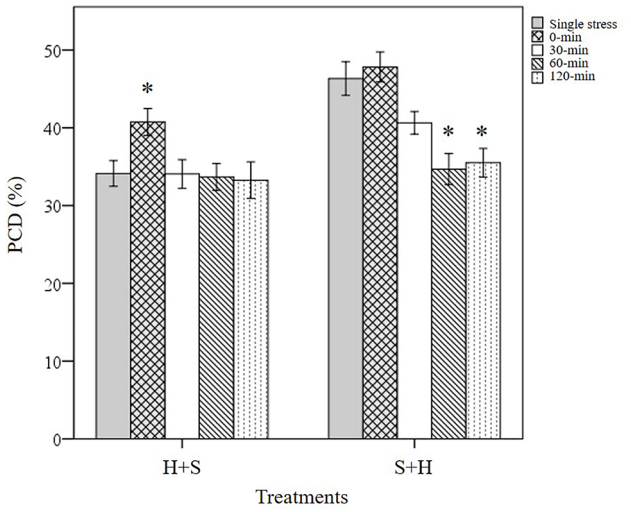

FIGURE 7 | Overall trends noted in stressed wheat seedlings by varying the initial stress cue. (*) marks PCD results significantly ($p < 0.05$) different from the single-stress factor control (H-only or S-only), using a one-way ANOVA Dunnett post-hoc test (**Supplementary Table 5**). Values represent the average PCD levels across the eight varieties, where error bars = standard error of n ≥ 89 replicates.

showed that stress acclimation and priming were the predominant responses when seedlings were either first heat or salt-shocked, respectively. Second, under combined stress, seedlings that were first salt-shocked had similar PCD levels (47.8%) as the single stress-factor control (46.3%), but initially heat-shocked seedlings had statistically higher ($p < 0.05$) stress-induced PCD (40.8%) compared to the heat stressed only dataset (34.1%). Finally, salt stress had a dominating effect over heat stress, and that initial salt shock had a lagging PCD-suppressing effect.

T. aestivum Cross-Stress Tolerance Depends on the Initial Stress Cue

Cross-stress tolerance was evaluated in terms of priming (lower PCD levels), acclimation (neutral PCD levels) and predisposition (higher PCD levels) to the second applied stress type, compared to their respective single stress-factor datasets (**Figure 8**). When heat was applied at the first stimuli and followed by subsequent NaCl shock, only WW1 ($p < 0.05$) were grouped under the primed category, while the remaining varieties fell under the acclimation category. However, wheat varieties responded differently when they were first subjected to NaCl shock, followed by later heat stress. Despite maintaining identical stress doses, the varieties were re-shuffled into different categories: primed (SW2, SW4, WW1, and WW2) and acclimation (SW1, SW3, WW3, and WW4). Primed seedlings had statistically lower ($p < 0.05$) PCD levels compared to their respective S-only controls. Predisposition was not observed across both datasets, regardless of the initial stress cue. Thus, stress acclimation was the primary response (87.5%) when heat-shocked wheat varieties were assessed for their cross-stress tolerance to subsequent salt stress. Conversely, priming shared equal dominance (50%) with the acclimation mode when varieties were initially salt-shocked, even though identical stress doses were maintained.

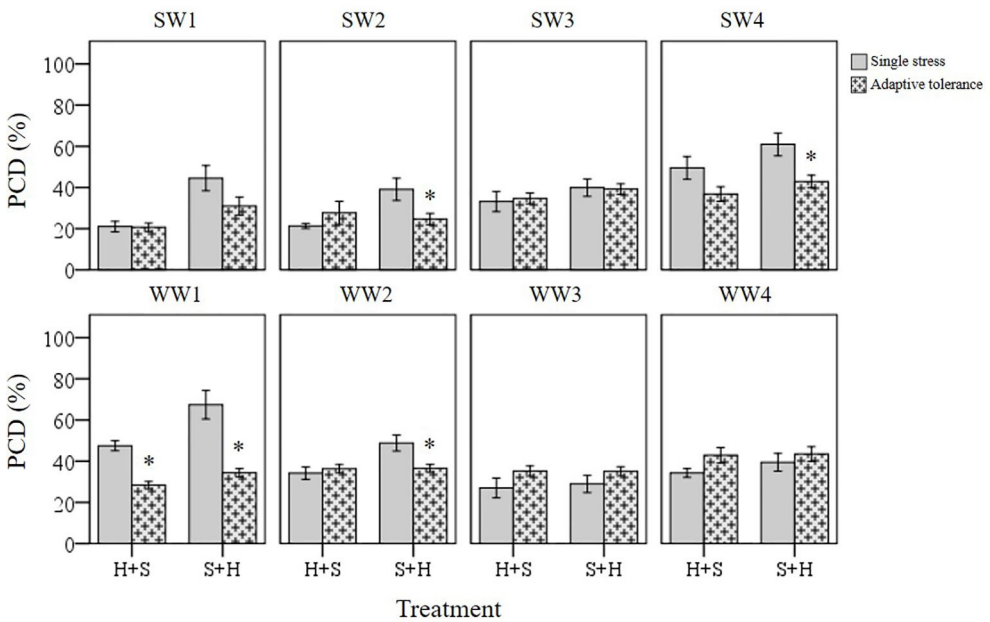

FIGURE 8 | Induced tolerance changes across individual wheat varieties and different initial stress cues. (*) marks PCD results significantly ($p < 0.05$) different from the single-stress factor control (H-only or S-only), using independent *t*-tests (**Supplementary Table 6**). Induced tolerance values represent the merged PCD levels across 30, 60 and 120-min datasets. Error bars = standard error of n ≥ 4 replicates.

The tendency for specific stress responses based on the initial stress cue (e.g. stress acclimation in H+S; priming in S+H) is illustrated in **Figure 7**, which depicts the average PCD values of all the varieties across both H+S and S+H datasets. When heat shock was the initial stress-cue, similar PCD levels (33-34%) were noted between the single heat stress-factor and the multiple stress (30, 60 and 120-min) dataset. This shows that additional salt stress did not negatively affect previously heat-shocked seedlings ($p > 0.05$), i.e. seedlings were stress-acclimatised against recurrent exposure. However, a different stress response pattern emerged when salt stress was the initial stress cue; exposure to NaCl successfully primed seedlings against subsequent heat damage as we recorded statistically lower ($p < 0.05$) PCD levels at the 60 and 120-min datasets compared to the single NaCl stress-factor dataset. Our results highlights the intricacy of supplying stresses in unique combinations as initial exposure to different stress cues causes divergent responses (**Table 3A**), despite exposure to identical stress dosages.

Individual *T. aestivum* Varieties Under Combined Stress Exposure Exhibit Varying Stress Responses

Basal tolerance to combined stress was assessed by examining the interactions between heat and salt stress in terms of synergistic (lower PCD levels), antagonistic (higher PCD levels), or neutral (no net changes in PCD levels) compared to their respective single stress-factor datasets. We organised the unique stress phenotypes displayed by the individual varieties into the form of a stress matrix (**Table 3B**), where most of the stress combination results (75%) fell under the neutral category. Under combined H+S stress, only SW3 and WW4 showed antagonistic interaction, i.e. statistically higher ($p < 0.05$) PCD levels from the H-only control. In contrast, different varieties such as WW1 (synergistic) and WW3 (antagonistic) responded towards S+H treatments. It was intriguing to note that varieties previously singled out as heat and salt tolerant (SW1 and SW2) by their performance at the viability/PCD inflection point (**Table 2**) displayed similar basal tolerance under combined stress exposure as illustrated in **Figure 9**. The inverse situation also held true as individual heat and salt-susceptible varieties (SW4 and WW1) also demonstrated a higher susceptibility to combined stress exposure. **Figure 9** depicts the role of basal tolerance in the correlation between single stress-factor and combined stress exposure; for example, in the S+H dataset, salt-tolerant varieties (SW1 and SW2) had the lowest PCD levels (36-38%), while the salt-susceptible line SW4 had the highest PCD levels (65%). The remaining varieties displayed varying degrees of tolerance: moderately tolerant (WW3 and WW4: 41-42%) and semi-susceptible (SW3, WW1, WW2: 50-54%). A similar scenario was observed in the H+S dataset; thermotolerant SW1 and SW2 varieties had the lowest PCD (24-26%), while the highest PCD levels were seen in SW3, SW4, and WW4 (50-53%). The remaining varieties (WW1, WW2, and WW3) showed varying degrees of tolerance, with PCD ranging from 35 to 43%.

Stress-Tolerant Varieties Responded Slower to Priming Compared to Stress-Susceptible Varieties

Stress-tolerant varieties were predicted to mount a faster counteracting response than stress-susceptible varieties, but this was not evident here. SW1 and SW2 retained similar PCD levels in the 30 min H+S dataset compared to their respective single (H only) stress-factor datasets (**Figure 10**). We only

TABLE 3 | Stress matrix summarizing the effect of (A) cross-stress tolerance and (B) the combined stress in response to heat and salt shock in wheat varieties. Symbols (+) denote a reduction in stress-induced PCD levels, (=) no substantial PCD changes and (-) a net rise in PCD levels from their respective single stress-factor controls.

A) Cross-stress tolerance

Treatment		SW1	SW2	SW3	SW4	WW1	WW2	WW3	WW4
H+S	Phenotype	=	=	=	=	+	=	=	=
	%PCD difference from H-only control	0%	7%	2%	-13%	-19%	2%	8%	9%
	p-value	0.926	0.278	0.785	0.064	0.001*	0.570	0.155	0.051
S+H	Phenotype	=	+	=	+	+	+	=	=
	%PCD difference from S-only control	-14%	-14%	-1%	-18%	-33%	-12%	6%	4%
	p-value	0.086	0.038*	0.894	0.010*	0.001*	0.012*	0.216	0.476

+ priming, ' = ' stress acclimation and '-' predisposition.

(B) Combined stress interactions

Treatment		SW1	SW2	SW3	SW4	WW1	WW2	WW3	WW4
H+S	Phenotype	=	=	-	=	=	=	=	-
	%PCD difference from H-only control	3%	5%	20%	0%	-4%	1%	11%	19%
	p-value	0.389	0.066	0.009*	0.959	0.401	0.8	0.085	0.002*
S+H	Phenotype	=	=	=	=	+	=	-	=
	%PCD difference from S-only control	-9%	-1%	12%	4%	-17%	5%	13%	2%
	p-value	0.253	0.873	0.064	0.553	0.044*	0.496	0.049*	0.818

'+' synergistic, ' = ' neutral and '-' antagonistic interactions.

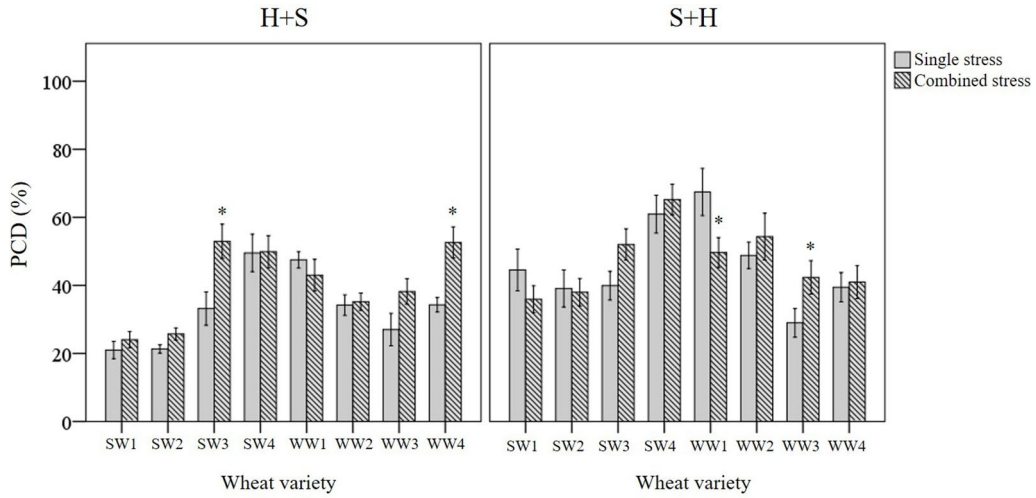

FIGURE 9 | Examining how basal tolerance varies across wheat varieties and different initial stress cues. (*) marks PCD results significantly ($p < 0.05$) different from the single-stress factor control (H-only or S-only), using independent *t*-tests (**Supplementary Table 7**). Combined stress PCD levels reflect the data recorded after simultaneous stress exposure (H+S or S+H) at the 0-min mark. Error bars = standard error of n ≥ 4 replicates.

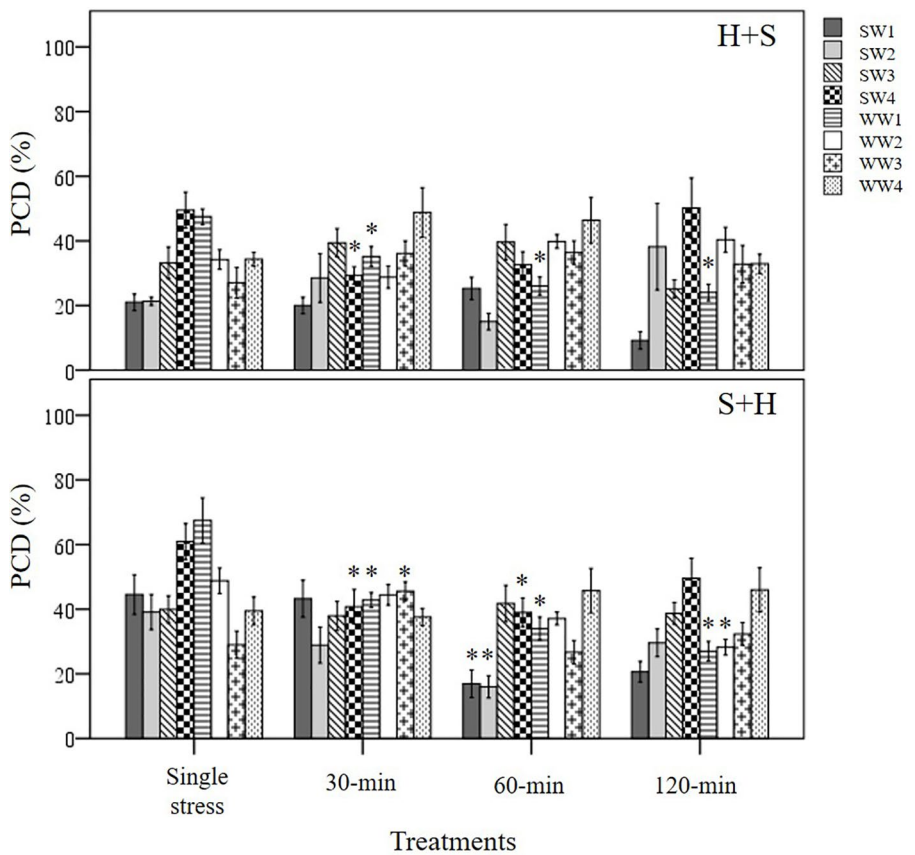

FIGURE 10 | Examining induced tolerance changes across eight individual wheat varieties after different initial stress cues. The initial stress cue (35°C heat or 150 mM NaCl) cue is applied at the 0-min mark, followed by the second stress application at different time-points (30, 60 and 120-min). (H+S) refers to heat stress as the initial cue, followed by salt stress, while (S+H) refers to salt stress as the first cue, followed by heat stress at the relevant time-points. (*) marks PCD results significantly ($p < 0.05$) different from the single-stress factor control (H-only or S-only), using a one-way ANOVA Dunnett post-hoc test (**Supplementary Table 4**). Error bars = standard error of n ≥4 replicates.

observed cross-stress tolerance to salt stress at the later stages as PCD levels only decreased at the 60-min (SW2) and 120-min (SW1) time-points. In contrast, stress-susceptible SW4 reacted faster as PCD levels declined by 21% ($p < 0.05$) at the 30-min H+S dataset compared to its single heat stress-factor dataset. A similar pattern, although to a lesser extent, appeared in heat primed WW1 seedlings whose PCD levels declined by 12% ($p < 0.05$) at the 30-min dataset compared to the H-only control. In view of the slower adaptive response in stress-tolerant varieties, heat priming enabled the stress susceptible SW4 line to maintain similar PCD levels (28%) in line with the tolerant SW2 variety, despite additional salt stress exposure at the 30-min time-point. Considering how the plant stress response is a combination of both basal and induced tolerance, our results suggests that a rapid induced response can partially make up for low basal tolerance, given successful priming and sufficient time-lag between repeated stresses.

We noted a similar temporal pattern when salt stress was the initial cue; significant cross-stress tolerance ($p < 0.05$) to heat stress only took place at the later stages (60-min) for both stress-tolerant SW1 and SW2 varieties. Like the heat priming treatment, salt priming rapidly suppressed PCD levels in varieties with a low basal tolerance (SW4 and WW1); both lines had statistically lower PCD levels ($p < 0.05$) at the 30-min mark compared to their respective S-only controls. Despite their slower adaptive response, SW1 and SW2 varieties still retained the lowest PCD levels out of all the varieties when the cross-stress tolerant effect finally took place. Regardless of the initial stress cue, PCD levels of the 60-min dataset for SW1 and SW2 initially primed with heat (15-24%) and salt (16-17%), were substantively lower than the average PCD values for the remaining varieties across heat (36.8%) and salt stress (37.5%) priming treatments. On balance, our results show that stress-susceptible varieties responded quicker than stress-tolerant varieties as illustrated in **Figure 10**.

Statistical Analysis of the Effect of Using Different Initial Stress Cues on Subsequent PCD Levels

Our results showed that applying salt stress as the initial cue followed by heat stress, exerted a stronger cytotoxic effect on PCD levels (p-value = 0.02) compared to the inverse scenario when heat was the first stress cue, despite maintaining identical stress dosages (**Table 4**). Only a small mean difference of 4.3% was observed between the overall (S+H) and (H+S) datasets. However, this only represents the average values across the eight varieties. When controlling for the individual varieties, we saw larger drifts between the H+S and S+H datasets. For example, statistically higher ($p < 0.05$) PCD levels in S+H datasets, compared to H+S datasets were seen in SW1 (11.4%), SW4 (8.5%) and WW1 (5.9%), (**Supplementary Table 8**). It is also worth noting that the stronger PCD-inducing signal in salt-shocked seedlings (S+H) largely disappeared at later time-points, 60 and 120-min. When controlling for PCD levels across the different stress-treatment time-points, the S+H datasets had higher PCD levels than their H+S counterparts at 0-min (S+H: 47.8%; H+S: 40.8%) and 30-min (S+H: 40.6%, H+S: 34.1%), but were similar at the later stages at 60-min (33-34%) and 120-min (33-35%). Hence, the longer the lag between stress applications, the better the priming effect as PCD levels decreased concurrently. One-way ANOVA analysis confirmed this as both the later datasets (60 and 120-min) were significantly lower ($p < 0.05$) than the single salt stress-factor dataset (**Figure 7**). Our results show that given sufficient time, the salt priming effect resulted in similar PCD-suppression rates with seedlings first subjected to heat shock. **Figure 7** illustrates the overall lagging PCD-suppressing effect of the initial salt shock cue, while **Figure 6** shows the how this general behaviour differs from variety to variety.

DISCUSSION

In this paper, we present three case studies to illustrate how stress-induced PCD levels can be used to investigate cereal stress tolerance. In the first instance, we directly scored *in vivo* PCD levels in heat-stressed barley and wheat seedlings. We observed mixed thermotolerance across the seasonal wheat varieties but noted a clear distinction between heat resistant spring and heat susceptible winter barley varieties. Without further investigations, it is difficult to determine why these differences exist, as thermotolerance is a spatially and temporally regulated polygenic trait that differs across development stages and plant genotype (Rejeb et al., 2014). However, evidence suggest that heat shock protein (HSP) diversity can be a marker for thermotolerance as Marmiroli et al. (1994) found that low-MW HSP expression patterns differ greatly across five heat-stressed barley varieties of varying thermotolerance. Plant HSPs are molecular chaperones that protect proteins under denaturing conditions and are divided into five families, Hsp100, Hsp90, Hsp70, Hsp60 and small Hsps (sHsp), that occasionally have overlapping functions (Wang et al., 2004). For example, Hsp70 and Hsp90 are engaged in the transcriptional activation of other HSPs, chaperone and stress-response proteins *via* heat-shock factors (HSFs), while sHsp and Hsp70 maintain protein conformation to prevent aggregation (Wang et al., 2004). Genetic HSP diversity might account for the intraspecies variances we

TABLE 4 | Independent samples t-test examining the effects of applying different stress cues as the initial cue on PCD levels. Inputted data consisted of PCD levels scored across 0, 30, 60 and 120-min.

Initial Stress cue	Group Statistics			*t*-test for Equality of Means		
	N	Mean	Std. Error Mean	Sig. (2-tailed)	Mean Difference	Std. Error Difference
Heat and Salt (H+S)	395	35.5	0.964	0.002	-4.31	1.35
Salt and Heat (S+H)	376	39.9	0.947			

noted between the seasonal barley varieties as Marmiroli et al. (1998) found a high degree of polymorphisms at the *Hvhsp17* gene locus that encoded for a low-MW HSP across winter and spring barley varieties. Restriction fragment length polymorphism analysis of two HSP genes (*TaHSP16.9* and *Hvhsp17*) in 27 barley varieties revealed that spring and winter barley varieties could be successfully partitioned into two dendrogram clusters, showing that polymorphisms in the HSP genes accurately predicted winter and spring barley varieties (Marmiroli et al., 1998).

Apart from predicting the divergent thermotolerance between spring and winter barley varieties, HSP molecular diversity might also account for the mixed tolerance of the seasonal wheat varieties we noticed here. Barley plants are diploid organisms, but wheat plants can either have diploid, tetraploid or hexaploid genomes; polyploid cereals have a higher HSP diversity than diploid cereals because of the additive effect of the subgenomes (Maestri et al., 2002). Perhaps this accounts for why mixed tolerance was seen across spring and winter wheat varieties, but not in barley as polyploidy affects HSP diversity and other stress-response genes, culminating in significantly divergent stress phenotypes from their original diploid parents (Arbona et al., 2017).

In the next case study, we examined how stress-induced PCD levels changed across eight salt-stressed wheat varieties. Like earlier heat stress experiments, we noted mixed salt tolerance, which was notably apparent when seedlings were subjected to salt stress at the viable/PCD inflection point. We confirmed the association between heat and salt stress-induced PCD levels with bivariate analysis, showing a statistically significant correlation of 0.333 ($p < 0.01$) between both variables. At this stress dosage, SW1 and SW2 were identified as salt tolerant varieties, SW3, WW3 and WW4 as moderately salt-tolerant, and SW4, WW1 and WW2 as salt susceptible lines. By comparing stress-induced PCD levels at the viable/PCD inflection point, we found striking parallels between heat and salt stress experiments as wheat varieties displayed similar tolerance to heat and salt shock - two seemingly distinct stresses. For example, thermotolerant varieties (SW1 and SW2) retained their robustness to low-to-medium salt stress, while heat susceptible SW4 and WW1 lines were similarly vulnerable to salt stress.

Stress exposure elicits primary and secondary damage (Munns, 2010) and we hypothesise that similar secondary-induced damages was the underlying reason behind the similar tolerance exhibited against heat and salt stress. Plants have evolved stress-specific pathways to deal with initial primary damage, while general 'housekeeping pathways' minimise the overlapping secondary damage effects (Munns, 2010). Examples of primary responses include HSP accumulation to counteract the elevated risk of protein misfolding (Wang et al., 2004) while salt-stressed plants upregulate ion transporters for Na^+ exclusion or sequestration (Wang et al., 2003; Kosová et al., 2015; Kosová et al., 2018). Despite these divergent responses, plants under heat or salt stress will manifest similar secondary damage symptoms in the form of elevated ROS, inhibition of key metabolic enzymes, and macromolecule denaturation (proteins, cell membranes and cytoskeleton) (Rivero et al., 2014). Hence, plants adopt similar downstream protective mechanisms against heat and salt stress because of overlapping secondary damage; examples of shared responses include cell volume regulation (osmolyte and hydrophilic protein accumulation) and upregulation of ROS and methylglyoxal-detoxifying pathways (Hoque et al., 2012; Rivero et al., 2014; Hossain et al., 2016). It is also interesting to note that sHsps are also upregulated during heat, salt and drought stress (Wang et al., 2004; Hossain et al., 2016); sHsps protects the mitochondrial Complex I electron transport chain from oxidative damage in salt-stressed *Z. mays* plants (Hamilton and Heckathorn, 2001), and inhibits PCD by regulating the intracellular redox state in mammalian cells (Arrigo, 1998). Collectively, the evidence suggests that similar tolerance to heat and salt stress by wheat varieties is likely due to higher expression of these conserved response pathways. Our results highlight the flexibility of using stress-induced PCD levels as a general maker for stress tolerance. Like heat tolerance, it is difficult to pinpoint salt tolerance to a single gene as both are polygenic traits controlled by multiple genes and signalling pathways (Zuther et al., 2007; Rejeb et al., 2014). Quantification of PCD levels avoid these problems as it integrates all these interacting networks to yield a useful single end-point measurement of the stress treatment effects. By identifying varieties with stress tolerant traits of interest, further testing using transcriptomics, proteomics and metabolomics can be performed to determine why different lines possess varying degrees of tolerance.

In the final case study, we used stress-induced PCD levels to assess basal, induced and cross-stress tolerance in heat and salt-stressed wheat seedlings. Basal tolerance refers to the innate plant capacity to withstand stress encounters without relying on priming or previous stress exposures, while induced tolerance reflects the adaptive capacity to mount a counteracting response to the initial stress stimuli (Arbona et al., 2017). Unlike genetically pre-determined basal tolerance, induced tolerance can be manipulated by non-lethal stress exposure or priming with chemical modulators for improved stress tolerance (Arbona et al., 2017). Non-lethal stress exposure can lead to improved resistance against additional stress factors, even that of different origins, (i.e. cross-stress tolerance), as the stress imprint can lead to a faster response to recurrent stress-factors compared to plants without a stress memory (Walter et al., 2013). But if the initial stress-factor undermines the plant defence or irreversibly disrupts cellular homeostasis, repeated stress exposure leads to an even greater harm (Walter et al., 2013). Therefore, depending on the adaptability of the induced tolerance response, the second stress application can either have a net positive, negative, or neutral effect on the plant stress response (**Supplementary Figure 1B**).

As illustrated in **Figure 1**, we assessed basal tolerance by subjecting seedlings to single and combined stress exposures, while induced and cross-stress tolerance were examined by applying recurrent stress cues of different origins. We subjected seedlings to different stress combinations because while individual stress exposures have been intensely researched over the years, plants continually experience unique stress combinations under field conditions (Mittler, 2006). For example, farmlands in the semi-arid regions of the world tend to face a combination of salt, heat and drought stress (Rivero et al., 2014). Evidence indicates that

plants under combined stress display a unique 'stress phenotype' that has little overlap with the phenotype exhibited under individual stresses. Hence, there are growing calls to study how plants respond under conditions that mimic field conditions, as the novel stress response under two different combined stresses cannot be merely extrapolated from studies where stresses were applied individually (Rasmussen et al., 2013; Rivero et al., 2014). This was demonstrated in a landmark study by Rasmussen et al. (2013) who discovered that 61% of the transcripts from double-combined stress exposure could not be anticipated from their individual stress treatments alone.

The survival of plants against stress depends on basal and adaptive tolerance and we noted a few interesting observations when screening seedlings for these attributes. First, varieties (SW1 and SW2) previously singled out as tolerant to single heat and salt stress exposure also exhibited similar resistance to combined and multiple individual stresses. In the case of SW1 and SW2, basal tolerance likely played a bigger initial role as both varieties had the lowest stress-induced PCD levels upon combined stress exposure, which did not significantly change from their respective single (heat or salt) stress-factor control. Thus, the single and combined stress-factor datasets strongly suggest that SW1 and SW2 have inherently high basal tolerance compared to the other varieties.

Cross-stress tolerance is the phenomenon where the initial stress exposure makes plants more resistant to other stress types, and SW1 and SW2 had an unexpectedly slower cross-tolerance response than their stress-susceptible counterparts. Both lines were initially hypothesised to have a rapidly induced tolerance response as Kawasaki et al. (2001) previously showed that salt-tolerant rice (Pokkali) responded faster to salt stress than the salt-sensitive (IR29) line. Transcription upregulation in Pokkali started a mere 15 min after the shock, while IR29 had a four-fold delayed response, suggesting that its slow ability to process stress cues was the underlying reason for its ineffective salt stress response (Kawasaki et al., 2001). However, we did not observe any significant changes in overall PCD levels in SW1 and SW2 when the secondary stress cue was applied at 30-min. Instead, the beneficial PCD-suppressing effects were only noted when the stress cue was applied at the later stages. This stands in contrast to stress-susceptible varieties with low basal tolerance, like SW4 and WW1, that adapted faster to recurrent stresses. Both lines had substantially lower PCD levels, even when the second stress cue was applied at the 30-min time-point, showing that the first non-lethal stress successfully primed SW4 and WW1 against additive damage from recurrent stress exposure. Collectively, our results show that stress-susceptible varieties responded faster than stress-tolerant varieties and evidence suggest that signalling components play a prominent role in this process as they control the reprogramming of cellular molecular machinery (Rejeb et al., 2014). For example, the transcriptional regulator MBF1c modulates basal thermotolerance but not induced tolerance (Ahammed et al., 2016), ABA-deficient *Arabidopsis* mutants had substantial losses of basal and acquired thermotolerance (Larkindale et al., 2005), while salicylic acid-dependent signalling increases basal thermotolerance but not induced tolerance (Clarke et al., 2004). Other studies have also shown that the signalling molecules ROS and methylglyoxal successfully imprinted cross-stress tolerance against drought and salt stress in *Brassica campestris* L. (Hossain et al., 2013; Hossain et al., 2016), while mechanical wounding increased salt tolerance in tomato plants because of cross-talk between the signalling pathways involving calmodulin-like activities, the signalling peptide systemin, and jasmonic acid biosynthesis (Capiati et al., 2006). Further work will be needed to deduce the role of these signalling molecules in the identified varieties of interest, but our results show that stress-induced PCD levels can be a useful marker of ecological stress memory. The identified stress-susceptible varieties had faster induced tolerance; despite the short time-lag between the two stress applications, both lines had not returned to their earlier homeostatic state and mounted a faster counteracting response and were consequently more tolerant against repeated stress - even that of a different origin (Walter et al., 2013).

It is also worth noting that the favoured modes of stress-response employed by stress-tolerant SW1 and SW2 (high basal tolerance, but slow induced response) and stress-susceptible SW4 and WW1 (low basal tolerance, but fast induced response) is remarkably similar to the strategies employed by two species of poplar tree: salt tolerant *Populus euphratica* and salt susceptible *Populus* × *canescens* (Janz et al., 2010). The elevated basal tolerance of *P. euphratica* was reflected in the high constitutive expression of salt sensitive genes but had comparatively low transcriptional responsiveness compared to *P.* x *canescens*. Salt-tolerant *P. euphratica* was slower to react to external changes in salt levels and did not rely on a global defence strategy unlike its salt-susceptible counterpart. Instead, *P. euphratica* were already pre-adapted to osmotic stress by the constitutive activation of cell protective mechanisms involved in ROS detoxification, osmolyte biosynthesis, Na^+ and K^+ ion carriers, and metabolite transporters. However, permanent activation of these pathways imposed a high metabolic burden and Janz et al. (2010) suggested this stress-anticipatory preparedness comes at the expense of diminished flexibility and a slower transcriptome response against fluctuating salt levels. Perhaps a comparable scenario is at play for SW1 and SW2 given that despite their slower induced tolerance, both varieties had the lowest overall PCD levels because of their inherently high basal tolerance.

Last, we observed an interesting phenomenon when different initial stress cues were used during combined and multiple individual stress experiments. Plants display a unique stress phenotype under combined stress that has little overlap with individual stress treatments (Mittler, 2006; Rasmussen et al., 2013; Rivero et al., 2014). Sometimes, combined stress can result in better plant robustness, e.g. mechanical injury increased salt tolerance of tomato plants (Capiati et al., 2006) or elevated vulnerability to the second stress, e.g. heavy metal exposure aggravated the effects of drought stress (Barceló and Poschenrieder, 1990). Based on the stress phenotype categories devised by Mittler (2006), we observed the dominance of salt stress over heat stress under combined stress exposure. Even though identical stress doses were maintained, salt stress

application followed by subsequent heat stress, exerted a stronger cytotoxic effect on PCD levels compared to the reverse scenario. Our results align with past *Arabidopsis* transcriptomic data showing that plants under combined stress prioritizes the salt-stress response over heat; Rasmussen et al. (2013) found that heat and salt-stressed plants had the highest level of prioritized transcripts (12.1%) out of six stress combinations. The greater response of salt transcripts compared to heat transcripts showed that the salt response dominated the heat stress response (Rasmussen et al., 2013). Taken together, our results with stress-induced PCD levels also accurately depicted the dominance of salt stress over heat stress, as shown in past transcriptomic data (Rasmussen et al., 2013). Nevertheless, we wish to reiterate that this finding simply reflects the overall trends as the individual stress response can vary between the varieties, as shown in the stress matrix (**Table 3**). Most varieties responded neutrally to combined heat and salt stress, although there were a few outliers for antagonistic (SW3, WW3, and WW4) and synergistic (WW1) interactions. Our results concur with past observations that plants display a unique stress phenotype when subjected to overlapping stress that is not necessarily additive, and that combined stress should be regarded as a new state of abiotic stress that requires a novel adaptive stress response (Mittler, 2006; Rasmussen et al., 2013; Rivero et al., 2014). Finally, we would like to extend an important caveat to the original hypothesis, as our results show that stress phenotypes can vary even within different varieties of the same species, and that caution should be exercised when extrapolating findings across different research groups. This intra-species diversity can be advantageous as the RHA enables agronomists to identify stress-tolerant varieties early in the screening process, without relying on exhaustive large-scale field trials or costly analytical chemistry and molecular biology techniques.

CONCLUSION

This paper demonstrates the use of root hairs as a model system for studying plant stress tolerance as direct scoring of stress-induced PCD levels integrates multiple stress-response pathways for a simple outcome, i.e. do plant cells stay alive or undergo PCD. A graphical summary of the findings obtained by the study is shown in **Supplementary Figure 3**. The RHA was originally developed in *Arabidopsis* and, in this study, the method was successfully applied on cereals to evaluate the heat and/or salt tolerance of barley and wheat varieties. By examining heat stress-induced PCD levels, a clear distinction between thermotolerant spring and thermo-susceptible winter barley varieties was determined. In addition, eight wheat varieties were examined for their tolerance to heat and salt stress; a comparison of their individual viability/PCD inflection points identified stress tolerant (SW1 and SW2) and stress susceptible (SW4 and WW1) varieties. Following this finding, stress-induced PCD levels were used to assess the basal, induced and cross-stress tolerance of the eight wheat varieties to heat and salt stress using single, multiple individual and combined stress exposures, respectively. Interesting parallels could be drawn from the earlier single-stress experiments as the same varieties demonstrated similar cross-stress tolerance (SW1 and SW2) and susceptibility (SW4 and WW1) to heat and salt stress.

Our results also show that stress-tolerant varieties (SW1 and SW2) had high basal tolerance, but a slower induced response compared to stress-susceptible varieties (SW4 and WW1). In addition, the dominant, more damaging effect of salt over heat stress was demonstrated; application of salt stress as the first stress cue induced a stronger cytotoxic effect than heat stress even though identical stress doses were maintained. The strength of the RHA lies in its simplicity and scalability as it can be easily adapted across various plant species and stress protocols in a simple 'plug-and-play' fashion. Last, we show that stress-induced PCD levels can be used for identifying cereal varieties with notable stress-tolerance traits for downstream work and for investigaing unique stress-phenotypes exhibited under combined stress, all in a fast and economical manner.

DATA AVAILABILITY STATEMENT

All datasets generated for this study are included in the article/ **Supplementary Material**.

AUTHOR CONTRIBUTIONS

AC designed and performed the experiments. LF and CD contributed to the discussion of the results. All authors reviewed and approved the final manuscript.

FUNDING

This work was supported by PhD scholarship awarded to AC by Waterford Institute of Technology. Cost of publishing was supported by the Waterford Institute of Technology, School of Science and Computing, Research Support Scheme.

ACKNOWLEDGMENTS

This work was supported by postgraduate scholarship awarded to AC by Waterford Institute of Technology, Ireland. Seeds were provided by Seedtech® and KWS UK®.

SUPPLEMENTARY MATERIAL

The Supplementary Material for this article can be found online at: https://www.frontiersin.org/articles/10.3389/fpls.2019.01539/full#supplementary-material

REFERENCES

Ahammed, G. J., Li, X., Zhou, J., Zhou, Y.-H., and Yu, J.-Q. (2016). "Role of hormones in plant adaptation to heat stress," in *Plant Hormones under Challenging Environmental Factors*. Eds. Ahammed, G. J., and Yu, J.-Q. (Dordrecht: Springer Netherlands), 1–21. doi: 10.1007/978-94-017-7758-2_1

Ahmad, P., Abdel Latef, A. A. H., Rasool, S., Akram, N. A., Ashraf, M., and Gucel, S. (2016). Role of proteomics in crop stress tolerance. *Front. Plant Sci.* 7, 1336. doi: 10.3389/fpls.2016.01336

Arbona, V., Manzi, M., Zandalinas, S. I., Vives-Peris, V., Pérez-Clemente, R. M., and Gómez-Cadenas, A. (2017). "Physiological, metabolic, and molecular responses of plants to abiotic stress," in *Stress Signaling in Plants: Genomics and Proteomics Perspective, Volume 2*. Eds. Sarwat, M., Ahmad, A., Abdin, M. Z., and Ibrahim, M. M. (Cham: Springer International Publishing), 1–35. doi: 10.1007/978-3-319-42183-4_1

Arrigo, A. P. (1998). Small stress proteins: chaperones that act as regulators of intracellular redox state and programmed cell death. *Biol. Chem.* 379, 19–26. doi: 10.1007/978-3-642-56348-5_9

Barceló, J., and Poschenrieder, C. (1990). Plant water relations as affected by heavy metal stress: a review. *J. Plant Nutr.* 13, 1–37. doi: 10.1080/01904169009364057

Capiati, D. A., País, S. M., and Téllez-Iñón, M. T. (2006). Wounding increases salt tolerance in tomato plants: evidence on the participation of calmodulin-like activities in cross-tolerance signalling. *J. Exp. Bot.* 57, 2391–2400. doi: 10.1093/jxb/erj212

Cattivelli, L., Baldi, P., Crosatti, C., Di Fonzo, N., Faccioli, P., Grossi, M., et al. (2002). Chromosome regions and stress-related sequences involved in resistance to abiotic stress in *Triticeae*. *Plant Mol. Biol.* 48, 649–665. doi: 10.1023/A:1014824404623

Chen, J., Bellin, D., and Vandelle, E. (2018). "Measurement of cyclic GMP during plant hypersensitive disease resistance response," in *Plant Programmed Cell Death*. Eds. De Gara, L., and Locato, V. (New York, NY: Springer New York), 143–151. doi: 10.1007/978-1-4939-7668-3_13

Chinnusamy, V., Zhu, J.-K., and Sunkar, R. (2010). "Gene regulation during cold stress acclimation in plants," in *Plant Stress Tolerance*. Ed. Sunkar, R. (Totowa, NJ: Humana Press), 39–55. doi: 10.1007/978-1-60761-702-0_3

Cimini, S., Ronci, M. B., Barizza, E., de Pinto, M. C., Locato, V., Lo Schiavo, F., et al. (2018). "Plant cell cultures as model systems to study programmed cell death," in *Plant Programmed Cell Death*. Eds. De Gara, L., and Locato, V. (New York, NY: Springer New York), 173–186. doi: 10.1007/978-1-4939-7668-3_16

Clarke, S. M., Mur, L. A. J., Wood, J. E., and Scott, I. M. (2004). Salicylic acid dependent signaling promotes basal thermotolerance but is not essential for acquired thermotolerance in *Arabidopsis thaliana*. *Plant J.* 38, 432–447. doi: 10.1111/j.1365-313X.2004.02054.x

Cockram, J., Chiapparino, E., Taylor, S. A., Stamati, K., Donini, P., Laurie, D. A., et al. (2007). Haplotype analysis of vernalization loci in European barley germplasm reveals novel *VRN-H1* alleles and a predominant winter *VRN-H1/VRN-H2* multi-locus haplotype. *Theor. Appl. Genet.* 115, 993–1001. doi: 10.1007/s00122-007-0626-x

Coleman-Derr, D., and Tringe, S. G. (2014). Building the crops of tomorrow: Advantages of symbiont-based approaches to improving abiotic stress tolerance. *Front. In Microbiol.* 5, 1–6. doi: 10.3389/fmicb.2014.00283

Distelfeld, A., Li, C., and Dubcovsky, J. (2009). Regulation of flowering in temperate cereals. *Curr. Opin. In Plant Biol.* 12, 178–184. doi: 10.1016/j.pbi.2008.12.010

Doccula, F. G., Luoni, L., Behera, S., Bonza, M. C., and Costa, A. (2018). "*In vivo* analysis of calcium levels and glutathione redox status in *Arabidopsis* epidermal leaf cells infected with the hypersensitive response-inducing bacteria *Pseudomonas syringae* pv. tomato *Avrb* (*PstAvrB*)," in *Plant Programmed Cell Death*. Eds. De Gara, L., and Locato, V. (New York, NY: Springer New York), 125–141. doi: 10.1007/978-1-4939-7668-3_12

Elavarthi, S., and Martin, B. (2010). "Spectrophotometric assays for antioxidant enzymes in plants," in *Plant Stress Tolerance*. Ed. Sunkar, R. (Totowa, NJ: Humana Press), 273–280. doi: 10.1007/978-1-60761-702-0_16

Hamilton, E. W., and Heckathorn, S. A. (2001). Mitochondrial adaptations to NaCl. Complex I is protected by anti-oxidants and small heat shock proteins, whereas Complex II is protected by proline and betaine. *Plant Physiol.* 126, 1266–1274. doi: 10.1104/pp.126.3.1266

Hatsugai, N., and Hara-Nishimura, I. (2018). "Measurement of the caspase-1-like activity of vacuolar processing enzyme in plants," in *Plant Programmed Cell Death*. Eds. De Gara, L., and Locato, V. (New York, NY: Springer New York), 163–171. doi: 10.1007/978-1-4939-7668-3_15

Hoang, T. M. L., Williams, B., and Mundree, S. G. (2016). "Manipulation of programmed cell death pathways enhances osmotic stress tolerance in plants: physiological and molecular insights," in *Drought Stress Tolerance in Plants*, vol. 1. Eds. Hossain, M. A., Wani, S. H., Bhattacharjee, S., Burritt, D. J., and Tran, L.-S. P. (Cham: Springer International Publishing), 439–464. doi: 10.1007/978-3-319-28899-4_19

Hogg, B. V., Kacprzyk, J., Molony, E. M., Reilly, C. O., Gallagher, T. F., Gallois, P., et al. (2011). An *in vivo* root hair assay for determining rates of apoptotic-like programmed cell death in plants. *Plant Methods* 7, 45. doi: 10.1186/1746-4811-7-45

Hoque, M. A., Uraji, M., Torii, A., Banu, M., Akhter, N., Mori, I. C., et al. (2012). Methylglyoxal inhibition of cytosolic ascorbate peroxidase from *Nicotiana tabacum*. *J. Biochem. Mol. Toxicol.* 26, 315–321. doi: 10.1002/jbt.21423

Hossain, M. A., Golam Mostofa, M., and Fujita, M. (2013). Heat-shock positively modulates oxidative protection of salt and drought-stressed mustard (*Brassica campestris* L.) seedlings. *J. Plant Sci. Mol. Breed.* 2, 2. doi: 10.7243/2050-2389-2-2

Hossain, M. A., Burritt, D. J., and Fujita, M. (2016). "Cross-stress tolerance in plants: Molecular mechanisms and possible involvement of reactive oxygen species and methylglyoxal detoxification systems," in *Abiotic Stress Response in Plants* (John Wiley & Sons, Ltd) (Weinheim, Germany: Wiley), 327–380. doi: 10.1002/9783527694570.ch16

Jambunathan, N. (2010). "Determination and detection of reactive oxygen species (ROS), lipid peroxidation, and electrolyte leakage in plants," in *Plant Stress Tolerance Methods in Molecular Biology*. Ed. Sunkar, R. (Totowa, NJ: Humana Press), 291–297. doi: 10.1007/978-1-60761-702-0_18

Janz, D., Behnke, K., Schnitzler, J.-P., Kanawati, B., Schmitt-Kopplin, P., and Polle, A. (2010). Pathway analysis of the transcriptome and metabolome of salt sensitive and tolerant poplar species reveals evolutionary adaption of stress tolerance mechanisms. *BMC Plant Biol.* 10, 150. doi: 10.1186/1471-2229-10-150

Kacprzyk, J., Daly, C. T., and McCabe, P. F. (2011). "The botanical dance of death: Programmed cell death in plants," in *Advances in Botanical Research* (San Diego, US: Elsevier), 169–261. doi: 10.1016/B978-0-12-385851-1.00004-4

Kacprzyk, J., Devine, A., and McCabe, P. F. (2014). The root hair assay facilitates the use of genetic and pharmacological tools in order to dissect multiple signalling pathways that lead to programmed cell death. *PloS One* 9, e94898. doi: 10.1371/journal.pone.0094898

Kacprzyk, J., Brogan, N. P., Daly, C. T., Doyle, S. M., Diamond, M., Molony, E. M., et al. (2017). The retraction of the protoplast during PCD is an active, and interruptible, calcium-flux driven process. *Plant Sci.* 260, 50–59. doi: 10.1016/j.plantsci.2017.04.001

Kawasaki, S., Borchert, C., Deyholos, M., Wang, H., Brazille, S., Kawai, K., et al. (2001). Gene expression profiles during the initial phase of salt stress in rice. *Plant Cell* 13, 889. doi: 10.1105/tpc.13.4.889

Kim, Y., Wang, M., Bai, Y., Zeng, Z., Guo, F., Han, N., et al. (2014). Bcl-2 suppresses activation of VPEs by inhibiting cytosolic Ca^{2+} level with elevated K^+ efflux in NaCl-induced PCD in rice. *Plant Physiol. Biochem.* 80, 168–175. doi: 10.1016/j.plaphy.2014.04.002

Kosová, K., Vítámvás, P., Urban, M., Klíma, M., Roy, A., and Prášil, I. (2015). Biological networks underlying abiotic stress tolerance in temperate crops—A proteomic perspective. *Int. J. Mol. Sci.* 16, 20913–20942. doi: 10.3390/ijms160920913

Kosová, K., Vítámvás, P., Urban, M. O., Prášil, I. T., and Renaut, J. (2018). Plant abiotic stress proteomics: The major factors determining alterations in cellular proteome. *Front. In Plant Sci.* 9, 122. doi: 10.3389/fpls.2018.00122

Larkindale, J., Hall, J. D., Knight, M. R., and Vierling, E. (2005). Heat stress phenotypes of *Arabidopsis* mutants implicate multiple signaling pathways in the acquisition of thermotolerance. *Plant Physiol.* 138, 882–897. doi: 10.1104/pp.105.062257

Lockshin, R. A., and Zakeri, Z. (2004). Apoptosis, autophagy, and more. *Int. J. Biochem. Cell Biol.* 36, 2405–2419. doi: 10.1016/j.biocel.2004.04.011

Maestri, E., Klueva, N., Perrotta, C., Gulli, M., Nguyen, H. T., and Marmiroli, N. (2002). Molecular genetics of heat tolerance and heat shock proteins in cereals. *Plant Mol. Biol.* 48, 667–681. doi: 10.1023/A

Mano, J., and Biswas, M. S. (2018). "Analysis of reactive carbonyl species generated under oxidative stress," in *Plant Programmed Cell Death*. Eds. De Gara, L., and Locato, V. (New York, NY: Springer New York), 117–124. doi: 10.1007/978-1-4939-7668-3_11

Marmiroli, N., Maestri, E., Terzi, V., Gulli, M., Pavesi, A., Raho, G., et al. (1994). "Genetic and molecular evidences of the regulation of gene expression during heat shock in plants," in *Biochemical and Cellular Mechanisms of Stress Tolerance in Plants NATO ASI Series*. Ed. Cherry, J. H. (Berlin, Germany: Springer), 157–190.

Marmiroli, N., Malcevschi, A., and Maestri, E. (1998). "Application of stress responsive genes RFLP analysis to the evaluation of genetic diversity in plants," in *Molecular Tools for Screening Biodiversity: Plants and Animals*. Eds. Karp, A., Isaac, P. G., and Ingram, D. S. (Dordrecht: Springer Netherlands), 464–470. doi: 10.1007/978-94-009-0019-6_82

Meena, K. K., Sorty, A. M., Bitla, U. M., Choudhary, K., Gupta, P., Pareek, A., et al. (2017). Abiotic stress responses and microbe-mediated mitigation in plants: the omics strategies. *Front. In Plant Sci.* 8, 172. doi: 10.3389/fpls.2017.00172

Mittler, R., and Blumwald, E. (2010). Genetic engineering for modern agriculture: challenges and perspectives. *Annu. Rev. Plant Biol.* 61, 443–462. doi: 10.1146/annurev-arplant-042809-112116

Mittler, R. (2006). Abiotic stress, the field environment and stress combination. *Trends In Plant Sci.* 11, 15–19. doi: 10.1016/j.tplants.2005.11.002

Munns, R., Wallace, P. A., Teakle, N. L., and Colmer, T. D. (2010). "Measuring soluble ion concentrations (Na^+, K^+, Cl^-) in salt-treated plants," in *Plant Stress Tolerance*. Ed. Sunkar, R. (Totowa, NJ: Humana Press), 371–382. doi: 10.1007/978-1-60761-702-0_23

Munns, R. (2010). Approaches to identifying genes for salinity tolerance and the importance of timescale. *Methods Mol. Biol.* 639, 25–38. doi: 10.1007/978-1-60761-702-0_2

Obata, T., and Fernie, A. R. (2012). The use of metabolomics to dissect plant responses to abiotic stresses. *Cell. Mol. Life Sci.* 69, 3225–3243. doi: 10.1007/s00018-012-1091-5

Pandey, P., Irulappan, V., Bagavathiannan, M. V., and Senthil-Kumar, M. (2017). Impact of combined abiotic and biotic stresses on plant growth and avenues for crop improvement by exploiting physio-morphological traits. *Front. Plant Sci.* 8, 537. doi: 10.3389/fpls.2017.00537

Petrov, V., Hille, J., Mueller-Roeber, B., and Gechev, T. S. (2015). ROS-mediated abiotic stress-induced programmed cell death in plants. *Front. Plant Sci.* 6, 1–16. doi: 10.3389/fpls.2015.00069

Rasmussen, S., Barah, P., Suarez-Rodriguez, M. C., Bressendorff, S., Friis, P., Costantino, P., et al. (2013). Transcriptome responses to combinations of stresses in *Arabidopsis*. *Plant Physiol.* 161, 1783–1794. doi: 10.1104/pp.112.210773

Reape, T. J., Brogan, N. P., and McCabe, P. F. (2015). "Mitochondrion and chloroplast regulation of plant programmed cell death," in *Plant Programmed Cell Death*. Eds. Gunawardena, A. N., and McCabe, P. F. (Cham: Springer International Publishing), 33–53. doi: 10.1007/978-3-319-21033-9_2

Rejeb, I., Pastor, V., and Mauch-Mani, B. (2014). Plant responses to simultaneous biotic and abiotic stress: molecular mechanisms. *Plants* 3, 458–475. doi: 10.3390/plants3040458

Rivero, R. M., Mestre, T. C., Mittler, R., Rubio, F., Garcia-Sanchez, F., and Martinez, V. (2014). The combined effect of salinity and heat reveals a specific physiological, biochemical and molecular response in tomato plants: Stress combination in tomato plants. *Plant Cell Environ.* 37, 1059–1073. doi: 10.1111/pce.12199

Singh, B., Mishra, S., Bohra, A., Joshi, R., and Siddique, K. H. M. (2018). "Crop phenomics for abiotic stress tolerance in crop plants," in *Biochemical, Physiological and Molecular Avenues for Combating Abiotic Stress Tolerance in Plants*. Ed. Wani, S. H. (San Diego, US: Elsevier), 277–296. doi: 10.1016/B978-0-12-813066-7.00015-2

Tausz, M., Šircelj, H., and Grill, D. (2004). The glutathione system as a stress marker in plant ecophysiology: Is a stress-response concept valid? *J. Exp. Bot.* 55, 1955–1962. doi: 10.1093/jxb/erh194

Terrón-Camero, L. C., Molina-Moya, E., Sanz-Fernández, M., Sandalio, L. M., and Romero-Puertas, M. C. (2018). "Detection of reactive oxygen and nitrogen species (ROS/RNS) during hypersensitive cell death," in *Plant Programmed Cell Death*. Eds. De Gara, L., and Locato, V. (New York, NY: Springer New York), 97–105. doi: 10.1007/978-1-4939-7668-3_9

United Nations, Department of Economic and Social Affairs, Population Division (2017). World Population Prospects: The 2017 Revision, Key Findings and Advance Tables. Working Paper No. ESA/P/WP/248. Accessed 19th November 2019 at: https://population.un.org/wpp/Publications/Files/WPP2017_KeyFindings.pdf

Verslues, P. E. (2010). "Quantification of water stress-induced osmotic adjustment and proline accumulation for *Arabidopsis thaliana* molecular genetic studies," in *Plant Stress Tolerance Methods in Molecular Biology*. Ed. Sunkar, R. (Totowa, NJ: Humana Press), 301–315. doi: 10.1007/978-1-60761-702-0_19

Walter, J., Jentsch, A., Beierkuhnlein, C., and Kreyling, J. (2013). Ecological stress memory and cross stress tolerance in plants in the face of climate extremes. *Environ. Exp. Bot.* 94, 3–8. doi: 10.1016/j.envexpbot.2012.02.009

Wang, W., Vinocur, B., and Altman, A. (2003). Plant responses to drought, salinity and extreme temperatures: towards genetic engineering for stress tolerance. *Planta* 218, 1–14. doi: 10.1007/s00425-003-1105-5

Wang, W., Vinocur, B., Shoseyov, O., and Altman, A. (2004). Role of plant heat-shock proteins and molecular chaperones in the abiotic stress response. *Trends In Plant Sci.* 9, 244–252. doi: 10.1016/j.tplants.2004.03.006

Wituszynska, W., and Karpinski, S. (2013). "Programmed cell death as a response to high light, UV and drought stress in plants," in *Abiotic Stress - Plant Responses and Applications in Agriculture*. Ed. Vahdati, K. (London, UK: InTech). doi: 10.5772/53127

Wu, Q., and Jackson, D. (2018). "Detection of MAPK3/6 phosphorylation during hypersensitive response (HR)-associated programmed cell death in plants," in *Plant Programmed Cell Death*. Eds. De Gara, L., and Locato, V. (New York, NY: Springer New York), 153–161). doi: 10.1007/978-1-4939-7668-3_14

Xiao, D., He, H., Huang, W., Oo, T. L., Wang, A., and He, L.-F. (2018). Analysis of mitochondrial markers of programmed cell death. *Methods Mol. Biol.* 1743, 65–71. doi: 10.1007/978-1-4939-7668-3_6

Zuther, E., Koehl, K., and Kopka, J. (2007). "Comparative metabolome analysis of the salt response in breeding cultivars of rice," in *Advances in Molecular Breeding Toward Drought and Salt Tolerant Crops*. Eds. Jenks, M. A., Hasegawa, P. M., and Jain, S. M. (Dordrecht: Springer Netherlands), 285–315. doi: 10.1007/978-1-4020-5578-2_12

Conflict of Interest: The authors declare that the research was conducted in the absence of any commercial or financial relationships that could be construed as a potential conflict of interest.

frontiers in Plant Science

ORIGINAL RESEARCH
published: 03 February 2020
doi: 10.3389/fpls.2019.01805

Immunoprofiling of Cell Wall Carbohydrate Modifications During Flooding-Induced Aerenchyma Formation in Fabaceae Roots

Timothy Pegg[1], *Richard R. Edelmann*[1,2] *and Daniel K. Gladish*[1]*

[1] Department of Biology, Miami University, Oxford, OH, United States, [2] Center for Advance Microscopy & Imaging, Miami University, Oxford, OH, United States

Understanding plant adaptation mechanisms to prolonged water immersion provides options for genetic modification of existing crops to create cultivars more tolerant of periodic flooding. An important advancement in understanding flooding adaptation would be to elucidate mechanisms, such as aerenchyma air-space formation induced by hypoxic conditions, consistent with prolonged immersion. Lysigenous aerenchyma formation occurs through programmed cell death (PCD), which may entail the chemical modification of polysaccharides in root tissue cell walls. We investigated if a relationship exists between modification of pectic polysaccharides through de-methyl esterification (DME) and the formation of root aerenchyma in select Fabaceae species. To test this hypothesis, we first characterized the progression of aerenchyma formation within the vascular stele of three different legumes—*Pisum sativum*, *Cicer arietinum*, and *Phaseolus coccineus*—through traditional light microscopy histological staining and scanning electron microscopy. We assessed alterations in stele morphology, cavity dimensions, and cell wall chemistry. Then we conducted an immunolabeling protocol to detect specific degrees of DME among species during a 48-hour flooding time series. Additionally, we performed an enzymatic pretreatment to remove select cell wall polymers prior to immunolabeling for DME pectins. We were able to determine that all species possessed similar aerenchyma formation mechanisms that begin with degradation of root vascular stele metaxylem cells. Immunolabeling results demonstrated DME occurs prior to aerenchyma formation and prepares vascular tissues for the beginning of cavity formation in flooded roots. Furthermore, enzymatic pretreatment demonstrated that removal of cellulose and select hemicellulosic carbohydrates unmasks additional antigen binding sites for DME pectin antibodies. These results suggest that additional carbohydrate modification may be required to permit DME and subsequent enzyme activity to form aerenchyma. By providing a greater understanding of cell wall pectin remodeling among legume species, we encourage further investigation into the mechanism of carbohydrate modifications during aerenchyma formation and possible avenues for flood-tolerance improvement of legume crops.

Keywords: aerenchyma, pectin, de-methyl-esterification, PCD, homogalacturonan, root, lysigenous, legume

OPEN ACCESS

Edited by:
Francois Bouteau, Paris Diderot University, France

Reviewed by:
Takaki Yamauchi, Japan Science and Technology Agency, Japan
Alexis Peaucelle, INRA Centre Versailles-Grignon, France

***Correspondence:**
Daniel K. Gladish
gladisdk@miamioh.edu

Specialty section:
This article was submitted to Plant Cell Biology, a section of the journal Frontiers in Plant Science

Received: *12 July 2019*
Accepted: *24 December 2019*
Published: *03 February 2020*

Citation:
Pegg T, Edelmann RR and Gladish DK (2020) Immunoprofiling of Cell Wall Carbohydrate Modifications During Flooding-Induced Aerenchyma Formation in Fabaceae Roots. Front. Plant Sci. 10:1805. doi: 10.3389/fpls.2019.01805

INTRODUCTION

Flooding is among the most common and costly natural disasters inflicted upon agricultural lands (Doocy et al., 2013). Between 2005 and 2015, global economic losses of over $19 billion were incurred due to destruction of crops and erosion of arable land from flooding (Conforti et al., 2018). Increased coastal flooding and changes of annual precipitation are predicted to cause significant economic losses within the next century (Hirabayashi et al., 2013). To aid in mitigating the future economic impact of flooding damage on plants, significant research has been conducted in the field of crop improvement with regards to understanding plant adaptations to water immersion (Grover et al., 2000; Evans, 2004; Bailey-Serres et al., 2012; Valliyodan et al., 2016; Mustroph, 2018).

One adaptive mechanism plants utilize against flooding is the creation of aerenchyma (Drew et al., 1980; Jackson and Armstrong, 1999). Aerenchyma tissues are characterized by the formation of large, air-filled channels or cavities in the stems, leaves or roots in plant cortical or vascular tissues (Yamauchi et al., 2013; Takahashi et al., 2016). These cavities allow plants to tolerate hypoxic conditions induced through prolonged water immersion by maintaining oxygen levels sufficient for cellular respiration and reducing the number of cells utilizing oxygen (Evans, 2004; Postma and Lynch, 2011; Yamauchi et al., 2013). Additionally, oxygen from aerenchyma diffuses through the plant apoplast into the surrounding soil, which increases soil oxygen content and protects tissues from infection by bacteria and fungi favored by anaerobic conditions (Jackson and Armstrong, 1999; Cronk and Fennessy, 2009; Takahashi et al., 2016).

Aerenchyma is often classified as either primary aerenchyma, forming within cortical tissues, or secondary aerenchyma, forming from cell divisions of meristematic phellogen layers (Shimamura et al., 2010). Primary aerenchyma can be either schizogenous, forming through separation of middle lamella between cells, or lysigenous, utilizing programmed cell death (PCD) of specific cells and tissues to form new cavities (Gunawardena et al., 2001a; Evans, 2004; Ishizaki, 2015). Lysigenous aerenchyma may also be formed in non-cortical tissues, such as the stele of legume roots such as *Pisum sativum* (pea) (Rost et al., 1991; Gladish and Niki, 2000; Sarkar and Gladish, 2012; Pegg et al., 2018) and *Phaseolus coccineus* (scarlet runner bean) roots under conditions of flooding stress (Takahashi et al., 2016).

Lysigenous aerenchyma formation is known to involve PCD that utilizes modification and subsequent deconstruction of plant cell walls to create aerenchyma cavities (Gunawardena et al., 2001a; Sarkar and Gladish, 2012). The plant cell wall itself is a dynamic structure consisting of interlinking matrices of xyloglucan and cellulose microfibrils inside a network of hydrated pectic polysaccharides (i.e. pectins) (Carpita, 1996). Modification of cell wall pectic polysaccharides is of significance in many plant physiological processes, such as fruit ripening (Hyodo et al., 2013; Paniagua et al., 2014), leaf abscission (Lashbrook and Cai, 2008), pollen tube growth (Bosch and Hepler, 2005) and lateral root emergence (Vilches-Barro and Maizel, 2015).

The process of de-methyl esterification (DME) modifies the pectin backbone structure (i.e. homogalacturonan) within plant cell walls by removing methyl ester groups from α-(1–4)-linked D-galacturonic acid chains. (Wolf et al., 2009; Daher and Braybrook, 2015). As a result, negatively charged carboxyl groups are created that participate in cross-linking reactions with calcium cations (**Supplemental Figure 1**). These cross-linking interactions form an "egg box" structure of paired homogalacturonan chains that allows susceptibility to hydrolytic enzymatic degradation of the pectin backbone from polygalacturonase (**Supplemental Figure 2**) and pectate lyase activity that destabilizes the cell wall matrix (Ochoa-Villarreal et al., 2012; Pérez-Pérez et al., 2019).

DME activity has been previously identified during cortical aerenchyma development in several crop species such as *Zea mays* (maize) (Gunawardena et al., 2001a), *Oryza sativa* (rice) (Qu et al., 2016) and *Saccharum* sp. (sugarcane) (Leite et al., 2017). Aerenchyma development is suspected to rely on DME to initiate degradation of the cell wall matrix by forming homogalacturonan residues susceptible to enzymatic hydrolytic cleavage (Gunawardena et al., 2001b; Pegg et al., 2018). However, an investigation into the chemical structure of the DME residues near aerenchyma cavities has been performed on relatively few plants species (Sarkar et al., 2008; Leite et al., 2017; Pegg et al., 2018).

In this project, we addressed the potential role of pectin modification during root aerenchyma formation in three members of the legume family (Fabaceae): *P. sativum*, *Cicer arietinum*, and *P. coccineus*. Our results indicated that pectin DME occurs in select cell regions prior to or during the formation of lysigenous aerenchyma in these legume species and that variation in the degree of pectin methyl-esterification (ME) is significant to cavity formation. Additionally, evidence exists for the removal of associated cell wall polymers such as cellulose and xylan as a potential requirement for DME activity to occur during aerenchyma formation.

MATERIALS AND METHODS

Seedling Growth and Flooding Treatment

Seedlings were grown according to method of Gladish and Niki (2000). For each species 20 seeds (*P. sativum* and *C. arietinum*), or 10 seeds (*P. coccineus*), were sown, per beaker, into 2 l beakers filled with 1800 ml of sterile, super-coarse vermiculite (Perlite Vermiculite Packaging Industries, Inc., USA), moistened with 650 ml of deionized water, and covered with aluminum foil. Beakers were placed into 25°C growth chambers for 5 d in complete darkness to initiate root growth. Three replicates for each flooding treatment (12, 24, and 48 h water immersion) and each control (0, 12, 24, 48 h without flooding) were created using a separate 2 l beaker for each replicate.

To perform flooding treatments, three sets of beakers (12, 24, and 48 h water immersion) were removed from growth

chambers, placed under a laminar flow hood, and filled with sterile deionized water to the surface level of the vermiculite substrate. An additional three sets of beakers (12, 24, and 48 h non-flooded) corresponding to the same timepoint as the flooding treatments were also removed from growth chambers but were not flooded to serve as control samples. Three non-flooded beakers representing the 0-hour timepoint were harvested at that time. Remaining beakers were returned to 25°C growth chambers and removed at either 12 h, 24, or 48 h after flooding to be harvested for sectioning.

Sectioning, Fixation and Embedding

Five to ten root segments were harvested from each species per flooding treatment or non-flooding control. Segments were cut with carbon steel razor blades (Electron Microscopy Services, USA) from either 1.5–5 cm (*P. sativum* and *P. coccineus*) or 3–7 cm (*C. arietinum*) away from root tips. Segments were fixed in 1% paraformaldehyde and 2% glutaraldehyde solution in deionized water for 24 h at 5°C. Segments were then washed 3× with deionized water (15 min per wash), embedded in 3.5% agarose (Sigma-Aldrich, CAS 9012-36-6, USA) at 40°C, solidified, mounted on stubs of epoxy resin, and sectioned at 100 µm thickness on a Vibratome Series 1000 Sectioning System (Ted Pella, Inc., Redding, CA, USA). Sections from each root were stored separately in three separate pools (per treatment, per species) in 0.1M tris-buffered saline solution (pH 7.4) with 0.1% sodium azide at 5°C.

Histological Staining and Area Measurement

Randomly selected root sections from each species pool were stained with 0.1% toluidine blue O stain (Electron Microscopy Sciences, RT26074-05, Hatfield, PA, USA) for 20 s, then washed three times with deionized water. Sections were placed in deionized water on standard 1 mm glass slides, flanked by two 22 × 22 mm, No. 1 coverslips serving as spacers, and covered with a 24 × 60 mm, No. 1.5 coverslip. A minimum of three sections (one section per individual root) from each species were observed per time point using bright field illumination on a Nikon Eclipse E200 upright binocular light microscope (Nikon, USA) with a 20× dry objective. Each section was photographed with a 12.2-megapixel CMOS digital camera (Samsung Galaxy S8 SM-G950U, Samsung, USA). Average area for aerenchyma cavities (n = 3) in each legume species was calculated for 12, 24 and 48 h flooding timepoints by measuring the 2D surface area of sections at each timepoint with ImageJ software (National Institutes of Health, USA). Data was plotted as a bar chart displaying average values with standard error bars using Microsoft Excel (Microsoft, USA).

Scanning Electron Microscopy

Randomly selected root sections from each species pool were placed in 1% osmium tetroxide in deionized water for 24 h. Sections were washed 3× with deionized water (15 min per wash), following by an ethanol dehydration series. Samples in

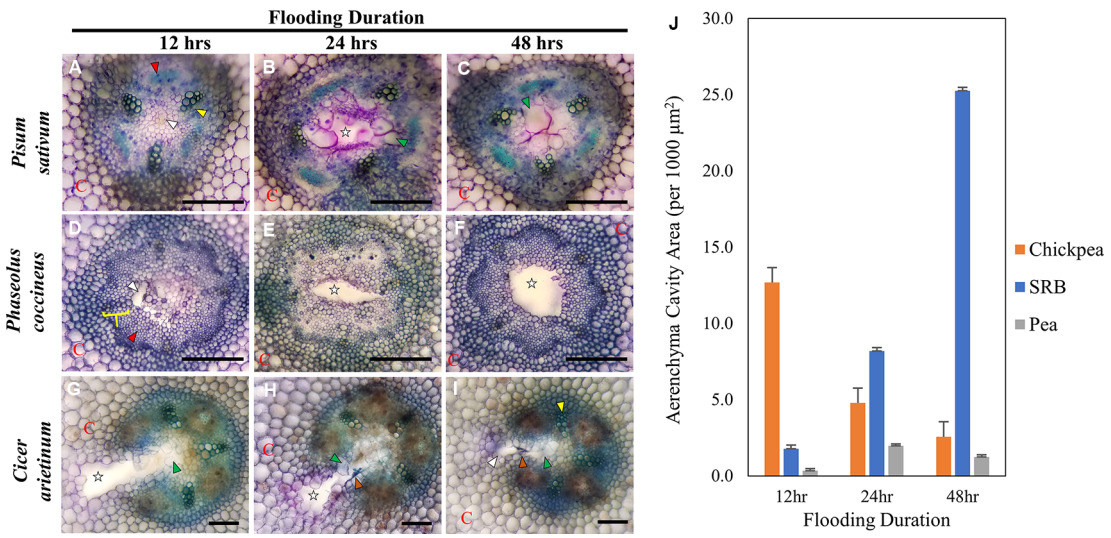

FIGURE 1 | Toluidine Blue Staining of three Fabaceae root species during a 48-hour flooding time course: **(A–C)** *Pisum sativum* (pea), **(D–F)** *Phaseolus coccineus* (scarlet runner bean, SRB), **(G–I)** *Cicer arietinum* (chickpea). **(J)** Average area measurement of aerenchyma cavities across legume species and flooding timepoints with standard error bars (n = 3). Aerenchyma cavities indicted with white stars and wedges. Xylem and phloem indicated with yellow wedges/brackets and red wedges, respectively. C = cortex. Tylose-like cells (TLCs) indicated with green wedges. Degraded cell wall components (dark blue accumulations) indicated with orange arrows. Scale Bars = 100 µm.

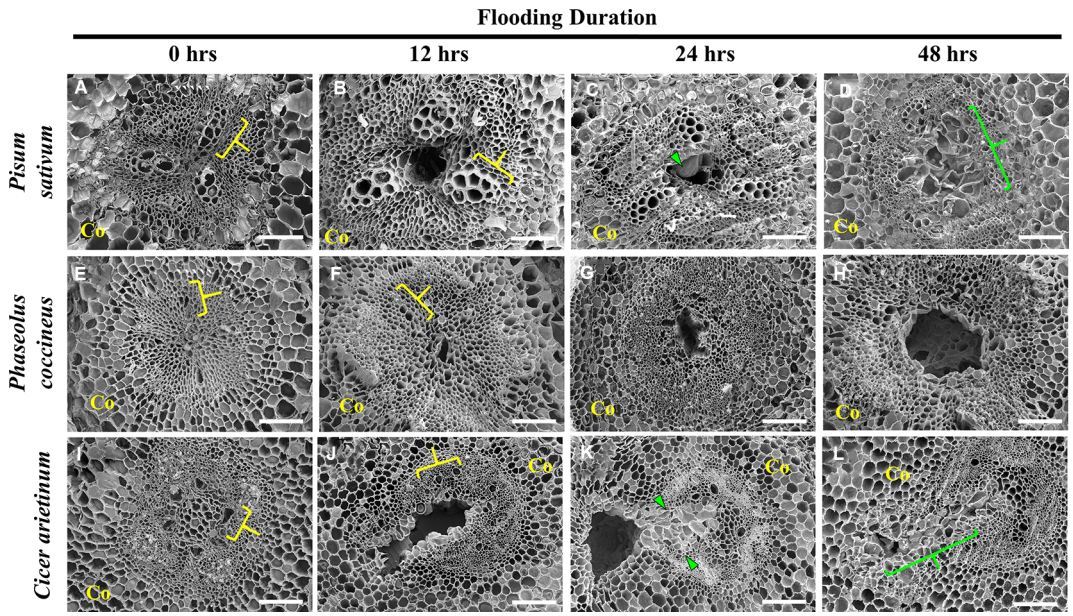

FIGURE 2 | Scanning electron micrographs of aerenchyma formation in the Fabaceae species. **(A–D)** *Pisum sativum*, **(E–H)** *Phaseolus coccineus*, and **(I–L)** *Cicer arietinum* root cross sections displaying cavity formation in vascular tissue over a 48-hour flooding time course. Xylem indicated by yellow brackets. Tylose-Like Cells (TLCs) indicated with green wedges and brackets. Co = cortex. Scale bars = 100 μm.

100% ethanol were CO_2 critical point drying, and then gold sputter-coated for 90 s to obtain a coating of 20 nm thickness. Samples were viewed on a Zeiss Supra 35 VP FEG SEM at 10 keV and 7.4 mm working distance.

Immunolocalization

Ten randomly selected sections from each species pool, for control (five sections) and experimental treatments (five sections), were placed into sterile 24-well cell culture plates and blocked with 7% normal goat serum (Thermo Fisher Scientific, USA) for 24 h at 5°C. Samples were washed 3× (15 min per wash) with 10 mM Tris-buffered saline (pH 7.4) containing 0.1% TWEEN-20 (TBST) then incubated with 1/20 dilutions of LM19 (PlantProbes, University of Leeds, UK), JIM7 or JIM5 (CCRC, University of Georgia, USA) monoclonal antibodies for 24 h at 5°C (**Supplemental Table 1**). After incubation, samples were washed three times with TBST buffer and treated with 1/500 dilution of IgG goat anti-rat secondary antibody conjugated to Alexa Fluor™ 647 fluorescent dye (Thermo Fisher Scientific, USA) for 24 h at 5°C while wrapped with Parafilm M sealing film and covered in aluminum foil. Samples were washed a final time with three changes of TBST buffer and mounted in 100% glycerol (Sigma-Aldrich, CAS 56-81-5, USA) on standard 1 mm glass slides. Slides were covered with 24 x 60 mm, No.1 coverslips with two 22 × 22 mm, No. 1 coverslips applied underneath to serve as spacers. Samples were stored at 5°C in darkness when not in use.

Enzyme Treatment

Randomly selected roots sections from each species pool for the 48-hour flooding treatment timepoint were incubated according to vendor instructions in the following enzyme solutions at 50°C for 2 h: 4% Cellulase, 1% xylanase, 3% pectinase, and 4% Viscoenzyme L (Sigma-Aldrich, USA) in 0.05 M citrate buffer (pH 5.0). Positive control treatment entailed incubation of samples in 0.1 M sodium carbonate (pH 11.4) at 50°C for 2 h to fully de-methyl-esterify homogalacturonan on exposed surfaces of the sample and ensure binding by LM19 antibody. Negative control treatment entailed incubation of samples in 0.05 M citrate buffer (pH 5.0) at 50°C for 2 h to replicate standard LM19 binding pattern observed without enzyme pretreatments. Samples were then washed three times with TBST buffer, treated with LM19 primary monoclonal antibody, and incubated with secondary antibody conjugated to Alexa Fluor® 647 (Thermo Fisher Scientific, USA) prior to mounting in 100% glycerol on 1 mm glass slides covered with 24 × 60 mm No.1 coverslips.

Fluorescence Microscopy

Autofluorescence and immunostained tissue sections were observed on an Olympus FV500 Laser Scanning Confocal system (Olympus Corporation, USA) using 20×/0.70 NA and 40×/0.75 NA dry objectives. Excitation of aldehyde-induced autofluorescence and Alexa Fluor® 647 dye was achieved with 405 nm and 633 nm laser diodes, respectively. Images were recorded using a Photometric HQ cooled CCD camera.

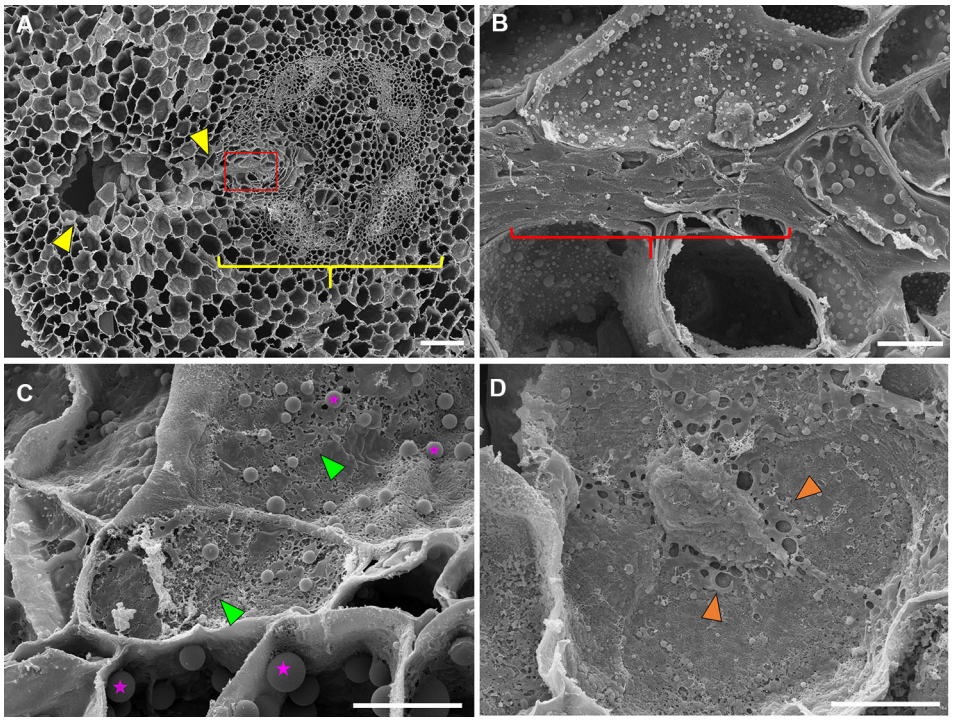

FIGURE 3 | Scanning electron microscopy images of 48 hr-flooded *Cicer arietinum* (chickpea) root sections during aerenchyma formation. **(A)** Vascular stele (yellow bracket) with region of active cavity formation (yellow wedges), 100×. **(B)** Collapse and compression of cell walls near the edge of the vascular stele (yellow bracket) as seen in the magnified area highlighted in red from **(A)**, 1,500×. **(C)** Degradation of cell walls indicated by "pock-mocked" appearance (green wedges) and increased abundance of suspected storage plastids (magenta stars). **(D)** Accumulation of cell wall components in apoplast space (orange wedges) at 2,000× magnification. Scale bars at **(A)** 100 μm and **(B–D)** 10 μm.

RESULTS

Distinct Morphological Characteristics Accompany Aerenchyma Development in Select Fabaceae Species

In this study, we used histological staining and scanning electron microscopy (SEM) to examine the morphogenesis of aerenchymatous cavities in Fabaceae. Toluidine blue staining and SEM of three species, *P. sativum*, *C. arietinum* (chickpea), and *P. coccineus*, during a 48-hour flooding time course revealed similarities and differences in cell wall chemistry and morphological dimensions (**Figures 1** and **2**, **Supplemental Table 2**) experienced by the root vascular stele.

P. sativum aerenchyma formation was consistently observed at 12 h after flooding stress was induced (**Figures 1A** and **2B**). Cavity formation began near the metaxylem of one xylem pole within the stele and expanded to form a transversely circular aerenchymatous space that occupied the center of the stele (**Figure 2B**). Release of large bubbles during cross sectioning of *P. sativum* suggests these cavities were filled with air. Consistent with previous reports (Lu et al., 1991; Niki et al., 1998) aerenchyma became partly occluded with new tissue expanding from the margin of the vascular cavity within 24-48 h of flooding (**Figures 1B, C, J** and **2C, D**). We described these tissues as being composed of large, nucleated "bubble-like" cells that we name "tylose-like cells" (TLCs) due to their cosmetic resemblance to tyloses found in xylem vessels of various hardwoods (Esau, 1965; Carlquist, 2013; Leśniewska et al., 2017). Interestingly, toluidine blue stained tissue near the margins of the aerenchyma and the TLCs a bright magenta color that was not found elsewhere in the root cross section (**Figures 1B, C**).

P. coccineus aerenchyma formation followed a similar pattern as *P. sativum* with initiation adjacent to metaxylem (**Figures 1D** and **2F**) and creation of a transversely ovoid or circular cavity that occupied the center of the stele (**Figures 1F** and **2G, H**). Release of large bubbles from the aerenchyma during cross sectioning suggests these cavities were filled with air, similar to observations made in *P. sativum*. Unlike *Pisum*, *Phaseolus* aerenchyma formation did not entail creation of TLCs at any point within a 48-hour flooding treatment (**Figures 1F, J** and **2H**). Occasionally, *Phaseolus* sections showed large, circular remains of degraded cell tissue deep within aerenchyma (**Figure 1H**). Similar to *P. sativum*, application of toluidine blue resulted in cells bordering the aerenchyma staining a bright magenta color (**Figures 1D–F**).

C. arietinum aerenchyma formation was quite distinct from either *P. sativum* or *P. coccineus*. Large, transversely oblong

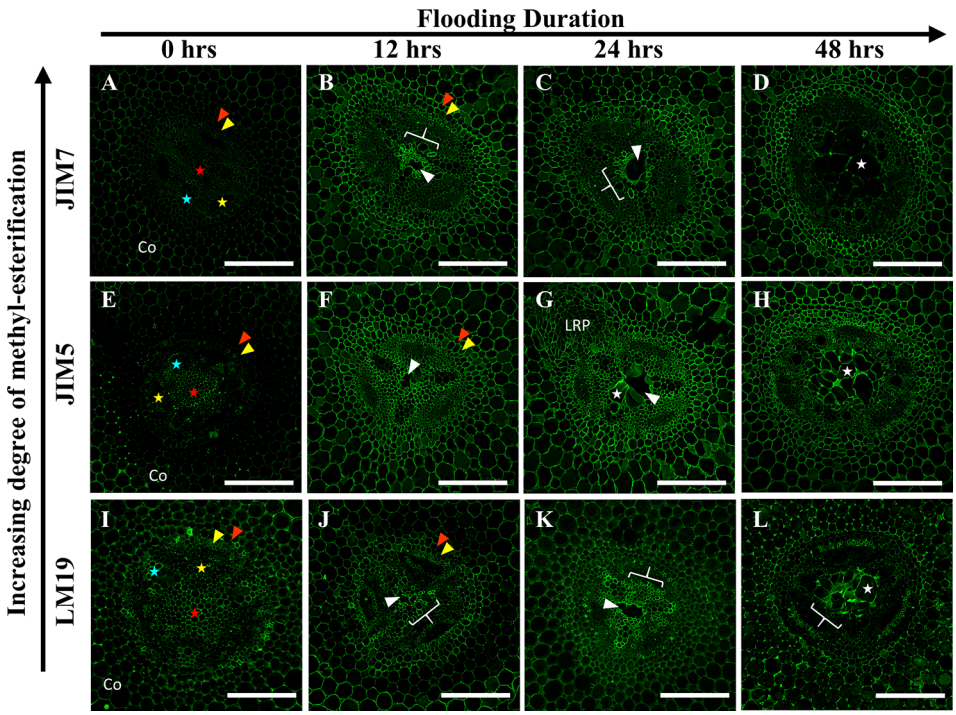

FIGURE 4 | Localization patterns of ME and DME homogalacturonan in *Pisum sativum* during aerenchyma formation. Micrographs demonstrating monoclonal antibody labeling of **(A–D)** JIM7, **(E–H)** JIM5, and **(I–L)** LM19 on cortex, endodermis (red wedge), pericycle (yellow wedge), xylem (blue star), phloem sieve tube elements (yellow star), and pith (red star) of root cross sections. Areas with prominent antibody labeling indicated with white brackets. Aerenchyma cavities indicated with white edges. Tylose-Like Cells indicated with white stars. Co, cortex, LRP, lateral root primordia. Scale bars = 100 μm.

cavities were observed as early as 12 h after flooding (**Figure 1**, **Supplemental Table 2**), with a unidirectional expansion of aerenchyma over time, which began near the stele xylem poles and extended into the root cortex (**Figures 1G** and **2J**), though notable examples were observed of aerenchyma formation remaining confined within the stele (**Supplemental Figure 3**). Formation of a cavity appeared to separate and split portions of the xylem poles (**Supplemental Figures 4B–D**) that were previously intact (**Supplmental Figure 4A**). Closer examination of TLCs formed during periods of flooding stress revealed occasional accumulations of collapsed cells surrounded by TLC walls (**Figure 3B**) and characteristic signs of enzymatic activity, as indicated by "pooling" of degraded cellular components (**Figure 3D**). Degradation of these cells appeared to occur concurrently with TLC formation within the stele (**Figures 1H, I** and **2K, L**). Endodermis and pericycle layers appeared to be more resistant to degradation compared to other cortical and vascular tissues, which resulted in an "hourglass-shaped" aerenchyma cavity observed in some cross sections (**Figures 1H** and **2K, L**). Air most likely fills the aerenchyma due to bubble release during sectioning, similar to observations made earlier in the experiment for *P. sativum* and *P. coccineus*. By 48 h after initial exposure to flooding aerenchyma had been mostly filled with TLCs (**Figures 1I** and **2L**), resulting in severely diminished cavity size (**Figure 1J**), in a fashion similar to *P. sativum*. In addition, near the margins of aerenchyma within the cortex of *C. arietinum* roots toluidine blue stained cells a bright magenta (**Figures 1G–I**), similar to observations made in TLCs of *P. sativum* (**Figures 1B, C**) and borders of aerenchyma in *P. coccineus* (**Figures 1D–F**), which suggests a similar chemical modification has occurred in these cell walls.

Immunolabeling of Fabaceae Root Radial Sections Indicates Specific Degrees of Pectin De-Methyl Esterification Adjacent to Aerenchyma

To evaluate the significance of cell wall pectin modification during aerenchyma formation, we labeled each Fabaceae species with three monoclonal antibodies targeting homogalacturonan pectin residues with differing degrees of de-methyl esterification (DME): LM19 (DME homogalacturonan), JIM5 (partially DME homogalacturonan), and JIM7 (fully methylated homogalacturonan). Immunolabeling of *P. sativum* flooding-time course series sections showed binding by LM19, JIM5 and JIM7 antibodies within central parenchyma, metaxylem, cortical apoplast and cells near phloem sieve tube elements (**Figure 4**). During aerenchyma formation, 12 and 24 h after flooding, binding by LM19 and JIM5 antibodies was detected within the cell walls and middle lamella of four to six cell layers adjacent to forming aerenchyma cavities (**Figures 4F, G, J, K**). Binding of JIM7 appeared to indicate a similar

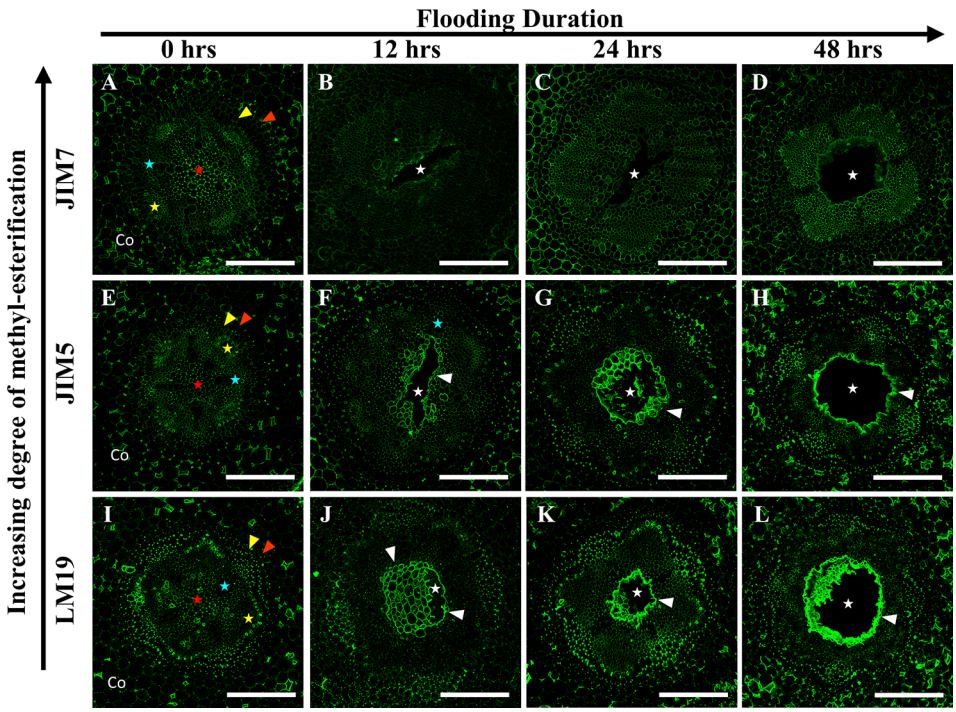

FIGURE 5 | Localization patterns of ME and DME homogalacturonan in *Phaseolus coccineus* during aerenchyma formation. Micrographs demonstrating monoclonal antibody labeling of **(A–D)** JIM7, **(E–H)** JIM5, and **(I–L)** LM19 on cortex, endodermis (red wedge), pericycle (yellow edge), xylem (blue star), phloem sieve tube elements (yellow star), and pith (red star) of root cross sections. Cell layers prominently labeled with antibodies are indicated with white wedges. Aerenchyma cavities indicated with white stars. Co, cortex. Scale bars = 100 μm.

localization pattern within cells adjacent to aerenchyma but was more restricted and localized to three cell layers or less adjacent to the aerenchyma cavity (**Figures 4B, C**). All three antibodies labeled TLCs produced by roots flooded for 48 h, suggesting the presence of multiple DME and methyl esterified homogalacturonan epitopes (**Figures 4D, H, L**). Interestingly, the availability of the epitopes may be different based on chemical composition due to the observed "spottiness" of the JIM7 antibody binding pattern (**Figure 4D**) compared to JIM5 (**Figure 4H**) and JIM7 (**Figure 4L**).

In *P. coccineus*, LM19, JIM5 and JIM7 antibodies displayed specific localization patterns within central parenchyma, cortical tissue apoplast, and cell walls of peripheral regions bordering the sieve tube elements (**Figures 5** and **7G–I**). By 12 h of flooding, all antibodies showed localization within cell walls and middle lamellas of central parenchyma cells within three to four cell layers of the aerenchyma, which suggests that de-methyl-esterification had probably begun. At 24–48 h after flooding, LM19 and JIM5 labeling was localized to most of the cell walls and middle lamellas of the root central parenchyma due to the increasing size of the aerenchyma cavity (**Figures 5G, H, K, L**). Similar to results seen in *P. sativum* (**Figure 4**), the binding pattern of JIM7 was noticeably less consistent and uniform compared to JIM5 and LM19 despite having shared localization patterns (**Figures 5A–D**).

Immunolabeling patterns for *C. arietinum* (**Figure 6**) were quite distinct from either *Pisum sativum* or *P. coccineus* (**Figures 4** and **5**). General localization patterns for LM19, JIM5 and JIM7 indicated the presence of all three antibody epitope structures in cortical apoplast, pericycle layer, xylem and cells bordering sieve tube elements of *Cicer* (**Figure 6**). Interestingly, LM19 and JIM7 antibody labeling was also prevalent on 0.5–1.0 μm membrane-bound bodies (MBB) found within cells of the pericycle, endodermis and inner cortical cell layers (**Figures 6A–D, I–L**), while it was mostly absent from similar tissues when labeled with JIM5 (**Figures 6E–H**). During aerenchyma formation, antibody labeling was limited to cell walls immediately adjacent to the cavity (**Supplemental Figures 3A–C**), newly formed TLCs (**Figures 6B–D, F–H, J–L**), or cell MBBs in the case of LM19 and JIM7 (**Figures 6B–D, J–L** and **7D, F**). Less consistent antibody binding patterns for LM19 and JIM7, compared to JIM5, was observed in cells adjacent to aerenchyma extending into the root cortex and TLCs developing within that region (**Figures 6B, C, J, K** and **7A, C**), which suggests an absence of fully DME and ME homogalacturonan. By comparison, JIM5 binding was prominent in cortical cells adjacent to aerenchyma, which implies the presence of partially DME homogalacturonan in these same cortical areas (**Figures 6F–H** and **7B**). However, JIM5 poor binding in the MBB of the inner cortex and stele, which contrasted with the consistent labeling observed from LM19 and JIM7 (**Figures 7D–F**).

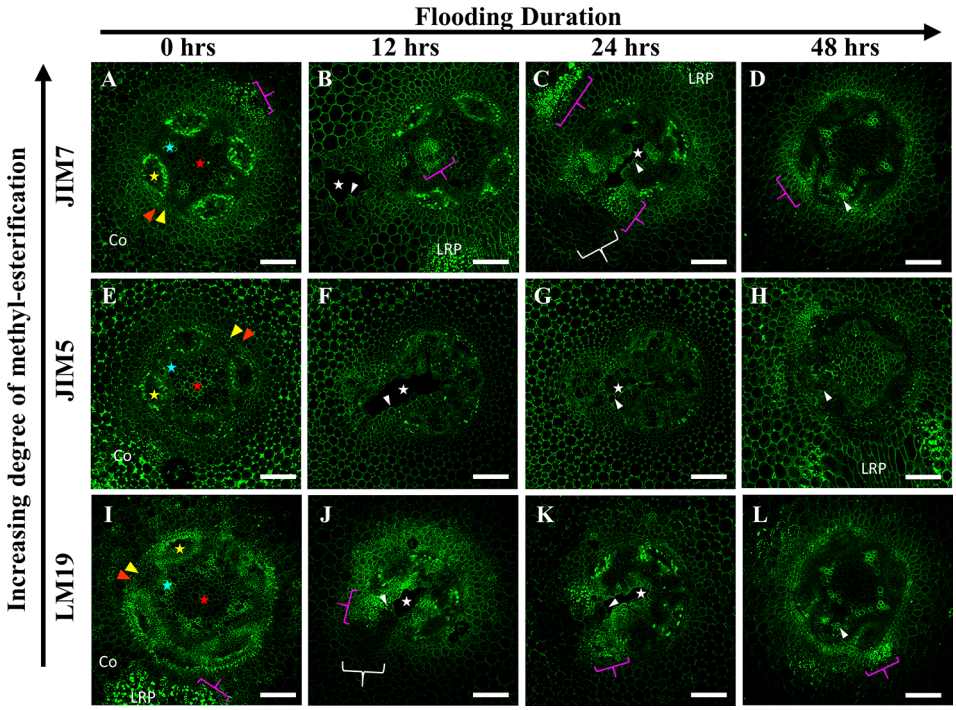

FIGURE 6 | Localization patterns of ME and DME homogalacturonan in *Cicer arietinum* during aerenchyma formation. Micrographs demonstrating monoclonal antibody labeling of **(A–D)** JIM7, **(E–H)** JIM5, and **(I–L)** LM19 on cortex, endodermis (red wedge), pericycle (yellow edge), xylem (blue star), phloem sieve tube elements (yellow star), and pith (red star) of root cross sections. Speckling pattern (magenta brackets) indicate cells containing membrane-bound bodies (MBBs). Aerenchyma cavities indicated with white stars. Areas with poor or non-existent antibody labeling indicated with white brackets. Tylose-Like Cells (TLCs) indicated with white wedges. Co, cortex, LRP, lateral root primordia. Scale bars = 100 μm.

Enzyme Treatments Suggest Cell Wall Components Mask LM19 Epitope by Cell Wall Matrix

Enzyme pretreatments of root sections before staining with LM19 antibody for DME homogalacturonan allowed evaluation of possible epitope site "masking" by other cell wall matrix components. Removal of cellulose prior to antibody labeling did not significantly alter LM19 localization pattern in either *P. sativum* or *C. arietinum* compared to sodium carbonate (**Figures 8A, D, E, H**) or citrate buffer control treatments (**Figures 8A, E–G, K, L**). However, cellulose removal in *P. coccineus* (**Figure 8M**) did increase LM19 localization pattern coverage in cell walls and middle lamella bordering the aerenchyma cavity and cortical apoplast when compared to sodium carbonate (**Figure 8Q**) and citrate buffer control treatments (**Figure 8R**). Xylan removal expanded LM19 binding pattern to cover the cortical apoplast in all species (**Figures 8B, H, N**) compared to control treatments (**Figures 8E, F, K, L, Q, R**) with visual changes in cortical apoplast binding consistency in *Pisum* and *Phaseolus*, and cell walls in tissue adjacent to aerenchyma in *Cicer*. Negative control treatments with pectinase (**Figures 8C, I, O**) and Viscoenzyme® L enzyme cocktail (**Figures 8D, J, P**) resulted in removal of LM19 binding pattern for *Pisum* and *Phaseolus* (**Figures 8D, P**), but had little effect on *Cicer* outside of loss of antibody binding in cell walls of the outer cortical cell layers (**Figure 8J**). Interestingly, treatment with Viscoenzyme® L enzyme cocktail altered the binding pattern of LM19 to permit labeling of xylem in *Phaseolus*, which suggests that removal of several cell wall polysaccharides is required for pectin in similarly lignified cell walls of this species to become available for antibody binding (**Figure 8P**).

DISCUSSION

The present study described shared characteristics, and notable differences among aerenchyma formation as a result of sudden flooding in three members of Fabaceae: *P. sativum*, *P. coccineus*, and *C. arietinum*. A unique characteristic of aerenchyma formation in Fabaceae is the location of the aerenchyma cavity within the root stele (Lu et al., 1991; Rost et al., 1991; Niki et al., 1995; Niki and Gladish, 2001). In all three species studied, aerenchyma formation was detected in stele tissues within 1.5–3 cm of the root apical meristem and became increasingly visible in older tissue zones away from the root tip. Similar to previous research (Gladish et al., 2006), we observed initiation of aerenchyma formation in the stele in central parenchyma cells adjacent to metaxylem followed by transverse expansion of the cavity to occupy most of the central parenchyma region in each species (**Figures 1** and **2**). However, in *C. arietinum* we observed

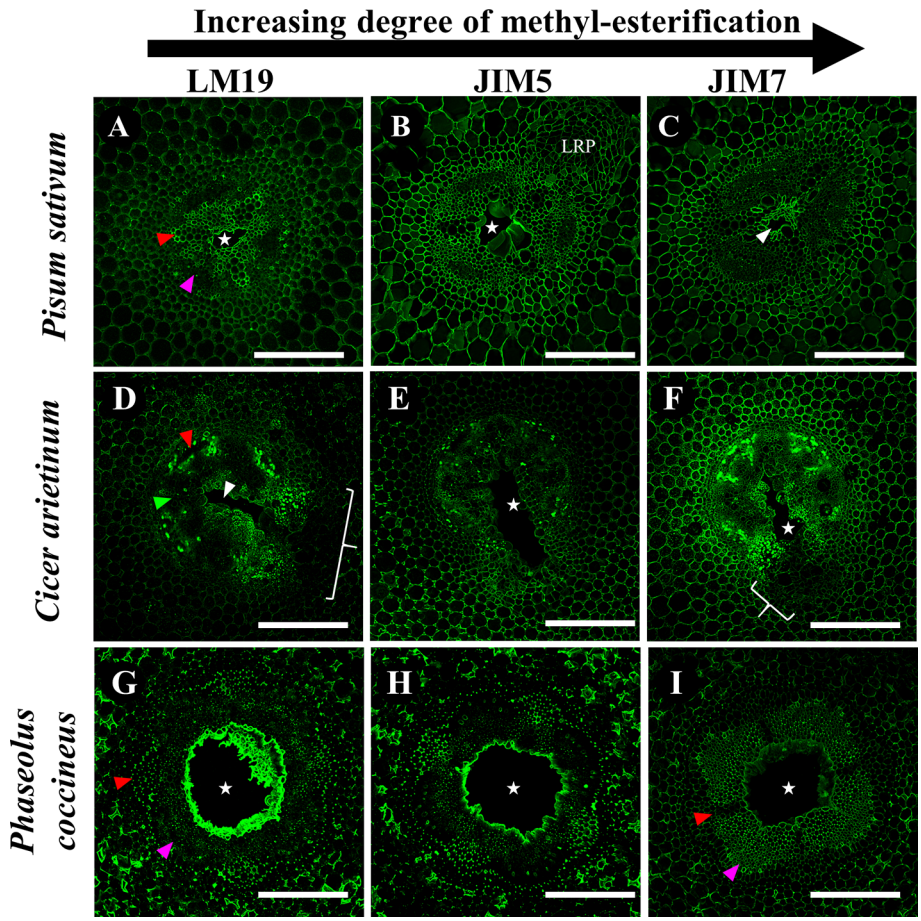

FIGURE 7 | Immunolabeling of three Fabaceae species with monoclonal antibodies targeting pectin residues with varying degrees of de-methyl-esterification. **(A–C)** *Pisum sativum*, **(D–F)** *Cicer arietinum*, **(G–I)** *Phaseolus coccineus* root cross sections. Antibody labeling indicated with green false color. Areas with loss of antibody labeling signal indicated with white brackets. Micrographs contain labeled aerenchyma cavities (white stars and wedges), xylem (red wedges), and phloem (magenta wedges) in cross-sections from root segments. LRP, lateral root primordia. Scale bars = 100 μm.

a unique aerenchyma formation pattern characterized by cavity formation continuing into the inner cortex and resulting in a large, rectangular or hourglass-shaped cavity when viewed in cross section (**Figures 1G, H** and **2J, K**). The biological significance of the aerenchyma pattern in *C. arietinum*, and why it differs from that of *P. sativum* and *P. coccineus*, is unknown but it may influence survival time of *C. arietinum* in hypoxic conditions by reducing the number of extraneous, oxygen-consuming cells in roots, as has been noted in other work in *Z. mays* and *O. sativa* (Drew et al., 2000; Evans, 2004). Furthermore, extending the aerenchyma cavity into the root cortex may increase the volume of air that *C. arietinum* can conduct during hypoxic conditions as compared to *P. sativum* and *P. coccineus*. Aerenchyma of all three species contain air, as indicated by the release of bubbles during cross-sectioning of root tissues, along with confirmation of oxygen content in *P. coccineus* aerenchyma in intact roots by previous research (Takahashi et al., 2016). This suggests the possibility that increases in aerenchyma air volume, due to changes in aerenchyma cavity dimensions, may enable prolonged functioning of aerobic metabolic processes in root tissues exposed to low-oxygen conditions.

Our study also described the formation of previously reported space-filling parenchyma cells (Lu et al., 1991; Niki et al., 1998; Pegg et al., 2018) during periods of prolonged flooding stress that cosmetically resemble tyloses found in hardwood plants (Esau, 1965; Carlquist, 2013; Leśniewska et al., 2017). The biological significance of these "tylose-like cells" (TLCs) forming in *Pisum* and *Cicer* samples is unclear with respect to formation and eventual filling of aerenchyma cavities during periods of flooding stress. Tyloses are often observed within older xylem tissues of vascular plants as ingrowths of parenchyma cells that prevent or limit water transport as a response to drought stress or pathogenic infection (Pallardy, 2008; Zhao et al., 2014; Micco et al., 2016). In some species of Fabaceae, TLCs may serve a similar purpose by removing the airspace within the stele

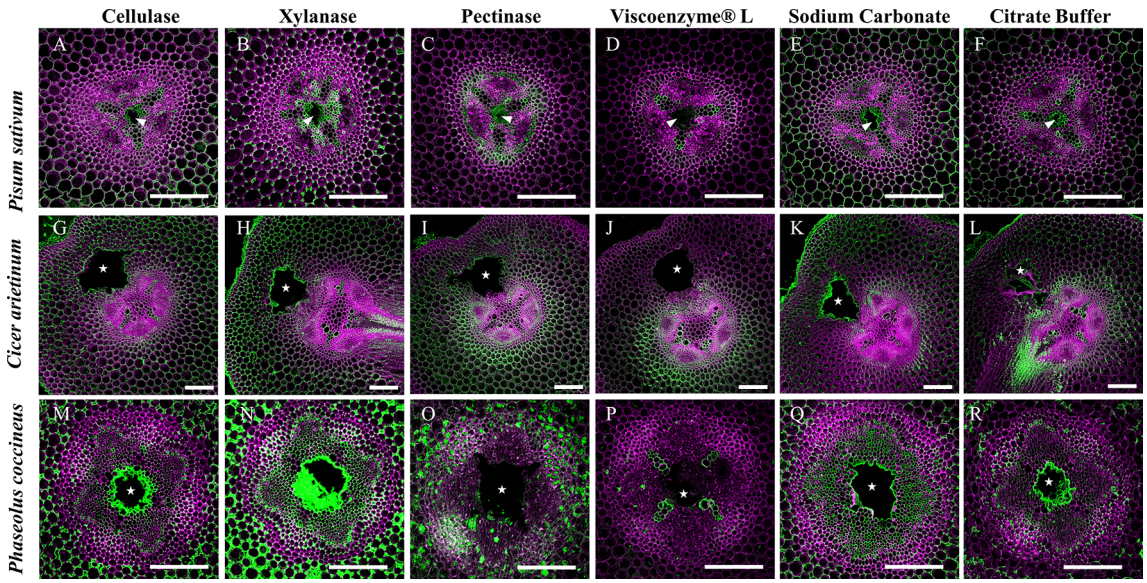

FIGURE 8 | Effect of enzymatic pretreatments on LM19 labelling pattern in Fabaceae roots with aerenchyma. Fluorescent antibody labeling pattern of LM19 (green), composited with aldehyde induced fluorescence (magenta), to show distribution of de-methyl esterified homogalacturonan pectin in root cross sections. **(A, G, M)** Treatment of 2% cellulase, **(B**, **H**, **N)** 1% xylanase, **(C**, **I**, **O)** and 1% pectinase solutions. **(D**, **J**, **P)** Treatment of Viscoenzyme® L enzyme solution (i.e. combination of cellulase, lichenase, pectinase, xylanase, etc.) to act as a negative control. **(E**, **K**, **Q)** Treatment of 0.1 M sodium carbonate, pH 11.4 solution to enhance LM19 binding pattern as a positive control. **(F**, **L**, **R)** Treatment of 0.05 M citrate buffer (negative control). White stars and wedges represent aerenchyma cavities. Scale bars = 100 μm.

through replacement with parenchyma and repairing a structural weakness induce by prolonged presence of aerenchyma cavities (citation).

Further observation of legume root sections with scanning electron microscopy revealed characteristic signs of cell wall collapse and enzymatic degradation in cells adjacent to expanding cavities (**Figure 3**). This supports previous research which proposed that root aerenchyma formation in certain members of Fabaceae (Lu et al., 1991; Rost et al., 1991; Niki et al., 1995; Niki and Gladish, 2001), rice (Joshi and Kumar, 2012) and tomato (Kawase, 1981) is lysigenous in nature. Furthermore, our study noted that cell wall degradation was very localized within one to three cell layers of forming aerenchyma (**Figure 3**), and suggests that a carefully regulated and localized PCD mechanism is required to form aerenchyma in this plant family (Sarkar et al., 2008b; Sarkar and Gladish, 2012) while preventing an uncontrolled enlargement that would consume essential xylem and phloem vasculature within the root stele (Sarkar et al., 2008b; Sarkar and Gladish, 2012). This may be particularly important in the case of *C. arietinum* since the expanding cavity partially removes one of xylem poles in the tetrarch stele, which could require the conservation of the remaining three xylem bundles to ensure proper water conduction through the root. Development of lysigenous aerenchyma may also prevent inhibition of aerobic cellular respiration in legume roots by creating an internal oxygen-containing channel when the rhizosphere environment becomes hypoxic due to flooding (Drew et al., 2000; Evans, 2004; Takahashi et al., 2016).

Our research also revealed the presence of de-methyl-esterified (DME), partially DME and fully methyl-esterified (ME) pectin residues in the cell walls and middle lamella of stele and cortical tissues involved in aerenchyma formation. Previous research proposed that removal of methyl ester substitutions from the homogalacturonan domains of pectin enables degradation of cell walls by unblocking cleavage sites between pectin residues, which are then targeted by polygalacturonases, pectin lyases and similar hydrolytic enzymes (Dheilly et al., 2016). Our observations showed that DME pectin is spatially localized within one to three cell layers around aerenchyma and increases from partial and fully DME during aerenchyma development (**Figures 4–7**). This indicates a direct correlation between DME pectin formation and degradation of root cell walls. Furthermore, DME process may also strengthen the plant primary cell wall pectin matrix through interactions with calcium cations (Hocq et al., 2016), benefitting roots by increasing cell wall mechanical strength (Celus et al., 2018) near the forming aerenchyma to compensate for the structural weakness caused by a large air channel within the stele. This enhancement of cell wall strength would be particularly advantageous for plants such as *C. arietinum* which have non-symmetrical aerenchyma extending into cortex tissues with thin primary cell walls.

Notable changes in pectin methyl-esterification were also noted in TLCs in *P. sativum* and *C. arietinum*. Similar to cells and middle lamella destined for degradation, the TLCs were thoroughly labeled with antibodies against DME (LM19) and partially DME (JIM5) homogalacturonan (**Figures 4** and **6**). The presence of DME homogalacturonan in TLCs primary walls has not been previously described and is likely due to action of pectin methylesterase activity upon the homogalacturonan backbone. Removal of methyl esters from homogalacturonan promotes hydrolytic enzyme activity required for "loosening" of primary cell walls prior to wall expansion (Foster, 1967; Micco et al., 2016; Wu et al., 2018) and is a possible prerequisite for expansion of TLCs into the aerenchyma cavity. Additionally, de-methyl-esterification of pectin may permit enlargement of TLCs prior to development of secondary wall patterning (Goulao et al., 2011), as suggested by cell wall morphology observed in the present study (**Supplemental Figure 5**)

Enzyme treatments performed in this study indicated that hemicelluloses such as xylan, along with cellulose, may "mask" pectin from recognition by monoclonal antibodies targeting de-methyl esterified homogalacturonan residues (**Figure 8**, **Supplemental Figure 6**). Previous research suggests that "masking" occurs due to pectin and xylan binding to each other within primary cell wall matrices and physically blocking access of antibodies to epitope binding sites (Marcus et al., 2008). The presence of masking effects in our root samples suggests the possibility that pectin de-methyl-esterification may occur in a wider region of the central parenchyma than previously observed in the present study. This prediction was supported by results in *P. sativum* and *P. coccineus* (**Figures 8B, F, N, R**) where removal of xylan expanded LM19 antibody labeling into stele tissue further away from aerenchyma cavities. Non-flooded control samples also manifested this labeling pattern, but to a less consistent degree, suggesting that the flooding treatment itself may alter effectiveness of xylanase enzymatic pretreatment (**Supplemental Figures 6B, F, N, R**). Interestingly, antibody binding patterns for DME pectin do not appear to change noticeably following removal of either cellulose or xylan in *C. arietinum* root sections when compared to non-enzyme-treated controls in either flooded samples (**Figures 8G, H, L**) or non-flooded samples (**Supplemental Figures 6G, H, L**). These observations suggest that primary cell wall polysaccharides in *C. arietinum* may be organized differently compared to *P. sativum* and *P. coccineus*, thereby preventing or limiting masking effects on pectin residues. Additionally, small differences in LM19 binding pattern contiguity between flooded (**Figure 8**) and non-flooded (**Supplemental Figure 6**) samples indicate that immersion in water may subtly alter cell wall chemistry throughout root segments from these legumes. One possible consequence is an increase in the hydration of the primary cell wall, resulting in changes to molecular rigidity of the pectin cross-linking network (Vicré et al., 1999; Bidhendi and Geitmann, 2015; Lampugnani et al., 2018) and potential alteration of enzyme penetration and activity that would explain the differences observed in the pre-treatment protocol (**Figure 8**, **Supplemental Figure 6**).

Our research also suggests the possibility of stele regions with strong antibody labeling having masking effects negated by previous removal of other cell wall components. Removal of xylan, and to a lesser extent cellulose, in areas adjacent to forming aerenchyma appears to eliminate masking and create the DME pectin antibody binding patterns seen in this study (**Figures 8F, L, R**). This hypothesis is supported in our study by observations that LM19 binding patterns in root cross-sections treated with cellulase, xylanase, and sodium carbonate (**Figures 8A, B, E, G, H, K, M, N, Q**) are greatly expanded throughout root stele compared to control treatments (**Figures 8F, L, R**) with DME pectin localized near the aerenchyma cavity. As a result of our observations, we propose that aerenchyma formation may depend on activity of multiple cell wall remodeling enzymes (i.e. cellulase, xylanase) working together to achieve cell wall degradation. Specifically, xylanases and cellulases may degrade xylan and cellulose polysaccharides in advance of de-methyl-esterification of pectin by PME enzymes and subsequent degradation by pectinases.

Our findings in the present study provide directions for future research into regulation and localization of components essential to DME during aerenchyma formation. For example, we observed that fragments of degraded root stele tissue may be found inside aerenchyma during cavity formation (**Supplemental Figure 7**), yet the destination of pectins from degraded cells is unclear. In the case of *C. arietinum*, degraded pectin residues with specific degrees of DME may accumulate within MBB and be utilized to construct TLCs during later stages of flooding. Pectin residues may also enter the apoplast (de Freitas et al., 2012; Anderson, 2016) and may become incorporated into the primary walls and middle lamella of cells adjacent to forming aerenchyma cavities. Observed differential metachromatic staining of toluidine blue near aerenchyma cavities (**Figure 1**) could be the result of pH changes (O'Brien et al., 1964; Niki et al., 2014; Bergholt et al., 2018) in the apoplast and indicate liberated, negatively charged DME pectin residues forming during cell wall or middle lamella degradation (Yamada et al., 2015; Printz et al., 2016).

Additionally, the localization of calcium and cell wall remodeling enzymes (i.e. pectin methylesterase and pectin lyase) within legume stele tissues during aerenchyma formation requires elucidation. Calcium is mainly localized in the cell walls of plant tissues, accounting for 60–75% total calcium content (Demarty et al., 1984), though it is also present in the surrounding, fluid-filled apoplast (de Freitas et al., 2012). High localization of calcium ions could indicate susceptibility to enzyme degradation of cell walls by virtue of Ca^{2+} linkages between DME homogalacturonan residues (Grant et al., 1973; Wolf et al., 2009) and by serving as a signaling molecule in proposed ethylene signal transduction pathways that initiate PCD in cells adjacent to forming aerenchyma (He et al., 1996; Gunawardena et al., 2001b). Similarly, confirmation of elevated pectin methylesterase in cells fated to be degraded was found to correlate with high calcium concentrations: this provides supporting evidence in legume roots for extensive pectin DME during aerenchyma

expansion (Goulao et al., 2007; Rajhi et al., 2011; de Freitas et al., 2012)

The regulation of gene expression leading to pectin DME during Fabaceae aerenchyma formation also remains unclear. Previous work in plants such as *Arabidopsis thaliana* (Mühlenbock et al., 2007) and *O. sativa* (Yamauchi et al., 2017) suggests the involvement of hydrogen peroxide (H_2O_2) in the formation of cortical lysigenous aerenchyma. Additional research involving *Z. mays* (Drew et al., 1980), *P. sativum* (Gladish and Niki, 2008) and *O. sativa* (Yamauchi et al., 2017) suggests ethylene signaling pathways may also play a role in cortical aerenchyma formation. These pathways are initiated by exposure to hypoxic, waterlogged conditions and result in gene expression for cell wall remodeling enzymes such as cellulases, xylanases, and pectinases (i.e. polygalacturonase and pectin lyase)(Waldenmaier, 2011) through transcription factors such as RAVs (Related-to-ABI3/VP1) identified in sugarcane (Li et al., 2011; Tavares et al., 2019). Involvement of downstream components for these pathways is supported in the results of the present study (**Figure 8**), which indicate cellulase and xylanase activity may degrade cell wall polymers (i.e. cellulose and hemicellulose, respectively) that partially "mask" (protect) pectin from enzymatic activities such as de-methyl-esterification and hydrolytic cleavage of homogalacturonan by pectinases (Voragen et al., 2009; Xue et al., 2013).

Research into genes involved in alternative processes, such as lateral root emergence, may identify similar functions during aerenchyma formation due to both events requiring cell wall remodeling to accommodate new structures within root tissues (Péret et al., 2009; Ishizaki, 2015; Porco et al., 2016; Leite et al., 2017). Specifically, genes involved in the auxin signaling pathway and cell wall remodeling genes such as those for auxin response factors in *A. thaliana* (Sénéchal et al., 2014) and polygalacturonases (PGLR, PGAZAT) in *O. sativa* (Kumpf et al., 2013) may have orthologs in legumes that also regulate pectin modification during aerenchyma formation. The potential presence of conserved cell wall remodeling genes among disparate plant families encourages research into controlled induction of aerenchyma *via* manipulation of an existing genetic framework for pectin modification and subsequent cell wall degradation in root tissues. Benefits of such work could lead to crop improvement with respect to increased tolerance to flooding, and, potentially, drought by plant root systems (Zhu et al., 2010; Nord et al., 2013).

CONCLUSION

Initiation of aerenchyma formation in three Fabaceae species begins with degradation of root parenchyma cells near metaxylem of the stele. Expansion of aerenchyma cavities continues within the stele (*P. sativum* and *P. coccineus*) or from the stele and into cortical tissues (*C. arietinum*) unless halted by formation of tylose-like cells (TLCs) that fill aerenchyma of species such as *P. sativum* and *C. arietinum*. Modification of the pectin homogalacturonan backbone structure through de-methyl-esterification appears to be one mechanism by which cell walls and middle lamella of tissues in forming lysigenous aerenchyma are prepared for enzymatic degradation to permit PCD and enable cavity formation. Additionally, presence of fully and partially de-methyl-esterified homogalacturonan residues in cell walls of forming TLCs suggests these pectin structures are essential to development of TLCs that occlude aerenchyma of *P. sativum* and *C. arietinum*. Evidence exists for removal of cellulose and hemicellulose (xylan) in the cell walls of tissues adjacent to forming aerenchyma. Removal may occur prior to aerenchyma formation to allow de-methyl-esterification and/or enzyme access to pectin backbone structure.

DATA AVAILABILITY STATEMENT

The datasets generated for this study are available on request toeither the corresponding author, DG (gladisdk@miamioh.edu) or TP (peggtj@miamioh.edu).

AUTHOR CONTRIBUTIONS

TP performed the primary experimental work. TP performed seedling cultivation, tissue sectioning, absorbance dye staining, immunolabeling, enzyme treatments and image processing. RE provided technical assistance in microscope operation and protocol development. RE and DG evaluated experimental design, project progress and provided editing of manuscript. All authors performed data analysis, interpretation, and approved the final manuscript.

ACKNOWLEDGMENTS

We thank Matt Duley (Microscopy Specialist) at CAMI (Center for Advance Microscopy & Imaging) at Miami University for his material and technical support during immunolocalization and confocal imaging troubleshooting. We also thank Dr. Robert Baker (Assistant Professor) at Miami University (Oxford, Ohio) for input on overall project design and interpretation of imaging data.

SUPPLEMENTARY MATERIAL

The Supplementary Material for this article can be found online at: https://www.frontiersin.org/articles/10.3389/fpls.2019.01805/full#supplementary-material

REFERENCES

Anderson, C. T. (2016). We be jammin': an update on pectin biosynthesis, trafficking and dynamics. *J. Exp. Bot.* 67, 495–502. doi: 10.1093/jxb/erv501

Bailey-Serres, J., Lee, S. C., and Brinton, E. (2012). Waterproofing crops: effective flooding survival strategies. *Plant Physiol.* 160, 1698–1709. doi: 10.1104/pp.112.208173

Bergholt, N. L., Lysdahl, H., Lind, M., and Foldager, C. B. (2018). A standardized method of applying toluidine blue metachromatic staining for assessment of chondrogenesis. *Cartilage*, 10, 370–374. doi: 10.1177/1947603518764262

Bidhendi, A. J., and Geitmann, A. (2015). Relating the mechanics of the primary plant cell wall to morphogenesis. *J. Exp. Bot.* 67, 449–461. doi: 10.1093/jxb/erv535

Bosch, M., and Hepler, P. K. (2005). Pectin methylesterases and pectin dynamics in pollen tubes. *Plant Cell* 17, 3219–3226. doi: 10.1105/tpc.105.037473

Carlquist, S. (2013). *Comparative wood anatomy: systematic, ecological, and evolutionary aspects of dicotyledon wood* (Newyork NY: Springer Science & Business Media).

Carpita, N. C. (1996). Structure and biogenesis of the cell walls of grasses. *Annu. Rev. Plant Physiol. Plant Mol. Biol.* 47, 445–476. doi: 10.1146/annurev.arplant.47.1.445

Celus, M., Kyomugasho, C., Van Loey, A. M., Grauwet, T., and Hendrickx, M. E. (2018). Influence of Pectin Structural Properties on Interactions with Divalent Cations and Its Associated Functionalities. *Compr. Rev. Food Sci. Food Saf.* 17, 1576–1594. doi: 10.1111/1541-4337.12394

Conforti, P., Ahmed, S., and Markova, G. (2018). Impact of disasters and crises on agriculture and food security, 2017.

Cronk, J. K., and Fennessy, M. S. (2009). "Wetland Plants," in *Encyclopedia of Inland Waters* Editor: G. E. Likens (Oxford: Academic Press), 590–598. doi: 10.1016/B978-012370626-3.00060-0

Daher, F. B., and Braybrook, S. A. (2015). How to let go: pectin and plant cell adhesion. *Front. Plant Sci.* 6, 523. doi: 10.3389/fpls.2015.00523

de Freitas, S. T., Handa, A. K., Wu, Q., Park, S., and Mitcham, E. J. (2012). Role of pectin methylesterases in cellular calcium distribution and blossom-end rot development in tomato fruit. *Plant J.* 71, 824–835. doi: 10.1111/j.1365-313X.2012.05034.x

Demarty, M., Morvan, C., and Thellier, M. (1984). Calcium and the cell wall. *Plant Cell Environ.* 7, 441–448. doi: 10.1111/j.1365-3040.1984.tb01434.x

Dheilly, E., Gall, S., Le,, Guillou, M.-C., Renou, J.-P., Bonnin, E., et al. (2016). Cell wall dynamics during apple development and storage involves hemicellulose modifications and related expressed genes. *BMC Plant Biol.* 16, 201. doi: 10.1186/s12870-016-0887-0

Doocy, S., Daniels, A., Murray, S., and Kirsch, T. D. (2013). The human impact of floods: a historical review of events 1980-2009 and systematic literature review. *PloS Curr.* 5, 1–34. doi: 10.1371/currents.dis.f4deb457904936b07c09daa98ee8171a.

Drew, M. C., He, C.-J., and Morgan, P. W. (2000). Programmed cell death and aerenchyma formation in roots. *Trends Plant Sci.* 5, 123–127. doi: 10.1016/S1360-1385(00)01570-3

Drew, M. C., Jackson, M. B., and Giffard, S. (1980). Ethylene-promoted Adventitious Rooting and Development of Cortical Air Spaces (Aerenchyma) in Roots May be Adaptive Responses to Flooding in Zea mays L. *Planta* 147, 83–88. doi: 10.1007/BF00384595

Esau, K. (1965). Plant anatomy. *Plant Anatomy*.

Evans, D. E. (2004). Aerenchyma formation. *New Phytol.* 161, 35–49. doi: 10.1046/j.1469-8137.2003.00907.x

Foster, R. C. (1967). Fine structure of Tyloses in three species of the Myrtaceae. *Aust. J. Bot.* 15, 25–34. doi: 10.1071/BT9670025

Gladish, D. K., and Niki, T. (2000). Factors inducing cavity formation in the vascular cylinders of pea roots (Pisum sativum L., cv. Alaska). *Environ. Exp. Bot.* 43, 1–9. doi: 10.1016/S0098-8472(99)00038-6

Gladish, D. K., and Niki, T. (2008). Ethylene is involved in vascular cavity formation in pea (Pisum sativum) primary roots. *Plant root* 2, 38–45. doi: 10.3117/plantroot.2.38

Gladish, D. K., Xu, J., and Niki, T. (2006). Apoptosis-like programmed cell death occurs in procambium and ground meristem of pea (Pisum sativum) root tips exposed to sudden flooding. *Ann. Bot.* 97, 895–902. doi: 10.1093/aob/mcl040

Goulao, L. F., Santos, J., de Sousa, I., and Oliveira, C. M. (2007). Patterns of enzymatic activity of cell wall-modifying enzymes during growth and ripening of apples. *Postharvest Biol. Technol.* 43, 307–318. doi: 10.1016/j.postharvbio.2006.10.002

Goulao, L. F., Vieira-Silva, S., and Jackson, P. A. (2011). Association of hemicellulose- and pectin-modifying gene expression with Eucalyptus globulus secondary growth. *Plant Physiol. Biochem.* 49, 873–881. doi: 10.1016/j.plaphy.2011.02.020

Grant, G. T., Morris, E. R., Rees, D. A., Smith, P. J. C., and Thom, D. (1973). Biological interactions between polysaccharides and divalent cations: the egg-box model. *FEBS Lett.* 32, 195–198. doi: 10.1016/0014-5793(73)80770-7

Grover, A., Good, A. G., Dennis, E. S., Hoeren, F. U., Ismond, K. P., Ellis, M., et al. (2000). Molecular strategies for improving waterlogging tolerance in plants. *J. Exp. Bot.* 51, 89–97. doi: 10.1093/jexbot/51.342.89

Gunawardena, A. H. L. A. N., Pearce, D. M. E., Jackson, M. B., Hawes, C. R., and Evans, D. E. (2001a). Rapid changes in cell wall pectic polysaccharides are closely associated with early stages of aerenchyma formation, a spatially localized form of programmed cell death in roots of maize (Zea mays L.) promoted by ethylene. *Plant Cell Environ.* 24, 1369–1375. doi: 10.1046/j.1365-3040.2001.00774.x

Gunawardena, A. H. L. A. N., Pearce, D. M., Jackson, M. B., Hawes, C. R., and Evans, D. E. (2001b). Characterisation of programmed cell death during aerenchyma formation induced by ethylene or hypoxia in roots of maize(Zea mays L.). *Planta* 212, 205–214. doi: 10.1007/s004250000381

He, C. J., Morgan, P. W., and Drew, M. C. (1996). Transduction of an ethylene signal is required for cell death and lysis in the root cortex of maize during Aerenchyma formation induced by hypoxia. *Plant Physiol.* 112, 463–472. 10.1104/pp.112.2.463

Hirabayashi, Y., Mahendran, R., Koirala, S., Konoshima, L., Yamazaki, D., Watanabe, S., et al. (2013). Global flood risk under climate change. *Nat. Clim. Change* 3, 816. doi: 10.1038/nclimate1911

Hocq, L., Pelloux, J., and Lefebvre, V. (2016). Connecting Homogalacturonan-type pectin remodeling to acid growth. doi: 10.1016/j.tplants.2016.10.009.

Hyodo, H., Terao, A., Furukawa, J., Sakamoto, N., Yurimoto, H., Satoh, S., et al. (2013). Tissue specific localization of pectin–Ca(2+) cross-linkages and pectin methyl-esterification during fruit ripening in tomato (Solanum lycopersicum). *PloS One* 8, e78949. doi: 10.1371/journal.pone.0078949

Ishizaki, K. (2015). Development of schizogenous intercellular spaces in plants. *Front. Plant Sci.* 6, 497. doi: 10.3389/fpls.2015.00497

Jackson, M. B., and Armstrong, W. (1999). Formation of aerenchyma and the processes of plant ventilation in relation to soil flooding and submergence. *Plant Biol.* 1, 274–287. doi: 10.1111/j.1438-8677.1999.tb00253.x

Joshi, R., and Kumar, P. (2012). Lysigenous aerenchyma formation involves non-apoptotic programmed cell death in rice (Oryza sativa L.) roots. *Physiol. Mol. Biol. Plants* 18, 1–9. doi: 10.1007/s12298-011-0093-3

Kawase, M. (1981). Effect of ethylene on aerenchyma development. *Am. J. Bot.* 68, 651–658. doi: 10.2307/2442791

Kumpf, R. P., Shi, C.-L., Larrieu, A., Stø, I. M., Butenko, M. A., Péret, B., et al. (2013). Floral organ abscission peptide IDA and its HAE/HSL2 receptors control cell separation during lateral root emergence. *Proc. Natl. Acad. Sci. U. S. A.* 110, 5235–5240. doi: 10.1073/pnas.1210835110

Lampugnani, E. R., Khan, G. A., Somssich, M., and Persson, S. (2018). Building a plant cell wall at a glance. *J. Cell Sci.* 131, jcs207373. doi: 10.1242/jcs.207373

Lashbrook, C. C., and Cai, S. (2008). Cell wall remodeling in Arabidopsis stamen abscission zones: Temporal aspects of control inferred from transcriptional profiling. *Plant Signal. Behav.* 3, 733–736. doi: 10.4161/psb.3.9.6489

Leśniewska, J., Öhman, D., Krzesłowska, M., Kushwah, S., Barciszewska-Pacak, M., Kleczkowski, L. A., et al. (2017). Defense responses in aspen with altered pectin methylesterase activity reveal the hormonal inducers of tyloses. *Plant Physiol.* 173, 1409–1419. doi: 10.1104/pp.16.01443

Leite, D. C. C., Grandis, A., Tavares, E. Q. P., Piovezani, A. R., Pattathil, S., Avci, U., et al. (2017). Cell wall changes during the formation of aerenchyma in sugarcane roots. *Ann. Bot.* 120, 693–708. doi: 10.1093/aob/mcx050

Li, C.-W., Su, R.-C., Cheng, C.-P., Sanjaya,, You, S.-J., Hsieh, T.-H., et al. (2011). Tomato RAV transcription factor is a pivotal modulator involved in the AP2/EREBP-mediated defense pathway. *Plant Physiol.* 156, 213–227. doi: 10.1104/pp.111.174268

Lu, P., Gladish, D., and Rost, T. L. (1991). Temperature-induced cavities and specialized parenchyma cells in the vascular cylinder of pea roots. *Am. J. Bot.* 78, 729–739. doi: 10.2307/2445064

Marcus, S. E., Verhertbruggen, Y., Hervé, C., Ordaz-Ortiz, J. J., Farkas, V., Pedersen, H. L., et al. (2008). Pectic homogalacturonan masks abundant sets of xyloglucan epitopes in plant cell walls. *BMC Plant Biol.* 8, 60. doi: 10.1186/1471-2229-8-60

Micco, V., Balzano, A., Wheeler, E., and Baas, P. (2016). Tyloses and gums: A review of structure, function and occurrence of vessel occlusions. doi: 10.1163/22941932-20160130.

Mühlenbock, P., Plaszczyca, M., Plaszczyca, M., Mellerowicz, E., and Karpinski, S. (2007). Lysigenous aerenchyma formation in Arabidopsis is controlled by LESION SIMULATING DISEASE1. *Plant Cell* 19, 3819–3830. doi: 10.1105/tpc.106.048843

Mustroph, A. (2018). Improving flooding tolerance of crop plants. *Agron* 8, 160. doi: 10.3390/agronomy8090160

Niki, T., and Gladish, D. K. (2001). Changes in Growth and Structure of Pea Primary Roots (Pisum sativum L. cv. Alaska) as a Result of Sudden Flooding. *Plant Cell Physiol.* 42, 694–702. doi: 10.1093/pcp/pce086

Niki, T., Gladish, D. K., Lu, P., and Rost, T. (1995). Cellular Changes Precede Cavity Formation in the Vascular Cylinders of Pea Roots (Pisum sativum L. cv Alaska). doi: 10.1086/297250.

Niki, T., Rost, T. L., and Gladish, D. K. (1998). Regeneration of tissue following cavity formation in the vascular cylinders of Pisum sativum (Fabaceae) primary roots. *Am. J. Bot.* 85, 17–24. doi: 10.2307/2446549

Niki, T., Saito, S., and K Gladish, ,. D. (2014). doi: 10.1007/s00709-014-0622-3. Granular bodies in root primary meristem cells of Zea mays L. var. Cuscoensis K. (Poaceae) that enter young vacuoles by invagination: a novel ribophagy mechanism.

Nord, E. A., Chimungu, J. G., Brown, K. M., Jaramillo, R. E., and Lynch, J. P. (2013). Root cortical burden influences drought tolerance in maize. *Ann. Bot.* 112, 429–437. doi: 10.1093/aob/mct069

O'Brien, T. P., Feder, N., and McCully, M. E. (1964). Polychromatic staining of plant cell walls by toluidine blue O. *Protoplasma* 59, 368–373. doi: 10.1007/BF01248568

Ochoa-Villarreal, M., Aispuro, E., Vargas-Arispuro, I., and Martínez-Téllez, M. (2012). "Plant cell wall polymers: function, structure and biological activity of their derivatives,". doi: 10.5772/46094.

Pallardy, S. G. (2008). "CHAPTER 3 - Vegetative Growth," in *Physiology of Woody Plants*, *3rd ed*Ed. S. G. Pallardy (San Diego: Academic Press), 39–86. doi: 10.1016/B978-012088765-1.50004-X

Paniagua, C., Posé, S., Morris, V. J., Kirby, A. R., Quesada, M. A., and Mercado, J. A. (2014). Fruit softening and pectin disassembly: an overview of nanostructural pectin modifications assessed by atomic force microscopy. *Ann. Bot.* 114, 1375–1383. doi: 10.1093/aob/mcu149

Pegg, T. J., Edelmann, R. E., and Gladish, D. K. (2018). Progression of cell wall matrix alterations during Aerenchyma formation in Pisum sativum root cortical cells. doi: 10.1017/S1431927618007377.

Péret, B., Larrieu, A., and Bennett, M. J. (2009). Lateral root emergence: a difficult birth. *J. Exp. Bot.* 60, 3637–3643. doi: 10.1093/jxb/erp232

Pérez-Pérez, Y., Carneros, E., Berenguer, E., Solís, M.-T., Bárány, I., Pintos, B., et al. (2019). Pectin De-methylesterification and AGP increase promote cell wall remodeling and are required during somatic embryogenesis of quercus suber. *Front. Plant Sci.* 9, 1915. doi: 10.3389/fpls.2018.01915

Porco, S., Larrieu, A., Du, Y., Gaudinier, A., Goh, T., Swarup, K., et al. (2016). Lateral root emergence in Arabidopsis is dependent on transcription factor LBD29 regulation of auxin influx carrier LAX3. *Development* 143, 3340–3349. doi: 10.1242/dev.136283

Postma, J. A., and Lynch, J. P. (2011). Root cortical aerenchyma enhances the growth of maize on soils with suboptimal availability of nitrogen, phosphorus, and potassium. *Plant Physiol.* 156, 1190–1201. doi: 10.1104/pp.111.175489

Printz, B., Lutts, S., Hausman, J.-F., and Sergeant, K. (2016). Copper trafficking in plants and its implication on cell wall dynamics. *Front. Plant Sci.* 7, 601. doi: 10.3389/fpls.2016.00601

Qu, L., Wu, C., Zhang, F., Wu, Y., Fang, C., Jin, C., et al. (2016). Rice putative methyltransferase gene OsTSD2 is required for root development involving pectin modification. *J. Exp. Bot.* 67, 5349–5362. doi: 10.1093/jxb/erw297

Rajhi, I., Yamauchi, T., Takahashi, H., Nishiuchi, S., Shiono, K., Watanabe, R., et al. (2011). Identification of genes expressed in maize root cortical cells during lysigenous aerenchyma formation using laser microdissection and microarray analyses. *New Phytol.* 190, 351–368. doi: 10.1111/j.1469-8137.2010.03535.x

Rost, T. L., Lu, P., and Gladish, D. (1991). The occurrence of vascular cavities and specialized parenchyma cells in the roots of cool-season legumes. *Bot. Acta* 104, 300–305. doi: 10.1111/j.1438-8677.1991.tb00234.x

Sarkar, P., and Gladish, D. K. (2012). Hypoxic stress triggers a programmed cell death pathway to induce vascular cavity formation in Pisum sativum roots. *Physiol. Plant* 146, 413–426. doi: 10.1111/j.1399-3054.2012.01632.x

Sarkar, P., Niki, T., and Gladish, D. K. (2008). Changes in cell wall ultrastructure induced by sudden flooding at 25°C in Pisum sativum (Fabaceae) primary roots. *Am. J. Bot.* 95, 782–792. doi: 10.3732/ajb.2007381

Sénéchal, F., Wattier, C., Rustérucci, C., and Pelloux, J. (2014). Homogalacturonan-modifying enzymes: structure, expression, and roles in plants. *J. Exp. Bot.* 65, 5125–5160. doi: 10.1093/jxb/eru272

Shimamura, S., Yamamoto, R., Nakamura, T., Shimada, S., and Komatsu, S. (2010). Stem hypertrophic lenticels and secondary aerenchyma enable oxygen transport to roots of soybean in flooded soil. *Ann. Bot.* 106, 277–284. doi: 10.1093/aob/mcq123

Takahashi, M., Niki, T., Deem, K. D., and Gladish, D. K. (2016). Vascular cavity formation enhances oxygen availability during flooding in root tips of Phaseolus coccineus L. primary roots. *Int. J. Plant Sci.* 177, 277–286. doi: 10.1086/684524

Tavares, E. Q. P., De Souza, A. P., Romim, G. H., Grandis, A., Plasencia, A., Gaiarsa, J. W., et al. (2019). The control of endopolygalacturonase expression by the sugarcane RAV transcription factor during aerenchyma formation. *J. Exp. Bot.* 70, 497–506. doi: 10.1093/jxb/ery362

Valliyodan, B., Ye, H., Song, L., Murphy, M., Shannon, J. G., and Nguyen, H. T. (2016). Genetic diversity and genomic strategies for improving drought and waterlogging tolerance in soybeans. *J. Exp. Bot.* 68, 1835–1849. doi: 10.1093/jxb/erw433

Vicré, M., Sherwin, H. W., Driouich, A., Jaffer, M. A., and Farrant, J. M. (1999). Cell wall characteristics and structure of hydrated and dry leaves of the resurrection plant craterostigma wilmsii, a microscopical study. *J. Plant Physiol.* 155, 719–726. doi: 10.1016/S0176-1617(99)80088-1

Vilches-Barro, A., and Maizel, A. (2015). Talking through walls: mechanisms of lateral root emergence in Arabidopsis thaliana. *Curr. Opin. Plant Biol.* 23, 31–38. doi: 10.1016/j.pbi.2014.10.005

Voragen, A. G. J., Coenen, G.-J., Verhoef, R. P., and Schols, H. A. (2009). Pectin, a versatile polysaccharide present in plant cell walls. *Struct. Chem.* 20, 263. doi: 10.1007/s11224-009-9442-z

Waldenmaier, H. E. (2011). Transcriptome analysis of vascular cavity formation in soybean cv. "Yukihomare" seedlings in response to flooding. Available at: http://rave.ohiolink.edu/etdc/view?accnum=miami1313012579 . .

Wolf, S., Mouille, G., and Pelloux, J. (2009). Homogalacturonan methyl-esterification and plant development. *Mol. Plant* 2, 851–860. doi: 10.1093/mp/ssp066

Wu, H.-C., Bulgakov, V. P., and Jinn, T.-L. (2018). Pectin methylesterases: cell wall remodeling proteins are required for plant response to heat stress. *Front. Plant Sci.* 9, 1612. doi: 10.3389/fpls.2018.01612

Xue, J., Bosch, M., and Knox, J. P. (2013). Heterogeneity and glycan masking of cell wall microstructures in the stems of miscanthus x giganteus, and its Parents M. sinensis and M. sacchariflorus. *PloS One* 8, e82114. doi: 10.1371/journal.pone.0082114

Yamada, Y., Koibuchi, M., Miyamoto, K., Ueda, J., and Uheda, E. (2015). Breakdown of middle lamella pectin by •OH during rapid abscission in Azolla. *Plant Cell Environ.* 38, 1555–1564. doi: 10.1111/pce.12505

Yamauchi, T., Shimamura, S., Nakazono, M., and Mochizuki, T. (2013). Aerenchyma formation in crop species: a review. *F. Crop Res.* 152, 8–16. doi: 10.1016/j.fcr.2012.12.008

Yamauchi, T., Yoshioka, M., Fukazawa, A., Mori, H., Nishizawa, N. K., Tsutsumi, N., et al. (2017). An NADPH oxidase RBOH functions in rice roots during lysigenous aerenchyma formation under oxygen-deficient conditions. *Plant Cell* 29, 775–790. doi: 10.1105/tpc.16.00976

Zhao, X. H., Liu, L. Y., Nan, L. J., Wang, H., and Li, H. (2014). Development of tyloses in the xylem vessels of Meili grapevine and their effect on water transportation. *Russ. J. Plant Physiol.* 61, 194–203. doi: 10.1134/S1021443714020198

Zhu, J., Brown, K. M., and Lynch, J. P. (2010). Root cortical aerenchyma improves the drought tolerance of maize (Zea mays L.). *Plant Cell Environ.* 33, 740–749. doi: 10.1111/j.1365-3040.2009.02099.x

Conflict of Interest: The authors declare that the research was conducted in the absence of any commercial or financial relationships that could be construed as a potential conflict of interest.

frontiers in Plant Science

REVIEW
published: 12 August 2020
doi: 10.3389/fpls.2020.01235

Stressed to Death: The Role of Transcription Factors in Plant Programmed Cell Death Induced by Abiotic and Biotic Stimuli

*Rory Burke, Johanna Schwarze†, Orla L. Sherwood†, Yasmine Jnaid, Paul F. McCabe and Joanna Kacprzyk**

School of Biology and Environmental Science, University College Dublin, Dublin, Ireland

Programmed cell death (PCD) is a genetically controlled pathway that plants can use to selectively eliminate redundant or damaged cells. In addition to its fundamental role in plant development, PCD can often be activated as an essential defense response when dealing with biotic and abiotic stresses. For example, localized, tightly controlled PCD can promote plant survival by restricting pathogen growth, driving the development of morphological traits for stress tolerance such as aerenchyma, or triggering systemic pro-survival responses. Relatively little is known about the molecular control of this essential process in plants, especially in comparison to well-described cell death models in animals. However, the networks orchestrating transcriptional regulation of plant PCD are emerging. Transcription factors (TFs) regulate the clusters of stimuli inducible genes and play a fundamental role in plant responses, such as PCD, to abiotic and biotic stresses. Here, we discuss the roles of different classes of transcription factors, including members of NAC, ERF and WRKY families, in cell fate regulation in response to environmental stresses. The role of TFs in stress-induced mitochondrial retrograde signaling is also reviewed in the context of life-and-death decisions of the plant cell and future research directions for further elucidation of TF-mediated control of stress-induced PCD events are proposed. An increased understanding of these complex signaling networks will inform and facilitate future breeding strategies to increase crop tolerance to disease and/or abiotic stresses.

Keywords: programmed cell death, abiotic stress, biotic stress, transcription factors, plants

OPEN ACCESS

Edited by:
Diane C. Bassham,
Iowa State University, United States

Reviewed by:
Caiji Gao,
South China Normal University, China
Zhixiang Chen,
Purdue University, United States

***Correspondence:**
Joanna Kacprzyk
joanna.kacprzyk@ucd.ie

†These authors have contributed equally to this work

Specialty section:
This article was submitted to Plant Cell Biology, a section of the journal Frontiers in Plant Science

Received: *26 May 2020*
Accepted: *28 July 2020*
Published: *12 August 2020*

Citation:
Burke R, Schwarze J, Sherwood OL, Jnaid Y, McCabe PF and Kacprzyk J (2020) Stressed to Death: The Role of Transcription Factors in Plant Programmed Cell Death Induced by Abiotic and Biotic Stimuli. Front. Plant Sci. 11:1235. doi: 10.3389/fpls.2020.01235

INTRODUCTION

Programmed cell death (PCD) is a genetically controlled pathway of organized cell destruction (Danon et al., 2000). PCD is not only an essential element of plant development (Daneva et al., 2016), but also a part of the arsenal of defense responses against biotic and abiotic environmental stresses (Locato and De Gara, 2018). The classic example is the hypersensitive response (HR), a rapid cell death at the initial infection site activated to restrict the growth of biotrophic pathogens (Heath, 2000). Localized PCD events can also improve the plant's ability to withstand abiotic

stresses, for example, selective cell death triggered in the root stem cell niche was recently identified as an integral part of the cold acclimation process (Hong et al., 2017). Likewise, PCD plays a central role in plant adaptation to hypoxic conditions by mediating the formation of lysigenous aerenchyma, a porous tissue comprising internal spaces and channels to transport gases between plant shoots and roots (Evans, 2004). While aerenchyma formation is the key adaptive trait for waterlogging tolerance (Mustroph, 2018), it can also be induced under aerobic conditions by other abiotic stresses. Its formation converts living cortical tissue to air volume, thereby improving plant carbon economy, and reducing the respiratory and nutrient cost of soil exploration. Aerenchyma formation has also been reported to enhance nutrient stress adaptation (Fan et al., 2003; Saengwilai et al., 2014), as well as improve drought (Zhu et al., 2010) and salt (Saqib et al., 2005; Akcin et al., 2015) tolerance in different plant species. PCD can be also considered a protective mechanism when triggered by the excess excitation energy stress, leading to signal transduction to systemic cells and their acclimation to high light (Wituszyńska and Karpiński, 2013). However, PCD is not always beneficial to the plant: its activation can be an infection strategy for necrotrophic pathogens (Coll et al., 2011) and extensive PCD caused by severe abiotic stress may result in crop yield losses. Climate change is associated with increasing frequency of extreme weather events such as heavy rainfall, droughts, and heatwaves (USGCRP et al., 2017) that exacerbate abiotic stresses and plant diseases, challenging the global crop productivity. Therefore, there is a growing pressure to elucidate the complex regulatory networks behind plant pro-survival strategies, including those involving the tightly controlled activation of PCD in specific cells in response to environmental stimuli. Our understanding of plant PCD is still lagging behind that of animal cell death programs. Although recent progress in the field has identified a plethora of new PCD regulators, the complex molecular networks responsible for coordinating plant PCD are only just beginning to emerge (Daneva et al., 2016). In animals, the *bona fide* core PCD machinery is mainly regulated post-translationally (Fuchs and Steller, 2011), however, there are exceptions: *egl-1*, the key activator of the execution phase of apoptotic cell death in *Caenorhabditis elegans* (Horvitz, 2003) is expressed at a detectable level predominantly in cells programmed to die (Conradt et al., 2016). Additionally, the cell death pathway can be promoted and repressed by transcriptional regulators (Zhai et al., 2012; Aubrey et al., 2018). At least some level of transcriptional control of the cell death process is also likely in plants, where blocking transcription using *de novo* RNA synthesis inhibitor actinomycin D can both alleviate (Masuda et al., 2003; Vacca et al., 2004) and induce PCD (Ning et al., 2001). Transcription factors (TFs) are central players in eukaryotic gene regulation, binding to DNA in a sequence specific manner and promoting or inhibiting the activity of a transcription initiation complex (Voss and Hager, 2014). TFs may therefore act as molecular switches to regulate clusters of stimuli responsive genes (Pradhan et al., 2019). The involvement of major plant TF classes in a range of developmentally controlled PCD events was recently comprehensively discussed (Cubría-Radío and Nowack, 2019). Here, our aim is to discuss the role of TFs in PCD induced by various environmental stimuli, both abiotic and biotic in nature (**Figure 1**).

NAC TRANSCRIPTION FACTORS

NAC TFs comprise one of the largest and most studied TFs families in plants. They contain a conserved DNA binding N-terminus and a more variable, transcription regulating, C-terminus (Ooka et al., 2003; Olsen et al., 2005). Several NACs have been linked to regulation of PCD triggered by abiotic and biotic stresses. NAC TFs have been implicated in regulation of the HR (Yuan et al., 2019). For example, OsNAC4 has been shown to positively regulate the HR by modulating the expression of almost 150 genes in rice (Kaneda et al., 2009). The OsNAC4 regulome included OsHSP90 and IREN, that act in parallel to induce HR PCD. Expression of *OsHSP90* is associated with the loss of plasma membrane integrity but not DNA fragmentation, while IREN, an endonuclease, is responsible for DNA degradation but alone does not affect plasma membrane integrity or induce cell death (Kaneda et al., 2009). The *Arabidopsis* NAC4 homologue, ANAC080 promotes cell death in response to bacterial infection by suppressing the transcription of three target genes; *LURP1*, *WRKY40*, and *WRKY54*, which negatively regulate PCD (Lee et al., 2017). The leaves of *ANAC080* overexpressing plants display accelerated and rapidly spreading PCD following infection with *Pseudomonas syringae*, while in null mutants cell death spread was delayed. *ANAC080* itself is negatively regulated by a microRNA 164, allowing fine-tuning of the appropriate immune response and ensuring that PCD is tightly controlled (Lee et al., 2017).

Several NAC TFs are also involved in cell death induced by ER stress. The accumulation of misfolded proteins in the ER triggers the unfolded protein response (UPR), a widely conserved pro-survival mechanism (Calfon et al., 2002). However, extreme, or prolonged ER stress can lead to the activation of PCD (Zuppini et al., 2004). Many environmental stimuli, such as salinity, heat, drought, osmotic stress, and pathogens, can evoke the ER stress responses (Park and Park, 2019). In soybean, programmed cell death induced by both ER and osmotic stress was linked to GmNAC30 and GmNAC81 (Faria et al., 2011; Mendes et al., 2013). The GmNAC30 and GmNAC81TFs form homo- or heterodimers and may act as both transcriptional activators or repressors, with their ability to promote PCD linked to transactivation of the *vacuolar processing enzyme* (*VPE*) gene by a NAC81/NAC30 heterodimer (Mendes et al., 2013). VPE is responsible for the caspase-1 activity and may contribute to PCD *via* the activation of vacuolar proteases and subsequent vacuole collapse (Hatsugai et al., 2006). Another NAC, NAC089 was implicated in ER stress induced PCD in *Arabidopsis* (Yang et al., 2014). Similarly to NAC81/NAC30 dimer, ANAC089 promotes the induction of caspase-like activity during ER stress induced PCD, and also appears to regulate other downstream PCD-

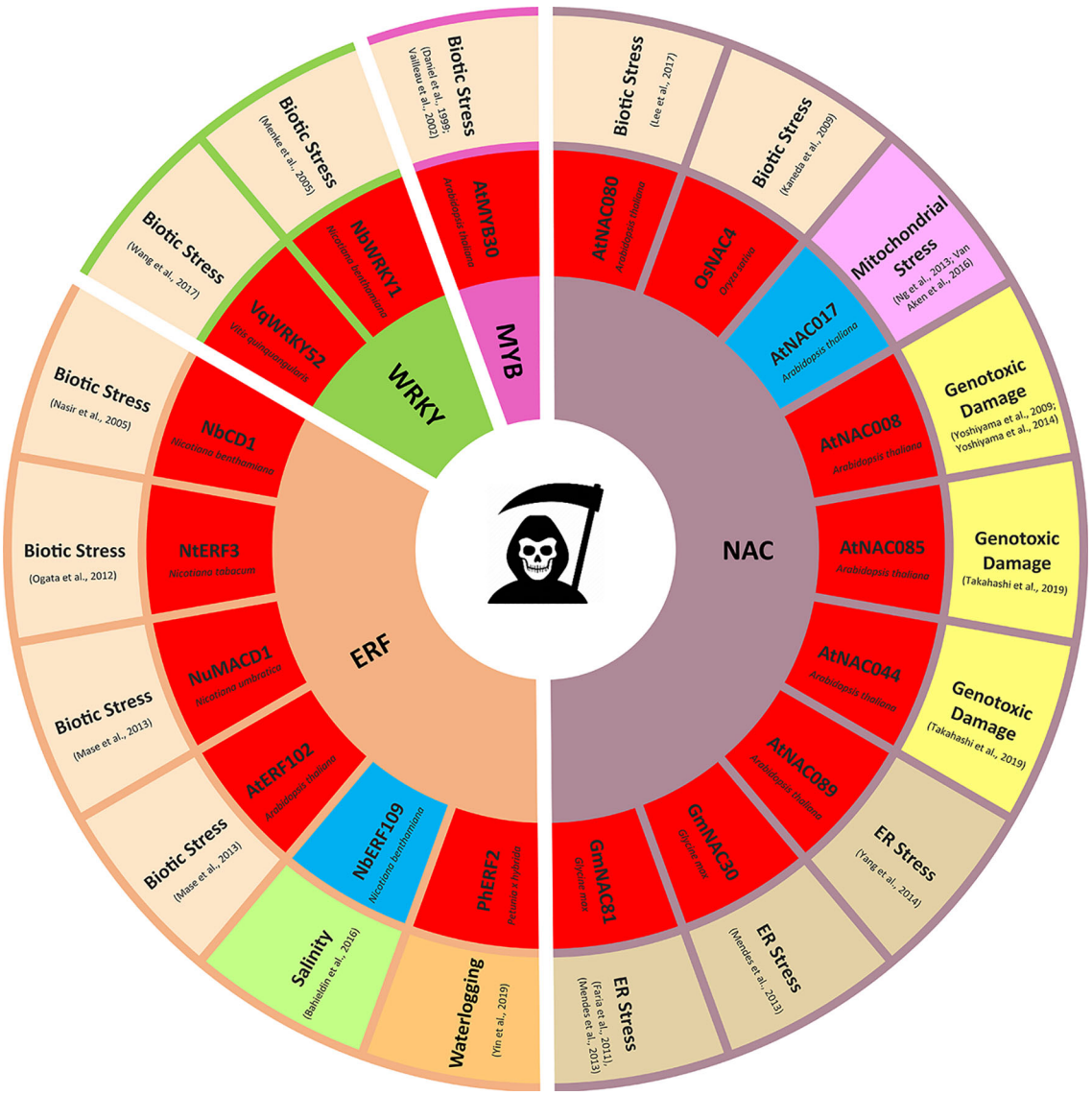

FIGURE 1 | Transcription factors regulating stress induced programmed cell death (PCD). Only transcription factors (TFs) with experimentally validated role in PCD regulation are presented. TFs promoting PCD are highlighted in red, TFs suppressing PCD are highlighted in blue.

associated genes including *BAG6* (*Bcl-2-associated athanogene family member*) and *MC5* (*metacaspase 5*). The transcription of *NAC089* is itself promoted by two membrane bound TFs, bZIP28 and bZIP60, highlighting the multiple levels of regulation involved in initiating the PCD cascade (Yang et al., 2014). In rapeseed, four NAC TFs (BnaNAC55, BnaNAC56, BnaNAC87, and BnaNAC103) have separately been shown to be involved in PCD following treatment with diverse abiotic stressors (Niu et al., 2014; Niu et al., 2016; Chen et al., 2017; Yan et al., 2017). In all cases, expression of the respective TF resulted in the development of HR-like lesions, reactive oxygen species (ROS) accumulation, and DNA degradation, however, the molecular mechanisms by which these TFs induce cell death has not been examined.

PCD is commonly induced following severe genotoxic stress in order to protect the organism from deleterious DNA mutations. This process initially involves cell cycle arrest and attempts at DNA repair, with apoptosis initiated if the damage is too severe (Norbury and Zhivotovsky, 2004). In animals this DNA damage response is largely coordinated by p53, a constitutively expressed TF that is stabilized *via* phosphorylation by four DNA damage sensing kinases; ATM, ATR, CHK1, and CHK2 (Lavin and Gueven, 2006). p53 not only induces apoptosis by regulating the transcription of apoptotic genes but also translocates to the mitochondria where it can modulate mitochondrial outer membrane permeabilization (MOMP) *via* direct interactions with pro- and anti-apoptotic proteins (Vaseva and Moll, 2009). Although several key DNA damage response genes such as *ATM*

and *ATR* are conserved across plants and animals, *p53* is not (Culligan et al., 2006). Instead, plants have developed a functional homolog of p53, SOG1/ANAC008, which fulfills similar functions in coordinating the DNA damage response (Yoshiyama et al., 2009; Yoshiyama et al., 2014). The root meristematic stem cell niche and its early descendants are hypersensitive to genotoxic stress (Fulcher and Sablowski, 2009), and undergo a selective type of PCD that is mediated by SOG1 and requires *de novo* protein synthesis (Furukawa et al., 2010). More recently it has been established that SOG1/ANAC008 is necessary not only to trigger PCD in these cell populations but also to mediate a regenerative response in meristematic tissue for the stem cell niche replenishment (Johnson et al., 2018). The SOG1 direct targets include genes implicated in response to abiotic stresses and pathogen infection (Ogita et al., 2018). Two of SOG1 targets, *ANAC044* and *ANAC085*, are its closest relatives in the NAC TF family and were suggested to also participate in SOG1-mediated induction of stem cell death (Takahashi et al., 2019). However, it is not clear which key downstream PCD effectors are controlled by SOG1/ANAC008 signaling. Chilling stress was shown to induce DNA damage dependent cell death of columella stem cell daughters (Hong et al., 2017). This highly localized cell death appeared to protect the stem cell niche from chilling stress and improve the root's ability to withstand the accompanying environmental stresses and resume growth (Hong et al., 2017). Considering the role of SOG1/ANAC008, ANAC044, and ANAC085 in regulation of PCD induced by DNA damage, it would be interesting to test the effect of these TFs on adaptation and survival of roots under the chilling stress.

The role of NAC TFs in lysigenous aerenchyma formation is also slowly emerging. The meta-analysis of quantitative trait loci (QTL) associated with abiotic stress tolerance identified a NAC domain TF as a key candidate gene for aerenchyma formation in barley (*Hordeum vulgare*) under waterlogging conditions (Zhang et al., 2017b). Several NAC TFs were linked to aerenchyma formation also in rice (*Oryza sativa*). For example, transgene overexpression of stress-inducible *OsNAC5* and *OsNAC9* resulted in enhanced aerenchyma formation in rice, especially under the root-specific promoter, and correlated with enhanced drought and salinity tolerance (Redillas et al., 2012; Jeong et al., 2013). Rice offers an interesting model for further studies delineating the transcriptional regulation of developmental and environmentally induced lysigenous aerenchyma, as this tissue forms constitutively in rice roots but is further induced by flooding (Yamauchi et al., 2013).

ETHYLENE RESPONSIVE ELEMENT BINDING FACTORS TRANSCRIPTION FACTORS IN THE REGULATION OF PLANT PROGRAMMED CELL DEATH

The ethylene responsive element binding factors (ERFs) belong to the AP2/ERF superfamily, characterized by the presence of one (in ERF) or two (in AP2) 60-70 residue AP2/ERF DNA binding domains (Nakano et al., 2006). This expansive group of transcriptional regulators display a wide range of roles in responding to various forms of abiotic stress (Mizoi et al., 2012; Li et al., 2017; Najafi et al., 2018). MACD1 and ERF102 are two ERFs linked to phytotoxin induced cell death (Mase et al., 2013) and both act downstream of ethylene signaling and are positive regulators of programmed cell death induced by the phytotoxins AAL and fumonisin B1. ERF TFs are also involved in regulation of HR PCD, for example NbCD1 is an ERF that is expressed in response to multiple HR elicitors, and its conditional expression is sufficient to induce cell death (Nasir et al., 2005). Expression of *NbCD1* also results in high levels of H_2O_2 generation, ion leakage, and DNA fragmentation. Additionally, NbCD1 modulates transcription *via* its ERF-associated amphiphilic repression (EAR) motif. NbCD1 positively regulates HR cell death by suppressing the transcription of almost 60 genes, including *HSR203*, a negative regulator of the HR (Nasir et al., 2005). The tobacco transcriptional repressor NtERF3 is another EAR motif containing TF that has been identified as an inducer of HR-associated PCD following Tobacco mosaic virus infection (Ogata et al., 2012). As with *NbCD1*, overexpression of *NtERF3* was sufficient to induce HR-like lesions on tobacco leaves, while deletion of the EAR motif from this TF prevented the HR cell death. Subsequent analysis of the *Arabidopsis*, rice, and tobacco genomes enabled the identification of dozens of closely related group VIII ERF genes (Ogata et al., 2013). Interestingly, overexpression of several group VIII-a ERFs (containing an EAR-motif) induced cell death, while overexpression of group VIII-b ERFs (lacking an EAR-motif) failed to induce cell death morphology in *Arabidopsis* (Ogata et al., 2013). However, the degree of cell death induced by different EAR-motif containing ERFs varied significantly, and the expression of fusion proteins consisting of group VIII-b ERFs fused to EAR motifs also failed to induce cell death, suggesting that the presence of an EAR motif alone is not sufficient to induce a transcriptional program resulting in PCD (Ogata et al., 2013).

ERF TFs are also involved in the regulation of PCD induced by abiotic stress. For example, ERF109 is implicated in salt stress tolerance, acting as a negative regulator of PCD in *Arabidopsis* (Bahieldin et al., 2016). This TF prevents PCD by inducing expression of *Bax-inhibitor 1*, which inhibits the pro-apoptotic Bax protein (Bahieldin et al., 2016). Ethylene is involved in lysigenous aerenchyma formation (Yamauchi et al., 2013) and treatment with ethylene inhibitors decreases aerenchyma formation under hypoxia (Drew et al., 1981; Gunawardena et al., 2001a). ERFs have been linked to both aerenchyma formation and waterlogging tolerance in several species and recently, the PhERF2 TF was found to modulate PCD during waterlogging response in petunia (Yin et al., 2019). Overexpression of *PhERF2* increased survival of waterlogged seedlings while the silencing lines exhibited compromised waterlogging tolerance with increased leaf chlorosis and necrosis. The root cells of *PhERF2* overexpressor plants displayed condensed, moon-shaped nuclei, characteristic of PCD, suggesting that this TF may positively regulate aerenchyma formation (Yin et al., 2019). Multiple transcriptome profiling analyses reported differential expression of ERFs in response to conditions inducing aerenchyma, such as waterlogging and hypoxia (Rajhi et al., 2011; Safavi-Rizi et al.,

2020) or in tissues undergoing developmental aerenchyma formation (Yoo et al., 2015; Du et al., 2018). However, functional validation studies are required to determine if the identified ERFs indeed contribute to aerenchyma induction. RAV1 seems to be a promising candidate, as the *RAV1-like* gene was induced specifically in maize cortical cells (aerenchyma-forming tissue) in response to waterlogging and this up-regulation was blocked upon pretreatment with ethylene perception inhibitor 1-methylcyclo-propene (1-MCP) (Rajhi et al., 2011). *RAV1* was later proposed to underlie Subtol6, a major QTL associated with submergence tolerance in maize (Campbell et al., 2015). The RAV1 TF was also suggested to regulate the initial steps of constitutive aerenchyma formation in sugarcane that involve cell wall polysaccharide modifications (Tavares et al., 2019). This is in line with work by Gunawardena et al. (2001b) who proposed that one of the earliest, ethylene-promoted, changes associated with aerenchyma formation are the alterations to cell wall polysaccharides. The role of RAV1 in regulation of PCD is plausible, as RAV1 overexpression in *Arabidopsis* results in accelerated senescence (Woo et al., 2010) and a *RAV1* homologue was strongly induced in pepper leaves during the early response to pathogen infection, abiotic elicitors, and environmental stresses (Sohn et al., 2006). *RAV1* itself might be regulated post-transcriptionally by microRNAs (Tavares Queiroz de Pinho et al., 2020), allowing tightly controlled expression of its target genes.

WRKY TRANSCRIPTION FACTORS IN PROGRAMMED CELL DEATH REGULATION

WRKY transcription factors are a diverse group of transcriptional regulators that integrate plant responses to environmental stress and regulate development (Bakshi and Oelmuller, 2014). WRKY TFs are categorized by the presence of 60 conserved amino acid residues at the N-terminus (Bakshi and Oelmüller, 2014; Phukan et al., 2016). The WRKY TF family targets genes containing a CRE containing W-box element (TGAC) (Eulgem et al., 2000). Several WRKY TFs are involved in the regulation of cell death during biotic stress. In tobacco, WRKY1 was first identified as a positive regulator of HR PCD, following its phosphorylation and activation by the salicylic acid (SA) induced kinase SIPK (Menke et al., 2005). WRKY18, WRKY40, and WRKY60 also modulate transcription of pathogen responsive genes *via* the formation of homo- or heterodimers (Xu et al., 2006). A triple knockout *Arabidopsis* line lacking all three TFs was more susceptible to infection by *Botrytis cinerea*, a necrotrophic fungal pathogen that promotes host cell death in a HR-like manner. The same KO line displayed increased resistance to *P. syringae*, a bacterial pathogen that is biotrophic during the early stages of infection (Xu et al., 2006). This suggests that this network of WRKY TFs may function to suppress HR cell death during the initial infection, although the transcriptional program they promote to achieve this has not yet been identified. The WRKY52 TF from the grapevine (*Vitis quinquangularis*) has the opposite role, as transgenic expression of *VqWRKY52* in *Arabidopsis* results in significantly greater cell death following infection by both *B. cinerea* and *P. syringae*, and thus increased and reduced susceptibility to the necrotrophic and biotrophic pathogens respectively (Wang et al., 2017). Finally, transient expression of phospho-mimicking mutants of *WRKY7*, *8*, *9*, *11*, *12*, and *14* is sufficient to induce cell death in *Nicotiana benthamiana*, with these TFs appearing to act downstream of a MAPK phosphorylation cascade (Adachi et al., 2015). Interestingly, the degree of cell death induced by these TFs was correlated to their ability to induce a respiratory burst oxidase homologue (RBOH) derived ROS burst, which has previously been shown to be required for resistance to biotic and abiotic stress, and for certain forms of PCD (Xie et al., 2014; Li et al., 2015). However, the relevance of such experiments involving phospho-mutants to physiological HR mechanisms is not clear.

Transcriptomic analyses suggested that WRKY TFs can regulate constitutive and environmentally induced lysigenous aerenchyma induction in rice (Yoo et al., 2015; Viana et al., 2018). However, *WRKY53* and *WRKY33* showed higher expression under submergence conditions in the waterlogging sensitive maize genotypes compared to tolerant lines (Campbell et al., 2015). Further research is therefore required to delineate the role of WRKYs in aerenchyma formation, which may differ between developmentally or environmentally induced aerenchyma. Interestingly, *HaWRKY76*, a divergent transcription factor from sunflower, conferred submergence tolerance when overexpressed in *Arabidopsis*, which in part can be linked to enhanced formation of lysigenous stem aerenchyma (Raineri et al., 2015).

OTHER TRANSCRIPTION FACTORS CONTRIBUTING TO MODULATION OF ENVIRONMENTALLY INDUCED PROGRAMMED CELL DEATH

Several other TF classes are also likely to contribute to the transcriptional regulation of life-and-death decisions in response to environmental stress. Auxin response factors (ARFs), which bind to auxin response elements (Li et al., 2016) and similarly to other TF families, possess an N-terminal DNA binding domain combined with a C-terminal domain suited to protein-protein interactions (Ulmasov et al., 1997). Although ARFs are typically associated with growth and developmental processes, their involvement in PCD regulation is possible, as supplementation of auxin or auxin analogues has been shown to block PCD following biotic and abiotic stresses such as exposure to the bacterial effector thaxtomin A or photorespiratory induced oxidative stress (Kerchev et al., 2015; Awwad et al., 2019). The molecular mechanisms responsible for this death-suppressing effect and potential involvement of ARFs require further research. The interplay between auxin and ethylene was suggested to regulate aerenchyma formation in maize under waterlogging stress where the auxin associated genes such as *IAA3*, *IAA14*, and *IAA16* were shown to be upregulated in the tolerant genotypes (Thirunavukkarasu et al., 2013). The IAAs are the short-lived, early auxin response proteins that interact with

ARFs and inhibit the transcription of their target genes (Luo et al., 2018). The IAAs- and ARFs- dependent auxin signaling was also linked to formation of constitutive aerenchyma in rice (Yoo et al., 2015; Yamauchi et al., 2019).

Another family of TFs linked to plant PCD modulation are the MYBs, a diverse family of eukaryotic transcription modulators with roles in both development and stress responses (Dubos et al., 2010). In *Arabidopsis*, AtMYB30 is a positive regulator of HR cell death, that was initially discovered due to its strong upregulation immediately following infection with HR inducing bacterial effectors (Daniel et al., 1999; Vailleau et al., 2002). The expression of *AtMYB30* is dependent on SA accumulation, and plants with knock-down, knock-out, or overexpression mediated perturbations in AtMYB30 levels in turn display altered SA levels, suggesting that the TF functions at least partially as an SA signaling amplification loop (Raffaele et al., 2006). It has been subsequently shown that AtMYB30 enhances the expression of several genes involved in very long chain fatty acid (VLCFA) synthesis and may also promote PCD by utilizing VLCFAs or their derivatives as cell death messaging molecules (Raffaele et al., 2008). The ectopic expression of rapeseed (*Brassica napus*) *BnaMYB78* in *N. benthamiana* has also been shown to induce a form of HR-like cell death associated with H_2O_2 production, although the function of this TF in *B. napus* or indeed of its *Arabidopsis* homologue remain to be investigated (Chen et al., 2016). Many MYB TFs have been proposed as putative regulators of aerenchyma formation by transcriptome profiling studies (Thirunavukkarasu et al., 2013; Valliyodan et al., 2014) and a meta-analysis of major QTL for waterlogging tolerance (Zhang et al., 2017b). During hypoxic treatment of wheat roots, expression of the *TaMyb1*, when analyzed using *in situ* hybridization, was elevated in root epidermal, endodermal, and cortex tissue peripheral to aerenchyma containing cortex (Lee et al., 2006). Further examination of the expression pattern of this TF sequentially during aerenchyma formation may provide more insights into its role in hypoxia responses. The MYB transcription factors *S4877491* and *S4910460* showed higher expression during flooding in waterlogging tolerant soybean genotype with enhanced aerenchyma formation (Valliyodan et al., 2014). Moreover, four MYBs were differentially expressed in rice root tissue forming constitutive aerenchyma (Yoo et al., 2015). However, functional studies are required in order to determine if MYB TFs indeed play a role in the regulation of cell death during aerenchyma formation in response to environmental stimuli.

MITOCHONDRIA, TRANSCRIPTION FACTORS, AND CELL FATE REGULATION

The role of mitochondria in plant PCD has been widely documented (Van Aken and Van Breusegem, 2015) although details of this involvement have not yet been fully elucidated. Mitochondria act as stress sensing organelles, with both extrinsic (environmental) and intrinsic (cellular) stimuli affecting the mitochondrial respiratory status (Schwarzlander and Finkemeier, 2013). Such changes can trigger signaling pathways, that either regulate mitochondria directly, which may result in events leading to PCD activation (Garmier et al., 2007; Gao et al., 2008; Scott and Logan, 2008; Bi et al., 2009; Wu et al., 2015; Zancani et al., 2015), or induce changes to nuclear gene expression *via* retrograde signaling (Rhoads, 2011; Schwarzlander and Finkemeier, 2013). The output of mitochondrial retrograde signaling not only feeds back to the mitochondrion but also regulates the functions of other cellular compartments (Schwarzlander et al., 2012; Schwarzlander and Finkemeier, 2013), thereby ensuring a coordinated response to environmental or intrinsic perturbations. The role of mitochondrial retrograde signaling in fine-tune regulation of cell fate decisions in plants is emerging, with transcription factors mediating some of the key pathways. Stress responsive mitochondrial proteins were identified by transcriptomic meta-analyses of the mitochondrial protein transcript abundance under a variety of stress conditions or during genetically or chemically induced mitochondrial dysfunction (Van Aken et al., 2009b; Schwarzlander et al., 2012; Wang et al., 2018). Alternative oxidase (AOX), probably the most widely studied stress induced mitochondrial protein and a classical marker of mitochondrial retrograde signaling (Van Aken et al., 2009a; Wang et al., 2018), has been implicated in the negative regulation of PCD response. AOX is a non-proton-pumping, terminal oxidase in the mitochondrial electron transport chain (ETC) (Vanlerberghe, 2013). By uncoupling the electron flow and ATP production, AOX acts as a safety valve, preventing over-reduction of ETC components and dampening the generation of O_2^- and nitric oxide in the mitochondria (Vanlerberghe, 2013). Unsurprisingly for a regulator of mitochondrial and cellular homeostasis, numerous studies report stress-induced PCD phenotypes in plants with altered AOX levels in response to miscellaneous abiotic and biotic factors (Ordog et al., 2002; Lei et al., 2003; Mizuno et al., 2005; Amirsadeghi et al., 2006; Kiba et al., 2008; Li and Xing, 2011; Liu et al., 2014). The pro-survival role of AOX conserved across the plant kingdom; it was recently shown to protect the unicellular algae *Chlamydomonas reinhardtii* from cell death induced by high light (Kaye et al., 2019) and *AOX* isoforms are induced by chemical and environmental stresses in cereal species such as rice and barley (Wanniarachchi et al., 2018). Indeed, the modulation of the AOX pathway has been recently proposed to offer crop protection against the challenges imposed by climate change (Florez-Sarasa et al., 2020). More recently, another stress-responsive mitochondrial protein has been linked to PCD regulation. *Om66* (*outer mitochondrial membrane protein of 66 kDa*), previously annotated as *AtBCS1* (*cytochrome BC1 synthase 1*), is induced by SA (Ho et al., 2008), mitochondrial and chloroplast perturbations (Van Aken and Whelan, 2012) and by biotic stress signals and UV light (Zhang et al., 2014). Interestingly, the OM66 transcript is also rapidly induced by the touch stimulus (Van Aken et al., 2016a), a mechanism that has not yet been investigated in the PCD context. *Arabidopsis thaliana* protoplasts treated with UV light exhibited increased cell death rates when *OM66* was overexpressed, and reduced cell death in the loss of function mutants; the *OM66* overexpressor (*OM66* OE) plants also demonstrated accelerated senescence and

increased drought tolerance (Zhang et al., 2014). The *OM66* OE was more tolerant to the biotrophic *P. syringae* but showed increased susceptibility to the necrotroph *B. cinerea* (Zhang et al., 2014). In line with the observed PCD phenotypes, the gene expression analysis revealed changes in pathogen defense signaling, cell death, and senescence in *OM66* OE lines (Zhang et al., 2014).

While the molecular mechanisms behind the regulation of cell death-suppressing AOX and cell death-promoting OM66 are still being uncovered, several TFs were demonstrated to play a role. There is an overlap between *AOX* and *OM66* regulation in response to mitochondrial dysfunction, although the rapid touch induction of *OM66* seems to be mediated by a distinct signal transduction pathway (Van Aken et al., 2016a). Under non-stress conditions, the TF abscisic acid insensitive 4 (ABI4) acts as *AOX1a* repressor in *A. thaliana*, with de-repression induced by rotenone or abscisic acid (ABA) itself (Giraud et al., 2009) suggesting that additional ABA response factors may regulate *AOX1a*, both positively and negatively (Wang et al., 2018). MYB29 is a general negative regulator of mitochondrial stress response, repressing both *AOX1a* and *OM66* indirectly *via* regulation of the expression of various *ERF* and *WRKY* transcription factors (Zhang et al., 2017a). The expression of *OM66* and *AOX1a* under mitochondrial stress conditions is also regulated by WRKY transcription factors, with likely functional redundancy suggested between them (Van Aken et al., 2013; Van Aken et al., 2016a). Knockout and overexpressor studies suggest that under stress conditions such as high light or actinomycin treatment, WRKY40 generally acts as a repressor of genes commonly affected by both chloroplast and mitochondrial perturbation, while WRKY63 is their activator (Van Aken et al., 2013). Interestingly, under no stress conditions, *OM66* but not *AOX1a* was induced in *WRKY63* OE line, highlighting differences in the pathways involved in regulation of these mitochondrial stress signaling genes (Van Aken et al., 2013). ANAC017 is an ER-tethered transcription factor and among the best characterized positive regulators of mitochondrial retrograde signaling (Ng et al., 2013). Once released from the ER, ANAC017 modulates the transcription of hundreds of nuclear and mitochondrial encoded genes, involved in energy metabolism, redox balance, mitochondrial fission, and hormone signaling, with both *AOX1a* and *OM66* among its target genes (Ng et al., 2013; Van Aken et al., 2016a). ANAC017 creates a positive feedback loop by inducing the expression of another ER bound TF, ANAC013, which activates its own expression, as well as promoting expression of the same target genes as ANAC017 (Van Aken and Pogson, 2017). The *anac017* knockout plants show a complete loss of *OM66* and *AOX1a* induction by mitochondrial perturbation, while the rapid touch induction of OM66 remains unchanged in *anac017* background, and instead is regulated by a complex signaling network involving WRKY40 and WRKY15, which themselves are also induced by touch, suggesting a negative feedback loop (Van Aken et al., 2016a; Xu et al., 2019). Moreover, the presence of OM66 is required for the touch induction of *WRKY40* (Xu et al., 2019). While the PCD rates induced by environmental factors have not been investigated in *ANAC017* mutant/transgenic lines, the overexpression of ANAC017 causes reduced cell viability and expansion, as well as early senescence, likely due to disturbed mitochondrial signaling (Meng et al., 2019). Moreover, the *anac017* knockout mutants are more sensitive to drought stress (Ng et al., 2013) and submergence (Meng et al., 2020) and show increased accumulation of ROS under stress conditions (Meng et al., 2020). Additionally, the double mutants with loss of function in both *ANAC017* and mitochondrial RNA polymerase (resulting in reduced activity of ETC complexes I and IV) display distinctive PCD-associated lesions (Van Aken et al., 2016b).

To conclude, mitochondria integrate stress signals and environmental stimuli resulting in perturbation of mitochondrial function (Rhoads, 2011; Schwarzlander and Finkemeier, 2013). The mitochondrial stress responsive proteins, such as AOX1a and OM66, can modulate cell fate decisions, and are regulated by complex, partially overlapping retrograde signaling networks involving numerous TFs, including WRKY15, WRKY40, MYB29 and ABI4, WRKY63, ANAC013, ANAC017. Detailed PCD phenotyping, in both abiotic and biotic context, is required for plants with reduced/enhanced expression of these TFs in order to further elucidate their role in modulation of cell death pathways, ideally in combination with monitoring of mitochondrial retrograde signaling. Methods such as root hair assay (Kacprzyk et al., 2014; Kacprzyk et al., 2016) or measurements of aerenchyma formation may provide useful tools to easily obtain quantitative information on the rates of PCD induced by numerous environmental stimuli in such mutants/transgenes. Finally, it remains to be established if the touch signaling, involving rapid upregulation of cell death promoting *OM66*, and activation regulatory network that mediates the responses to abiotic and biotic stresses, has an effect on plant's susceptibility to subsequent PCD triggers by environmental stimuli.

CONCLUSION AND PERSPECTIVES

Our understanding of PCD regulation in response to environmental stimuli is expanding. Increasing numbers of TFs are implicated in the transcriptional control of stress-induced cell fate decisions in plants. Details of the signaling pathways associated with the individual TFs are also emerging (**Table S1**), however, an integrative (meta)-analysis of gene regulatory network activated during PCD induced by abiotic and biotic stresses is required. Approaches allowing quantitative assessment of rates and timing of PCD, occurring in response to abiotic and biotics stresses will support further elucidation of TF mediated control of cell death processes in plants. The complex regulatory networks activated in response to environmental stresses need to be studied in the PCD context, including delineation of the cooperative action between individual TFs and detailed characterization of their targetomes. Furthermore, exploring the interplay between microRNAs and TFs implicated in stress induced PCD will reveal another layer of gene regulatory network(s) involved. Such research will be expedited by

technological advances, like ultra-affordable transcriptomics (Alpern et al., 2019) and resources such as AtTORF-Ex seed collections (*Arabidopsis thaliana TF ORF* over-*Ex*pression) (Weiste et al., 2007). Cautious, fine-tuned control of PCD activation is required in plants to successfully cope with the environmental challenges they cannot escape. In particular, recent advances in the understanding of organellar retrograde signaling highlight the ability of TFs to act as molecular switches between pro-death and pro-survival responses. Further research into these PCD regulatory nodes is thus crucially important for future crop improvement strategies.

AUTHOR CONTRIBUTIONS

JK and RB conceived an original idea for a review. RB, JS, OS, and JK drafted the initial version and RB prepared the figure. All authors contributed to the article and approved the submitted version.

FUNDING

RB was funded by University College Dublin PhD Advance grant awarded to JK and PM. JS was funded by the School of Biology and Environmental Science. OS was funded by Environmental Protection Agency-Irish Research Council (EPA-IRC) Postgraduate Scholarship. YJ was funded by Newman Fellowship Programme and Council for At-Risk Academics (CARA).

ACKNOWLEDGMENTS

We thank University College Dublin for providing funding to RB (PhD Advance Scheme) and YJ (Newman Fellowship Programme). We also thank School of Biology and Environmental Science for PhD funding provided to JS. We are grateful to Environmental Protection Agency and Irish Research Council for PhD funding provided to OS, and to Council for At-Risk Academics for supporting YJ.

SUPPLEMENTARY MATERIAL

The Supplementary Material for this article can be found online at: https://www.frontiersin.org/articles/10.3389/fpls.2020.01235/full#supplementary-material

REFERENCES

Adachi, H., Nakano, T., Miyagawa, N., Ishihama, N., Yoshioka, M., Katou, Y., et al. (2015). WRKY Transcription Factors Phosphorylated by MAPK Regulate a Plant Immune NADPH Oxidase in *Nicotiana benthamiana*. *Plant Cell* 27 (9), 2645–2663. doi: 10.1105/tpc.15.00213

Akcin, T. A., Akcin, A., and Yalcin, E. (2015). Anatomical Adaptations to Salinity in *Spergularia marina* (Caryophyllaceae) from Turkey. *Proc. Natl. Acad. Sci. India B* 85 (2), 625–634. doi: 10.1007/s40011-014-0386-8

Alpern, D., Gardeux, V., Russeil, J., Mangeat, B., Meireles-Filho, A. C. A., Breysse, R., et al. (2019). BRB-seq: ultra-affordable high-throughput transcriptomics enabled by bulk RNA barcoding and sequencing. *Genome Biol.* 20 (1), 71. doi: 10.1186/s13059-019-1671-x

Amirsadeghi, S., Robson, C. A., McDonald, A. E., and Vanlerberghe, G. C. (2006). Changes in plant mitochondrial electron transport alter cellular levels of reactive oxygen species and susceptibility to cell death signaling molecules. *Plant Cell Physiol.* 47 (11), 1509–1519. doi: 10.1093/pcp/pcl016

Aubrey, B. J., Kelly, G. L., Janic, A., Herold, M. J., and Strasser, A. (2018). How does p53 induce apoptosis and how does this relate to p53-mediated tumour suppression? *Cell Death Differ.* 25 (1), 104–113. doi: 10.1038/cdd.2017.169

Awwad, F., Bertrand, G., Grandbois, M., and Beaudoin, N. (2019). Auxin protects *Arabidopsis thaliana* cell suspension cultures from programmed cell death induced by the cellulose biosynthesis inhibitors thaxtomin A and isoxaben. *BMC Plant Biol.* 19 (1), 512. doi: 10.1186/s12870-019-2130-2

Bahieldin, A., Atef, A., Edris, S., Gadalla, N. O., Ali, H. M., Hassan, S. M., et al. (2016). Ethylene responsive transcription factor ERF109 retards PCD and improves salt tolerance in plant. *BMC Plant Biol.* 16 (1), 216. doi: 10.1186/s12870-016-0908-z

Bakshi, M., and Oelmuller, R. (2014). WRKY transcription factors: Jack of many trades in plants. *Plant Signal Behav.* 9 (2), e27700. doi: 10.4161/psb.27700

Bakshi, M., and Oelmüller, R. (2014). WRKY transcription factors. *Plant Signal Behav.* 9 (2), e27700. doi: 10.4161/psb.27700

Bi, Y., Chen, W., Zhang, W., Zhou, Q., Yun, L., and Xing, D. (2009). Production of reactive oxygen species, impairment of photosynthetic function and dynamic changes in mitochondria are early events in cadmium-induced cell death in Arabidopsis thaliana. *Biol. Cell* 101 (11), 629–643. doi: 10.1042/BC20090015

Bourbousse, C., Vegesna, N., and Law, J. A. (2018). SOG1 activator and MYB3R respressors regulate a complex DNA damage network in. *Arabidopsis PNAS* 115 (52), E12453–E12462. doi: 10.1073/pnas.1810582115

Cai, X., Xu, P., Zhao, P., Liu, R., Yu, L. H., and Xiang, C. B. (2014). *Arabidopsis* ERF109 mediates cross-talk between jasmonic acid and auxin biosynthesis during lateral root formation. *Nat. Commun.* 5, 5833. doi: 10.1038/ncomms6833

Calfon, M., Zeng, H., Urano, F., Till, J. H., Hubbard, S. R., Harding, H. P., et al. (2002). IRE1 couples endoplasmic reticulum load to secretory capacity by processing the XBP-1 mRNA. *Nature* 415 (6867), 92–96. doi: 10.1038/415092a

Campbell, M. T., Proctor, C. A., Dou, Y., Schmitz, A. J., Phansak, P., Kruger, G. R., et al. (2015). Genetic and molecular characterization of submergence response identifies Subtol6 as a major submergence tolerance locus in maize. *PLoS One* 10 (3), e0120385. doi: 10.1371/journal.pone.0120385

Chen, B., Niu, F., Liu, W. Z., Yang, B., Zhang, J., Ma, J., et al. (2016). Identification, cloning and characterization of R2R3-MYB gene family in canola (Brassica napus L.) identify a novel member modulating ROS accumulation and hypersensitive-like cell death. *DNA Res.* 23 (2), 101–114. doi: 10.1093/dnares/dsv040

Chen, Q., Niu, F., Yan, J., Chen, B., Wu, F., Guo, X., et al. (2017). Oilseed rape NAC56 transcription factor modulates reactive oxygen species accumulation and hypersensitive response-like cell death. *Physiol. Plant* 160 (2), 209–221. doi: 10.1111/ppl.12545

Coll, N. S., Epple, P., and Dangl, J. L. (2011). Programmed cell death in the plant immune system. *Cell Death Differ.* 18 (8), 1247–1256. doi: 10.1038/cdd.2011.37

Conradt, B., Wu, Y. C., and Xue, D. (2016). *P*rogrammed Cell Death During Caenorhabditis elegans Development. *Genetics* 203 (4), 1533. doi: 10.1534/genetics.115.186247

Cubría-Radío, M., and Nowack, M. K. (2019). Transcriptional networks orchestrating programmed cell death during plant development. *Curr. Top Dev. Biol.* 131, 161–184. doi: 10.1016/bs.ctdb.2018.10.006

Culligan, K. M., Robertson, C. E., Foreman, J., Doerner, P., and Britt, A. B. (2006). ATR and ATM play both distinct and additive roles in response to ionizing radiation. *Plant J.* 48 (6), 947–961. doi: 10.1111/j.1365-313X.2006.02931.x

Daneva, A., Gao, Z., Van Durme, M., and Nowack, M. K. (2016). Functions and Regulation of Programmed Cell Death in Plant Development. *Annu. Rev. Cell Dev. Biol.* 32 (1), 441–468. doi: 10.1146/annurev-cellbio-111315-124915

Daniel, X., Lacomme, C., Morel, J. B., and Roby, D. (1999). A novel myb oncogene homologue in Arabidopsis thaliana related to hypersensitive cell death. *Plant J.* 20 (1), 57–66. doi: 10.1046/j.1365-313x.1999.00578.x

Danon, A., Delorme, V., Mailhac, N., and Gallois, P. (2000). Plant programmed cell death: A common way to die. *Plant Physiol. Biochem.* 38 (9), 647–655. doi: 10.1016/s0981-9428(00)01178-5

De Clercq, I., Vermeirssen, V., Van Aken, O., Vandepoele, K., Murcha, M. W., Law, S. R., et al. (2013). The membrane-bound NAC transcription factor ANAC013 functions in mitochondrial retrograde regulation of the oxidative stress response in Arabidopsis. *Plant Cell* 25 (9), 3472–3490. doi: 10.1105/tpc.113.117168

Drew, M. C., Jackson, M. B., Giffard, S. C., and Campbell, R. (1981). Inhibition by silver ions of gas space (aerenchyma) formation in adventitious roots of Zea mays L. subjected to exogenous ethylene or to oxygen deficiency. *Planta* 153 (3), 217–224. doi: 10.1007/BF00383890

Du, X. M., Ni, X. L., Ren, X. L., Xin, G. L., Jia, G. L., Liu, H. D., et al. (2018). De novo transcriptomic analysis to identify differentially expressed genes during the process of aerenchyma formation in Typha angustifolia leaves. *Gene* 662, 66–75. doi: 10.1016/j.gene.2018.03.099

Dubos, C., Stracke, R., Grotewold, E., Weisshaar, B., Martin, C., and Lepiniec, L. (2010). MYB transcription factors in Arabidopsis. *Trends Plant Sci.* 15 (10), 573–581. doi: 10.1016/j.tplants.2010.06.005

Eulgem, T., Rushton, P. J., Robatzek, S., and Somssich, I. E. (2000). The WRKY superfamily of plant transcription factors. *Trends Plant Sci.* 5 (5), 199–206. doi: 10.1016/s1360-1385(00)01600-9

Evans, D. E. (2004). Aerenchyma formation. *New Phytol.* 161 (1), 35–49. doi: 10.1046/j.1469-8137.2003.00907.x

Fan, M., Zhu, J., Richards, C., Brown, K. M., and Lynch, J. P. (2003). Physiological roles for aerenchyma in phosphorus-stressed roots. *Funct. Plant Biol.: FPB* 30 (5), 493–506. doi: 10.1071/fp03046

Faria, J. A. Q. A., Reis, P. A. B., Reis, M. T. B., Rosado, G. L., Pinheiro, G. L., Mendes, G. C., et al. (2011). The NAC domain-containing protein, GmNAC6, is a downstream component of the ER stress- and osmotic stress-induced NRP-mediated cell-death signaling pathway. *BMC Plant Biol.* 11 (1), 129. doi: 10.1186/1471-2229-11-129

Florez-Sarasa, I., Fernie, A. R., and Gupta, K. J. (2020). Does the alternative respiratory pathway offer protection against the adverse effects resulting from climate change. *J. Exp. Bot.* 71 (2), 465–469. doi: 10.1093/jxb/erz428

Froidure, S., Canonne, J., Daniel, X., Jauneau, A., Brière, C., Roby, D., et al. (2010). AtsPLA2-alpha nuclear relocalization by the Arabidopsis transcription factor AtMYB30 leads to repression of the plant defense response. *PNAS* 107 (34), 15281–15286. doi: 10.1073/pnas.1009056107

Fuchs, Y., and Steller, H. (2011). Programmed Cell Death in Animal Development and Disease. *Cell* 147 (4), 742–758. doi: 10.1016/j.cell.2011.10.033

Fulcher, N., and Sablowski, R. (2009). Hypersensitivity to DNA damage in plant stem cell niches. *Proc. Natl. Acad. Sci. U. S. A.* 106 (49), 20984–20988. doi: 10.1073/pnas.0909218106

Furukawa, T., Curtis, M. J., Tominey, C. M., Duong, Y. H., Wilcox, B. W. L., Aggoune, D., et al. (2010). A shared DNA-damage-response pathway for induction of stem-cell death by UVB and by gamma irradiation. *DNA Repair* 9 (9), 940–948. doi: 10.1016/j.dnarep.2010.06.006

Gao, C., Xing, D., Ling, L., and Zhang, L. (2008). Implication of reactive oxygen species and mitochondrial dysfunction in the early stages of plant programmed cell death induced by ultraviolet-C overexposure. *Planta* 227 (4), 755–767. doi: 10.1007/s00425-007-0654-4

Garmier, M., Priault, P., Vidal, G., Driscoll, S., Djebbar, R., Boccara, M., et al. (2007). Light and oxygen are not required for harpin-induced cell death. *J. Biol. Chem.* 282 (52), 37556–37566. doi: 10.1074/jbc.M707226200

Giraud, E., Van Aken, O., Ho, L. H., and Whelan, J. (2009). The Transcription Factor ABI4 Is a Regulator of Mitochondrial Retrograde Expression of ALTERNATIVE OXIDASE1a1[C][W][OA]. *Plant Physiol.* 150 (3), 1286–1296. doi: 10.1104/pp.109.139782

Gunawardena, A. H. L. A. N., Pearce, D. M. E., Jackson, M. B., Hawes, C. R., and Evans, D. E. (2001a). Rapid changes in cell wall pectic polysaccharides are closely associated with early stages of aerenchyma formation, a spatially localized form of programmed cell death in roots of maize (Zea mays L.) promoted by ethylene. *Plant Cell Environ.* 24 (12), 1369–1375. doi: 10.1046/j.1365-3040.2001.00774.x

Gunawardena, A. H., Pearce, D. M., Jackson, M. B., Hawes, C. R., and Evans, D. E. (2001b). Characterisation of programmed cell death during aerenchyma formation induced by ethylene or hypoxia in roots of maize (Zea mays L.). *Planta* 212 (2), 205–214. doi: 10.1007/s004250000381

Hatsugai, N., Kuroyanagi, M., Nishimura, M., and Hara-Nishimura, I. (2006). A cellular suicide strategy of plants: vacuole-mediated cell death. *Apoptosis* 11 (6), 905–911. doi: 10.1007/s10495-006-6601-1

Heath, M. C. (2000). Hypersensitive response-related death. *Plant Mol. Biol.* 44 (3), 321–334. doi: 10.1023/A:1026592509060

Ho, L. H., Giraud, E., Uggalla, V., Lister, R., Clifton, R., Glen, A., et al. (2008). Identification of regulatory pathways controlling gene expression of stress-responsive mitochondrial proteins in Arabidopsis. *Plant Physiol.* 147 (4), 1858–1873. doi: 10.1104/pp.108.121384

Hong, J. H., Savina, M., Du, J., Devendran, A., Ramakanth, K. K., Tian, X., et al. (2017). A Sacrifice-for-Survival Mechanism Protects Root Stem Cell Niche from Chilling Stress. *Cell* 170 (1), 102–113.e14. doi: 10.1016/j.cell.2017.06.002

Horvitz, H. R. (2003). Worms, Life, and Death (Nobel Lecture). *ChemBioChem* 4 (8), 697–711. doi: 10.1002/cbic.200300614

Jeong, J. S., Kim, Y. S., Redillas, M. C., Jang, G., Jung, H., Bang, S. W., et al. (2013). OsNAC5 overexpression enlarges root diameter in rice plants leading to enhanced drought tolerance and increased grain yield in the field. *Plant Biotechnol. J.* 11 (1), 101–114. doi: 10.1111/pbi.12011

Johnson, R. A., Conklin, P. A., Tjahjadi, M., Missirian, V., Toal, T., Brady, S. M., et al. (2018). SUPPRESSOR OF GAMMA RESPONSE1 Links DNA Damage Response to Organ Regeneration. *Plant Physiol.* 176 (2), 1665. doi: 10.1104/pp.17.01274

Kacprzyk, J., Devine, A., and McCabe, P. F. (2014). The Root Hair Assay Facilitates the Use of Genetic and Pharmacological Tools in Order to Dissect Multiple Signalling Pathways That Lead to Programmed Cell Death. *PLoS One* 9 (4), e94898. doi: 10.1371/journal.pone.0094898

Kacprzyk, J., Dauphinee, A. N., Gallois, P., Gunawardena, A. H., and McCabe, P. F. (2016). Methods to Study Plant Programmed Cell Death. *Methods Mol. Biol.* 1419, 145–160. doi: 10.1007/978-1-4939-3581-9_12

Kaneda, T., Taga, Y., Takai, R., Iwano, M., Matsui, H., Takayama, S., et al. (2009). The transcription factor OsNAC4 is a key positive regulator of plant hypersensitive cell death. *EMBO J.* 28 (7), 926–936. doi: 10.1038/emboj.2009.39

Kaye, Y., Huang, W., Clowez, S., Saroussi, S., Idoine, A., Sanz-Luque, E., et al. (2019). The mitochondrial alternative oxidase from Chlamydomonas reinhardtii enables survival in high light. *J. Biol. Chem.* 294 (4), 1380–1395. doi: 10.1074/jbc.RA118.004667

Kerchev, P., MÜHlenbock, P. E. R., Denecker, J., Morreel, K., Hoeberichts, F. A., Van Der Kelen, K., et al. (2015). Activation of auxin signalling counteracts photorespiratory H2O2-dependent cell death. *Plant Cell Environ.* 38 (2), 253–265. doi: 10.1111/pce.12250

Kiba, A., Lee, K. Y., Ohnishi, K., and Hikichi, Y. (2008). Comparative expression analysis of genes induced during development of bacterial rot and induction of hypersensitive cell death in lettuce. *J. Plant Physiol.* 165 (17), 1757–1773. doi: 10.1016/j.jplph.2007.10.010

Lavin, M. F., and Gueven, N. (2006). The complexity of p53 stabilization and activation. *Cell Death Differ.* 13 (6), 941–950. doi: 10.1038/sj.cdd.4401925

Lee, T. G., Jang, C. S., Kim, J. Y., Kim, D. S., Park, J. H., Kim, D. Y., et al. (2006). A Myb transcription factor (TaMyb1) from wheat roots is expressed during hypoxia: roles in response to the oxygen concentration in root environment and abiotic stresses. *Physiol. Plant* 129 (2), 375–385. doi: 10.1111/j.1399-3054.2006.00828.x

Lee, M. H., Jeon, H. S., Kim, H. G., and Park, O. K. (2017). An Arabidopsis NAC transcription factor NAC4 promotes pathogen-induced cell death under negative regulation by microRNA164. *New Phytol.* 214 (1), 343–360. doi: 10.1111/nph.14371

Lei, X. Y., Zhu, R. Y., Zhang, G. Y., and Dai, Y. R. (2003). Possible involvement of the mitochondrial alternative pathway in ethylene-induced apoptosis in tomato protoplasts. *Plant Growth Regul.* 41 (2), 111–116. doi: 10.1023/A:1027355502538

Li, Z., and Xing, D. (2011). Mechanistic study of mitochondria-dependent programmed cell death induced by aluminium phytotoxicity using fluorescence techniques. *J. Exp. Bot.* 62 (1), 331–343. doi: 10.1093/jxb/erq279

Li, L., Yu, X., Thompson, A., Guo, M., Yoshida, S., Asami, T., et al. (2009). Arabidopsis MYB30 is a direct target of BES1 and cooperates with BES1 to regulate brassinosteroid-induced gene expression. *Plant J.* 58, 275–286. doi: 10.1111/j.1365-313X.2008.03778.x

Li, X., Zhang, H., Tian, L., Huang, L., Liu, S., Li, D., et al. (2015). Tomato SlRbohB, a member of the NADPH oxidase family, is required for disease resistance against Botrytis cinerea and tolerance to drought stress. *Front. Plant Sci.* 6, 463. doi: 10.3389/fpls.2015.00463

Li, S. B., Xie, Z. Z., Hu, C. G., and Zhang, J. Z. (2016). A Review of Auxin Response Factors (ARFs) in Plants. *Front. Plant Sci.* 7, 47. doi: 10.3389/fpls.2016.00047

Li, H., Wang, Y., Wu, M., Li, L., Li, C., Han, Z., et al. (2017). Genome-Wide Identification of AP2/ERF Transcription Factors in Cauliflower and Expression Profiling of the ERF Family under Salt and Drought Stresses. *Front. Plant Sci.* 8, 946. doi: 10.3389/fpls.2017.00946

Liu, J., Li, Z., Wang, Y., and Xing, D. (2014). Overexpression of ALTERNATIVE OXIDASE1a alleviates mitochondria-dependent programmed cell death induced by aluminium phytotoxicity in Arabidopsis. *J. Exp. Bot.* 65 (15), 4465–4478. doi: 10.1093/jxb/eru222

Locato, V., and De Gara, L. (2018). "Programmed Cell Death in Plants: An Overview," in *Plant Programmed Cell Death: Methods and Protocols*. Eds. L. De Gara and V. Locato (New York, NY: Springer New York), 1–8.

Luo, J., Zhou, J. J., and Zhang, J. Z. (2018). Aux/IAA Gene Family in Plants: Molecular Structure, Regulation, and Function. *Int. J. Mol. Sci.* 19 (1), 259. doi: 10.3390/ijms19010259

Mabuchi, K., Maki, H., Itaya, T., Suzuki, T., Nomoto, M., Sakaoka, S., et al. (2018). MYB30 links ROS signaling, root cell elongation, and plant immune responses". *PNAS* 115 (20), E4710–E4719. doi: 10.1073/pnas.1804233115

Marino, D., Froidure, S., Canonne, J., Khaled, S. B., Khafif, M., Pouzet, C., et al. (2013). *Arabidopsis* ubiquitin ligase MIEL1 mediates degradation of the transcription factor MYB30 weakening plant defence". *Nat. Commun.* 4, 1476. doi: 10.1038/ncomms2479

Mase, K., Ishihama, N., Mori, H., Takahashi, H., Kaminaka, H., Kodama, M., et al. (2013). Ethylene-responsive AP2/ERF transcription factor MACD1 participates in phytotoxin-triggered programmed cell death. *Mol. Plant Microbe Interact.* 26 (8), 868–879. doi: 10.1094/MPMI-10-12-0253-R

Masuda, Y., Yamada, T., and Marubashi, W. (2003). Time Course Analysis of Apoptotic Cell Death during Expression of Hybrid Lethality in Hybrid Tobacco Cells (Nicotiana suaveolens × N. tabacum). *Plant Cell Physiol.* 44 (4), 420–427. doi: 10.1093/pcp/pcg055

Mendes, G. C., Reis, P. A., Calil, I. P., Carvalho, H. H., Aragao, F. J., and Fontes, E. P. (2013). GmNAC30 and GmNAC81 integrate the endoplasmic reticulum stress- and osmotic stress-induced cell death responses through a vacuolar processing enzyme. *Proc. Natl. Acad. Sci. U. S. A.* 110 (48), 19627–19632. doi: 10.1073/pnas.1311729110

Meng, X., Li, L., De Clercq, I., Narsai, R., Xu, Y., Hartmann, A., et al. (2019). ANAC017 Coordinates Organellar Functions and Stress Responses by Reprogramming Retrograde Signaling. *Plant Physiol.* 180 (1), 634. doi: 10.1104/pp.18.01603

Meng, X., Li, L., Narsai, R., De Clercq, I., Whelan, J., and Berkowitz, O. (2020). Mitochondrial signalling is critical for acclimation and adaptation to flooding in Arabidopsis thaliana. *Plant J.* 103, (1), 227–247. doi: 10.1111/tpj.14724

Menke, F. L. H., Kang, H. G., Chen, Z., Park, J. M., Kumar, D., and Klessig, D. F. (2005). Tobacco Transcription Factor WRKY1 Is Phosphorylated by the MAP Kinase SIPK and Mediates HR-Like Cell Death in Tobacco. *Mol. Plant Microbe Interact.* 18 (10), 1027–1034. doi: 10.1094/MPMI-18-1027

Mizoi, J., Shinozaki, K., and Yamaguchi-Shinozaki, K. (2012). AP2/ERF family transcription factors in plant abiotic stress responses. *BBA Gene Regul. Mech.* 1819 (2), 86–96. doi: 10.1016/j.bbagrm.2011.08.004

Mizuno, M., Tada, Y., Uchii, K., Kawakami, S., and Mayama, S. (2005). Catalase and alternative oxidase cooperatively regulate programmed cell death induced by beta-glucan elicitor in potato suspension cultures. *Planta* 220 (6), 849–853. doi: 10.1007/s00425-004-1402-7

Mustroph, A. (2018). Improving Flooding Tolerance of Crop Plants. *Agronomy* 8, 160. doi: 10.3390/agronomy8090160

Najafi, S., Sorkheh, K., and Nasernakhaei, F. (2018). Characterization of the APETALA2/Ethylene-responsive factor (AP2/ERF) transcription factor family in sunflower. *Sci. Rep.* 8 (1), 11576. doi: 10.1038/s41598-018-29526-z

Nakano, T., Suzuki, K., Fujimura, T., and Shinshi, H. (2006). Genome-Wide Analysis of the ERF Gene Family in Arabidopsis and Rice. *Plant Physiol.* 140 (2), 411. doi: 10.1104/pp.105.073783

Nasir, K. H. B., Takahashi, Y., Ito, A., Saitoh, H., Matsumura, H., Kanzaki, H., et al. (2005). High-throughput in planta expression screening identifies a class II ethylene-responsive element binding factor-like protein that regulates plant cell death and non-host resistance. *Plant J.* 43 (4), 491–505. doi: 10.1111/j.1365-313X.2005.02472.x

Ng, S., Ivanova, A., Duncan, O., Law, S. R., Van Aken, O., De Clercq, I., et al. (2013). A membrane-bound NAC transcription factor, ANAC017, mediates mitochondrial retrograde signaling in Arabidopsis. *Plant Cell* 25 (9), 3450–3471. doi: 10.1105/tpc.113.113985

Ning, S. B., Wang, L., Li, Z. Y., Jin, W. W., and Song, Y. C. (2001). Apoptotic Cell Death and Cellular Surface Negative Charge Increase in Maize Roots Exposed to Cytotoxic Stresses. *Ann. Bot.* 87 (5), 575–583. doi: 10.1006/anbo.2001.1370

Niu, F., Wang, B., Wu, F., Yan, J., Li, L., Wang, C., et al. (2014). Canola (Brassica napus L.) NAC103 transcription factor gene is a novel player inducing reactive oxygen species accumulation and cell death in plants. *Biochem. Biophys. Res. Commun.* 454 (1), 30–35. doi: 10.1016/j.bbrc.2014.10.057

Niu, F., Wang, C., Yan, J., Guo, X., Wu, F., Yang, B., et al. (2016). Functional characterization of NAC55 transcription factor from oilseed rape (Brassica napus L.) as a novel transcriptional activator modulating reactive oxygen species accumulation and cell death. *Plant Mol. Biol.* 92 (1), 89–104. doi: 10.1007/s11103-016-0502-7

Norbury, C. J., and Zhivotovsky, B. (2004). DNA damage-induced apoptosis. *Oncogene* 23 (16), 2797–2808. doi: 10.1038/sj.onc.1207532

Ogata, T., Kida, Y., Arai, T., Kishi, Y., Manago, Y., Murai, M., et al. (2012). Overexpression of tobacco ethylene response factor NtERF3 gene and its homologues from tobacco and rice induces hypersensitive response-like cell death in tobacco. *J. Gen. Plant Pathol.* 78 (1), 8–17. doi: 10.1007/s10327-011-0355-5

Ogata, T., Kida, Y., Tochigi, M., and Matsushita, Y. (2013). Analysis of the cell death-inducing ability of the ethylene response factors in group VIII of the AP2/ERF family. *Plant Sci.* 209, 12–23. doi: 10.1016/j.plantsci.2013.04.003

Ogata, T., Okada, H., Kawaide, H., Takahashi, H., Seo, S., Mitsuhara, I., et al. (2015). Involvement of NtERF 3 in the cell death signalling pathway mediated by SIPK/WIPK and WRKY 1 in tobacco plants". *Plant Biol. J.* 17, 962–972. doi: 10.1111/plb.12349

Ogita, N., Okushima, Y., Tokizawa, M., Yamamoto, Y. Y., Tanaka, M., Seki, M., et al. (2018). Identifying the target genes of SUPPRESSOR OF GAMMA RESPONSE 1, a master transcription factor controlling DNA damage response in Arabidopsis. *Plant J.* 94 (3), 439–453. doi: 10.1111/tpj.13866

Ohme-Takagi, M., and Shinshi, H. (1995). Ethylene-inducible DNA binding proteins that interact with an ethylene-responsive element. *Plant Cell* 7 (2), 173–182. doi: 10.1105/tpc.7.2.173

Olsen, A. N., Ernst, H. A., Leggio, L. L., and Skriver, K. (2005). NAC transcription factors: structurally distinct, functionally diverse. *Trends Plant Sci.* 10 (2), 79–87. doi: 10.1016/j.tplants.2004.12.010

Ooka, H., Satoh, K., Doi, K., Nagata, T., Otomo, Y., Murakami, K., et al. (2003). Comprehensive Analysis of NAC Family Genes in Oryza sativa and Arabidopsis thaliana. *DNA Res.* 10 (6), 239–247. doi: 10.1093/dnares/10.6.239

Ordog, S. H., Higgins, V. J., and Vanlerberghe, G. C. (2002). Mitochondrial alternative oxidase is not a critical component of plant viral resistance but may play a role in the hypersensitive response. *Plant Physiol.* 129 (4), 1858–1865. doi: 10.1104/pp.003855

Park, C. J., and Park, J. M. (2019). Endoplasmic Reticulum Plays a Critical Role in Integrating Signals Generated by Both Biotic and Abiotic Stress in Plants. *Front. Plant Sci.* 10, 399. doi: 10.3389/fpls.2019.00399

Phukan, U. J., Jeena, G. S., and Shukla, R. K. (2016). WRKY Transcription Factors: Molecular Regulation and Stress Responses in Plants. *Front. Plant Sci.* 7, 760. doi: 10.3389/fpls.2016.00760

Pradhan, S. K., Pandit, E., Nayak, D. K., Behera, L., and Mohapatra, T. (2019). Genes, pathways and transcription factors involved in seedling stage chilling stress tolerance in indica rice through RNA-Seq analysis. *BMC Plant Biol.* 19 (1), 352–352. doi: 10.1186/s12870-019-1922-8

Raffaele, S., Rivas, S., and Roby, D. (2006). An essential role for salicylic acid in AtMYB30-mediated control of the hypersensitive cell death program in

Arabidopsis. *FEBS Lett.* 580 (14), 3498–3504. doi: 10.1016/j.febslet.2006.05.027

Raffaele, S., Vailleau, F., Leger, A., Joubes, J., Miersch, O., Huard, C., et al. (2008). A MYB transcription factor regulates very-long-chain fatty acid biosynthesis for activation of the hypersensitive cell death response in Arabidopsis. *Plant Cell* 20 (3), 752–767. doi: 10.1105/tpc.107.054858

Raineri, J., Ribichich, K. F., and Chan, R. L. (2015). The sunflower transcription factor HaWRKY76 confers drought and flood tolerance to Arabidopsis thaliana plants without yield penalty. *Plant Cell Rep.* 34 (12), 2065–2080. doi: 10.1007/s00299-015-1852-3

Rajhi, I., Yamauchi, T., Takahashi, H., Nishiuchi, S., Shiono, K., Watanabe, R., et al. (2011). Identification of genes expressed in maize root cortical cells during lysigenous aerenchyma formation using laser microdissection and microarray analyses. *New Phytol.* 190 (2), 351–368. doi: 10.1111/j.1469-8137.2010.03535.x

Redillas, M. C., Jeong, J. S., Kim, Y. S., Jung, H., Bang, S. W., Choi, Y. D., et al. (2012). The overexpression of OsNAC9 alters the root architecture of rice plants enhancing drought resistance and grain yield under field conditions. *Plant Biotechnol. J.* 10 (7), 792–805. doi: 10.1111/j.1467-7652.2012.00697.x

Rhoads, D. M. (2011). "Plant Mitochondrial Retrograde Regulation," in *Plant Mitochondria* (SpringerLink), 411–437. doi: 10.1007/978-0-387-89781-3_16

Ryu, T. H., Go, Y. S., Choi, S. H., Kim, J.-I., Chung, B. Y., and Kim, J.-H. (2019). SOG 1-dependent NAC 103 modulates the DNA damage response as a transcriptional regulator in Arabidopsis. *Plant J.* 98, 83–96. doi: 10.1111/tpj.14201

Saengwilai, P., Nord, E. A., Chimungu, J. G., Brown, K. M., and Lynch, J. P. (2014). Root Cortical Aerenchyma Enhances Nitrogen Acquisition from Low-Nitrogen Soils in Maize. *Plant Physiol.* 166 (2), 726. doi: 10.1104/pp.114.241711

Safavi-Rizi, V., Herde, M., and Stöhr, C. (2020). RNA-Seq reveals novel genes and pathways associated with hypoxia duration and tolerance in tomato root. *Sci. Rep.* 10 (1), 1692. doi: 10.1038/s41598-020-57884-0

Saqib, M., Javaid, A., and Qureshi, R. (2005). Na+ Exclusion and Salt Resistance of Wheat (Triticum aestivum) in Saline-Waterlogged Conditions are Improved by the Development of Adventitious Nodal Roots and Cortical Root Aerenchyma. *Plant Sci.* 169, 125–130. doi: 10.1016/j.plantsci.2005.03.003

Schwarzlander, M., and Finkemeier, I. (2013). Mitochondrial energy and redox signaling in plants. *Antioxid. Redox Signal* 18 (16), 2122–2144. doi: 10.1089/ars.2012.5104

Schwarzlander, M., Konig, A. C., Sweetlove, L. J., and Finkemeier, I. (2012). The impact of impaired mitochondrial function on retrograde signalling: a meta-analysis of transcriptomic responses. *J. Exp. Bot.* 63 (4), 1735–1750. doi: 10.1093/jxb/err374

Scott, I., and Logan, D. C. (2008). Mitochondrial morphology transition is an early indicator of subsequent cell death in Arabidopsis. *New Phytol.* 177 (1), 90–101. doi: 10.1111/j.1469-8137.2007.02255.x

Serrano, I., Buscaill, P., Audran, C., Pouzet, C., Jauneau, A., and Rivas, S. (2016). A non canonical subtilase attenuates the transcriptional activation of defence responses in *Arabidopsis thaliana*. *Elife* 5, e19755. doi: 10.7554/eLife.19755

Sohn, K. H., Lee, S. C., Jung, H. W., Hong, J. K., and Hwang, B. K. (2006). Expression and functional roles of the pepper pathogen-induced transcription factor RAV1 in bacterial disease resistance, and drought and salt stress tolerance. *Plant Mol. Biol.* 61 (6), 897–915. doi: 10.1007/s11103-006-0057-0

Takahashi, N., Ogita, N., Takahashi, T., Taniguchi, S., Tanaka, M., Seki, M., et al. (2019). A regulatory module controlling stress-induced cell cycle arrest in Arabidopsis. *eLife* 8, e43944. doi: 10.7554/eLife.43944

Tavares, E. Q. P., De Souza, A. P., Romim, G. H., Grandis, A., Plasencia, A., Gaiarsa, J. W., et al. (2019). The control of endopolygalacturonase expression by the sugarcane RAV transcription factor during aerenchyma formation. *J. Exp. Bot.* 70 (2), 497–506. doi: 10.1093/jxb/ery362

Tavares Queiroz de Pinho, E., Martins Camara Mattos, M., Grandis, A., Romim, G. H., Rusiska Piovezani, A., Weissmann Gaiarsa, J., et al. (2020). Newly identified miRNAs may contribute to aerenchyma formation in sugarcane roots. *Plant Direct* 4 (3), e00204. doi: 10.1002/pld3.204

Thirunavukkarasu, N., Hossain, F., Mohan, S., Shiriga, K., Mittal, S., Sharma, R., et al. (2013). Genome-wide expression of transcriptomes and their co-expression pattern in subtropical maize (Zea mays L.) under waterlogging stress. *PLoS One* 8 (8), e70433. doi: 10.1371/journal.pone.0070433

Ulmasov, T., Hagen, G., and Guilfoyle, T. J. (1997). ARF1, a transcription factor that binds to auxin response elements. *Science* 276 (5320), 1865–1868. doi: 10.1126/science.276.5320.1865

USGCRP, Wuebbles, D. J., Fahey, D. W., Hibbard, K. A., Dokken, D. J., Stewart, B. C., et al. (2017). *USGCRP, 2017: Climate Science Special Report: Fourth National Climate Assessment, Volume I* (Washington, DC, USA: U.S. Global Change Research Program).

Vacca, R. A., Concetta de Pinto, M., Valenti, D., Passarella, S., Marra, E., and De Gara, L. (2004). Production of reactive oxygen species, alteration of cytosolic ascorbate peroxidase, and impairment of mitochondrial metabolism are early events in heat shock-induced programmed cell death in tobacco Bright-Yellow 2 cells. *Plant Physiol.* 134 (3), 1100–1112. doi: 10.1104/pp.103.035956

Vailleau, F., Daniel, X., Tronchet, M., Montillet, J. L., Triantaphylides, C., and Roby, D. (2002). A R2R3-MYB gene, AtMYB30, acts as a positive regulator of the hypersensitive cell death program in plants in response to pathogen attack. *Proc. Natl. Acad. Sci. U. S. A.* 99 (15), 10179–10184. doi: 10.1073/pnas.152047199

Valliyodan, B., Van Toai, T. T., Alves, J. D., Goulart P. de Fatima, P., Lee, J. D., Fritschi, F. B., et al. (2014). Expression of root-related transcription factors associated with flooding tolerance of soybean (Glycine max). *Int. J. Mol. Sci.* 15 (10), 17622–17643. doi: 10.3390/ijms151017622

Van Aken, O., and Pogson, B. J. (2017). Convergence of mitochondrial and chloroplastic ANAC017/PAP-dependent retrograde signalling pathways and suppression of programmed cell death. *Cell Death Differ.* 24 (6), 955–960. doi: 10.1038/cdd.2017.68

Van Aken, O., and Van Breusegem, F. (2015). Licensed to Kill: Mitochondria, Chloroplasts, and Cell Death. *Trends Plant Sci.* 20 (11), 754–766. doi: 10.1016/j.tplants.2015.08.002

Van Aken, O., and Whelan, J. (2012). Comparison of transcriptional changes to chloroplast and mitochondrial perturbations reveals common and specific responses in Arabidopsis. *Front. Plant Sci.* 3, 281. doi: 10.3389/fpls.2012.00281

Van Aken, O., Zhang, B., Carrie, C., Uggalla, V., Paynter, E., Giraud, E., et al. (2009a). Defining the mitochondrial stress response in Arabidopsis thaliana. *Mol. Plant* 2 (6), 1310–1324. doi: 10.1093/mp/ssp053

Van Aken, O., Giraud, E., Clifton, R., and Whelan, J. (2009b). Alternative oxidase: a target and regulator of stress responses. *Physiol. Plant* 137 (4), 354–361. doi: 10.1111/j.1399-3054.2009.01240.x

Van Aken, O., Zhang, B., Law, S., Narsai, R., and Whelan, J. (2013). AtWRKY40 and AtWRKY63 modulate the expression of stress-responsive nuclear genes encoding mitochondrial and chloroplast proteins. *Plant Physiol.* 162 (1), 254–271. doi: 10.1104/pp.113.215996

Van Aken, O., De Clercq, I., Ivanova, A., Law, S. R., Van Breusegem, F., Millar, A. H., et al. (2016a). Mitochondrial and Chloroplast Stress Responses Are Modulated in Distinct Touch and Chemical Inhibition Phases. *Plant Physiol.* 171 (3), 2150–2165. doi: 10.1104/pp.16.00273

Van Aken, O., Ford, E., Lister, R., Huang, S., and Millar, A. H. (2016b). Retrograde signalling caused by heritable mitochondrial dysfunction is partially mediated by ANAC017 and improves plant performance. *Plant J.* 88 (4), 542–558. doi: 10.1111/tpj.13276

Vanlerberghe, G. C. (2013). Alternative oxidase: a mitochondrial respiratory pathway to maintain metabolic and signaling homeostasis during abiotic and biotic stress in plants. *Int. J. Mol. Sci.* 14 (4), 6805–6847. doi: 10.3390/ijms14046805

Vaseva, A. V., and Moll, U. M. (2009). The mitochondrial p53 pathway. *BBA Bioenerg.* 1787 (5), 414–420. doi: 10.1016/j.bbabio.2008.10.005

Viana, V. E., Marini, N., Busanello, C., Pegoraro, C., Fernando, J. A., Da Maia, L. C., et al. (2018). Regulation of rice responses to submergence by WRKY transcription factors. *Biol. Plant.* 62 (3), 551–560. doi: 10.1007/s10535-018-0806-3

Voss, T., and Hager, G. L. (2014). Dynamic regulation of transcriptional states by chromatin and transcription factors. *Nat. Rev. Genet.* 15 (2), 69–81. doi: 10.1038/nrg3623

Wang, X., Guo, R., Tu, M., Wang, D., Guo, C., Wan, R., et al. (2017). Ectopic Expression of the Wild Grape WRKY Transcription Factor VqWRKY52 in Arabidopsis thaliana Enhances Resistance to the Biotrophic Pathogen Powdery Mildew But Not to the Necrotrophic Pathogen Botrytis cinerea. *Front. Plant Sci.* 8, 97. doi: 10.3389/fpls.2017.00097

Wang, Y., Berkowitz, O., Selinski, J., Xu, Y., Hartmann, A., and Whelan, J. (2018). Stress responsive mitochondrial proteins in Arabidopsis thaliana. *Free Radic. Biol. Med.* 122, 28–39. doi: 10.1016/j.freeradbiomed.2018.03.031

Wanniarachchi, V. R., Dametto, L., Sweetman, C., Shavrukov, Y., Day, D. A., Jenkins, C. L. D., et al. (2018). Alternative Respiratory Pathway Component Genes (AOX and ND) in Rice and Barley and Their Response to Stress. *Int. J. Mol. Sci.* 19 (3), 915. doi: 10.3390/ijms19030915

Weiste, C., Iven, T., Fischer, U., Oñate-Sánchez, L., and Dröge-Laser, W. (2007). In planta ORFeome analysis by large-scale over-expression of GATEWAY®-compatible cDNA clones: screening of ERF transcription factors involved in abiotic stress defense. *Plant J.* 52 (2), 382–390. doi: 10.1111/j.1365-313X.2007.03229.x

Wituszyńska, W., and Karpiński, S. (2013). *Programmed Cell Death as a Response to High Light, UV and Drought Stress in Plants, Abiotic Stress - Plant Responses and Applications in Agriculture*. Eds. K. Vahdati and C. Leslie. doi: 10.5772/53127

Woo, H. R., Kim, J. H., Kim, J., Kim, J., Lee, U., Song, I. J., et al. (2010). The RAV1 transcription factor positively regulates leaf senescence in Arabidopsis. *J. Exp. Bot.* 61 (14), 3947–3957. doi: 10.1093/jxb/erq206

Wu, J., Sun, Y., Zhao, Y., Zhang, J., Luo, L., Li, M., et al. (2015). Deficient plastidic fatty acid synthesis triggers cell death by modulating mitochondrial reactive oxygen species. *Cell Res.* 25 (5), 621–633. doi: 10.1038/cr.2015.46

Xie, H. T., Wan, Z. Y., Li, S., and Zhang, Y. (2014). Spatiotemporal Production of Reactive Oxygen Species by NADPH Oxidase Is Critical for Tapetal Programmed Cell Death and Pollen Development in Arabidopsis. *Plant Cell* 26 (5), 2007–2023. doi: 10.1105/tpc.114.125427

Xu, X., Chen, C., Fan, B., and Chen, Z. (2006). Physical and functional interactions between pathogen-induced Arabidopsis WRKY18, WRKY40, and WRKY60 transcription factors. *Plant Cell* 18 (5), 1310–1326. doi: 10.1105/tpc.105.037523

Xu, Y., Berkowitz, O., Narsai, R., De Clercq, I., Hooi, M., Bulone, V., et al. (2019). Mitochondrial function modulates touch signalling in Arabidopsis thaliana. *Plant J.* 97 (4), 623–645. doi: 10.1111/tpj.14183

Yamauchi, T., Shimamura, S., Nakazono, M., and Mochizuki, T. (2013). Aerenchyma formation in crop species: A review. *Field Crops Res.* 152, 8–16. doi: 10.1016/j.fcr.2012.12.008

Yamauchi, T., Tanaka, A., Inahashi, H., Nishizawa, N. K., Tsutsumi, N., Inukai, Y., et al. (2019). Fine control of aerenchyma and lateral root development through AUX/IAA- and ARF-dependent auxin signaling. *Proc. Natl. Acad. Sci. U. S. A.* 116 (41), 20770. doi: 10.1073/pnas.1907181116

Yan, J., Tong, T., Li, X., Chen, Q., Dai, M., Niu, F., et al. (2017). A Novel NAC-Type Transcription Factor, NAC87, from Oilseed Rape Modulates Reactive Oxygen Species Accumulation and Cell Death. *Plant Cell Physiol.* 59 (2), 290–303. doi: 10.1093/pcp/pcx184

Yang, P., Chen, C., Wang, Z., Fan, B., and Chen, Z. (1999). A pathogen- and salicylic acid-induced WRKY DNA-binding activity recognizes the elicitor response element of the tobacco class I chitinase gene promoter. *Plant J.* 18, 141–149. doi: 10.1046/j.1365-313X.1999.00437.x

Yang, Z. T., Wang, M. J., Sun, L., Lu, S. J., Bi, D. L., Sun, L., et al. (2014). The Membrane-Associated Transcription Factor NAC089 Controls ER-Stress-Induced Programmed Cell Death in Plants. *PLoS Genet.* 10 (3), e1004243. doi: 10.1371/journal.pgen.1004243

Yin, D., Sun, D., Han, Z., Ni, D., Norris, A., and Jiang, C. Z. (2019). PhERF2, an ethylene-responsive element binding factor, plays an essential role in waterlogging tolerance of petunia. *Hortic. Res.* 6 (1), 83. doi: 10.1038/s41438-019-0165-z

Yoo, Y. H., Choi, H. K., and Jung, K. H. (2015). Genome-wide identification and analysis of genes associated with lysigenous aerenchyma formation in rice roots. *J. Plant Biol.* 58, 117–127. doi: 10.1007/s12374-014-0486-2

Yoshiyama, K., Conklin, P. A., Huefner, N. D., and Britt, A. B. (2009). Suppressor of gamma response 1 (SOG1) encodes a putative transcription factor governing multiple responses to DNA damage. *Proc. Natl. Acad. Sci. U. S. A.* 106 (31), 12843–12848. doi: 10.1073/pnas.0810304106

Yoshiyama, K. O., Kobayashi, J., Ogita, N., Ueda, M., Kimura, S., Maki, H., et al. (2013). ATM-mediated phosphorylation of SOG1 is essential for the DNA damage response in Arabidopsis. *EMBO Rep.* 14 (9), 817–822. doi: 10.1038/embor.2013.112

Yoshiyama, K. O., Kimura, S., Maki, H., Britt, A. B., and Umeda, M. (2014). The role of SOG1, a plant-specific transcriptional regulator, in the DNA damage response. *Plant Signal Behav.* 9 (4), e28889. doi: 10.4161/psb.28889

Yuan, X., Wang, H., Cai, J., Li, D., and Song, F. (2019). NAC transcription factors in plant immunity. *Phytopathol. Res.* 1 (1), 3. doi: 10.1186/s42483-018-0008-0

Zancani, M., Casolo, V., Petrussa, E., Peresson, C., Patui, S., Bertolini, A., et al. (2015). The Permeability Transition in Plant Mitochondria: The Missing Link. *Front. Plant Sci.* 6, 1120. doi: 10.3389/fpls.2015.01120

Zhai, Z., Ha, N., Papagiannouli, F., Hamacher-Brady, A., Brady, N., Sorge, S., et al. (2012). Antagonistic Regulation of Apoptosis and Differentiation by the Cut Transcription Factor Represents a Tumor-Suppressing Mechanism in Drosophila. *PLoS Genet.* 8 (3), e1002582. doi: 10.1371/journal.pgen.1002582

Zhang, B., Van Aken, O., Thatcher, L., De Clercq, I., Duncan, O., Law, S. R., et al. (2014). The mitochondrial outer membrane AAA ATPase AtOM66 affects cell death and pathogen resistance in *Arabidopsis thaliana*. *Plant J.* 80 (4), 709–727. doi: 10.1111/tpj.12665

Zhang, X., Ivanova, A., Vandepoele, K., Radomiljac, J., Van de Velde, J., Berkowitz, O., et al. (2017a). The Transcription Factor MYB29 Is a Regulator of ALTERNATIVE OXIDASE1a. *Plant Physiol.* 173 (3), 1824–1843. doi: 10.1104/pp.16.01494

Zhang, X., Shabala, S., Koutoulis, A., Shabala, L., and Zhou, M. (2017b). Meta-analysis of major QTL for abiotic stress tolerance in barley and implications for barley breeding. *Planta* 245 (2), 283–295. doi: 10.1007/s00425-016-2605-4

Zhu, J., Brown, K. M., and Lynch, J. P. (2010). Root cortical aerenchyma improves the drought tolerance of maize (*Zea mays* L.). *Plant Cell Environ.* 33 (5), 740–749. doi: 10.1111/j.1365-3040.2009.02099.x

Zuppini, A., Navazio, L., and Mariani, P. (2004). Endoplasmic reticulum stress-induced programmed cell death in soybean cells. *J. Cell Sci.* 117 (12), 2591. doi: 10.1242/jcs.01126

Conflict of Interest: The authors declare that the research was conducted in the absence of any commercial or financial relationships that could be construed as a potential conflict of interest.

frontiers in Plant Science

ORIGINAL RESEARCH
published: 14 December 2020
doi: 10.3389/fpls.2020.490075

Cyanobacteria-Derived Proline Increases Stress Tolerance in *Arabidopsis thaliana* Root Hairs by Suppressing Programmed Cell Death

*Alysha Chua[1,2,3], Orla L. Sherwood[4,5,6], Laurence Fitzhenry[1,2], Carl K.-Y. Ng[4,5,6], Paul F. McCabe[4,5,6] and Cara T. Daly[1,2,3]**

[1] Department of Science, Waterford Institute of Technology, Waterford, Ireland, [2] Pharmaceutical and Molecular Biotechnology Research Centre (PMBRC), Waterford Institute of Technology, Waterford, Ireland, [3] Eco-Innovation Research Centre (EIRC), Waterford Institute of Technology, Waterford, Ireland, [4] UCD School of Biology and Environmental Science, University College Dublin, Dublin, Ireland, [5] UCD Centre for Plant Science, University College Dublin, Dublin, Ireland, [6] UCD Earth Institute, University College Dublin, Dublin, Ireland

Nitrogen-fixing heterocystous cyanobacteria are used as biofertilizer inoculants for stimulating plant growth but can also alleviate plant stress by exometabolite secretion. However, only a small number of studies have focused on elucidating the identity of said bioactives because of the wide array of exuded compounds. Here, we used the root hair assay (RHA) as a rapid programmed cell death (PCD) screening tool for characterizing the bioactivity of cyanobacteria *Nostoc muscorum* conditioned medium (CM) on *Arabidopsis thaliana* root hair stress tolerance. We found that heat-stressed *A. thaliana* pre-treated with *N. muscorum* CM fractions exhibited significantly lower root hair PCD levels compared to untreated seedlings. Treatment with CM increased stress tolerance by suppressing PCD in root hairs but not necrosis, indicating the bioactive compound was specifically modulating the PCD pathway and not a general stress response. Based on documented *N. muscorum* exometabolites, we identified the stress-responsive proline as a compound of interest and strong evidence from the ninhydrin assay and HPLC indicate that proline is present in *N. muscorum* CM. To establish whether proline was capable of suppressing PCD, we conducted proline supplementation experiments. Our results showed that exogenous proline had a similar effect on root hairs as *N. muscorum* CM treatment, with comparable PCD suppression levels and insignificant necrosis changes. To verify proline as one of the biologically active compounds in *N. muscorum* CM, we used three mutant *A. thaliana* lines with proline transporter mutations (*lht1*, *aap1* and *atprot1-1::atprot2-3::atprot3-2*). Compared with the wild-type seedlings, PCD-suppression in *lht1*and *aap1* mutants was significantly reduced when supplied with low proline (1–5 μM) levels. Similarly, pre-treatment with *N. muscorum* CM resulted in elevated PCD levels in all three mutant lines compared to wild-type seedlings. Our results show that plant uptake of cyanobacteria-derived proline alters their root hair PCD sensitivity threshold. This offers evidence of a novel biofertilizer mechanism for reducing stress-induced PCD levels, independent of the existing mechanisms documented in the literature.

Keywords: programmed cell death (PCD), proline, biofertiliser, cyanobacteria exometabolites, root hair assay (RHA), *Nostoc muscorum*, plant stress tolerance

OPEN ACCESS

Edited by:
Julian Eaton-Rye, University of Otago, New Zealand

Reviewed by:
Vijay Pratap Singh, University of Allahabad, India
Dietmar Funck, University of Konstanz, Germany

***Correspondence:**
Cara T. Daly
CDALY@wit.ie

Specialty section:
This article was submitted to Plant Cell Biology, a section of the journal Frontiers in Plant Science

Received: *06 August 2019*
Accepted: *25 November 2020*
Published: *14 December 2020*

Citation:
Chua A, Sherwood OL, Fitzhenry L, Ng CK-Y, McCabe PF and Daly CT (2020) Cyanobacteria-Derived Proline Increases Stress Tolerance in Arabidopsis thaliana Root Hairs by Suppressing Programmed Cell Death. Front. Plant Sci. 11:490075. doi: 10.3389/fpls.2020.490075

INTRODUCTION

Cyanobacteria are adaptable organisms found in aquatic and terrestrial ecosystems. Their ability to inhabit most environments is attributed to the diverse range of exuded metabolites, termed exometabolites that can have antiviral, antibacterial, antifungal, antitumoral and anti-inflammatory properties (Singh et al., 2005; Jaiswal et al., 2008; Prasanna et al., 2010). In agriculture, nitrogen-fixing heterocystous cyanobacteria are often used as biofertiliser inoculants to stimulate plant growth. For example, *Anabaena*-inoculated wheat seedlings had improved shoot length, grain weight and phytohormone (cytokinin and indole-3-acetic acid) levels compared to untreated controls (Hussain and Hasnain, 2011). Biofertiliser inoculants contain little macro- and micro-nutrients as they are catalysts for mobilizing nutrients into metabolically accessible forms that are otherwise unavailable to plants (Kennedy, 2008). Depending on the functional characteristics of the inoculant, biofertilizers can either directly or indirectly provide yield gain. Direct benefits make essential macronutrients available for plant growth via nitrogen fixation and phosphate solubilization, while indirect benefits rely on assorted mechanisms to safeguard against abiotic and biotic stresses (Barreto et al., 2011).

Nostoc is a genus of blue-green, N_2-fixing bacteria which can be free-living but can form symbiotic relationships with fungi (Rai et al., 2000) and several plant species, such as the hornwort *Anthoceros punctatus* (Campbell and Meeks, 1989) and the angiosperm *Gunnera* (Rasmussen et al., 1994). *Nostoc muscorum* is the model organism for studying heterocyst differentiation but it cannot differentiate into akinetes and hormogonia, unlike other taxonomically defined *Nostoc* species (Meeks et al., 2002). A wide range of compounds have been found in *N. muscorum* extracellular filtrate, termed conditioned media (CM), such as amino acids (Picossi et al., 2005; Pernil et al., 2008), exopolysaccharides (EPS) (Mehta and Vaidya, 1978), auxin (Mirsa and Kaushik, 1989; Karthikeyan et al., 2009), abscisic acid (ABA) (Maršálek et al., 1992) and phenolics and alkaloids (Abdel-Hafez et al., 2015). Previous work (unpublished data) showed that *Nostoc muscorum* sp.7120 (hereafter, *N. muscorum*) CM suppresses root hair programmed cell death (PCD) in heat-stressed *Arabidopsis* seedlings, but the identity of these pro-survival signals were not identified. Considered the model organism for studying heterocyst differentiation, *N. muscorum* has undergone many name changes over the years. *Nostoc* sp. strain PCC 7120 was originally named *Nostoc muscorum*, before being classified as *Anabaena* and finally renamed as *Nostoc* sp. strain PCC 7120 based on DNA–DNA hybridization data and short tandem repeated repetitive fingerprinting (Svenning et al., 2005).

Chen and Dickman (2005) have shown that exogenous proline inhibits stress-induced PCD levels in *Colletotrichum trifolii* and *Saccharomyces cerevisiae* by quenching reactive oxygen species (ROS). Proline might have a similar role in plants as it is a stress-responsive amino acid that indirectly scavenges ROS by stimulating the plant antioxidant defense and glyoxalase system (Hossain et al., 2014, 2016; Rejeb et al., 2014). Studies have reported the presence of proline in *N. muscorum* extracellular medium (Picossi et al., 2005; Pernil et al., 2008) and plants have three root-localized transporters for importing proline: amino acid permease 1 (AAP1), lysine-histidine transporter 1 (LHT1) and proline transporter (ProT) (Lehmann et al., 2010).

AAP1 is an intermediate-affinity transport system for neutral amino acids (i.e., proline), glutamate and aspartate (Svennerstam et al., 2011). Expressed in the *Arabidopsis* root epidermis and tips, AAP1 imports extracellular amino acids into the vascular system for long-distance transport (Lee et al., 2007). LHT1 is a broad-specificity, high-affinity transporter for histidine, acidic and neutral amino acids like proline (Hirner et al., 2006). During the early developmental stage, LHT1 is expressed in the rhizodermis of emerging and lateral roots to import soil amino acids (Hirner et al., 2006). In later stages, LHT1 supplies leaf mesophylls with xylem-derived amino acids and is expressed throughout the root epidermis and tips, leaf mesophyll, stem, petals and sepals (Hirner et al., 2006). In contrast to both general amino acid transporters, the ProT subfamily only imports proline, but can also transport stress-induced compounds such as glycine betaine and γ-aminobutyric acid (Schwacke et al., 1999; Grallath et al., 2005). Three subfamily members have been characterized in *Arabidopsis* (AtProT1, AtProT2 and AtProT3) and they are expressed differently all over the plant (Lehmann et al., 2011). Phloem-localized AtProT1 is expressed in the vascular tissue of leaves, petioles, roots, flowers, siliques, and stems (Rentsch et al., 1996). However, AtProT1 expression is absent in root tips and has weak expression levels in emerging lateral roots. Conversely, AtProT2 expression is mostly present in the root cortex and epidermis, while AtProT3 expression is only found in leaf epidermis (Grallath et al., 2005). As external proline can be assimilated by *Arabidopsis*, it is a possible candidate for the bioactive PCD-suppressing effect noted in *N. muscorum* CM.

PCD is activated by developmental and environmental factors as it plays an important role in vegetative and reproductive tissue development (Kacprzyk et al., 2011; Daneva et al., 2016). However, plant cells also undergo PCD to mitigate stress effects, such as hypoxia (Lenochová et al., 2009), salinity (Shabala, 2009), drought (Nguyen et al., 2009), UV overexposure (Ferreyra et al., 2016), heavy metal exposure (Xu et al., 2013), heat (Vacca et al., 2004) and pathogen infection (Lam et al., 2001). PCD is a methodical process of cellular destruction characterized by the distinctive retraction of the cytoplasm; this active and interruptible process is driven by cellular Ca^{2+} influx (Kacprzyk et al., 2017). Conversely, necrosis is associated with uncontrolled cell death that occurs when cells cannot withstand overwhelming cellular stress (Reape et al., 2008). As substantial differences in signaling, morphology and regulation exist between PCD and necrosis (Kacprzyk et al., 2017), assessing the stress response only using a single parameter loses context as to whether cells are dying by activated PCD or uncontrolled necrotic death. Therefore, it is important to differentiate between both death modes to paint an accurate picture of plant cell death studies across different research groups (Reape et al., 2008; Reape and McCabe, 2013).

In this study, we used the root hair assay (RHA) to demonstrate the PCD-suppressing bioactivity of *N. muscorum* CM. 5-day old *Arabidopsis* seedlings were pre-treated with

N. muscorum CM fractions and heat stress applied. Using a combination of viability staining and death morphologies, the RHA was used to quantify the root hair stress response in terms of cell viability, PCD, and necrosis. This was done to test if the bioactive compound was affecting the PCD pathway or modulating a general stress response. Based on documented *N. muscorum* exometabolites, the stress-responsive amino acid proline was highlighted as a compound of interest. Proline was detected in *N. muscorum* CM using the ninhydrin assay and HPLC. Following that, we confirmed the bioactivity of proline by assessing how exogenous proline affected heat-shocked wild-type *Arabidopsis* seedlings. Finally, we also compared the performance of *Arabidopsis* proline transporter mutants (*lht1*, *aap1* and *atprot1-1::atprot2-3::atprot3-2*) against stress-induced PCD levels of wild-type seedlings pre-treated with proline before heat shock exposure. To the best of our knowledge, this study is the first instance to show that proline enhances *in vivo* root hair stress tolerance by modifying the PCD activation threshold.

MATERIALS AND METHODS

Growth and Sterilization Procedures for Seedlings

Seeds of *Arabidopsis thaliana* L. ecotype Columbia (Col-0) were soaked in 20% bleach (Domestos® disinfectant: sodium hypochlorite −4.5 g per 100 g) aseptically, the bleach solution was removed, and the seeds were rinsed five times with sterilized deionised water (SDW). Sterilized seeds (15–20) were placed in a straight line on germination medium comprising ½-strength Murashige and Skoog (MS) agar plates, adjusted to pH 5.8 with NaOH and solidified with 6 g/L Duchefa® plant agar. The composition of the ½ MS plates were as follows: 0.0125 mg/L $CoCl_2.6H_2O$, 0.0125 mg/L μM $CuSO_4.5\ H_2O$, 18.4 mg/L FeNaEDTA, 3.10 mg/L H_3BO_3, 0.415 mg/L KI, 8.45 mg/L $MnSO_4.\ H_2O$, 0.125 mg/L $Na_2MoO_4.2\ H_2O$, 4.30 mg/L $ZnSO_4.7\ H_2O$, 0.166 g/L $CaCl_2$, 0.085 g/L KH_2PO_4, 0.950 g/L KNO_3, 0.090 g/L $MgSO_4$, and 0.825 g/L NH_4NO_3. Plates were stratified at 4°C for 24 h to synchronize germination and placed vertically under light (33 μmol m^{-2} s^{-1}, 16-h light: 8-h darkness) in a 21°C growth chamber to germinate seeds. *Arabidopsis* seedlings developed sufficient root hair density after five days of growth and were then used for stress assays.

Heat Stressing of *Arabidopsis thaliana* Seedlings

Arabidopsis seedlings (5-day old) were transferred using sterile forceps into individual wells of a sterile 24-well plate (Sarstedt® Tissue Culture Plate) containing 1 ml SDW. Seedlings were handled with care during the transfer process to avoid mechanical damage to root hairs and elevated background death levels. 24-well plates were sealed using autoclave tape, placed in a Grant SUB Aqua Pro 26 water bath already stabilized at the desired heat stress temperature (25, 35, 45, 50, 55, 65, 75, or 85°C), and heat stressed for 10 min. Seedlings were returned to the 21°C growth chamber and scored 14–16 h after stress application to allow PCD morphology to fully develop. The RHA was used to quantify the stress response in terms of viability, PCD and necrosis as described by Hogg et al. (2011).

Assessing the Plant Stress Response Using PCD Morphology and Viability Stain

Direct scoring of root hairs relied on a combination of the fluorescein diacetate (FDA) viability stain and cell corpse morphology (PCD and necrotic root hairs) as visual indicators. *Arabidopsis* seedlings were placed on microscope slides, stained with a 0.001% w/v FDA solution for 2 min and examined using an Olympus BX61 microscope with a FITC filter. The root hairs were scored as follows: (A) viable when exhibiting positive FDA staining, (B) PCD if exhibiting a negative FDA stain and retracted cytoplasm and (C) necrotic if the FDA stain is negative and the protoplast is not retracted (**Figure 1A**; Hogg et al., 2011). At least 100 root hairs were scored per seedling to give an accurate representation of the levels of viable cells and dead cells (PCD + necrosis). The proportions of cells in each state is expressed as percentage of the total number of analyzed root hairs.

For additional evidence (**Supplementary Figure 1**) to confirm heat-exposed root hairs were dead and not merely dehydrated, whole trichoblast cells were stained with Evans Blue indicating the whole cell was dead, and not just the cytoplasmic extension that forms the root hair. To this end, a 5 day old *A. thaliana* Col-0 seedling was heat stressed at 49 °C for 10 min, incubated for 30 h under constant illumination and then stained for 1 h in 0.25% Evans Blue stain.

Profiling Bioactive *Nostoc* spp. Exometabolites in Conditioned Medium (CM)

Nostoc muscorum cultures from the Pasteur Culture Collection of Cyanobacteria Paris, France (PCC 7120 available for order from the following link: https://catalogue-crbip.pasteur.fr/recherche_catalogue.xhtml), were grown in BG11 media at 25 °C (light intensity of 30 μmol m^{-2} s^{-1}, 16-h light: 8-h darkness) and shaken at 110 rpm under sterile conditions to maintain axenic cultures. Culture growth was monitored by measuring optical density (Myers et al., 2013), chl-*a*, and carotenoid concentration by methanol extraction according to Zavřel et al. (2015). *N. muscorum* CM was harvested in the deceleration phase [OD_{730} (1.17), chl-*a* (14.14 μg ml^{-1}), carotenoid (3 μg ml^{-1})] after two cycles of centrifugation (Eppendorf Centrifuge 5810 R®) at 3000 × *g* for 20 min. After each cycle, the supernatant was collected, and the pellet discarded to eliminate leftover cells. The resulting cell-free supernatant was sterile-filtered through a 0.45 μm PES filter; half of the filtered supernatant was autoclaved (121°C for 15 min) while the other half remained unautoclaved. *Nostoc* CM fractions (autoclaved and non-autoclaved) were diluted in BG11 at various concentrations and screened for PCD-suppressing bioactivity by pre-treating *Arabidopsis* seedlings with CM fractions for 3 h in 24-well plates, followed by 50°C exposure for 10 min in the water

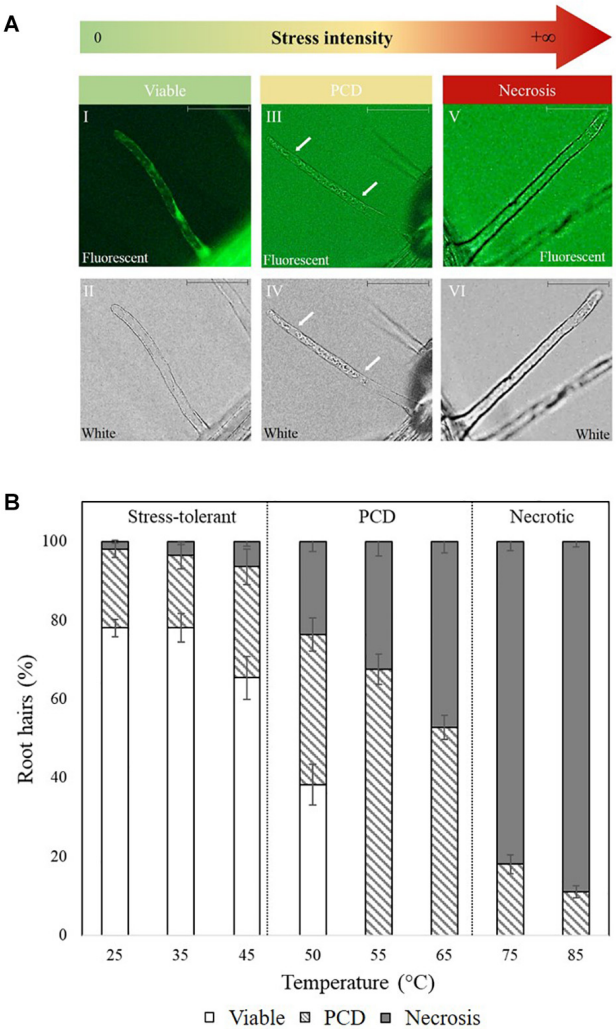

FIGURE 1 | (A) Cell morphology of FDA-stained root hairs of heat shocked *Arabidopsis* seedlings under fluorescent (I, III, and V) and white light (II, IV, and VI). Viable root hairs are FDA positive and exhibit fluorescence (I and II – no heat shock), PCD root hairs are FDA negative and have a retracted cytoplasm indicated by white arrows (III and IV – 50°C heat shock), and necrotic root hairs are FDA negative but do not have a retracted cytoplasm (V and VI – 80°C heat shock). Scale bars: I–VI 10 μm. **(B)** Effect of heat stress on *Arabidopsis* root hair viability and cell death (PCD and necrosis) levels. The bars represent viable (white), PCD (hatched) and necrosis (gray) root hairs, each expressed as a percentage of cell mode over total number of root hairs. Values are means ± SE ($n \geq 12$) and represent the merged results of 3 experiments.

bath. Viability, PCD, and necrosis levels were scored 14–16 h later using the RHA.

Ninhydrin Assay

A modified ninhydrin-based protocol (Bates et al., 1973) that did not rely on the use of toluene was adapted from Claussen (2005), who used it to determine stress-induced proline levels in tomato plants. The protocol from Claussen (2005) was used to quantify proline levels in autoclaved and non-autoclaved CM. A mixture containing 400 μl of CM, 400 μl of glacial acetic acid, and 400 μl ninhydrin mixture (2.5% ninhydrin dissolved in 6:3:1 ratios of glacial acetic acid, SDW and 85% orthophosphoric acid) were vortexed and heated at 100°C for 1 h in a block heater (Stuart® SBH130D). The reaction was terminated by incubation at 21°C for 5 min, followed by quantification at 546 nm using an Ultrospec 2000® spectrophotometer. Proline concentration was determined from a proline standard curve.

Detection of Amino Acids Using Reverse-Phase HPLC

A modified protocol from Heinrikson and Meredith (1984) and Kwanyuen and Burton (2010) was adapted to detect amino acids in *N. muscorum* CM. Phenyl isothiocyanate (PITC) was chosen as the precolumn derivatization agent as it reacts with both primary and secondary amines such as proline and hydroxyproline, unlike other derivatizing agents such as *o*-phthalaldehyde (Walker and Mills, 1995). Amino acid standards (TCI Chemicals), each corresponding to 1.5 mM,

were prepared individually and in a mixture in 0.1 M HCl. *N. muscorum* CM was harvested in the deceleration phase [OD_{730} (1.67), chl-*a* (33.19 μg ml^{-1}) and carotenoid (9.77 μg ml^{-1}) after two cycles of centrifugation at 3000 × *g* for 20 min. After each cycle, the supernatant was collected and sterile-filtered through a 0.45 μm PES filter. Following that, 40 μl of the amino acid mixture or 200 μl of filtered *N. muscorum* CM sample was added to 100 μl of coupling buffer (acetonitrile: pyridine: triethylamine: H_2O, 10:5:2:3) and dried under vacuum by rotary evaporation (ScanSpeed 32®) at 85°C. Derivatization was performed by adding 20 μl of a 7:1:1:1 ratio mixture of ethanol: water: triethylamine: PITC (v/v). The resultant mixture was incubated for 20 min in the dark at room temperature to form phenylthiocarbamyl derivatives (PTC-amino acid) that were quantified using reverse-phase HPLC. Samples were then dried under vacuum at 35°C because of PTC amino acid sensitivity to light and high temperature. The pellet was re-suspended in 100 μl of 4 mM sodium phosphate (pH 7.4) and 2% (v/v) acetonitrile and was injected into a Symmetry® C18 column (3.99 mm × 15 cm, 5 μm particle size) in a HPLC system (Agilent Technologies 1200 Series). An injection volume of 14 μl was used for the amino acid mixture, while 70 μl was injected for the *N. muscorum* CM sample. The mobile phase consisted of two solvents: Solvent A was 70 mM sodium phosphate (pH 6.55, adjusted by NaOH) and 2% acetonitrile (v/v); solvent B comprised 50% (v/v) acetonitrile. The following step-wise gradient was used to separate the amino acid peaks: 0–1 min [0% Solvent B; 5.5–7 min (15% B); 8.5–13.5 min (30% B); 14 min (35% B); 15.5 min (42% B); 16 min (43% B); 20 min (60%); 22 min 0% B]. Absorbance of the PTC-amino acid adducts was monitored at 254 nm.

Evaluating the Effect of Exogenous Proline and *N. muscorum* CM in Root Hairs of Wild-Type and Mutant *Arabidopsis* Lines

Two proline solutions were established in BG11 at identical concentrations previously measured in autoclaved CM (1.94 μM) and non-autoclaved CM (1.83 μM), with the former solution autoclaved at 121°C for 15 min. Both proline solutions (autoclaved and non-autoclaved) were diluted in BG11 at various concentrations. Five-day old *Arabidopsis* seedlings were incubated for 3 hr in the proline solutions and seedlings were then heat stressed at 50°C for 10 min. We chose 50°C as it is a stress intensity that can either give rise to high levels of PCD or cell survival, depending on the elicitor treatment. Therefore, stress exposure at this viability/PCD inflection point informs us on the effect of various treatments on the perturbation of cell death or survival signaling pathways. Seedlings were returned to the 21°C growth chamber and scored for viability, and death via necrosis or PCD 14–16 h after heat stress application. This protocol was repeated with *Arabidopsis* lines with proline transporter mutations: *lht1* (Hirner et al., 2006), *aap1* (Lee et al., 2007) and the *atprot* triple knockout (*atprot1-1::atprot2-3::atprot3-2)* (Lehmann et al., 2011). Five-day old *Arabidopsis* mutant seedlings were treated with exogenous proline (1, 2, 5, or 100 μM) or fresh 100% *N. muscorum* CM (OD_{730} = 1.43), chl-*a* = 18.9 μg ml^{-1} and carotenoid = 4.67 μg ml^{-1}) for 3 h, heat stressed at 50°C for 10 min and returned to the 21°C growth chamber. The RHA was used to score viable, PCD and necrotic root hairs of the mutants after 14–16 h of stress application.

Statistical Analysis

IBM® SPSS® Version 24 (RRID:SCR_002865) was used to analyze results for significant changes ($p < 0.05$) across elicitor treatment and mutant *Arabidopsis* lines. Statistical tests used include one-way (Tukey or Dunnett *Post-hoc* Test) and two-way ANOVA analysis.

RESULTS

The Arabidopsis Heat Stress Baseline Response

Baseline heat stress responses were established in *Arabidopsis thaliana* and two distinctive stress-response thresholds were detected: stress-tolerant, PCD and necrosis (**Figure 1B**). Most of the root hairs remained viable (65–75%) at 25–45°C, but at 50–65°C, cell death accumulated at greater rates, with PCD being the predominant cell death form. This changed under overwhelming heat stress (75–85°C) as root hairs primarily died by necrosis, instead of PCD. Based on the dose-dependent response, 50°C was identified as the inflection point as it was located at the stress-tolerant/PCD threshold, i.e., the transition border between the majority of root hairs remaining alive versus PCD activation.

Screening *N. muscorum* CM for PCD-Suppression

The secretion of pro-survival signals into extracellular filtrate have been observed in animal (Barres et al., 1992) and plant cells (McCabe et al., 1997), and similar observations by C.T. Daly (unpublished data) suggest that *N. muscorum* CM also contains pro-survival signals. To identify the pro-survival signals, the RHA was used as a high-throughput system for screening *N. muscorum* CM for PCD-suppressing activity. *N. muscorum* was cultured in a closed batch system and the harvested CM diluted with fresh BG11 to generate a concentration range (20–100%) to determine the optimum CM% for the strongest PCD-suppressing effect at the 50°C inflection point. We used a two-way ANOVA test to analyze if increasing the *N. muscorum* CM concentration and autoclaving fractions would influence stress-induced PCD levels. Each individual variable had a strong significant ($p < 0.01$) effect on PCD levels and the adjusted r-squared value (0.333) shows that 33.3% of the variance in PCD levels can be attributed to autoclave treatment and CM% fraction. The interaction effect was non-significant, F (4, 121) = 0.49, p = 0.743.

For example, CM treatment exerted a statistically significant dose-dependent effect, where F (4, 121) = 0.49, p = 0.000. As shown in **Figure 2**, the strongest protection effect was offered by 60–100% non-autoclaved CM treatment (38–42% PCD), which equates to an approximate 30% decrease in PCD levels compared to SDW and BG11 (75–78% PCD)

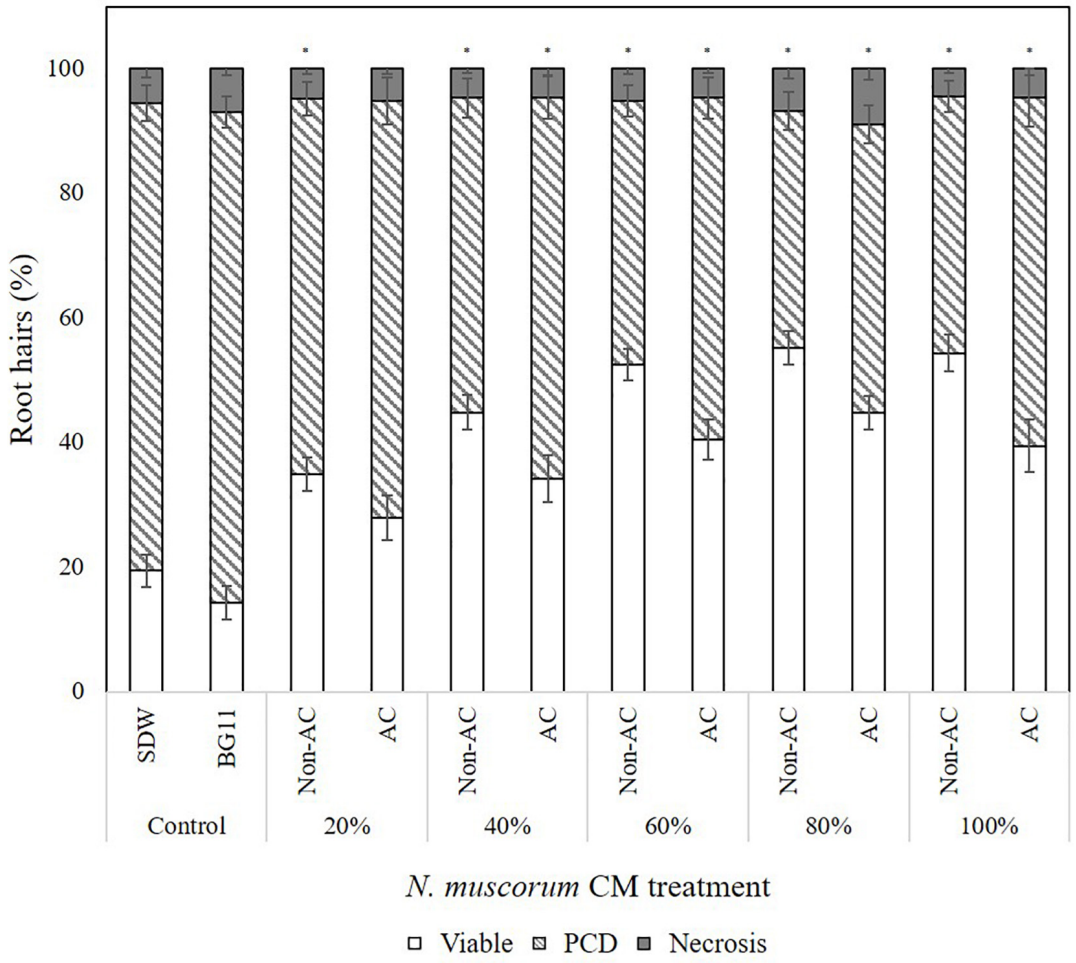

FIGURE 2 | Effect of autoclaved (AC) and non-autoclaved *N. muscorum* CM on *Arabidopsis* root hair viability and death (PCD and necrosis) levels at 50°C heat stress. The bars represent viable (white), PCD (hatched) and necrosis (gray) root hairs, each expressed as a percentage of cell mode over total number of root hairs. Values are the average of $n \geq 8$ (±SE) and represent the merged results of 3 experiments. (*) marks PCD levels significantly ($p < 0.05$) different from the BG11 control using a Dunnett t-test (**Supplementary Table 1**).

controls. All tested *N. muscorum* CM fractions, apart from the 20% autoclaved treatment, were significantly different ($p < 0.05$) from the BG11 control (**Supplementary Table 1**). Similarly, autoclaved CM treatments resulted in higher mean PCD levels ($M = 57.1\%$, $SE = 1.46$) over non-autoclaved CM supplementation ($M = 46.5\%$, $SE = 1.52$), where F (1, 121) = 25.4, $p = 0.000$. We tested autoclaved and non-autoclaved CM fractions to determine if the PCD-suppressing compound was thermolabile; both treatments suppressed PCD in treated root hairs showing that the major compound was thermostable. However, the PCD-suppression effect in autoclaved *N. muscorum* CM was consistently lower than non-autoclaved CM across all five tested CM concentrations (20–100%). Autoclaved *N. muscorum* CM treated seedlings had significantly ($p < 0.05$) higher PCD levels, with an average difference of 10.6%, compared to their non-autoclaved treated counterparts. Lastly, *N. muscorum* CM treatment shifted the PCD activation threshold, as a proportion of root hairs normally dying by PCD in treated seedlings were now viable. There were negligible changes in necrosis levels across all tested CM concentrations as improvements in viability levels corresponded to increasing PCD suppression.

Identification and Quantification of Proline as the Compound of Interest

Our findings from the initial *N. muscorum* CM screening process showed that the bioactive compound was thermostable and directly modulating the PCD pathway. This information was cross-referenced with data from a literature review on *N. muscorum* exometabolites and used as input for building a framework to identify possible bioactive candidates (see "Discussion"). The resultant framework highlighted proline as a candidate of interest as it accumulates in plants under abiotic and biotic stress (Abrahám et al., 2010; Hayat et al., 2012). Proline was detected in *N. muscorum* CM using two separate

assays: the ninhydrin assay and reverse-phase HPLC. Using the ninhydrin assay, similar proline concentrations (1.83–1.94 μM) were detected in autoclaved and non-autoclaved CM used in the screening experiments, which had insignificant variability once the standard error was considered (**Table 1**). The ninhydrin assay is a colorimetric method for quantifying proline as ninhydrin produces a distinctive red chromophore when reacting with proline under acidic conditions. While the other proteinogenic amino acids give no color (Friedman, 2004), the ninhydrin assay can overestimate proline levels when high levels of structurally related amino acids are present, as ornithine, D-proline and δ^1-pyrroline-5-carboxylic acid (P5C) produces a similar red color (Forlani and Funck, 2020).

For these reasons, a reverse-phase HPLC method was developed for additional evidence of proline and the other amino acids in *N. muscorum* CM. We utilized a different *N. muscorum* CM batch for HPLC analysis, separate from the batch originally used in the bioactivity screening and ninhydrin assay. Older cultures in the deceleration phase were specifically chosen for better amino acid detection sensitivity as culture age significantly influences the composition of cyanobacteria exometabolites (Volk, 2007). Separation of the amino acid standard mixture was achieved under the run conditions, with proline achieving a satisfactory peak resolution of 4.61 with alanine, its adjacent peak (**Figure 3A**, red lines). 200 μL of *N. muscorum* CM was concentrated (a 5-fold concentration factor) and analyzed for amino acid content. Proline was successfully detected in the 200 μL *N. muscorum* CM sample as a peak (70.73 mAU) that eluted at the 7.87-minute mark (**Figure 3B**) and its presence demonstrated by spiking the 200 μL *N. muscorum* CM with an internal 100 μM proline standard (**Figure 3C**). After overlaying the *N. muscorum* sample with the amino acid standard mixture, we detected the following amino acids in *N. muscorum* CM: glutamic acid, serine, asparagine/glycine, glutamine, histidine, arginine, threonine, alanine, tyrosine, valine, methionine, isoleucine/leucine, phenylalanine, tryptophan and lysine.

Confirming the Bioactive PCD-suppressing Effect of Proline

Evaluating the Effect of Exogenous Proline and *N. muscorum* CM in Wild-type (Col-0) *Arabidopsis* Lines

We prepared two proline solutions in BG11, at concentrations identical to that measured using the ninhydrin assay in autoclaved CM (1.94 μM) and non-autoclaved CM (1.83 μM). The former solution was autoclaved at 121°C for 15 min to determine if proline was the thermostable bioactive compound in *N. muscorum* CM. Both proline solutions were diluted across a similar concentration gradient (20–100%) to assess if proline elicits a dose-dependent response. The SDW control was omitted for this series of experiments as past results and statistical analysis (**Supplementary Table 1**) show that BG11 and SDW treatment results in similar PCD levels, with no bioactive effect noted in treated wild-type *Arabidopsis* seedlings.

We also applied a two-way ANOVA test to assess if proline was thermostable and if exogenous proline treatment exerted a dose-dependent effect. This was done by assessing if autoclave treatment and diluted proline fractions (20–100%) affected stress-induced PCD levels. Both variables did not have a significant effect and the interaction effect was also non-significant, where F (4, 115) = 2.14, p = 0.08. Autoclave treatment had an F ratio of F (4, 115) = 0.347, p = 0.557, indicating that proline was thermostable. There was no significant ($p > 0.05$) differences between autoclaved (M = 46.1%, SE = 1.49) and non-autoclaved (M = 47.4%, SE = 1.57) proline treatments, with an average mean difference of 1.28%. Our results confirmed that proline was thermostable as all tested proline fractions (autoclaved and non-autoclaved) significantly reduced ($p < 0.05$) stress-induced PCD levels of treated *Arabidopsis* seedlings, with up to a 24% mean difference from the BG11 control (**Supplementary Table 2**). Moreover, proline treated seedlings exhibited a similar stress-response profile as *N. muscorum* CM treatment: treated seedlings had lower stress-induced PCD levels, but negligible changes to necrosis levels (**Figure 4**), demonstrating the PCD-suppressing ability of proline. Unlike *N. muscorum* CM though, exogenous proline did not inhibit PCD in a dose-dependent manner, where F ratio of F (1, 115) = 0.195, p = 0.941. Overall, we show that proline was thermostable and suppressed *Arabidopsis* stress-induced PCD levels as necrosis changed negligibly across the entire treatment range.

Comparing the Effect of *N. muscorum* CM and Exogenous Proline in Heat-Stressed *Arabidopsis* Seedlings

We examined the extent of PCD-suppression between *N. muscorum* CM and exogenous proline treatments at each dilution factor from 20–100% (**Figure 5**). One-way ANOVA analysis at each % of CM/proline fraction revealed two key trends: (1) the greatest variations primarily affected autoclaved *N. muscorum* CM treated seedlings as they had higher PCD levels compared to the other treatments and (2) significant differences ($p < 0.05$) between *N. muscorum* CM and exogenous proline datasets predominantly occurred at the lower concentrations, but largely disappeared at the more concentrated doses (**Supplementary Table 3**). The largest fluctuation in root hair PCD levels were observed for dilutions of CM and proline solutions in the range of 20–40%, but dilutions from 60–100% did not have significant differences ($p > 0.05$) between *N. muscorum* CM and exogenous proline datasets. This shows that comparable PCD-suppression occurs at concentrated doses between proline-treated root hairs and their corresponding CM fractions – offering preliminary evidence for proline as the bioactive compound.

TABLE 1 | Quantification of proline in autoclaved and non-autoclaved *N. muscorum* CM [OD_{730} (1.17), chl-*a* (14.14 μg ml^{-1}) and carotenoid (3 μg ml^{-1})].

N. muscorum Conditioned Media (CM)	Proline concentration (μM)
Autoclaved	1.83 ± 0.26
Non-autoclaved	1.94 ± 0.22

Values are the average of n = 16 (±SE) and represent the merged results of 2 experiments.

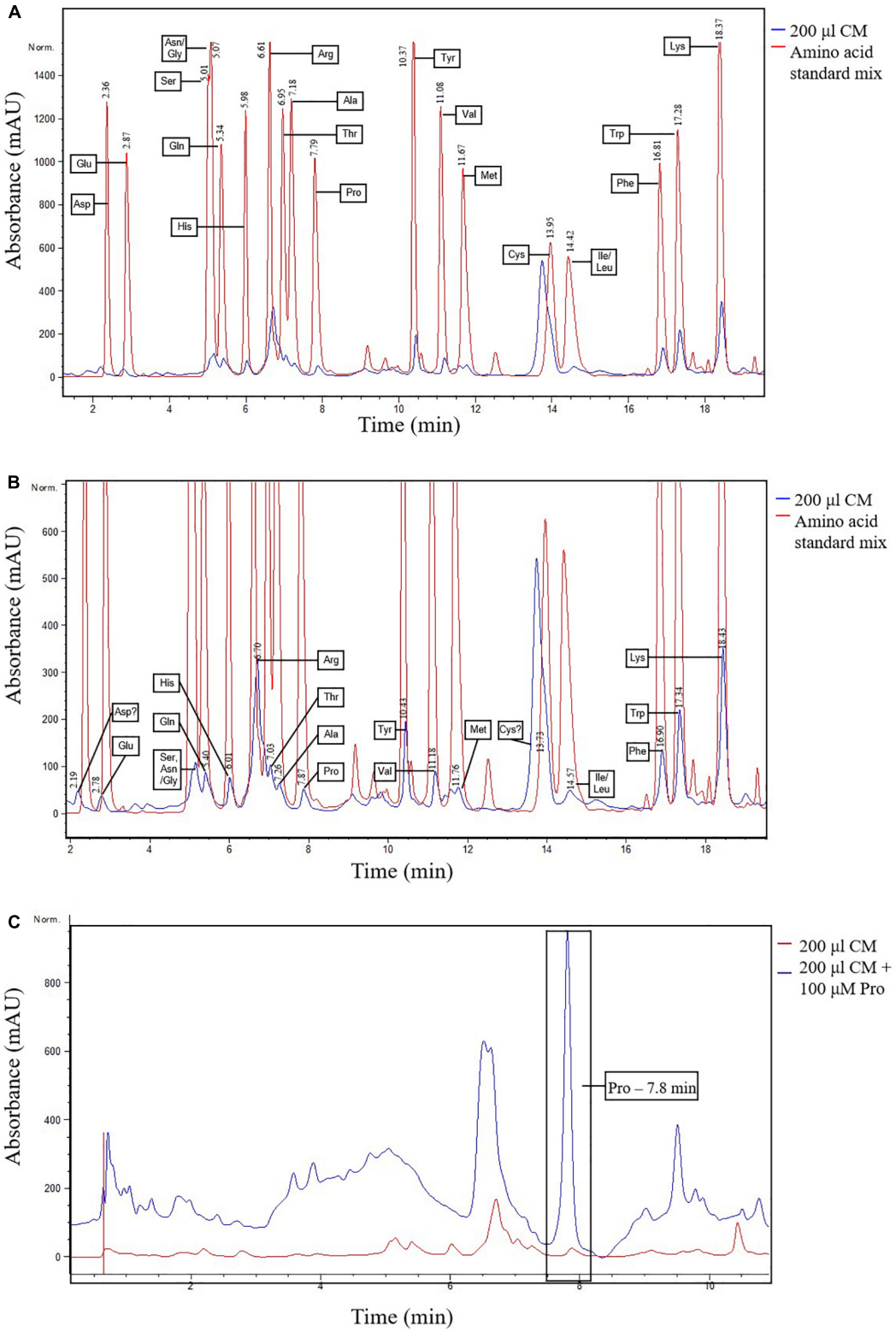

FIGURE 3 | Detection of proline and other amino acids in *N. muscorum* CM sample. **(A)** Overlaid chromatogram of *N. muscorum* CM and amino acid standard mix and **(B)** its close-up view of the individual amino acid peaks. **(C)** Confirmation of the elution of proline at the 7.8 min point by spiking *N. muscorum* CM with an internal 100 µM proline standard. Asp, Aspartic acid, Glu, Glutamic acid, Ser, Serine, Asn, Asparagine, Gly, Glycine, Gln, Glutamine, His, Histidine, Arg, Arginine, Thr, Threonine, Ala, Alanine, Pro, Proline, Tyr, Tyrosine, Val, Valine, Met, Methionine, Cys, Cysteine, Ile, Isoleucine, Leu, Leucine, Phe, Phenylalanine, Trp, Tryptophan, and Lys, Lysine.

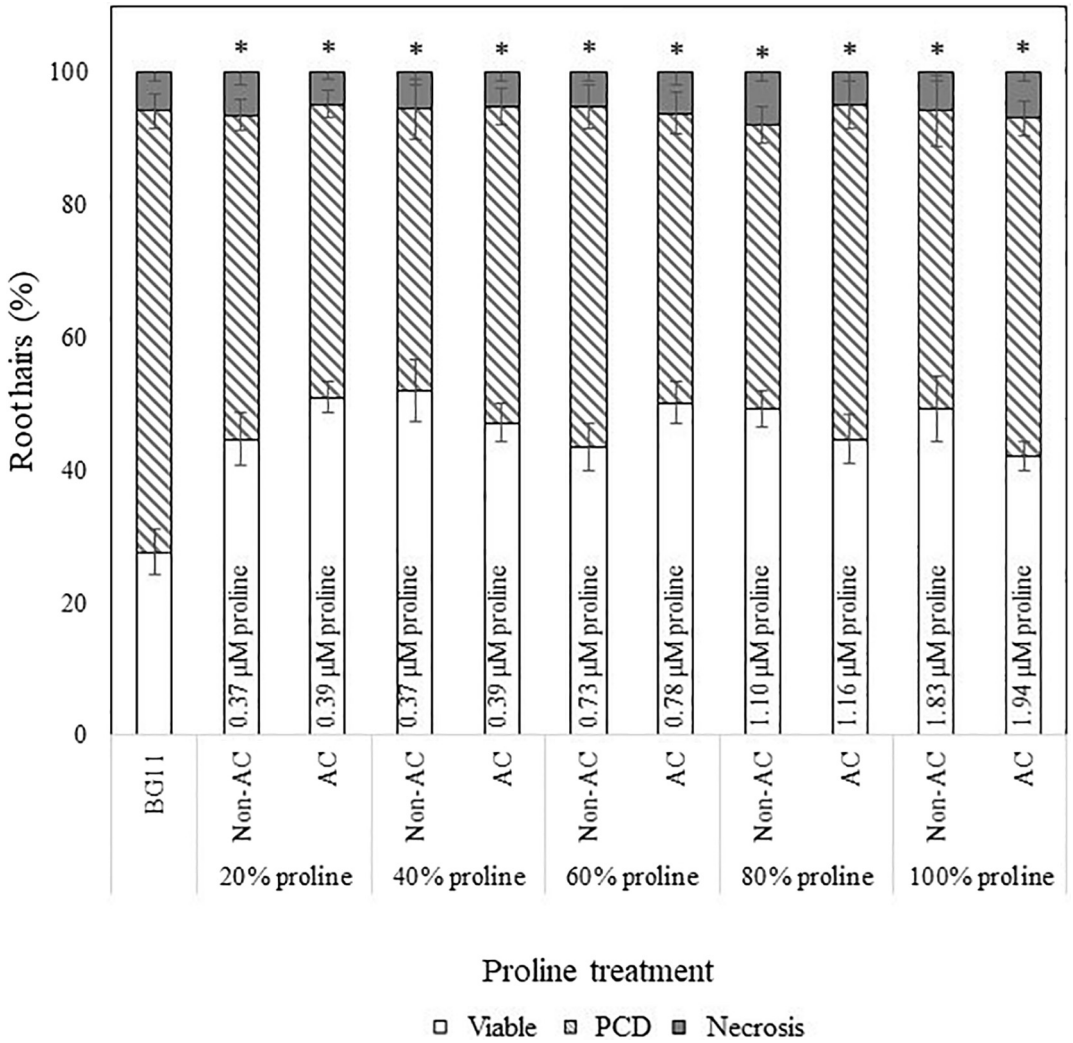

FIGURE 4 | Effect of autoclaved (AC) and non-autoclaved exogenous proline on root hair viability and cell death modes of *Arabidopsis* at 50°C. A proline gradient (20–100%) was made up to assess its similarity to the *N. muscorum* gradient in **Figure 2**. Solutions labeled '100% proline' corresponded to proline levels previously measured in undiluted *N. muscorum* CM. The remaining gradient (20–80%) was established in BG11, where 80% proline = 80% proline + 20% BG11, 60% proline = 60% proline + 40% BG11, etc., (*) marks PCD levels significantly ($p < 0.05$) different from the BG11 control (**Supplementary Table 2**). The bars represent viable (white), PCD (hatched) and necrosis (gray) root hairs, each expressed as a percentage of cell mode over total number of root hairs. Values are the average of $n \geq 12$ (±SE) and represent the merged results of 3 experiments.

Evaluating the Effect of Exogenous Proline and *N. muscorum* CM in Mutant *Arabidopsis* Lines

We evaluated the stress response profile of three proline transporter mutants against wild-type seedlings after *N. muscorum* CM and exogenous proline treatment. Due to differences in the ages of wild-type seed batches and their storage conditions, we obtained different PCD levels in the BG11 controls in **Figures 6A,B** (∼50%), compared to a different experimental set in **Figure 5** (65–80%). All four *Arabidopsis* lines (wild-type, *lht1*, *aap1* and the *atprot* triple knockout mutant line) were treated with undiluted *N. muscorum* CM (100% CM), low (1 μM), medium (2–5 μM), or high (100 μM) proline levels and two controls (SDW and BG11). For clarity, the SDW dataset is omitted here as it has no significant ($p > 0.05$) differences with the BG11 control but is displayed in **Supplementary Table 4**.

Wild-type seedlings benefited the most out of the four tested *Arabidopsis* lines, whether they were treated with exogenous proline or *N. muscorum* CM (**Figure 6**). An overall trend of lower stress-induced PCD levels were observed with proline treatments from 1–5 μM, and significant reductions ($p < 0.05$) were noted with 1 μM and 5 μM compared to the BG11 control (**Supplementary Table 4**). Biological variability probably accounts for weak effect at 2 μM proline as the −3.94% reduction was not sufficiently high enough to be significant. *N. muscorum* CM-treated wild-type plants also had the lowest

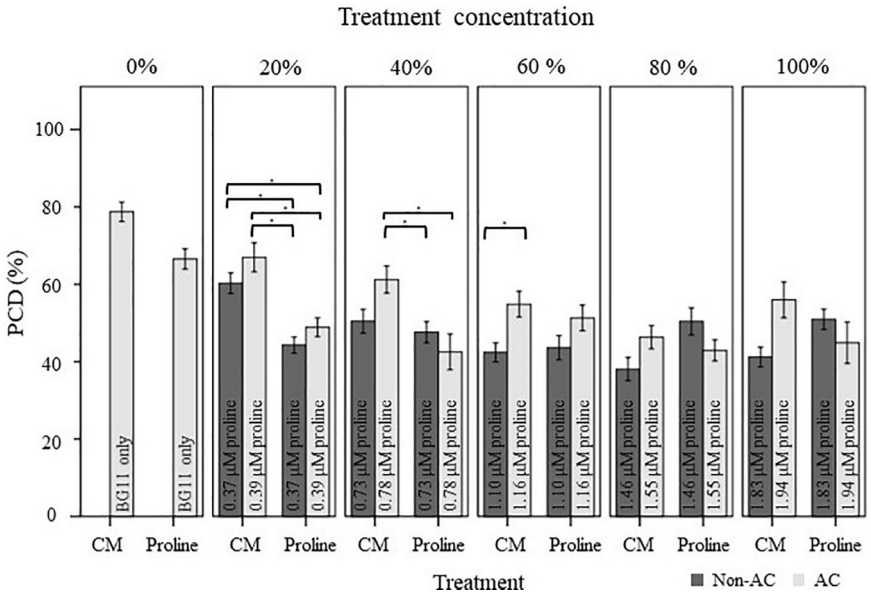

FIGURE 5 | Comparison of the stress-induced PCD levels of autoclaved (AC) and non-autoclaved *N. muscorum* CM and exogenous proline in 50 °C-heat shocked *Arabidopsis* seedlings. Samples were diluted in BG11 across a concentration gradient (0–100%). Solutions labeled '100% proline' corresponded to proline levels previously measured in undiluted *N. muscorum* CM, while the remaining solutions were diluted in BG11, where 80% proline = 80% proline + 20% BG11, 60% proline = 60% proline + 40% BG11, etc., Values for each dataset represent the average of $n \geq 8$ (±SE) and represent the merged results of 3 experiments. Datasets marked with an (*) are statistically different ($p < 0.05$) to each other using a one-way ANOVA Tukey *post-hoc* test (**Supplementary Table 3**).

PCD levels (26.7%) of all four *Arabidopsis* lines which equated to approximately 21.4% lower than its untreated control. However, a cytotoxic effect was noted when proline was supplemented at high (100 μM) doses; proline lost its protective effects as stress-induced PCD levels rose to 44.5% and was not statistically ($p = 0.894$) different from the BG11 control seedlings. A similar effect took place when proline was supplemented at 1000 μM, resulting in 54% PCD (data not shown), showing that excessive proline doses have a cytotoxic effect.

There were a number of interesting observations from the mutant supplementation study: (1) the PCD-suppressing effects of proline was attenuated in proline transporter mutants, (2) the *atprot* triple knockout mutant displayed a stress phenotype more similar to wild-type seedlings, (3) differences between *atprot* triple knockout mutant with *aap1* and *lht1* mutants only becomes apparent at different proline doses, and (4) priming mutants with *N. muscorum* CM eliminated differences between mutants.

First, proline transporter mutants responded differently to exogenous proline treatment (**Figure 6A**). Statistical analysis confirmed that all three mutant lines had no significant differences ($p > 0.05$) across the entire 1–100 μM proline treatment compared to their respective BG11 controls (**Supplementary Table 4**). This was reflected in the stability of their PCD levels, as the biggest mean differences from their respective BG11 controls were insignificant, e.g., the *atprot* triple knockout mutant (4.6%), *lht1* (4.8%), and to a lesser extent *aap1* (11.1%). Thus, the PCD-suppressing effects observed in proline-treated wild-type seedlings were lost in the proline transporter mutants.

Nevertheless, we also observed a marked difference between the stress-response of proline-specific (*atprot* triple knockout) and the general amino acid transporter (*lht1* and *aap1*) mutants. The *atprot* triple knockout mutant displayed a stress phenotype more akin to wild-type seedlings, unlike the *lht1* and *aap1* knockout mutants (**Figure 6B**). The *atprot* triple knockout mutant had negligible changes to PCD (43–48%) levels across all proline treatments and were not statistically different ($p > 0.05$) from the wild-type seedlings at identical proline doses (**Supplementary Table 5**). In contrast, *aap1* and *lht1* mutants shared a similar stress phenotype, with higher PCD levels than wild-type and the *atprot* triple knockout mutant.

Next, the variances between the *atprot* triple knockout and both general amino acid transporter mutants were apparent at medium (2–5 μM) and high (100 μM) proline doses, but had little differences at low (1 μM) proline treatment (**Figure 6B**). At low proline levels, all three mutants had similar PCD levels (41–50%) to each other but a different pattern emerged when they were supplied with medium and high proline doses. The *atprot* triple knockout mutant only had slightly higher PCD levels (up to a 9.5% increase) than wild-type lines at medium and high proline doses. In contrast, both general amino acid transporter mutants were more susceptible to death and displayed up to a 19% increase in PCD levels compared to wild-type seedlings. This was reflected in statistical analysis showing that *aap1* and *lht1* mutants were significantly different ($p < 0.05$) from wild-type seedlings at 5 μM and 100 μM proline doses (**Supplementary Table 5**).

Finally, priming with *N. muscorum* CM eliminated the phenotypic difference between the *atprot* triple knockout and general amino acid transporter mutants as we detected similar

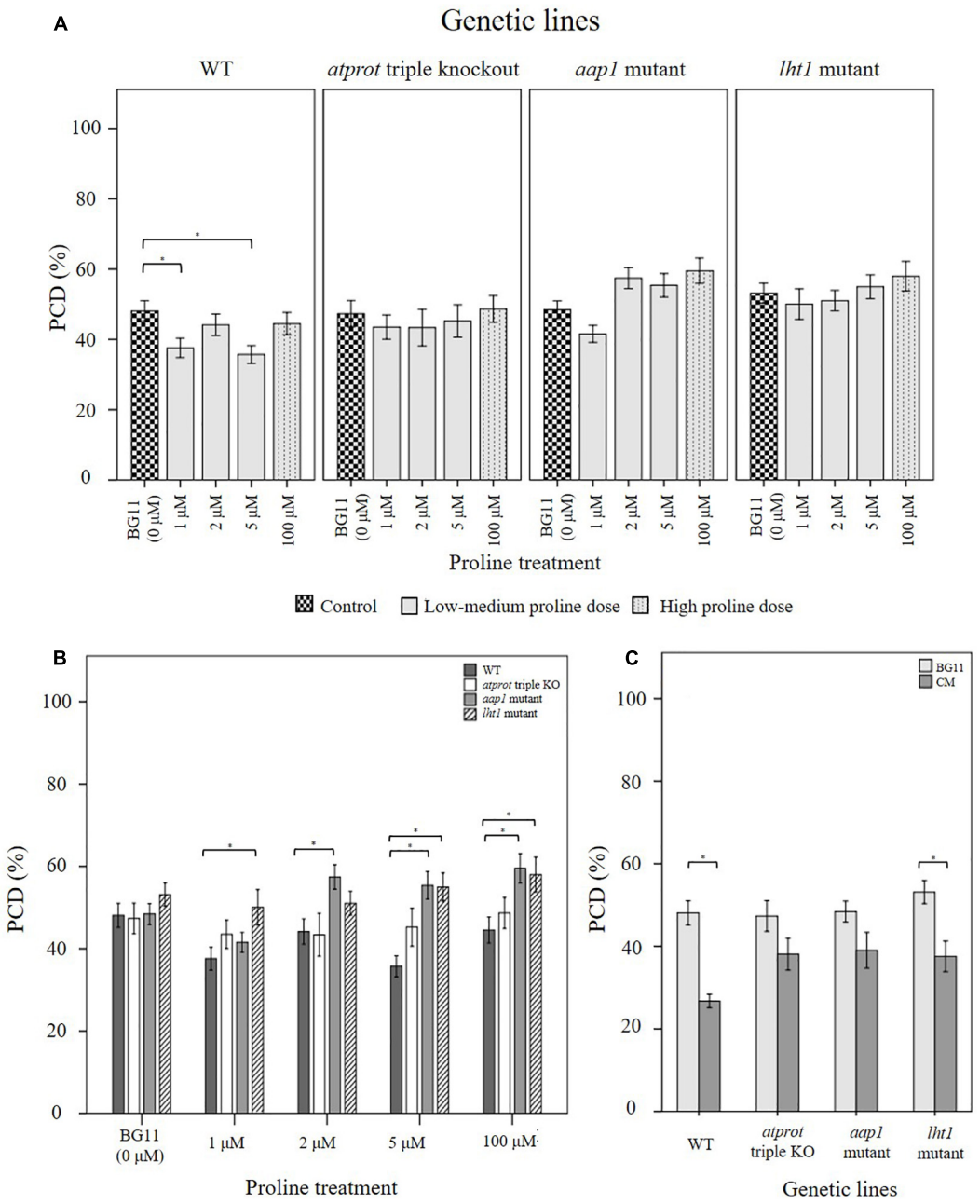

FIGURE 6 | Examining how proline bioactivity differs between 50°C-heat shocked wild-type and proline transporter mutants (*atprot1-1::atprot2-3::atprot3-2*, *aap1*, and *lht1*) upon **(A, B)** proline or **(C)** *N. muscorum* CM treatment. Figures **A and B** are the same data collated into different groupings. Datasets marked with an (*) are statistically different ($p < 0.05$) to each other (**Supplementary Tables 4, 5**). Values are the average of $n \geq 12$ (± SE) and represent the merged results of 3 experiments.

PCD levels (35–39%) across all three mutant lines (**Figure 6C**). The CM bioactive effect was weaker in mutant lines as CM-treated mutants had a higher average of PCD levels (8–12%) than wild-type seedlings, but only the *app1* mutants were significantly different ($p = 0.032$) (**Supplementary Table 5**). It appears than even in mutant lines, the accompanying bioactive compounds in *N. muscorum* CM were likely acting synergistically to exert a stronger PCD-suppressing effect than proline alone.

DISCUSSION

Survival signals such as platelet-derived and insulin-like growth factors can inhibit PCD in animal cells (Barres et al., 1992) and similar observations have been noted in plants as McCabe et al. (1997) showed that carrot cell CM inhibits stress-induced PCD at low cell densities. Previous work by C.T. Daly (unpublished data) suggest that *N. muscorum* CM contains pro-survival signals

that exert a similar bioactive effect in *Arabidopsis* root hairs but attempts to identify the compound are difficult as *N. muscorum* exudes a broad range of exometabolites. Here, the RHA was used as a rapid screening tool to characterize *N. muscorum* CM bioactivity on root hair stress tolerance in terms of viability, PCD and necrosis. By using this high-throughput method, we developed a workflow for identifying and assessing the validity of the main bioactive compound in *N. muscorum* CM, as summarized in **Figure 7**.

To achieve this, we first established the baseline stress response in untreated wild-type (Col-0) *Arabidopsis* root hairs and identified similar thresholds (**Figure 1B**), first reported by Hogg et al. (2011). For example, root hairs primarily underwent PCD when subjected to heat stress within the temperature range in which cells die predominantly of PCD. At this stage, root hairs either survive if the cellular protective mechanisms can repair the heat-induced damage or activate PCD if the response is insufficient. By identifying the PCD threshold, 50 °C was chosen as the set-point for screening *N. muscorum* CM. Beyond this temperature, root hairs cannot survive and crossing the necrotic threshold causes necrosis to replace PCD as the primary cell death mode because of excessive cellular damage. This biphasic cell death motif concurs with past *in vivo* (Hogg et al., 2011) and *in vitro* (Lennon et al., 1991; McCabe et al., 1997; Mammone et al., 2000; Burbridge et al., 2007) studies showing that the severity of an insult governs the fate of the cell.

In the initial *N. muscorum* CM screening, our results yielded a few key observations. Firstly, the main PCD-suppressing bioactive compound in *N. muscorum* CM was thermostable as autoclaving did not attenuate the pro-survival signal in treated *Arabidopsis* seedlings. Additional thermolabile bioactives were likely acting in synergy with the main bioactive to suppress PCD as stress-induced PCD levels in root hairs were consistently lower in non-autoclaved CM treated seedlings than their autoclaved CM-treated counterparts. Furthermore, *N. muscorum* secretes EPS into their growth medium (Mehta and Vaidya, 1978) and autoclaving sugars with phosphate (BG11 medium contains high K_2HPO_4 concentrations) generates cytotoxic products (Finkelstein and Lankford, 1957; Wang and Hsiao, 1995). Therefore, the diminished capacity of autoclaved CM to suppress PCD was likely a combination of the destruction of synergistic thermolabile bioactive compounds and leftover cytotoxic by-products from the autoclaving process. Lastly, the main bioactive compound in *N. muscorum* CM shifted the PCD threshold instead of decreasing necrosis levels. Distinguishing whether the pro-survival signal affects PCD or necrosis is important as modulation of a general stress response affects necrosis, while treatments targeting the PCD pathway itself lowers PCD levels, but not necrosis (Reape et al., 2008). Thus, the main bioactive compound appeared to be directly affecting the PCD pathway and not a general stress response. Collectively, these observations were used to narrow the list of bioactive candidates as a literature review of *N. muscorum* exometabolites showed that they can be grouped into the following categories: exoproteins (Oliveira et al., 2015), EPS (Mehta and Vaidya, 1978), amino acids (Picossi et al., 2005; Pernil et al., 2008), the phytohormones auxin (Mirsa and Kaushik, 1989; Karthikeyan et al., 2009) and ABA (Maršálek et al., 1992), phenolics and alkaloids (Abdel-Hafez et al., 2015), and fatty acid derivatives (Abdel-Hafez et al., 2015).

Compounds were grouped into orders of importance based on their ability to withstand thermal degradation. This eliminated thermolabile groups such as EPS and exoproteins as primary candidates, while phytohormones (Sigma-Aldrich, 2019) and phenolics (Zainol et al., 2009; Igual et al., 2011; Sharma and Gujral, 2011) were considered secondary candidates as thermal processing results in a significant loss of biological activity. After filtering candidates based on their thermostability, the remaining candidate groups were amino acids, and fatty acid derivatives. By considering three factors (mechanism of PCD inhibition, cyanobacteria release and plant uptake), proline arose as a promising candidate as it accumulates in plants under abiotic and biotic stress (Abrahám et al., 2010; Hayat et al., 2012).

Proline protects against oxidative damage by upregulating the antioxidant defense and glyoxalase system (Hossain et al., 2014, 2016; Rejeb et al., 2014). Growth medium supplementation of 5–20 mM proline upregulated flux through the influential H_2O_2-detoxifying ascorbate-glutathione (AsA-GSH) cycle and methylglyoxal-detoxification pathways for increased tolerance to salt (Hoque et al., 2008; Hossain and Fujita, 2010) and cold stress (Kumar and Yadav, 2009). Both pathways are linked by GSH, a redox buffer that modulates the stress acclimation response as efficient GSH recycling through the glyoxalase and AsA-GSH cycle lessens the oxidative load on plant cells (Yadav et al., 2005; Hossain et al., 2016). This holds important significance for our work as ROS signaling is complicit in PCD activation in animals and plants (Doyle et al., 2010; Wang et al., 2013; Gutiérrez et al., 2014). Moreover, exogenous proline was effective at quenching ROS and inhibiting PCD in *Colletotrichum trifolii* and *Saccharomyces cerevisiae* under a range of stress elicitors (UV radiation, salt, heat, H_2O_2 and paraquat) (Chen and Dickman, 2005). Proline appears to have an important protective role in suppressing ROS-mediated PCD (Chen and Dickman, 2005) and here we report a similar effect *N. muscorum* CM has in plants.

The evidence points towards cyanobacteria-derived proline as the main bioactive ingredient as proline buffers against oxidative damage by indirectly scavenging ROS in stressed plants (Hossain et al., 2014, 2016; Rejeb et al., 2014). Additionally, unspecific leakage of proline through the *natH* transporter enables its release by *N. muscorum* cells into the extracellular medium (Picossi et al., 2005). Finally, plants have three amino acid transporter subfamilies (two general and one proline-specific) that can import proline from their surroundings into plant roots (Lehmann et al., 2010). On the whole, this offers a working paradigm as to how cyanobacteria-derived proline can prime the root hair stress response in heat-shocked *Arabidopsis* seedlings.

Following this, we used two assays to provide evidence for the presence of proline in *N. muscorum*. The ninhydrin assay was first used to quantify the proline levels, but the assay may provide false positives or overestimate the proline concentration in CM as it side-reacts with hydroxyproline and pipecolic acid. Therefore, we used the HPLC for additional proof and found similar retention times of the putative proline peak in the CM sample with both the proline standard and proline-spiked CM

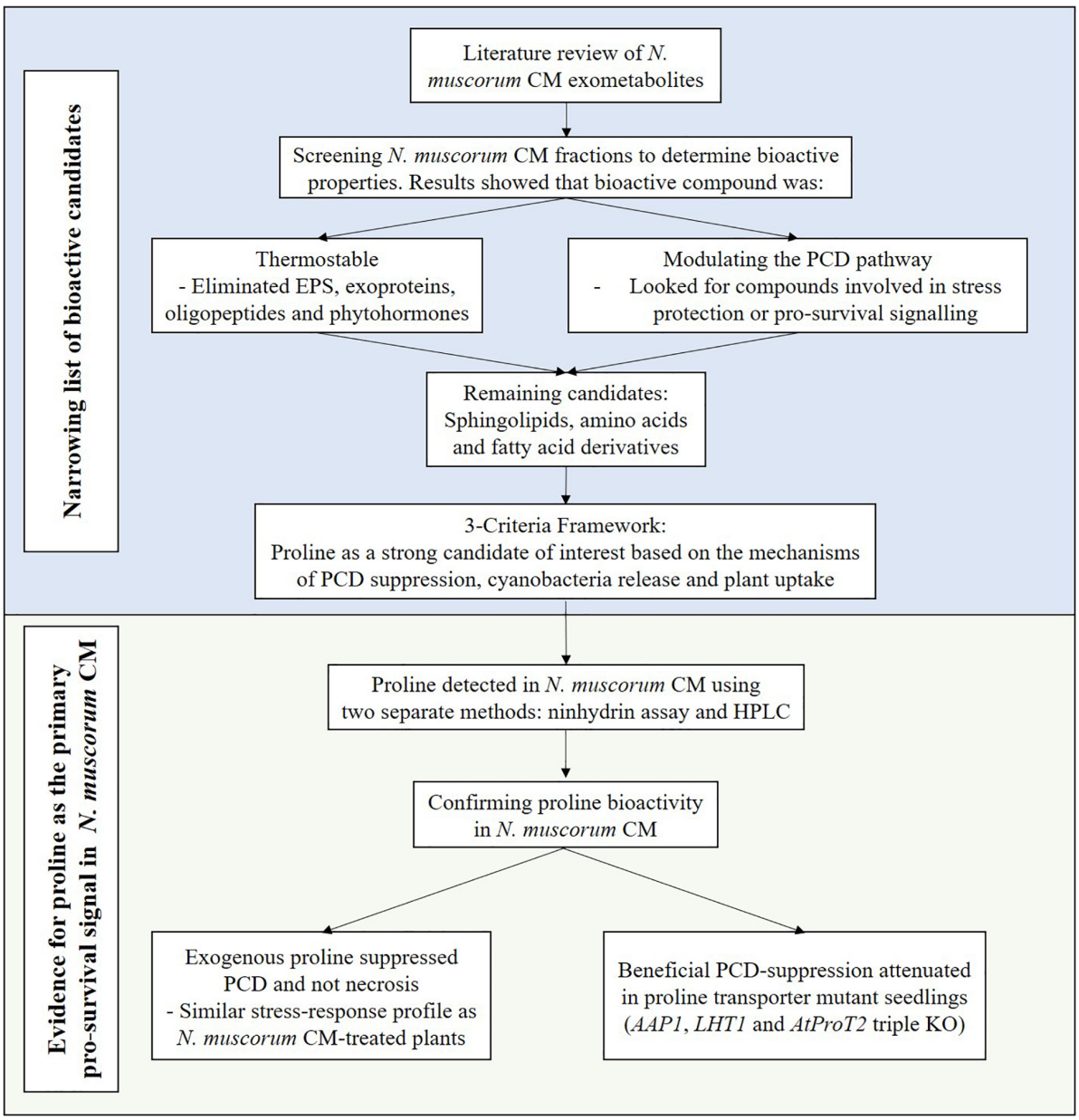

FIGURE 7 | Workflow for identifying the pro-survival signal in *N. muscorum* CM.

samples. Collectively, our results offer strong evidence for proline in the CM. We then followed-up with two sets of experiments to determine if proline was the main bioactive compound in CM. In the first experimental series, we supplied wild-type *Arabidopsis* seedlings with exogenous proline at the concentrations measured in *N. muscorum* CM. Our results showed that exogenous proline elicited a similar stress response profile to *N. muscorum* CM treatment by increasing viability levels by inhibiting PCD, but not necrosis. All ten proline fractions (autoclaved and non-autoclaved) significantly reduced the proportion of root hairs initiating PCD in treated *Arabidopsis* seedlings compared to the BG11 control. Moreover, autoclaving proline did not attenuate its PCD suppressing effects, showing that the main bioactive compound was highly thermostable. Interestingly, exogenous proline did not suppress PCD in a dose-dependent manner as seen in the *N. muscorum* CM fractions, at least not in the current tested range. Proline likely acts in synergy with the accompanying bioactive exometabolites in *N. muscorum* CM to exert a stronger PCD-suppressing effect than individual proline treatments alone. Moreover, we observed a cytotoxic effect when seedlings were supplemented with overtly high proline doses. This was reminiscent of past studies reporting the cytotoxic effects of over-supplying proline in *Distichlis spicata* suspension cultures (2–10 mM) (Rodriguez and Heyser, 1988)

and *Arabidopsis (*5–20 mM) (Hare et al., 2002) and rice seedlings (5–10 mM) (Chen and Kao, 1995). For example, Hellmann et al. (2000) showed that *Arabidopsis* (ecotype C24) plants developed lesions after prolonged incubation on agar plates containing 200 mM proline (48 h).

Next, we investigated how *Arabidopsis* wild-type and proline transporter (*lht1*, *aap1* and *atprot* triple knockout) mutants responded towards proline and *N. muscorum* CM treatment. A proline gradient was used as all three transporter subfamilies possess varying affinities for proline; heterologous *Saccharomyces cerevisiae* expression showed that *ProT* transporters had the lowest proline affinity, e.g., AtProT1 (427 μM), AtProT2 (500 μM), AtProT3 (999 μM), AAP1 (60 μM), and LHT1 (10 μM) (Lehmann et al., 2010). By comparing the performance of the mutant lines against wild-type seedlings, we sought to confirm if proline was one of the major bioactive ingredients in *N. muscorum* CM, while discerning the role of each transporter in stress tolerance.

Our results showed that the beneficial PCD-suppressing proline effect seen in wild-type seedlings was lost in all three mutant lines. Similarly, the bioactive effect of CM treatment was weaker across the mutant lines, although only the *aap1* mutant was statistically different ($p = 0.032$) from the wild-type seedlings. Under low to medium proline doses, PCD was inhibited in wild-type seedlings, but this effect was lost in the mutant lines, especially in *aap1* and *lht1* mutants. Statistical analysis confirmed this as all three mutants had no significant ($p > 0.05$) PCD deviations across all proline treatments, compared to their respective BG11 controls. A similar root hair stress-response profile was observed when the mutants were treated with *N. muscorum* CM: all mutants had higher PCD and lower viability levels than wild-type seedlings under identical treatments. As the mutant lines have an impaired ability to import proline, their subsequent higher root hair PCD levels offered further evidence that proline was an important bioactive compound in *N. muscorum* CM.

It must be noted that we did not assess the mutants at other temperatures in the absence of CM or proline treatments. As of now, no study has investigated the possible effect of the amino transporter mutations on temperature sensitivity; current studies include exposure of *aap1* mutants to toxic levels of amino acids (2–100 mM) (Lee et al., 2007), *atprot* mutants to salt stress (Lehmann et al., 2011) and *lht1* mutants grown with elevated inorganic nitrogen levels (Hirner et al., 2006). In future experiments, it would be interesting to explore if the mutations would have an impact on temperature sensitivity, i.e., if the threshold for PCD induction would shift to another temperature because of possible deleterious effects from impaired proline transport. Also, we acknowledge that stressed plants can elevate internal proline levels by upregulating proline biosynthesis instead of relying on external proline uptake. However, prokaryotic studies show that proline uptake is preferred over biosynthesis if the osmolyte is already readily available (Roesser and Müller, 2001). Similar findings have been shown in plants; osmotic stressed maize (Verslues and Sharp, 1999) and salt stressed barley roots (Ueda et al., 2007) contain elevated proline levels, despite low levels of proline biosynthesis in the root tips. This was further underscored by elevated *HvProT* expression in barley root cap cells under salt stress and minimal pyrroline-5-carboxylate synthetase (P5CS1) activity (Ueda et al., 2001). Taken together, this implies that stressed plants also prefer importing proline compared to the biosynthesis route as it enables metabolic resources to be channeled towards other cell protective mechanisms for improved survival rates (Verslues and Sharma, 2010).

Although all three mutants did not respond to the PCD-suppressing effects of proline, a distinct root hair stress-response profile was observed between the general amino acid transporter (*lht1* and *aap1*) and *atprot* triple knockout mutants. The *atprot* triple knockout mutant displayed a stress phenotype more reminiscent to wild-type seedlings than the mutant lines. Lehmann et al. (2011) showed that single, double and *atprot* triple knockout mutants had no discernible changes between the shoot size, root length and flowering time, compared to wild-type seedlings grown under axenic conditions or in the soil. This was also reflected in salt-stress treatments as they noted similar leaf proline distribution levels between the wild-type and *atprot3-2* and the authors concluded that the lack of the strong phenotype of the *atprot* triple knockout mutants lines is due to compensation by the other root-localized proline transporters (LHT1 and APP1). Our results also reflected this as significant deviations in PCD levels from wild-type seedlings only occurred when either LHT1 or AAP1 are inactivated. Phloem-localized AtProT1 is responsible for long-distance proline translocation and can be replaced by the AAP1 transporter, while AtProT2 is found in the root epidermis and imports extracellular proline into the root cortex; this can be replaced by both LHT1 and AAP1 transporters (Perchlik et al., 2014). Thus, our work provides reinforcing evidence of the functional overlap shared between ProT and other proline transporters (Lehmann et al., 2011).

Between exogenous proline and *N. muscorum* CM treatments, the latter resulted in the lowest stress-induced PCD levels across wild-type and mutant lines. The biological matrix likely contains additional bioactive compounds that act synergistically to exert a stronger PCD-suppressing effect than individual proline treatments alone. We did not confirm the identity of these additional compounds, but candidates include EPS, phytohormones, ROS-detoxifying exoproteins and phenolics. EPS such as arabinose, glucose, galactose, rhamnose, xylose and ribose have been detected in *N. muscorum* CM (Mehta and Vaidya, 1978) and carbohydrates are organic osmolytes that protect macromolecule structure against denaturing stress conditions (Yancey, 2005; Judy and Kishore, 2016). Microbial-derived phytohormones have been suggested to play an important role in plant survival fitness (Fahad et al., 2015; Egamberdieva et al., 2017). A substantial portion of *N. muscorum* exoproteins were associated with ROS detoxification, suggesting the importance of maintaining redox homeostasis even outside the cell (Oliveira et al., 2015). Moreover, the high concentrations of phenolics and alkaloids in *N. muscorum* CM may buffer against oxidative damage (El-Sheekh et al., 2006; Abdel-Hafez et al., 2015). Collectively, reduction of ROS damage may suppress activation of PCD-inducing signals.

CONCLUSION

In this study, we provide evidence that cyanobacteria-derived proline suppressed PCD in *Arabidopsis* root hairs. By using the RHA to characterize *N. muscorum* CM bioactivity, we found that a major bioactive compound was thermostable and directly affecting PCD levels but not necrosis. Proline was identified as a potential candidate and strong evidence using the ninhydrin assay and HPLC suggest that proline is present in *N. muscorum* CM. Subsequent testing with exogenous proline showed a similar root hair stress-response profile with *N. muscorum* CM treatment (higher viability, lower PCD and unaffected necrosis levels), showing that both treatments altered the PCD sensitivity threshold. However, the lower PCD rates observed in *N. muscorum* CM treatment is likely because of synergistic interactions between additional thermolabile bioactive compounds. We provide additional evidence for proline as the bioactive compound using three proline transporter mutants (*lht1*, *aap1* and *atprot* triple knockout). Both general amino acid transporter mutants (*lht1* and *aap1*) displayed similar stress phenotypes to each other, with consistently higher PCD levels than wild-type seedlings at medium to high proline doses. All three mutant lines had higher PCD levels when treated with *N. muscorum* CM compared to wild-type seedlings, providing additional evidence for proline as an important bioactive compound present in *N. muscorum* CM. Data from the mutant lines also reinforce earlier findings that the accompanying bioactive compounds in *N. muscorum* CM were strongly inhibiting PCD over proline treatment alone, which warrants further research in the future. Collectively, this offers preliminary evidence of an unconventional biofertiliser method for inhibiting environmentally induced PCD, distinct from the known mechanisms in literature.

DATA AVAILABILITY STATEMENT

All datasets generated for this study are included in the manuscript/**Supplementary Material**.

AUTHOR CONTRIBUTIONS

AC designed and performed the majority of the experiments. OS prepared and captured the **Supplementary F1 image**. CN, PM, and CD conceived several of the preliminary hypotheses. LF and CD contributed to the discussion of the results. All authors reviewed and approved the final manuscript.

FUNDING

This work was supported by the Ph.D. scholarship awarded to AC by Waterford Institute of Technology, Ireland, an Irish Research Council for Science Engineering and Technology (IRCSET) Ph.D. scholarship awarded to CD, and an Irish Research Council – Environmental Protection Agency (IRC-EPA) Ph.D. scholarship awarded to OS. Publishing costs have been partially funded by the Waterford Institute of Technology 'Research Connexions' Research Support Scheme through the WIT School of Science, and the School of Biology and Environmental Science, University College Dublin.

ACKNOWLEDGMENTS

We would like to thank Professor Mechthild Tegeder (Washington State University, United States) who gifted us the *lht1* and *aap1* mutants and Professor Doris Rentsch (University of Bern, Switzerland) who kindly gave us the *1::atprot2-3::atprot3-2* mutant.

SUPPLEMENTARY MATERIAL

The Supplementary Material for this article can be found online at: https://www.frontiersin.org/articles/10.3389/fpls.2020.490075/full#supplementary-material

REFERENCES

Abdel-Hafez, S. I. I., Abo-Elyousr, K. A. M., and Abdel-Rahim, I. R. (2015). Fungicidal activity of extracellular products of cyanobacteria against *Alternaria porri*. *Eur. J. Phycol.* 50, 239–245. doi: 10.1080/09670262.2015.1028105

Abrahám, E., Hourton-Cabassa, C., Erdei, L., and Szabados, L. (2010). "Methods for determination of proline in plants," in *Plant Stress Tolerance: Methods in Molecular Biology*, ed. R. Sunkar (Totowa, NJ: Humana Press), 317–331. doi: 10.1007/978-1-60761-702-0_20

Barres, B. A., Hart, I. K., Coles, H. S., Burne, J. F., Voyvodic, J. T., Richardson, W. D., et al. (1992). Cell death and control of cell survival in the oligodendrocyte lineage. *Cell* 70, 31–46. doi: 10.1016/0092-8674(92)90531-g

Barreto, V., Seldin, L., and Araujo, F. F. D. (2011). Plant growth and health promoting bacteria. *Microbiol. Monogr.* 18, 21–44. doi: 10.1007/978-3-642-13612-2

Bates, L. S., Waldren, R. P., and Teare, I. D. (1973). Rapid determination of free proline for water-stress studies. *Plant Soil* 39, 205–207. doi: 10.1007/BF00018060

Burbridge, E., Diamond, M., Dix, P. J., and McCabe, P. F. (2007). Use of cell morphology to evaluate the effect of a peroxidase gene on cell death induction thresholds in tobacco. *Plant Sci.* 172, 853–860. doi: 10.1016/j.plantsci.2006.03.024

Campbell, E. L., and Meeks, J. C. (1989). Characteristics of hormogonia formation by symbiotic *Nostoc* spp. in response to the presence of *Anthoceros punctatus* or its extracellular products. *Appl. Environ. Microbiol.* 55, 125–131. doi: 10.1128/aem.55.1.125-131.1989

Chen, C., and Dickman, M. B. (2005). Proline suppresses apoptosis in the fungal pathogen *Colletotrichum trifolii*. *Proc. Natl. Acad. Sci. U.S.A.* 102, 3459–3464. doi: 10.1073/pnas.0407960102

Chen, S. L., and Kao, C. H. (1995). Cd induced changes in proline level and peroxidase activity in roots of rice seedlings. *Plant Growth Regul.* 17, 67–71. doi: 10.1007/BF00024497

Claussen, W. (2005). Proline as a measure of stress in tomato plants. *Plant Sci.* 168, 241–248. doi: 10.1016/j.plantsci.2004.07.039

Daneva, A., Gao, Z., Van Durme, M., and Nowack, M. K. (2016). Functions and regulation of programmed cell death in plant development. *Annu.*

Rev. Cell Dev. Biol. 32, 441–468. doi: 10.1146/annurev-cellbio-111315-124915

Doyle, S. M., Diamond, M., and McCabe, P. F. (2010). Chloroplast and reactive oxygen species involvement in apoptotic-like programmed cell death in *Arabidopsis* suspension cultures. *J. Exp. Bot.* 61, 473–482. doi: 10.1093/jxb/erp320

Egamberdieva, D., Wirth, S. J., Alqarawi, A. A., Abd Allah, E. F., and Hashem, A. (2017). Phytohormones and beneficial microbes: essential components for plants to balance stress and fitness. *Front. Microbiol.* 8:2104. doi: 10.3389/fmicb.2017.02104

El-Sheekh, M. M., Osman, M. E. H., Dyab, M. A., and Amer, M. S. (2006). Production and characterization of antimicrobial active substance from the cyanobacterium *Nostoc muscorum*. *Environ. Toxicol. Pharmacol.* 21, 42–50. doi: 10.1016/j.etap.2005.06.006

Fahad, S., Hussain, S., Bano, A., Saud, S., Hassan, S., Shan, D., et al. (2015). Potential role of phytohormones and plant growth-promoting rhizobacteria in abiotic stresses: consequences for changing environment. *Environ. Sci. Pollut. Res.* 22, 4907–4921. doi: 10.1007/s11356-014-3754-2

Ferreyra, M. L. F., Casadevall, R., D'Andrea, L., Abd Elgawad, H., Beemster, G. T. S., and Casati, P. (2016). AtPDCD5 plays a role in programmed cell death after UV-B exposure in Arabidopsis. *Plant Physiol.* 170, 2444–2460. doi: 10.1104/pp.16.00033

Finkelstein, R. A., and Lankford, C. E. (1957). A bacteriotoxic substance in autoclaved culture media containing glucose and phosphate. *Appl. Microbiol.* 5, 74–79. doi: 10.1128/aem.5.2.74-79.1957

Forlani, G., and Funck, D. (2020). A specific and sensitive enzymatic assay for the Quantitation of L-Proline. *Front. Plant Sci.* 11:582026. doi: 10.3389/fpls.2020.582026

Friedman, M. (2004). Applications of the ninhydrin reaction for analysis of amino acids, peptides, and proteins to agricultural and biomedical sciences. *J. Agric. Food Chem.* 52, 385–406. doi: 10.1021/jf030490p

Grallath, S., Weimar, T., Meyer, A., Gumy, C., Suter-Grotemeyer, M., Neuhaus, J.-M., et al. (2005). The AtProT family. Compatible solute transporters with similar substrate specificity but differential expression patterns. *Plant Physiol.* 137, 117–126. doi: 10.1104/pp.104.055079

Gutiérrez, J., González-Pérez, S., García-García, F., Daly, C. T., Lorenzo, Ó., Revuelta, J. L., et al. (2014). Programmed cell death activated by Rose Bengal in *Arabidopsis thaliana* cell suspension cultures requires functional chloroplasts. *J. Exp. Bot.* 65, 3081–3095. doi: 10.1093/jxb/eru151

Hare, P., Cress, W., and Staden, J. V. (2002). Disruptive effects of exogenous proline on chloroplast and mitochondrial ultrastructure in Arabidopsis leaves. *S. Afr. J. Bot.* 393–396. doi: 10.1016/S0254-6299(15)30405-1

Hayat, S., Hayat, Q., Alyemeni, M. N., Wani, A. S., Pichtel, J., and Ahmad, A. (2012). Role of proline under changing environments. *Plant Signal. Behav.* 7, 1456–1466. doi: 10.4161/psb.21949

Heinrikson, R. L., and Meredith, S. C. (1984). Amino acid analysis by reverse-phase high-performance liquid chromatography: precolumn derivatization with phenylisothiocyanate. *Anal. Biochem.* 136, 65–74. doi: 10.1016/0003-2697(84)90307-5

Hellmann, H., Funck, D., Rentsch, D., and Frommer, W. B. (2000). Hypersensitivity of an Arabidopsis sugar signaling mutant toward exogenous proline application. *Plant Physiol.* 123, 779–789. doi: 10.1104/pp.123.2.779

Hirner, A., Ladwig, F., Stransky, H., Okumoto, S., Keinath, M., Harms, A., et al. (2006). Arabidopsis LHT1 is a high-affinity transporter for cellular amino acid uptake in both root epidermis and leaf mesophyll. *Plant Cell* 18, 1931–1946. doi: 10.1105/tpc.106.041012

Hogg, B. V., Kacprzyk, J., Molony, E. M., Reilly, C. O., Gallagher, T. F., Gallois, P., et al. (2011). An *in vivo* root hair assay for determining rates of apoptotic-like programmed cell death in plants. *Plant Methods* 7:45. doi: 10.1186/1746-4811-7-45

Hoque, M. A., Banu, M. N. A., Nakamura, Y., Shimoishi, Y., and Murata, Y. (2008). Proline and glycinebetaine enhance antioxidant defense and methylglyoxal detoxification systems and reduce NaCl-induced damage in cultured tobacco cells. *J. Plant Physiol.* 165, 813–824. doi: 10.1016/j.jplph.2007.07.013

Hossain, M. A., Burritt, D. J., and Fujita, M. (2016). "Cross-stress tolerance in plants: molecular mechanisms and possible involvement of reactive oxygen species and methylglyoxal detoxification systems," in *Abiotic Stress Response in Plants*, eds N. Tuteja and S. S. Gill (Weinheim: John Wiley & Sons, Ltd), 327–380. doi: 10.1002/9783527694570.ch16

Hossain, M. A., and Fujita, M. (2010). Evidence for a role of exogenous glycinebetaine and proline in antioxidant defense and methylglyoxal detoxification systems in mung bean seedlings under salt stress. *Physiol. Mol. Biol. Plants* 16, 19–29. doi: 10.1007/s12298-010-0003-0

Hossain, M. A., Hoque, M. A., Burritt, D. J., and Fujita, M. (2014). "Proline protects plants against abiotic oxidative stress: biochemical and molecular mechanisms," in *Oxidative Damage to Plants*, ed. P. Ahmad (San Diego, CA: Academic Press), 477–522. doi: 10.1016/B978-0-12-799963-0.00016-2

Hussain, A., and Hasnain, S. (2011). Phytostimulation and biofertilization in wheat by cyanobacteria. *J. Ind. Microbiol. Biotechnol.* 38, 85–92. doi: 10.1007/s10295-010-0833-3

Igual, M., García-Martínez, E., Camacho, M. M., and Martínez-Navarrete, N. (2011). Changes in flavonoid content of grapefruit juice caused by thermal treatment and storage. *Innov. Food Sci. Emerg. Technol.* 12, 153–162. doi: 10.1016/j.ifset.2010.12.010

Jaiswal, P., Singh, P. K., and Prasanna, R. (2008). Cyanobacterial bioactive molecules: an overview of their toxic properties. *Can. J. Microbiol.* 54, 701–717. doi: 10.1139/W08-034

Judy, E., and Kishore, N. (2016). Biological wonders of osmolytes: the need to know more. *Biochem. Anal. Biochem.* 05:1000304. doi: 10.4172/2161-1009.1000304

Kacprzyk, J., Brogan, N. P., Daly, C. T., Doyle, S. M., Diamond, M., Molony, E. M., et al. (2017). The retraction of the protoplast during PCD is an active, and interruptible, calcium-flux driven process. *Plant Sci.* 260, 50–59. doi: 10.1016/j.plantsci.2017.04.001

Kacprzyk, J., Daly, C. T., and McCabe, P. F. (2011). The botanical dance of death: programmed cell death in plants. *Adv. Bot. Res.* 60, 169–261. doi: 10.1016/B978-0-12-385851-1.00004-4

Karthikeyan, N., Prasanna, R., Sood, A., Jaiswal, P., Nayak, S., and Kaushik, B. D. (2009). Physiological characterization and electron microscopic investigation of cyanobacteria associated with wheat rhizosphere. *Folia Microbiol.* 54, 43–51. doi: 10.1007/s12223-009-0007-8

Kennedy, I. (2008). *Efficient Nutrient Use in Rice Production in Vietnam Achieved Using Inoculant Biofertilisers*. Canberra: Australian Centre for International Agricultural Research.

Kumar, V., and Yadav, S. K. (2009). Proline and betaine provide protection to antioxidant and methylglyoxal detoxification systems during cold stress in *Camellia sinensis* (L.) O. Kuntze. *Acta Physiol. Plant.* 31, 261–269. doi: 10.1007/s11738-008-0227-6

Kwanyuen, P., and Burton, J. W. (2010). A modified amino acid analysis using PITC derivatization for soybeans with accurate determination of cysteine and half-cystine. *J. Am. Oil Chem. Soc.* 87, 127–132. doi: 10.1007/s11746-009-1484-2

Lam, E., Kato, N., and Lawton, M. (2001). Programmed cell death, mitochondria and the plant hypersensitive response. *Nature* 411, 848–853. doi: 10.1038/35081184

Lee, Y.-H., Foster, J., Chen, J., Voll, L. M., Weber, A. P. M., and Tegeder, M. (2007). AAP1 transports uncharged amino acids into roots of Arabidopsis. *Plant J.* 50, 305–319. doi: 10.1111/j.1365-313X.2007.03045.x

Lehmann, S., Funck, D., Szabados, L., and Rentsch, D. (2010). Proline metabolism and transport in plant development. *Amino Acids* 39, 949–962. doi: 10.1007/s00726-010-0525-3

Lehmann, S., Gumy, C., Blatter, E., Boeffel, S., Fricke, W., and Rentsch, D. (2011). In planta function of compatible solute transporters of the AtProT family. *J. Exp. Bot.* 62, 787–796. doi: 10.1093/jxb/erq320

Lennon, S. V., Martin, S. J., and Cotter, T. G. (1991). Dose–dependent induction of apoptosis in human tumour cell lines by widely diverging stimuli. *Cell Prolif.* 24, 203–214. doi: 10.1111/j.1365-2184.1991.tb01150.x

Lenochová, Z., Soukup, A., and Votrubová, O. (2009). Aerenchyma formation in maize roots. *Biol. Plant.* 53, 263–270. doi: 10.1007/s10535-009-0049-4

Mammone, T., Gan, D., Collins, D., Lockshin, R. A., Marenus, K., and Maes, D. (2000). Successful separation of apoptosis and necrosis pathways in HaCaT keratinocyte cells induced by UVB irradiation. *Cell Biol. Toxicol.* 16, 293–302. doi: 10.1023/A:1026746330146

Maršálek, B., Zahradníčková, H., and Hronková, M. (1992). Extracellular abscisic acid produced by cyanobacteria under salt stress. *J. Plant Physiol.* 139, 506–508. doi: 10.1016/S0176-1617(11)80503-1

McCabe, P. F., Levine, A., Meijer, P. J., Tapon, N. A., and Pennell, R. I. (1997). A programmed cell death pathway activated in carrot cells cultured at low cell density. *Plant J.* 12, 267–280. doi: 10.1046/j.1365-313X.1997.12020267.x

Meeks, J. C., Campbell, E., Summers, M., and Wong, F. (2002). Cellular differentiation in the cyanobacterium *Nostoc punctiforme*. *Arch. Microbiol.* 178, 395–403. doi: 10.1007/s00203-002-0476-5

Mehta, V. B., and Vaidya, B. S. (1978). Cellular and extracellular polysaccharides of the blue green alga *Nostoc*. *J. Exp. Bot.* 29, 1423–1430. doi: 10.1093/jxb/29.6.1423

Mirsa, S., and Kaushik, B. D. (1989). Growth promoting substances of cyanobacteria, II. Detections of amino acids, sugars and auxin. *Proc. Indian Natl. Sci. Acad. B* 55, 499–504.

Myers, J. A., Curtis, B. S., and Curtis, W. R. (2013). Improving accuracy of cell and chromophore concentration measurements using optical density. *BMC Biophys.* 6:4. doi: 10.1186/2046-1682-6-4

Nguyen, G. N., Hailstones, D. L., Wilkes, M., and Sutton, B. G. (2009). Drought-induced oxidative conditions in rice anthers leading to a programmed cell death and pollen abortion. *J. Agron. Crop Sci.* 195, 157–164. doi: 10.1111/j.1439-037X.2008.00357.x

Oliveira, P., Martins, N., Santos, M., Couto, N., Wright, P., and Tamagnini, P. (2015). The *Anabaena* sp. PCC 7120 exoproteome: taking a peek outside the box. *Life* 5, 130–163. doi: 10.3390/life5010130

Perchlik, M., Foster, J., and Tegeder, M. (2014). Different and overlapping functions of *Arabidopsis* LHT6 and AAP1 transporters in root amino acid uptake. *J. Exp. Bot.* 65, 5193–5204. doi: 10.1093/jxb/eru278

Pernil, R., Picossi, S., Mariscal, V., Herrero, A., and Flores, E. (2008). ABC-type amino acid uptake transporters Bgt and N-II of *Anabaena* sp. strain PCC 7120 share an ATPase subunit and are expressed in vegetative cells and heterocysts. *Mol. Microbiol.* 67, 1067–1080. doi: 10.1111/j.1365-2958.2008.06107.x

Picossi, S., Montesinos, M. L., Pernil, R., Lichtlé, C., Herrero, A., and Flores, E. (2005). ABC-type neutral amino acid permease N-I is required for optimal diazotrophic growth and is repressed in the heterocysts of *Anabaena* sp. strain PCC 7120. *Mol. Microbiol.* 57, 1582–1592. doi: 10.1111/j.1365-2958.2005.04791.x

Prasanna, R., Sood, A., Jaiswal, P., Nayak, S., Gupta, V., Chaudhary, V., et al. (2010). Rediscovering cyanobacteria as valuable sources of bioactive compounds. *Appl. Biochem. Microbiol.* 46, 119–134. doi: 10.1134/S0003683810020018

Rai, A. N., Söderbäck, E., and Bergman, B. (2000). Cyanobacterium-plant symbioses. *New Phytol.* 147, 449–481. doi: 10.1046/j.1469-8137.2000.00720.x

Rasmussen, U., Bergman, B., and Johansson, C. (1994). Early communication in the Gunnera-Nostoc symbiosis plant-induced cell differentiation and protein synthesis in the cyanobacterium. *Mol. Plant Microbe Interact.* 7, 696–702. doi: 10.1094/mpmi-7-0696

Reape, T. J., and McCabe, P. F. (2013). Commentary: the cellular condensation of dying plant cells: Programmed retraction or necrotic collapse? *Plant Sci.* 207, 135–139. doi: 10.1016/j.plantsci.2013.03.001

Reape, T. J., Molony, E. M., and McCabe, P. F. (2008). Programmed cell death in plants: distinguishing between different modes. *J. Exp. Bot.* 59, 435–444. doi: 10.1093/jxb/erm258

Rejeb, K. B., Abdelly, C., and Savouré, A. (2014). How reactive oxygen species and proline face stress together. *Plant Physiol. Biochem.* 80, 278–284. doi: 10.1016/j.plaphy.2014.04.007

Rentsch, D., Hirner, B., Schmelzer, E., and Frommer, W. B. (1996). Salt stress-induced proline transporters and salt stress-repressed broad specificity amino acid permeases identified by suppression of a yeast amino acid permease-targeting mutant. *Plant Cell* 8, 1437–1446. doi: 10.1105/tpc.8.8.1437

Rodriguez, M. M., and Heyser, J. W. (1988). Growth inhibition by exogenous proline and its metabolism in saltgrass (*Distichlis spicata*) suspension cultures. *Plant Cell Rep.* 7, 305–308. doi: 10.1007/BF00269924

Roesser, M., and Müller, V. (2001). Osmoadaptation in bacteria and archaea: common principles and differences. *Environ. Microbiol.* 3, 743–754. doi: 10.1046/j.1462-2920.2001.00252.x

Schwacke, R., Grallath, S., Breitkreuz, K. E., Stransky, E., Stransky, H., Frommer, W. B., et al. (1999). LeProT1, a transporter for proline, glycine betaine, and γ-amino butyric acid in tomato pollen. *Plant Cell* 11, 377–392. doi: 10.1105/tpc.11.3.377

Shabala, S. (2009). Salinity and programmed cell death: unravelling mechanisms for ion specific signalling. *J. Exp. Bot.* 60, 709–712. doi: 10.1093/jxb/erp013

Sharma, P., and Gujral, H. S. (2011). Effect of sand roasting and microwave cooking on antioxidant activity of barley. *Food Res. Int.* 44, 235–240. doi: 10.1016/j.foodres.2010.10.030

Sigma-Aldrich (2019). *Growth Regulators - Plant Tissue Culture Protocol. Sigma-Aldrich*. Available online at: https://www.sigmaaldrich.com/technical-documents/protocols/biology/growth-regulators.html (accessed May 6, 2019).

Singh, S., Kate, B. N., and Banerjee, U. C. (2005). Bioactive compounds from cyanobacteria and microalgae: an overview. *Crit. Rev. Biotechnol.* 25, 73–95. doi: 10.1080/07388550500248498

Svennerstam, H., Jämtgård, S., Ahmad, I., Huss-Danell, K., Näsholm, T., and Ganeteg, U. (2011). Transporters in Arabidopsis roots mediating uptake of amino acids at naturally occurring concentrations. *New Phytol.* 191, 459–467. doi: 10.1111/j.1469-8137.2011.03699.x

Svenning, M. M., Eriksson, T., and Rasmussen, U. (2005). Phylogeny of symbiotic cyanobacteria within the genus *Nostoc* based on 16S rDNA sequence analyses. *Arch. Microbiol.* 183, 19–26. doi: 10.1007/s00203-004-0740-y

Ueda, A., Shi, W., Sanmiya, K., Shono, M., and Takabe, T. (2001). Functional analysis of salt-inducible proline transporter of barley roots. *Plant Cell Physiol.* 42, 1282–1289. doi: 10.1093/pcp/pce166

Ueda, A., Yamamoto-Yamane, Y., and Takabe, T. (2007). Salt stress enhances proline utilization in the apical region of barley roots. *Biochem. Biophys. Res. Commun.* 355, 61–66. doi: 10.1016/j.bbrc.2007.01.098

Vacca, R. A., de Pinto, M. C., Valenti, D., Passarella, S., Marra, E., and De Gara, L. (2004). Production of reactive oxygen species, alteration of cytosolic ascorbate peroxidase, and impairment of mitochondrial metabolism are early events in heat shock-induced programmed cell death in tobacco bright-yellow 2 cells. *Plant Physiol.* 134, 1100–1112. doi: 10.1104/pp.103.035956

Verslues, P. E., and Sharma, S. (2010). Proline metabolism and its implications for plant-environment interaction. *Arabidopsis Book* 8:e0140. doi: 10.1199/tab.0140

Verslues, P. E., and Sharp, R. E. (1999). Proline accumulation in maize (*Zea mays* L.) primary roots at low water potentials. II. Metabolic source of increased proline deposition in the elongation zone. *Plant Physiol.* 119, 1349–1360. doi: 10.1104/pp.119.4.1349

Volk, R. B. (2007). Studies on culture age versus exometabolite production in batch cultures of the cyanobacterium *Nostoc insulare*. *J. Appl. Phycol.* 19, 491–495. doi: 10.1007/s10811-007-9161-z

Walker, V., and Mills, G. A. (1995). Quantitative methods for amino acid analysis in biological fluids. *Ann. Clin. Biochem.* 32, 28–57. doi: 10.1177/000456329503200103

Wang, X. J., and Hsiao, K. C. (1995). Sugar degradation during autoclaving: effects of duration and solution volume on breakdown of glucose. *Physiol. Plant.* 94, 415–418. doi: 10.1111/j.1399-3054.1995.tb00947.x

Wang, Y., Loake, G. J., and Chu, C. (2013). Cross-talk of nitric oxide and reactive oxygen species in plant programed cell death. *Front. Plant Sci.* 4:314. doi: 10.3389/fpls.2013.00314

Xu, H., Xu, W., Xi, H., Ma, W., He, Z., and Ma, M. (2013). The ER luminal binding protein (BiP) alleviates Cd2+-induced programmed cell death through endoplasmic reticulum stress-cell death signaling pathway in tobacco cells. *J. Plant Physiol.* 170, 1434–1441. doi: 10.1016/j.jplph.2013.05.017

Yadav, S. K., Singla-Pareek, S. L., Ray, M., Reddy, M. K., and Sopory, S. K. (2005). Methylglyoxal levels in plants under salinity stress are dependent on glyoxalase I and glutathione. *Biochem. Biophys. Res. Commun.* 337, 61–67. doi: 10.1016/j.bbrc.2005.08.263

Yancey, P. H. (2005). Organic osmolytes as compatible, metabolic and counteracting cytoprotectants in high osmolarity and other stresses. *J. Exp. Biol.* 208, 2819–2830. doi: 10.1242/jeb.01730

Zainol, K., Abdul Hamid, A., Abu Bakar, F., and Dek, M. (2009). Effect of different drying methods on the degradation of selected flavonoids in *Centella asiatica*. *Int. Food Res. J.* 16, 531–537.

Zavřel, T., Sinetova, M., and Červený, J. (2015). Measurement of chlorophyll a and carotenoids concentration in cyanobacteria. *Bio Protoc.* 5, 1–5. doi: 10.21769/BioProtoc.1467

Conflict of Interest: The authors declare that the research was conducted in the absence of any commercial or financial relationships that could be construed as a potential conflict of interest.

Advantages of publishing in Frontiers

OPEN ACCESS
Articles are free to read for greatest visibility and readership

FAST PUBLICATION
Around 90 days from submission to decision

HIGH QUALITY PEER-REVIEW
Rigorous, collaborative, and constructive peer-review

TRANSPARENT PEER-REVIEW
Editors and reviewers acknowledged by name on published articles

Frontiers
Avenue du Tribunal-Fédéral 34
1005 Lausanne | Switzerland

Visit us: www.frontiersin.org
Contact us: frontiersin.org/about/contact

REPRODUCIBILITY OF RESEARCH
Support open data and methods to enhance research reproducibility

DIGITAL PUBLISHING
Articles designed for optimal readership across devices

FOLLOW US
@frontiersin

IMPACT METRICS
Advanced article metrics track visibility across digital media

EXTENSIVE PROMOTION
Marketing and promotion of impactful research

LOOP RESEARCH NETWORK
Our network increases your article's readership